UNIVERSIDAD DE SONORA

DIVISIÓN DE CIENCIAS BIOLÓGICAS Y DE LA SALUD

DEPARTAMENTO DE INVESTIGACIÓN Y POSGRADO EN ALIMENTOS

Programa de Posgrado en Ciencias y Tecnología de Alimentos

Biodisponibilidad *in vitro* de compuestos fenólicos extraídos de la mezcla hoja-tallo del cártamo (*Carthamus tinctorius* L.) nanoencapsulados en una matriz de zeína

TESIS

Como requisito parcial para obtener el grado de:

DOCTOR EN CIENCIAS DE LOS ALIMENTOS

Presenta:

M.C. José Agustín Tapia Hernández

Hermosillo, Sonora **Septiembre, 2019**

APROBACIÓN

Biodisponibilidad *in vitro* de compuestos fenólicos extraídos de la mezcla hoja-tallo del cártamo (*Carthamus tinctorius* L.) nanoencapsulados en una matriz de zeína

M.C José Agustín Tapia Hernández

_____

Dr. Francisco Rodríguez Félix
Director de Tesis

_____ _____

Dra. Carmen Lizette Del Toro Sánchez
Codirectora de Tesis

Dr. Francisco Javier Cinco Moroyoqui
Secretario de Tesis

_____ _____

Dr. Josué Elías Juárez Onofre
Sinodal de Tesis

Dr. Saúl Ruiz Cruz
Sinodal de Tesis

Hermosillo, Sonora Septiembre del 2019

Hermosillo, Sonora a 06 de agosto de 2019.

Asunto: Cesión de derechos

UNIVERSIDAD DE SONORA
P R E S E N T E.

Por este conducto hago constar que soy autor y titular de la obra denominada **Biodisponibilidad *in vitro* de compuestos fenólicos extraídos de la mezcla hoja-tallo del cártamo (*Carthamus tinctorius* L.) nanoencapsulados en una matriz de zeína**, en los sucesivo LA OBRA, realizada como trabajo terminal con el propósito de obtener el Grado de **Doctor en Ciencias de los Alimentos**, en virtud de lo cual autorizo a la Universidad de Sonora (UNISON) para que efectúe la divulgación, publicación, comunicación pública, distribución, distribución pública, distribución electrónica y reproducción, así como la digitalización de la misma, con fines académicos o propios de la institución y se integren a los repositorios de la universidad, estatales, regionales, nacionales e internacionales.

La UNISON se compromete a respetar en todo momento mi autoría y a otorgarme el crédito correspondiente en todas las actividades mencionadas anteriormente.

De la misma manera, manifiesto que el contenido académico, literario, la edición y en general cualquier parte de LA OBRA son de mi entera responsabilidad, por lo que deslindo a la UNISON por cualquier violación a los derechos de autor y/o propiedad intelectual y/o cualquier responsabilidad relacionada con la OBRA que cometa el suscrito frente a terceros.

A T E N T A M E N T E

LIC. GILBERTO LEÓN LEÓN
Abogado General
UNIVERSIDAD DE SONORA

José Agustín Tapia Hernández

RESUMEN

Hoy en día, se ha reportado que los compuestos fenólicos (CF) son moléculas con potencial aplicación en la disminución de enfermedades crónico degenerativas (ECD). Una fuente de CF es la mezcla hoja-tallo del Cártamo (*Carthamus tinctorius* L.). Sin embargo, para aplicaciones biológicas, la biodisponibilidad de estos compuestos es baja debido a factores fisiológicos como pH y enzimas. Por esta razón, una alternativa es la protección de los CF en matrices de biopolímeros como zeína. Con base en lo anterior, en el presente estudio se obtuvieron extractos a partir de la mezcla (hoja-tallo) de cártamo y se evaluó la actividad antioxidante por diferentes métodos, asimismo, se identificaron los compuestos fenólicos. Los resultados mostraron alta actividad antioxidante por DPPH, ABTS, FRAP y efecto protector de eritrocitos humanos con IC50 bajas. Los principales grupos de compuestos fenólicos identificados fueron pigmentos, flavonoides, lignanos, ácidos fenólicos y derivados de serotonina. Además, estos compuestos mostraron alta correlación ($R^2 > 89$) con la actividad antioxidante, lo cual fueron responsables de dicha actividad. Con la finalidad de proteger los compuestos fenólicos, se obtuvieron nanoencapsulados de zeína conteniendo los compuestos fenólicos del cártamo, por la técnica de electro-aspersión. Primeramente, se evaluaron las propiedades fisicoquímicas y reológicas de las soluciones formadoras de nanopartículas. Las soluciones a diferentes concentraciones de compuestos fenólicos mostraron diferencias significativas ($p<0.05$) en viscosidad, densidad, conductividad eléctrica y tensión superficial que tuvieron efecto sobre la formación del cono de Taylor, y las propiedades reológicas predijeron fluidos de tipo newtonianos (n=1). La encapsulación de estos compuestos, se corroboró por análisis de espectroscopia de infrarrojo (FT-IR) y por microscopia electrónica de transmisión (TEM). En la evaluación de distribución y tamaño de partícula e índice de polidispersidad se utilizó microscopia electrónica de barrido (SEM). Los resultados mostraron una interacción de la zeína con los compuestos fenólicos del cártamo vía puentes de hidrógeno, interacciones hidrofóbicas e interacciones electrostáticas. Por otra parte, el diámetro de los nanoencapsulados, fue en rango nanométrico con partículas esféricas lisas y compactas. Además, se determinó la eficiencia de encapsulación y biodisponibilidad *in vitro* de los nanoencapsulados. Los resultados mostraron que a menor concentración de compuestos fenólicos existía una mayor eficiencia de encapsulación, pero no fue estadísticamente significativa ($P<0.05$), sin embargo, la mejor concentración fue al de 1% (p/v), debido a que mayor cantidad de CF estaban encapsulados en la matriz de zeína. La biodisponibilidad *in vitro* de los compuestos fenólicos del cártamo fue mayor cuando estuvieron encapsulados que en su forma libre. Finalmente, se puede concluir que la encapsulación de los compuestos fenólicos del cártamo en matrices de zeína, promueve la protección a cambios de pH y enzimas, simulando su paso durante el tracto gastrointestinal aumentado su biodisponibilidad.

INTRODUCCIÓN

A nivel global, la sociedad actual demanda más atención a la salud, debido al aumento de las enfermedades causadas a su estilo vida. De estas enfermedades, un grupo que ha ido en aumento considerable, son las enfermedades crónico degenerativas (ECD). Se estima a nivel mundial que 41 millones de personas mueren cada año a raíz de una ECD y equivalen al 71% del total de defunciones (OMS, 2018). Las principales enfermedades son cardiovasculares, seguidas por el cáncer, enfermedades respiratorias y diabetes; y son responsables del más del 80 % de defunciones de este grupo de enfermedades (OMS, 2018). Por lo tanto, deben ser fomentadas estrategias, para disminuir la prevalencia de este grupo de enfermedades.

Una causa de la aparición de algún tipo de ECD es el estrés oxidativo en las células generado por los radicales libres (RL) (Gupta et al., 2019; Singh, 2019). Los RL son moléculas que tienen uno o más electrones desapareados en su último orbital de energía. El cuerpo humano tiene mecanismos para disminuir los RL mediante moléculas endógenas denominadas antioxidantes (Olson y Gao, 2019). Un antioxidante es cualquier sustancia que cuando está presente en bajas concentraciones en comparación con la de un sustrato oxidable retrasa significativamente o evita la oxidación de ese sustrato (Galano y Alvarez-Idaboy, 2019). Sin embargo, cuando la producción de RL es mayor a estas moléculas se genera el estrés oxidativo. Una estrategia es el consumo de antioxidantes exógenos proveniente de vegetales (Del Castillo; Neha et al., 2019).

Los compuestos fenólicos (CF) son una amplia familia de moléculas sintetizadas en plantas como defensa al medio ambiente (Rodríguez-Pérez et al., 2019), y son considerados moléculas antioxidantes, ya que tienen la capacidad de retardar o prevenir la oxidación en presencia de oxígeno (Jurikova et al., 2019), contrarrestando los efectos nocivos de los RL (Luna-Guevara, et al., 2019). Estos compuestos se pueden dividir en dos grupos, los flavonoides (flavona, flavanona, flavanol y antocianinas) y no flavonoides (ácidos fenólicos, xantenos, estilbenos y lignanos) (Vuolo et al., 2019). Diferentes estudios han investigado los efectos benéficos de los CF en disminuir o retardar la prevalencia de ECD (Golonko et al., 2019; Tohma et al., 2019; Zhang et al., 2019).

Una fuente de CF es la mezcla hoja-tallo del cártamo (*Carthamus tinctorius* L.). Ésta planta es cultivada principalmente por su semilla, que se usa para la producción de aceite comestible (Asgarpanah y Kazemivash, 2013). México se destaca por ser uno de los principales productores de cártamo a nivel mundial después de India y Estados Unidos. Además, el estado de Sonora es uno de los principales productores de este cultivo por las condiciones áridas y semiáridas de la región (SIAP, 2018), por lo cual, grandes cantidades de residuos de cártamo son generados siendo fuente potencial de CF.

Sin embargo, los CF tienen la desventaja de ser lábiles a cambios de pH, así como a enzimas, ocasionando la pérdida de su actividad antioxidante, al ser consumidos, ya sea frescos de

manera natural o procesados (Rostami et al., 2919). En este sentido, una estrategia para proteger estos compuestos, es la nanoencapsulación en matrices de biopolímeros, que evita la degradación de los CF, brindando protección y haciéndolos más biodisponibles para el organismo, desde su consumo hasta llegar al torrente sanguíneo con la dosis suministrada (Chen et al., 2019; Rehman et al., 2019).

Esta matriz biopolimérica se puede elaborar a partir de materiales biodegradables y biocompatibles, tales como los residuos de la industria agrícola y además se contribuye a disminuir la contaminación ambiental por los mismos (Fayaz et al., 2019; Moghbeli et al., 2019). Entre los componentes de estos residuos se encuentra la zeína proveniente del bagazo de maíz residual de las industrias de obtención de aceites y biodiesel (Santos et al., 2018; Gupta et al., 2019). La zeína es una proteína de tipo prolamina, que se encuentran en el endospermo del grano de maíz y en el bagazo generado de las diferentes industrias, es poco valorizada, por lo que se puede emplear para elaborar materiales biopoliméricos (Tapia-Hernández et al., 2019). Una de las ventajas de la zeína es que es generalmente reconocida como segura (GRAS) por la FDA (Tapia-Hernández et al., 2019), por lo cual, la hace un material atractivo para ser aplicado en la industria farmacéutica y alimentaria.

Para la elaboración de estos sistemas nanoencapsulados conteniendo los CF del cártamo se propone la técnica de electro-aspersión, ya que es de bajo costo, utiliza pocos solventes y no genera muchos residuos, comparado con las técnicas convencionales de nanoprecipitación o emulsión difusión (Hao *et al*., 2013). La técnica de electroaspersión, consiste en aplicar un campo eléctrico a una solución polimérica que se encuentra en una jeringa, cual venciendo la tensión superficial es formando el conocido cono de Taylor, generando nanopartículas (Tapia-Hernández *et al.*, 2015). Además, las nanopartículas contendiendo los CF de subproducto de cártamo y obtenidas por este método se les debe evaluar su digestión *in vitro* para observar la diferencia en biodisponibilidad comparado con su forma libre.

En este sentido, la biodisponibilidad es la integración de diversos procesos, mediante el cual una fracción de un nutriente ingerido está disponible para la digestión, absorción, transporte, utilización y eliminación (Haro et al., 2006; Hurrell et al., 2010). Los métodos para la determinación de la biodisponibilidad de CF incluyen experimentos humanos (*in vivo*), así como simulados, realizados en laboratorio (*in vitro*). Los métodos *in vivo* proporcionan datos directos de la biodisponibilidad y se han utilizado para una gran variedad de nutrientes. Por otro lado, los métodos *in vitro* tienen la ventaja de ser más rápidos, menos costosos, menor mano de obra, y no tienen restricciones éticas. Los métodos *in vitro* simulan la digestión gastrointestinal bajo condiciones controladas usando enzimas digestivas comerciales.

Con base a lo anterior, el presenta trabajo de tesis plantea la extracción e identificación de los compuestos fenólicos de cártamo (*Carthamus tinctorius* L.) y su nanoencapsulación en una matriz de zeína con la finalidad de aumentar su biodisponibilidad en un sistema *in vitro*.

HIPÓTESIS

Los compuestos fenólicos extraídos de la mezcla hoja-tallo de cártamo (*Carthamus tinctorius* L.) presentan mayor biodisponibilidad *in vitro* después de ser nanoencapsulados en una matriz de zeína

OBJETIVOS

Objetivo General

Evaluar la biodisponibilidad *in vitro* de compuestos fenólicos extraídos de la mezcla hoja-tallo de cártamo (*Carthamus tinctorius* L.) nanoencapsulados en una matriz de zeína.

Objetivos Específicos

1. Evaluar la actividad antioxidante e identificar los compuestos fenólicos de la mezcla hoja-tallo de cártamo (*Carthamus tinctorius* L.) por cromatografía de líquidos de ultra-resolución acoplado a iodos (UPLC-DAD-MS).

2. Determinar los parámetros para la obtención de nanopartículas de zeína con compuestos fenólicos extraídos de la mezcla hoja-tallo de cártamo (*Carthamus tinctorius* L.) utilizando el método de electro-aspersión.

3. Caracterizar química y estructuralmente los compuestos fenólicos extraídos de la mezcla hoja-tallo de cártamo (*Carthamus tinctorius* L.) encapsulados en una matriz de zeína.

4. Evaluar la biodisponibilidad *in vitro* de compuestos fenólicos extraídos de la mezcla hoja-tallo de cártamo (*Carthamus tinctorius* L.) libres y encapsulados en una matriz de zeína.

REFERENCIA BIBLIOGRÁFICA

Asgarpanah, J., & Kazemivash, N. (2013). Phytochemistry, pharmacology and medicinal properties of Carthamus tinctorius L. Chinese Journal of Integrative Medicine, 19(2), 153–159.

Chen, L., Gnanaraj, C., Arulselvan, P., El-Seedi, H., & Teng, H. (2019). A review on advanced microencapsulation technology to enhance bioavailability of phenolic compounds: Based on its activity in the treatment of Type 2 Diabetes. Trends in food science & technology, 85, 149-162.

Del Castillo, M. D., Iriondo-DeHond, A., Fernandez-Gomez, B., Martinez-Saez, N., Rebollo-Hernanz, M., Martín-Cabrejas, M. A., & Farah, A. (2019). Coffee antioxidants in chronic diseases. In Coffee (pp. 20-56).

Fayaz, G., Plazzotta, S., Calligaris, S., Manzocco, L., & Nicoli, M. C. (2019). Impact of high pressure homogenization on physical properties, extraction yield and biopolymer structure of soybean okara. LWT, 113, 108324.

Galano, A., & Raúl Alvarez-Idaboy, J. (2019). Computational strategies for predicting free radical scavengers' protection against oxidative stress: Where are we and what might follow?. International Journal of Quantum Chemistry, 119(2), e25665.

Golonko, A., Pienkowski, T., Swislocka, R., Lazny, R., Roszko, M., & Lewandowski, W. (2019). Another look at phenolic compounds in cancer therapy the effect of polyphenols on ubiquitin-proteasome system. European journal of medicinal chemistry.

Gupta, P., Jyoti, R. B., & Gupta, S. (2019). Free Radical Pharmacology and its role in various diseases. Journal of Drug Delivery and Therapeutics, 9(2-s), 690-694.

Gupta, J., Vadlani, P. V., Lau, C. S., Madl, R. L., & Shi, Y. C. (2019). Innovative zein extraction from distillers' grains with solubles: Process development and product characterization studies. Environmental Progress & Sustainable Energy, 38(4).

Hao, S., Wang, Y., Wang, B., Deng, J., Liu, X., & Liu, J. (2013). Rapid preparation of pH-sensitive polymeric nanoparticle with high loading capacity using electrospray for oral drug delivery. Materials Science and Engineering: C, 33(8), 4562-4567.

Haro, J. F., Martínez, C., Ros, G., & Vidal, M. L. (2006). Note: Stability of calcium bioaccessibility and sensory parameters during the storage of fortified juices. Food science and technology international, 12(4), 281-285.

Hurrell, R. (2010). Use of ferrous fumarate to fortify foods for infants and young children. Nutrition reviews, 68(9), 522-530.

Jurikova, T., Skrovankova, S., Mlcek, J., Balla, S., & Snopek, L. (2019). Bioactive compounds, antioxidant activity, and biological effects of european cranberry (vaccinium oxycoccos). Molecules, 24(1), 24.

Luna-Guevara, M. L., Luna-Guevara, J. J., Hernández-Carranza, P., Ruíz-Espinosa, H., & Ochoa-Velasco, C. E. (2019). Phenolic Compounds: A Good Choice Against Chronic Degenerative Diseases. In Studies in Natural Products Chemistry (Vol. 59, pp. 79-108). Elsevier.

Moghbeli, S., Jafari, S. M., Maghsoudlou, Y., & Dehnad, D. (2019). Influence of pectin-whey protein complexes and surfactant on the yield and microstructural properties of date powder produced by spray drying. Journal of food engineering, 242, 124-132.

Olson, K. R., & Gao, Y. (2019). Effects of inhibiting antioxidant pathways on cellular hydrogen sulfide and polysulfide metabolism. Free Radical Biology and Medicine, 135, 1-14.

OMS, (2018). Enfermedades no transmisibles. Consultado en: https://www.who.int/es/news-room/fact-sheets/detail/noncommunicable-diseases. Fecha 19 de agosto de 2018.

Neha, K., Haider, M. R., Pathak, A., & Yar, M. S. (2019). Medicinal prospects of antioxidants: A review. European journal of medicinal chemistry, 178, 687-704.

Rehman, A., Ahmad, T., Aadil, R. M., Spotti, M. J., Bakry, A. M., Khan, I. M., ... & Tong, Q. (2019). Pectin polymers as wall materials for the nano-encapsulation of bioactive compounds. Trends in Food Science & Technology, 90, 35-46.

Rodríguez-Pérez, C., Segura-Carretero, A., & del Mar Contreras, M. (2019). Phenolic compounds as natural and multifunctional anti-obesity agents: A review. Critical reviews in food science and nutrition, 59(8), 1212-1229.

Rostami, M. R., Yousefi, M., Khezerlou, A., Mohammadi, M. A., & Jafari, S. M. (2019). Application of different biopolymers for nanoencapsulation of antioxidants via electrohydrodynamic processes. Food Hydrocolloids, 97, 105170.

Santos, T. M., Men de Sá Filho, M. S., Silva, E. D. O., da Silveira, M. R., de Miranda, M. R. A., Lopes, M. M., & Azeredo, H. M. (2018). Enhancing storage stability of guava with tannic acid-crosslinked zein coatings. Food chemistry, 257, 252-258.

Singh, R. (2019). Impact of Free Radicals and Antioxidants on Human Health. Research & Reviews A Journal of Pharmacognosy, 3(2), 19-26.

Tapia-Hernandez, J. A., Torres-Chavez, P. I., Ramirez-Wong, B., Rascon-Chu, A., Plascencia-Jatomea, M., Barreras-Urbina, C. G., Rangel-Vázquez, N. A., & Rodriguez-Félix, F. (2015). Micro-and nanoparticles by electrospray: advances and applications in foods. Journal of agricultural and food chemistry, 63(19), 4699-4707.

Tapia-Hernández, J. A., Del-Toro-Sánchez, C. L., Cinco-Moroyoqui, F. J., Ruiz-Cruz, S., Juárez, J., Castro-Enríquez, D. D., Barreras-Urbina, C. G., López-Ahumada G. A., & Rodríguez-Félix, F. (2019). Gallic Acid-Loaded Zein Nanoparticles by Electrospraying Process. Journal of food science, 84(4), 818-831.

Tapia-Hernández, J. A., Del-Toro-Sánchez, C. L., Cinco-Moroyoqui, F. J., Juárez-Onofre, J. E., Ruiz-Cruz, S., Carvajal-Millan, E., López-Ahumada G. A., Castro-Enríquez, D. D., Barreras-Urbina, C. G., & Rodríguez-Félix, F. (2019). Prolamins from cereal by-products: Classification, extraction, characterization and its applications in micro-and nanofabrication. Trends in Food Science & Technology, 90, 111-132.

Tohma, H., Altay, A., Köksal, E., Gören, A. C., & Gülçin, İ. (2019). Measurement of anticancer, antidiabetic and anticholinergic properties of sumac (Rhus coriaria): analysis of its phenolic compounds by LC–MS/MS. Journal of Food Measurement and Characterization, 13(2), 1607-1619.

Vuolo, M. M., Lima, V. S., & Junior, M. R. M. (2019). Phenolic Compounds: Structure, Classification, and Antioxidant Power. In Bioactive Compounds (pp. 33-50). Woodhead Publishing.

Zhang, Q., de Mejia, E. G., Luna-Vital, D., Tao, T., Chandrasekaran, S., Chatham, L., ... & Kumar, D. (2019). Relationship of phenolic composition of selected purple maize (Zea mays L.) genotypes with their anti-inflammatory, anti-adipogenic and anti-diabetic potential. Food chemistry, 289, 739-750.

CAPÍTULO I

Zein-polysaccharide nanoparticles as matrices for antioxidant compounds: A strategy for prevention of chronic degenerative diseases

Food Research International 111 (2018) 451–471

Contents lists available at ScienceDirect

Food Research International

journal homepage: www.elsevier.com/locate/foodres

Review

Zein-polysaccharide nanoparticles as matrices for antioxidant compounds: A strategy for prevention of chronic degenerative diseases

José Agustín Tapia-Hernández[a], Francisco Rodríguez-Felix[a], Josué Elías Juárez-Onofre[b], Saúl Ruiz-Cruz[c], Miguel Angel Robles-García[d], Jesús Borboa-Flores[a], Francisco Javier Wong-Corral[a], Francisco Javier Cinco-Moroyoqui[a], Daniela Denisse Castro-Enríquez[a], Carmen Lizette Del-Toro-Sánchez[a,*]

[a] Department of Research and Posgraduate in Food (DIPA). University of Sonora, Blvd. Luis Encinas y Rosales, S/N, Colonia Centro, 83000 Hermosillo, Sonora, Mexico
[b] Department of Physics, University of Sonora, Blvd. Luis Encinas y Rosales, S/N, Colonia Centro, 83000 Hermosillo, Sonora, Mexico
[c] Department of Biotechnology and Food Science. Institute Technology of Sonora. 5 de febrero #818 sur, Colonia Centro, 85000 Ciudad Obregón, Sonora, Mexico
[d] Department of Medical Scinces and Life, University of Guadalajara, 1115. Ocotlán, Jalisco, Mexico

ARTICLE INFO

Keywords:
Zein
Polysaccharide
Antioxidants
Free radicals
Nanoparticles
Chronic degenerative diseases

ABSTRACT

Oxidative Stress (OS) produces the formation of free radicals and other reactive oxygen and nitrogen species that are intimately involved in many diseases, especially Chronic Degenerative Diseases (CDD) such as cancer, diabetes, cardiovascular diseases, and obesity, among others. Thus, reactive compounds need to be quenched by antioxidants. The problems of these compounds include that they are susceptible to degradation, have low bioavailability, and can lose their bioactivity in the gastroIntestinal tract. Therefore, an alternative is encapsulation. Zein is a protein used in nanotechnology as a polymer matrix because it can encapsulate different compounds such as antioxidants to provide stability and control of the release. The disadvantage of zein as a delivery vehicle is that it is limited by the low stability of aggregation when suspended in water, in addition to the conditions of acid pH or that higher ionic strength tends to destabilize. To reduce these limitations, the incorporation of polysaccharides as a second polymer matrix can provide stability in zein nanoparticles. In this review, we discuss OS as a source of CDD, the role of antioxidants in the prevention of these diseases, and the preparation, characterization, and application of antioxidant-zein-polysaccharide particles as delivery systems as well as possible mechanisms to control CDD.

1. Introduction

Free radicals and other Reactive Oxygen and Nitrogen Species (ROS and RNS) are products of normal cellular metabolism: however high levels of these molecules can be responsible for altering the structure and function of DNA, RNA, cell membranes, protein, carbohydrates, and lipids (Blomhoff et al., 2006). Consequently, this damage impacts directly on harm to human health and the formation and progression of Chronic Degenerative Diseases (CDD). These diseases provide the greatest amount of illnesses and are responsible for 43 million deaths per year, with 80% of all deaths (Castro et al., 2017). Some examples of CDD caused by free radicals or reactive species include neurologic diseases, cancer, diabetes, cardiovascular diseases, obesity, etc. (Bakrania et al., 2017; Bohnert et al., 2018; Kalita et al., 2015; Kelly and Fussell, 2017; Nosso et al., 2017; Oguntibeju et al., 2010; Salles et al., 2017). ROS are the predominant and principal reactive molecules in the organism. The most common are hydroxyl free radical, hydrogen peroxide, nitric oxide, singlet oxide, and superoxide radical (Schieber and Chandel, 2014). Hence, the use of the antioxidants for scavenging ROS is one of the most effective means of decreasing the level of Oxidative Stress (OS) (Huang, Huang, et al., 2016, Huang, Zhang & Chen, 2016).

The World Health Organization (WHO) has implemented strategies for the consumption of sources rich in antioxidant compounds such as vitamins, carotenoids, and phenolics, which contribute to their chemopreventive potential (Shashirekha et al., 2015). Their aromatic feature and their highly conjugated system with multiple hydroxyl groups render these compounds good electron or hydrogen-atom donors,

* Corresponding author.
E-mail addresses: francisco.rodriguezfelix@unison.mx (F. Rodríguez-Felix), josue.juarez@unison.mx (J.E. Juárez-Onofre), saul.ruiz@itson.edu.mx (S. Ruiz-Cruz), jesus.borboa@unison.mx (J. Borboa-Flores), francisco.wong@unison.mx (F.J. Wong-Corral), javier.cinco@unison.mx (F.J. Cinco-Moroyoqui), carmen.deltoro@unison.mx (C.L. Del-Toro-Sánchez).

https://doi.org/10.1016/j.foodres.2018.05.036
Received 22 August 2017; Received in revised form 14 May 2018; Accepted 18 May 2018
Available online 25 May 2018
0963-9969/

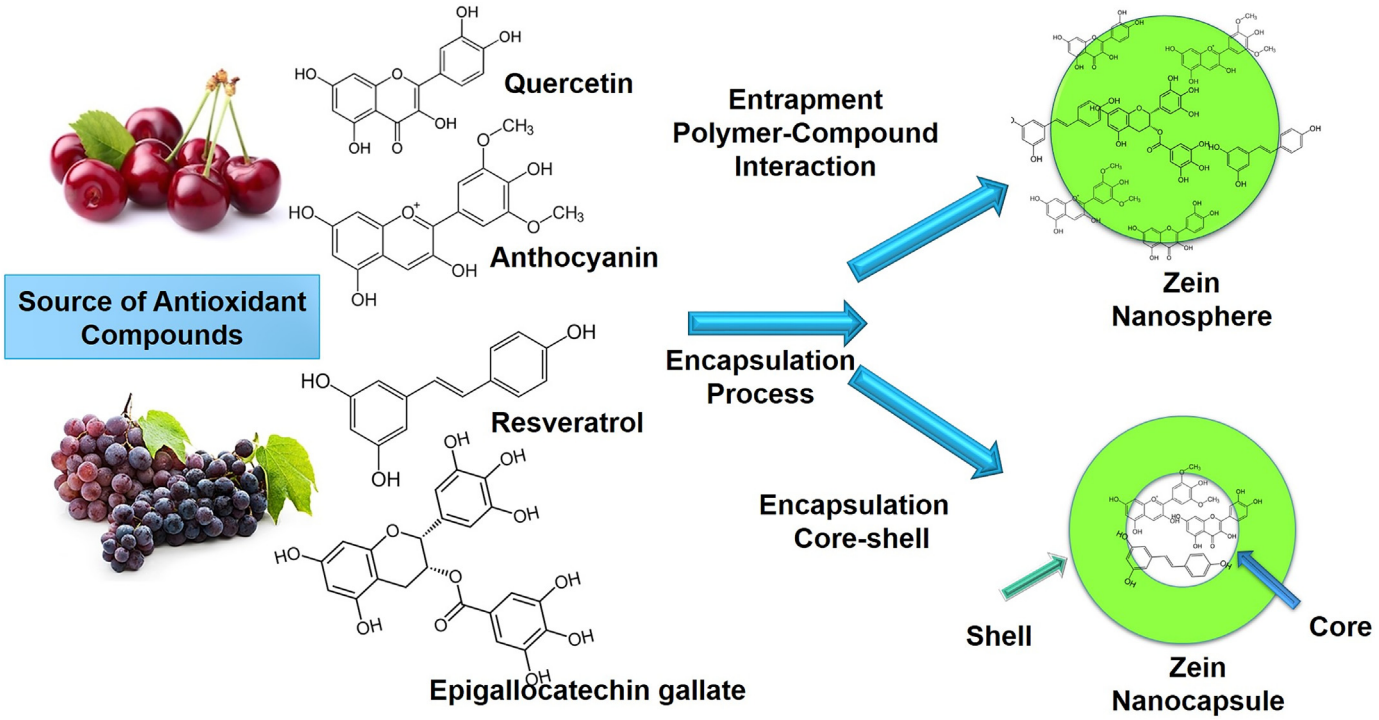

Fig. 1. Formation of zein-based nanoparticles by entrapment (nanosphere) and core-shell (nanocapsule) with antioxidant compounds.

neutralizing free radicals and other ROS or RNS (Zhang and Tsao, 2016). However, antioxidants possess low bioavailability and are very susceptible to degradation by environmental factors (photosensistive, thermolabile, etc.) or body factors (such as pH and enzymes). Hence, encapsulation could be a good option to avoid these disadvantages. Recently, research has focused on developing new technologies such as nanoencapsulation in different polymeric matrices (Li et al., 2017) including zein with polysaccharides (Bothelho et al., 2017; Li et al., 2015).

Zein is a protein classified within the group of prolamins. It is attractive for use in nanotechnology as a polymer matrix and is classified as Generally Recognized As Safe (GRAS) by the U.S. Food and Drug Administration (FDA). In addition, zein has promising characteristics, such as biocompatibility, biodegradability, and low toxicity (Luo and Wang, 2014). It is widely used in that it can encapsulate generally different insoluble compounds in water to provide stability and control of release when is in the GastroIntestinal Tract (GIT) (Luo et al., 2013). Therefore, current studies of zein nanoparticles are directed toward providing protection to antioxidant compounds as quercetin, anthocyanin, resveratrol and apigallocatechin gallate (Fig. 1). Some disadvantages of zein as a delivery vehicle comprise its low stability of aggregation when suspended in water and to conditions of acid pH or higher ionic strength that tend to destabilize it. Thus, at present, a strategy to reduce these limitations is the incorporation of polysaccharides as a second polymer matrix that provides stability to zein nanoparticles (Huang, Panagiotou, et al., 2017), (Huang, Dai, et al., 2017).

Among polysaccharides that interact to a greater degree with zein, we find anionic such as alginate, pectins, chitosan, and cellulose derivatives. Hydrogen bonds and electrostatic interactions among the reactive groups of both polymers are the main interactions in these systems. In this context, some electrostatic deposition techniques are used for obtaining antioxidant-zein-polysaccharide nanoparticles, such as liquid-liquid dispersion, anti-solvent co-precipitation, layer-by-layer deposition, and electrospray (Borges and Mano, 2014; Laelorspoen et al., 2014; Li, Wang, et al. 2016; Li, Dong, et al. 2016; Sun, Chen, et al. 2017; Sun, Xu, et al. 2017; Sun, Yang, et al. 2017; Sun, Liu, et al. 2017; Sun et al. 2017a, 2017b). Then, the formation of zein-polysaccharide nanoparticle is a novel alternative to conventional encapsulation (single zein nanoparticle) that presents new and better physicochemical properties, as well as improving the limitations of zein nanoparticles as antioxidant system for CDD (Zhang, Niu, et al. 2014; Zhang, Tong, et al. 2014). There are studies that demonstrate the benefits of antioxidants nanoencapsulated in a zein-polysaccharide matrix, especially those that provide greater stability and protection of the system, remaining in the GIT for a longer time until the bioactive compounds are released into the small intestine to control, reduce, or prevent CDD (Davidov-Pardo, Joye, Espinal-Ruiz, et al. 2015; Davidov-Pardo, Joye, McClements, 2015; Davidov-Pardo, Pérez-Ciordia, et al. 2015; Huang, Panagiotou et al., 2017; Huang, Dai et al.2017; Chang, Wang, Hu, & Luo, 2017; Chang, Wang, Hu, Zhou, et al. 2017).

This review provides a compilation of the mechanisms of the OS and antioxidants in CDD, as well as the preparation, characterization, and application of antioxidants nanoencapsulated in zein-polysaccharide matrices in order to obtain better benefits for combatting these diseases.

2. Oxidative stress as a source of chronic degenerative diseases

Normal cellular oxidative-metabolic reactions (endogenous) and other factors (exogenous) such as radiation, food constituents, tobacco smoke, and environmental pollutants form free radicals and other Reactive Oxygen and Nitrogen Species (ROS and RNS). These reactive compounds are atoms or molecules that contain an unpaired electron in their outer orbital; therefore, they alter the structure and function of proteins, lipoproteins, carbohydrates, cell membranes, RNA, and DNA (Blomhoff et al., 2006). To avoid these damages, reactive compounds need to be quenched by antioxidants. However, when there is an imbalance between free radicals and antioxidant, OS is generated. Thus, “a disturbance in the pro-oxidant/antioxidant systems in favor of the former may be denoted as an oxidative stress” (Sies, 1985).

OS is intimately involved in many diseases, especially Chronic Degenerative Diseases (CDD). For example cancer, heart diseases, diabetes, Acquired Immuno Deficiency Syndrome (AIDS), neurologic diseases (Parkinson disease, muscular dystrophy, Alzheimer disease,

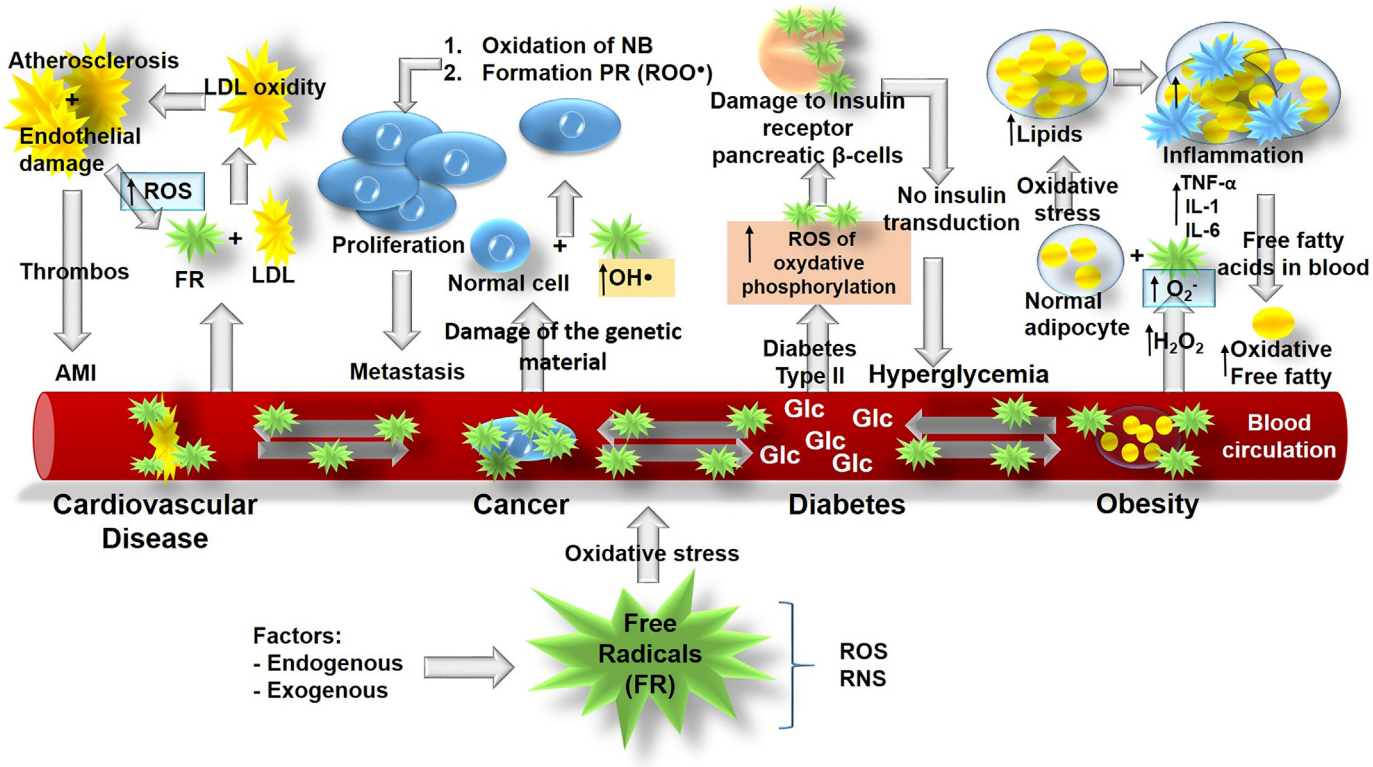

Fig. 2. Relation of free radicals in the prevalence of chronic degenerative diseases. Glc: Glucose, FR: free radicals; LDL: low density lipoprotein; AMI: acute myocardial infarction; NB: nitrogenous bases; PR: peroxyl radical; ROS: Reactive Oxygen Species; RNS: Reactive Nitrogen Species.

multiple sclerosis, amyotrophic lateral sclerosis), obesity, among others (Bakrania et al., 2017; Bohnert et al., 2018; Kalita et al., 2015; Kelly and Fussell, 2017; Nosso et al., 2017; Oguntibeju et al., 2010; Salles et al., 2017). Free radicals not only induce direct damage to critical biomolecules, but they also indirectly alter or deregulate cellular signaling events, consequently triggering the disorders previously mentioned, the most common being cardiovascular diseases, cancer, diabetes, and obesity (Fig. 2).

ROS are often associated with the principle of OS and include the superoxide anion (O_2^-), hydrogen peroxide (H_2O_2), and hydroxyl radicals (OH•) (Schieber and Chandel, 2014). Approximately 0.2% to −2% of oxygen consumed in the cell is emitted as ROS (Balaban et al., 2005). Physiologically produced ROS from various types of immune cells or respiratory burst in neutrophils are beneficial to human health because of their role in preventing pathogen invasion, depleting malignant cells, and improving wound healing. However, persistent and long-term immune responses can generate irreversible damage (Zhang and Tsao, 2016).

The increase of ROS production deriving from endothelial dysfunction is commonly engaged in developing typical characteristics of atherosclerosis (Fig. 2), such as a CardioVascular Disease (CVD). One of the critical steps in the development of atherosclerosis is when Low-Density-Lipoprotein (LDL) that entered the arterial wall is oxidized by excessive ROS and scavenged by macrophages, forming lipid drops, which are characterized as foam cells, clogging the blood vessels (Steinberg et al., 1989; Taverne et al., 2013). Hence, atherosclerosis is characterized as an accumulation of inflammatory cells in the arterial wall due to a variety of trauma to the endothelial and smooth-muscle cells. Then, atherosclerotic plaques are formed, decreasing the availability of oxygen and nutrients. A thrombus can be formed if the plaque is ruptured, which may occlude coronary and/or cerebral blood circulation, leading to Acute Myocardial Infarction (AMI) and stroke (He and Zuo, 2015).

On the other hand, ROS play an essential role in the initiation, development, and progression stages of some other CDD, such as cancer and diabetes (Fig. 2). Superoxide anion (O_2^-), hydrogen peroxide (H_2O_2), and hydroxyl radicals (OH·) are the most well studied ROS in both of these CDD (Panieri and Santoro, 2016). H_2O_2 is not very reactive toward DNA and the majority of damaging effects on DNA are due to hydroxyl ions (Imlay et al., 1988). Due to their high diffusibility, hydroxyl radicals attack DNA rapidly, oxidizing DNA bases (consequently forming peroxyl radicals ROO·), and single-strand, and double-strand breaks (Maynard et al., 2009). Cells attempt to repair these DNA lesions, but if cells were incapable of repairing them, they undergo programmed cell death (apoptosis). However, when cells with DNA mutations ellude apoptosis, they can give rise to a great opportunity for cancerous growth, proliferation, and metastasis (Liou and Storz, 2010). Cell proliferation is stimulated principally by low doses of superoxide and hydrogen peroxide in certain cancer cell types, such breast-cancer cells, through the translocation of estrogen to the mitochondria (Reddy and Glaros, 2007). Another example is the proliferation of pancreatic cancer, which is intensified due to the increase of the ROS level from endogenous OS (Storz, 2005). Some other studies demonstrated that hydrogen peroxide enhances metastasis and that ROS may also promote tumor-cell metastasis by increasing the vascular permeability (Brown and Bicknell, 2001; Kundu et al., 1995; Pelicano et al., 2009).

Diabetes, a group of metabolic diseases characterized by high blood sugar, is other important health issue worldwide (Fernandes, Silva, et al., 2017; Fernandes, Pérez-Gregorio, et al., 2017). There are two types: Type I (insulin-dependent), generated by beta-cell destruction, mediated by the immune system, producing insulin deficiency, and Type 2 (Non-insulin- dependent), which is due to insulin secretion defects and that results in insulin resistance (Salsali and Nathan, 2006). ROS toxicity remains an undisputed cause of a Type-2 Diabetes Mellitus (T2DM). Persons with T2DM are prone to the risk of Alzheimer disease (a neurological disorder) and other CDD (Ahmad et al., 2017). Injury induced by ROS of insulin-producing pancreatic β-cells or insulin sensitivity in adipose or muscle tissues generates a large amount of sugar in

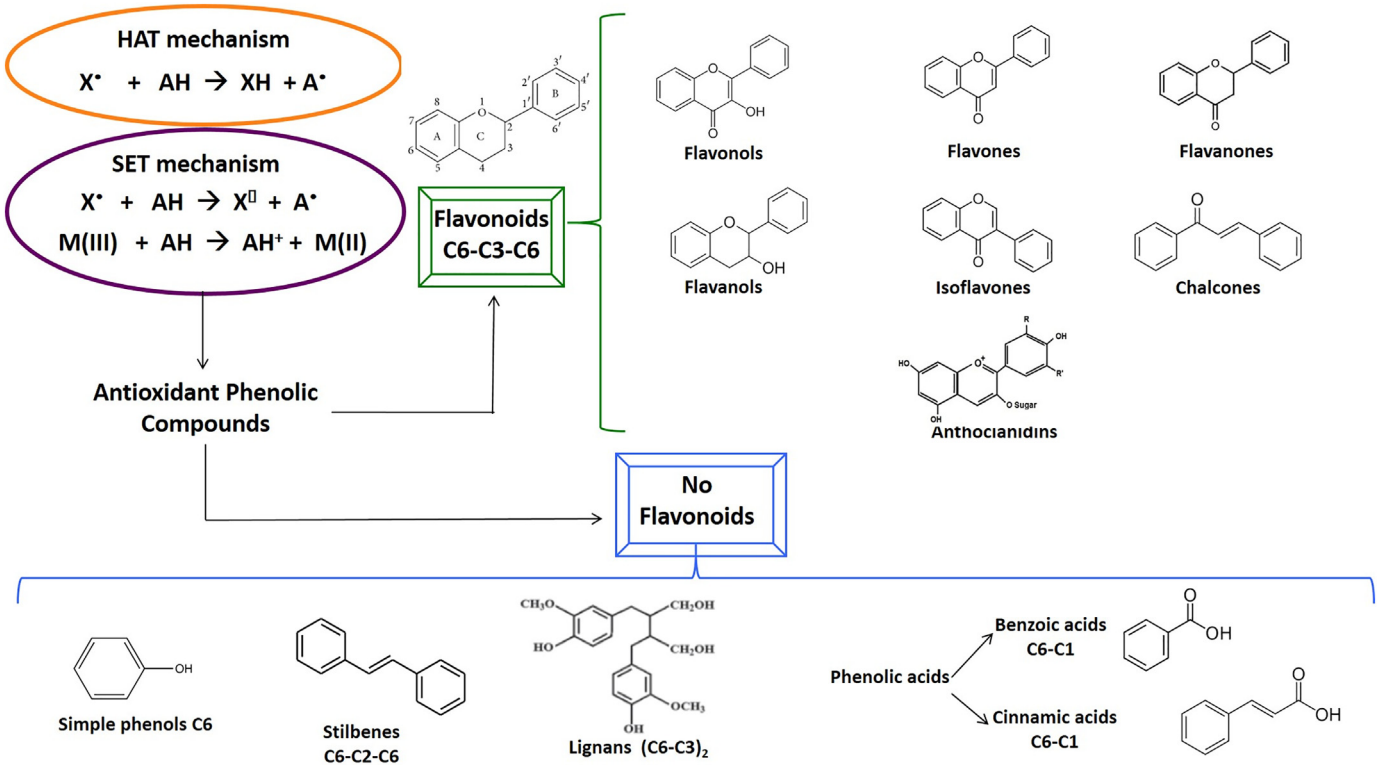

Fig. 3. Hydrogen Atom Transfer (HAT) and Single Electron Transfer (SET) mechanisms of phenolic antioxidant compounds and their classfication. X: Inticial free radical, AH: Antioxidant, M: Metal, C6: aromatic ring, C1, C2 or C3: refers to side chains or intermediate chains.

the blood (hyperglycemia), which is the main cause of T2DM (Fig. 2) (Butterfield et al., 2014). There is evidence that ROS and RNS are directly implicated in T2DM, and its complications are produced in mitochondria (Erejuwa, 2012; Moussa, 2008). When insulin is required to decrease blood sugar, it reacts with receptors that lead to the activation of Akt and the translocation of GLUT4 (GLUcose Transporter type 4) to the cell membrane. However, damage to or alteration in oxidative phosphorylation resulted in insulin resistance (Jahangir et al., 2014). Consequently, an increase occurs of ROS from oxidative phosphorylation, and the induction of fatty acid oxidation resulted in the activation of serine kinases followed by phosphorylation of insulin receptor substrates and interfering insulin signal transduction (Sorriento et al., 2014). Thus, the severity and pathogenesis of T2DM can depend on the production of ROS.

Moreover, OS establishes a vicious circle in which ROS provide obesity-related complications. Obesity is regulated by the renin/angiotensin system; consequently, an increase of O_2^- and LDL is produced due to NADPH oxidase stimulated by angiotensin II, in which they are taken up by macrophages (Fig. 2) (Edeas and Micol, 2007). In adipocytes, high levels of circulating glucose and lipid concentrations increase ROS generation owing to an excessive supply of energy substrates for metabolic pathways in these cells (McMurray et al., 2016). Furthermore, pro-inflammatory cytokines, including InterLeukin (IL)-1b, IL-6, IL-8, Tumor Necrosis Factor alpha (TNF)-α, and InterFeroN gamma (IFN-γ) are released into the circulation system which, if not properly regulated, can trigger irreversible systemic inflammation and disrupt immune homeostasis (Zhang and Tsao, 2016). There is evidence that OS affects adipocyte differentiation through a hydrogen peroxide-dependent mechanism in the 3 T3-L1 preadipocyte model (Lee et al., 2009). However, the precise roles of ROS in adipogenesis *in vivo* remain controversial. More studies are needed to delineate the roles of ROS and redox signaling mechanisms, which could be either positive or negative, in the pathogenesis of obesity and related metabolic disorders (Liu et al., 2012).

Several studies are focused on the detection, mainly of ROS, employing chemiluminescence, mass spectrometry probes, nanoparticles, and various fluorescence probes (Cochemé et al., 2011; Martins et al., 2014). However, Sarkar et al., 2018 indicated that, among the fluorescence probes, 2, 7-DiChlorodiHydroFluorescein (DCFH) is the most widely used probe for the detection of intracellular OS. For this reason, these authors developed a novel DNA-based fiber-optic sensor for direct *in-vivo* measurement of OS using DCFH. The sensor has been shown to monitor ROS/OS efficiently and continuously in aqueous medium as well as in biological samples, without forming any complexations or reactions with the biological samples. On the other hand, antioxidants have largely been considered as chain-breaking molecules, able to interrupt free radical reactions; thus, this compounds are important in the regulation and prevention of CDD, involving initiation, propagation, and termination. The following sections describe more details, such as antioxidant types, the mechanisms that they utilized, and their possible nanoencapsulation in controlled-release systems with different matrices.

3. Role of antioxidants in the prevention of chronic degenerative diseases

All aerobic organisms utilize a series of primary antioxidant defenses through enzymatic or non-enzymatic reactions in an attempt to protect themselves against oxidant damage (Davies, 2000). In this context, an antioxidant is defined as “a redox active compound that limits oxidative stress by reacting non-enzymatically with a reactive oxidant”, while an antioxidant enzyme is “a protein that limits oxidative stress by catalyzing a redox reaction with a reactive oxidant” (Blomhoff, 2005).

Our cells utilize a series of antioxidant compounds that can be both endogenous and/or exogenous, such as enzymes [SuperOxide Dismutases (SOD), Glutathione Peroxidases (GPx), CATalases (CAT), Glutathione Reductase (GR)], vitamins (C and E), proteins (ferritin,

ceruloplasmin, ubiquinone), uric acid, glutathione, carotenids (beta-carotene, beta-cryptoxanthin, lycopene, lutein and zeaxanthin), and phenolic compounds (flavonoids and non-flavonoids) (McEligot et al., 2005; Oguntibeju et al., 2010; Nirmala et al., 2014; Narra et al., 2015; Khan et al., 2016;, Matak et al., 2017; Coyago-Cruz et al., 2018). Exogenous antioxidants such as phenolic compounds are more usually studied for nanoencapsulation in different matrices in order to be used to prevent or decrease CDD. These compounds are considered the most potent exogenous antioxidants; hence, they exert several effects on human health and disease prevention (Fernandes, Silva, et al., 2017; Fernandes, Pérez-Gregorio, et al., 2017). The aromatic feature and highly conjugated system with multiple hydroxyl groups render these compounds good electron or hydrogen-atom donors, neutralizing free radicals and other ROS or RNS (Fig. 3) (Zhang and Tsao, 2016). Flavonols such as quercetin containing the 3-hydroxy group have demonstrated relatively higher antioxidant activity than those without the latter in neutralizing free radicals (Tsao, 2010). Therefore, the antioxidant potential primarily depends on the number and position of hydroxyl groups in the molecule, as well as on the degree of hydroxylation. In the case of phenolic acids, these appear to increase antioxidant activity if there is a longer distance of the carbonyl group and of the aromatic ring, as well as if the substitution phenol is in *ortho*-position and/or *para*-position (Göçer and Gülçin, 2011).

Phenols act as antioxidants via different mechanisms, such as inhibition of oxidative enzymes, quenching of ROS, chelation of transition metals, the scavenging of free radicals, or due to interaction with biomembranes (Nirmala et al., 2014). Antioxidant molecules may react directly with the reactive radicals and destroy them, while they may become new free radicals which are less active, longer-lived, and less dangerous than the radicals that they have neutralized. Other antioxidants can react with ROS and/or free radical intermediates induced by ROS and terminate the chain reaction (Lü et al., 2010). The neutralization of free radicals is carried out by accepting or donating electron(s) to eliminate the unpaired condition of the radical. The two major mechanisms that antioxidants employ are Hydrogen Atom Transfer (HAT) and Single Electron Transfer (SET). The HAT mechanism is the ability of an antioxidant to quench free radicals by hydrogen donation, while in the SET mechanism, the antioxidant transfers one electron to reduce any compound, including metals, carbonyls, and radicals (Fig. 3). Both may occur simultaneously; however, one of these can be the dominant but will depend on several factors, such as solubility, bond dissociation energy, ionization potential, antioxidant structure, and the system solvent (Prior et al., 2005).

There is evidence that the consumption of polyphenols (having one or more aromatic rings bearing more than one hydroxyl group) enhances the activities of antioxidant enzymes such as CAT, SOD, GR, and GPx, preventing systemic or localized inflammation in order to prevent the development of CDD, consequently affecting the transcription factors of various genes encoding these enzymes (Kansanen et al., 2013). Another way to reduce inflammatory responses is controlling the inflammatory signaling cascades throughout the interference of Nuclear Factor-kappa Beta (NF-kB) and Mitogen-Activated Protein Kinase (MAPK) (Chuang and McIntosh, 2011). In addition, polyphenols can reduce pro-inflammatory biomarkers ((IL)-1b, IL-6, IL-8, (TNF)-α, and (IFN)-γ); nevertheless, the underlying mechanisms of these compounds are still not well understood to date (Zhang and Tsao, 2016). The consumption of more than 1 g per day of phenolic compounds is considered safe and beneficial for CDD; however, we must be careful in terms of the doses because these can act as pro-oxidants at high doses (Scalbert and Williamson, 2000).

Polyphenols such as procyanidins have also been reported to affect lipid metabolism repressing the activity of pancreatic lipase (the enzyme that hydrolyzes triglycerides), limiting triglyceride absorption (Gonçalves et al., 2010). Several *in-vivo* studies have been carried out to demonstrate that procyanidins decreased body weight gain, reduced the adiposity index, and normalized plasma triglycerides and LDL-cholesterol (Bladé et al., 2010; Caimari et al., 2013; Quesada et al., 2009). On the other hand, phenolic compounds such as gallic acid and catechin, can interfere with some proteins, such as β-amyloid, inhibiting fibril and aggregate formation in Alzheimer disease (Ono et al., 2008; Smid et al., 2012).

To protect against CVD, antioxidants decrease LDL oxidation, diminish blood pressure, inhibit platelet aggregation, improve endothelial functionality, reduce anti-inflammatory actions through the inhibition of cyclooxygenase and 5-LipoOxygenase (5-LO) pathways, and reduce the release of pro-inflammatory cytokines (Apostolidou et al., 2015; Magrone and Jirillo, 2010; Mohanty et al., 2015; Votruba et al., 2009). To protect against cancer, antioxidants such as flavonoids can restore to a normal state some altered cell-signaling pathways acting as carcino-preventive agents. For example, flavones and flanonols inhibit breast cancers (Doo and Maskarinec, 2014), flanones inhibit cancer related to the upper aerodigestive tract (Woo and Kim, 2013), anthocyanins and flavonols inhibit colorectal cancer (Koosha et al., 2016), among others. One of the mechanisms utilized by these compounds is the inhibition of the proliferation of cancer cells (Song et al., 2015; Yu et al., 2016). Another mechanism comprises the modulation of proteins and enzymes that detoxify carcinogens (Jose et al., 2014).

In Diabetes Mellitus (DM) to avoid excessive glucose absorption or to suppress postprandial hyperglycemia, phenolic compounds can inhibit enzymes as α-glucosidase and α-amylase (Xia et al., 2017), as well as some glucose transporter, such as Sodium-dependent GLucose Transporter 1 (SGLT1) in the intestine (Johnston et al., 2005; Welsch et al., 1989). However, there is not sufficient information on polyphenols in glucose and insulin; hence, more studies must be conducted (Fernandes, Silva, et al., 2017; Fernandes, Pérez-Gregorio, et al., 2017). Obesity normally is related with high amounts of blood sugar and the signaling of these metabolic pathways. In this context, polyphenols can induce β-oxidation of fatty acids in the liver and suppress gluconeogenesis. Consequently, the blood-glucose level and lipid amount in liver are reduced; thus, glucose transporters are stimulated in adipose and muscle tissues, and finally, an improvement in insulin sensitivity is observed (Rupasinghe et al., 2016). The principal mechanism that antioxidants employ to prevent or reduce obesity is in the decrease of fat absorption, for example, with the inhibition of digestive enzymes (Tan et al., 2017).

In general, the application of antioxidants to prevent or protect against CDD is not easy, due to that antioxidants present some disadvantages, including that they are labile to environmental factors (photosensistive, thermolabile, etc.) and body factors (such as pH and enzymes). Therefore, recently, research has focused on developing new technologies to maintain their bioactivity, as is the case of the nanoencapsulation in different polymeric matrices such as zein with polysaccharides (Bothelho et al., 2017; Li et al., 2015).

4. Characteristics and properties of zein as encapsulant

A variety of nanoparticle-based systems have been investigated for their potential to encapsulate, protect, and deliver antioxidant compounds. Zein (a prolamin-type protein) has shown to be a suitable material for the development of nanoparticle delivery systems to encapsulate antioxidants (Huang, Panagiotou, et al., 2017; Huang, Dai, et al., 2017). This protein is found in the corn-grain endosperm, hence rendering this an inexpensive raw material and one that is easily removable in ethanol. Based on its solubility and sequence homology, zein can be separated into four classes: α-zein (19 and 22 kDa); β-zein (14 kDa); γ-zein (16 and 27 kDa), and δ-zein (10 kDa). All zein groups are abundant in hydrophobic and neutral amino acids (i.e., leucine, proline, and alanine) and also contain some polar amino-acid residues, such as glutamine (Lucio et al., 2017). The most abundant zein classes are α-Zein (70–85%) and γ-zein (10–20%) (Dong et al., 2016; Zhang et al., 2015). The former comprises two subunits: 19 KD (Z19) and 22 kD (Z22), which have been the most studied in terms of structure and

functionality. They contain hydrophobic residues such as leucine, proline, alanine, and phenylalanine (Righetti et al., 1977). According to its structure, approximately 50% correspond to α-helix and possesses nine adjacent helices that form an antiparallel ring with predominant glutamine turns (Argos et al., 1982). The secondary structure is provided by α-helix and β-sheet structures. Mejia et al. (2007) reported that, with regard to zein in 70% methanol, the most prevalent secondary forms comprise the α-zein fraction (approximately 65%), with some β-sheets (30%) at 25 °C. The β-conformation of zein is formed due to the amino-acid side chains, alternating to the right and left of the polypeptide chain. The β-structure of different polypeptide chains or of different regions of the same zein chain can react with each other via hydrogen bonds, resulting in laminar structures called β-sheets.

The tertiary structure of globular-type zein furnishes the facility of nanoparticle formation. In this globular structure, side chains with apolar character are oriented toward the interior of the molecule, avoiding interactions with the solvent, these forming a compact nucleus of hydrophobic character. The side chains of the polar amino acids are located on the surface of the molecule, interacting with polar solvents (water, ethanol) and allowing the protein to remain in solution (Guo et al., 2005). There are four general steps for the formation of zein nanoparticles. The first is the conformational transition from α-helix to β-sheets. Second is the packaging, where the β-sheets are folded antiparallel to each other due to the hydrophobic interaction of the adjacent β-sheets of zein. Third, we find the curl of β-sheet packaging, forming a toroid ring. Fourth, the center of the toroid hollow is closed and bioactive compounds are encapsulated (Fig. 4). In order to obtain nanometric-sized zein-based particles, the self-assembly of zein must be understood, in addition to controlling solvent-evaporation time (Luo and Wang, 2014).

The stability of zein will be a function of the covalent bonds of side chains such as disulfide bridges (S—S) and bond amides (—CO—NH—); however, non-covalent bonds such as those of the hydrophobic type can affect zein stability (Guo et al., 2005). Consequently, the formation of zein nanoparticles is due to the maximal change of α-helix into β-sheet in the globular structure. This is due to that α-helix forms disappear because they are unstable at the pH at which the ionizable amino acids are charged. Therefore, this type of nanoparticle possesses poor aggregation stability when exposed to pH values around the isoelectric point, elevated temperatures, and high salt levels. To minimize this instability, zein can be mixed with other polymers (polysaccharides), as suggested by Huang, Panagiotou, et al. (2017); Huang, Dai, et al. (2017).

5. Zein-polysaccharide nanoparticles

Antioxidants that have been encapsulated in zein-based nanoparticle matrices are very diverse; however, one of the priorities is to decrease or eliminate the free radicals that are involved in the formation of CDD. The advantage of zein-based nanoparticles is that their encapsulations can be of a hydrophobic and hydrophilic nature; hence, their use results as very attractive. One important point to consider is zein safety and tolerance in the human body or the possibility of producing an allergy; however, information on this is scarce. Vandenplas et al. (2014) showed that is better to use protein hydrolysates as vehicles as compared to proteins because of their low allergic characteristics and easy absorption properties. Lin et al. (2016) supported this same idea using corn-protein hydroslyate as a novel nanovehicle. Nevertheless, the majority of studies analysed in this review indicated that zein protect to a greater extent the bioactivity of antioxidants; chemically, encapsulation resulted in an optimal structure for the delivery of this type of compounds to prevent CDD. Table 1 presents some zein-based nanoparticles with antioxidant compounds related with the prevention or treatment of some CDD.

Deriving the limitations of zein in the GIT due to pH changes, strategies have been proposed to increase its efficiency as a carrier of antioxidant compounds to prevent or reduce CDD (Li et al., 2012). Among these strategies, we find the use of polysaccharides, mainly anionic in character, which permits their interaction with the amine groups of zein (Luo, Song, et al., 2011; Luo, Zhang, et al., 2011). This strategy is denominated the zein-polysaccharide strategy and it has currently undergone a boom as a composite nanoparticle, improving individual properties (Irache and González-Navarro, 2017). Hence, zein-polysaccharide polymer matrices for the formation of nanoparticles improve the physical properties of environmental stress and protect them within the GIT (Fig. 5) (Luo et al., 2013).

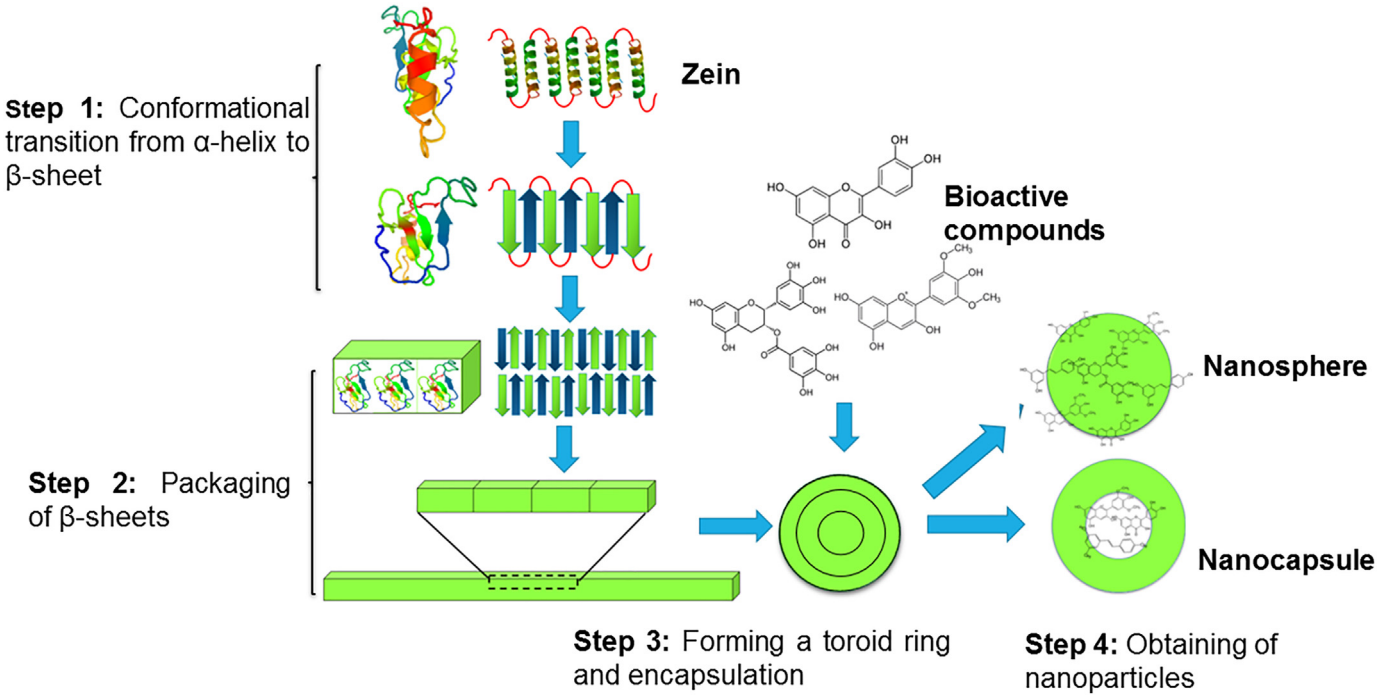

Fig. 4. Mechanism for the formation of zein-based nanoparticles encapsulating antioxidant compounds.

Table 1
Studies of Antioxidant-zein-polysaccharide nanoparticles in chronic degenerative diseases.

Zein-polysaccharide nanoparticles	Bioactive compounds	CDD[a]	Activity	References
Zein-pectin	Omega-3 polyunsaturated fatty	Heart disease	Antihypertensive	Soltani and Madadlou (2015)
Zein-pectin	Curcumin	Different diseases	Antioxidant, antiinflammatory, antimicrobial	Hu et al. (2015)
Zein-pectin	Resveratrol	Cancer	Antioxidant and anticancer	Huang, Panagiotou, et al. (2017); Huang, Dai, et al. (2017)
Zein-NaCas- Pectin[b]	Curcumin	Different diseases	Antioxidant	Chang, Wang, Hu, and Luo (2017); Chang, Wang, Hu, Zhou, et al. (2017)
Zein- NaCas -pectin	Eugenol	Possible application in CDD	Antioxidant and antimicrobial	Veneranda et al. (2018)
Zein-NaCas-Pectin and Zein-NaCas- carboxymethyl cellulose zein-NaCas-gum arabic	Curcumin	Different diseases	Antioxidant	Chang, Wang, Hu, and Luo (2017); Chang, Wang, Hu, Zhou, et al. (2017)
Zeinn-pectin-sodium alginate	Curcumin	Different diseases	Antioxidant	Huang, Huang, et al. (2016); Huang, Zhang, and Chen (2016)
Zein- carboxymethyl chitosan	Vitamin D3	Chronic diseases	Prevention	Luo et al. (2012)
Zein- carboxymethyl chitosan	Indole-3-carbinol and 3,30-diindolylmethane	Cancer	Anticancer	Luo et al. (2013)
Zein-chitosan	Vitmin E (α-tocopherol)	Different diseases	Antioxidant	Luo, Song, et al. 2011; Luo, Zhang, et al. 2011
Zein-chitosan	Epigallocatechin gallate	Possible application in CDD	Antioxidant	Liang et al. (2017)
Zein- carboxymethyl chitosan	Polyphenols and β-carotene	Cancer and Heart disease	Antioxidant	Wang et al. (2017)
Zein-quaternized chitosan	Curcumin	Possible application in CDD	Antioxidant	Liang, Huan, et al. 2015; Liang, Zhou, et al. 2015
Zein- Maillard conjugates[c] and zein-NaCas-Dextran	Resveratrol	Health	Nutraceutical	Davidov-Pardo, Joye, Espinal-Ruiz, and McClements (2015); Davidov-Pardo, Joye, and McClements (2015); Davidov-Pardo, Pérez-Ciordia, Marín-Arroyo, and McClements (2015)
Zein-Shellac	Curcumin	Possible application in CDD	Antioxidant, anti-inflammatory and anticancer	Sun, Chen, et al. (2017); Sun, Xu, et al. (2017); Sun, Yang, et al. (2017); Sun, Liu, et al. (2017); Sun et al. 2017a, 2017b
Zein-tea polysaccharide	Paclitaxel	Cancer	Anticancer	Li, Wang, et al. (2016); Li, Dong, et al. (2016)
zein–sodium carboxymethyl cellulose	Paclitaxel	Cancer	Anticancer	Liang, Huang, et al., 2015; Liang, Zhou, et al. 2015
Zein-chondroitin sulphate	Sorafenib	Cancer	Anticancer	Cheng et al. (2016)

[a] CDD: Chronic Degenerative Disease.
[b] NaCas: sodium caseinate.
[c] Maillard conjugates: reaction NaCas-Dextran.

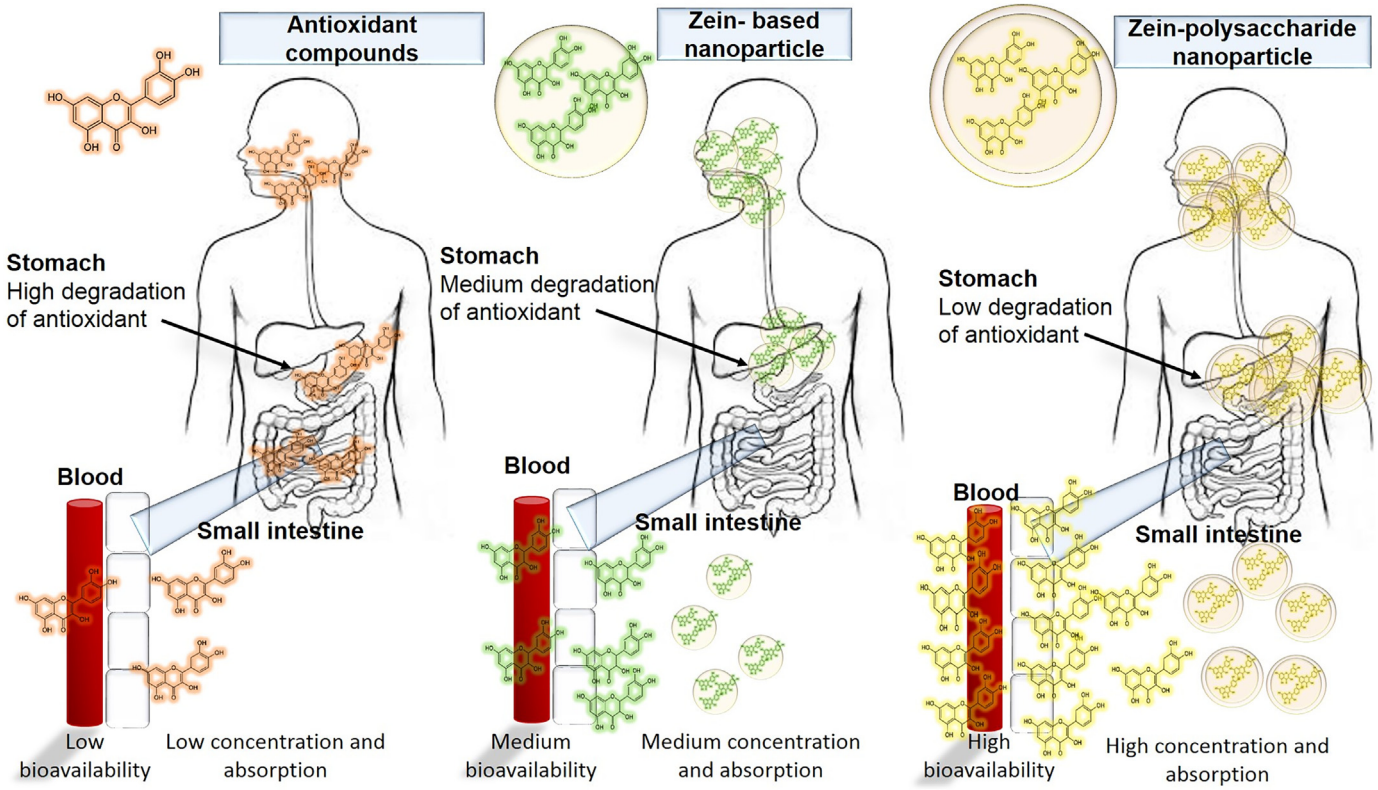

Fig. 5. Oral administration of antioxidant compounds to CDD. Conventional form with free antioxidant compounds with low bioavailability or encapsulated in a matrix of zein with médium bioavailability and zein-polysaccharide with higt bioavailability.

The formation of the polymer complex is due to the interaction of its ionized groups, mainly the zein amino group and the carboxyl group of the polysaccharide, also denominated polyelectrolytes (Dobrynin and Rubinstein, 2005). Therefore, the zein-polysaccharide nanoparticle provides a greater advantage over other zein-based nanoparticles and is much greater than antioxidant compounds without encapsulation. Among these, there is lower degradation of the antioxidant molecule and a higher concentration in the small intestine, which is reflected in high bioavailability in the bloodstream for eliminating free radicals.

A polyelectrolyte is a polymer that, at pH variations, produces the ionization or protonation of ionic functional groups. This property performs many opposing-charge polymers that are attractive, in that they can interact with each other by forming complexes such as gels or compound particles (Soltani and Madadlou, 2016). Polysaccharides are this type of biopolymer due to their large polymeric structures and natural origins (Le et al., 2017). The dissociation constant (pKa) is dependent on the polysaccharide type and will interact with zein at an acidic pH. Chitosan has a pKa range of 6.1–7.0, promoting electrostatic interaction. Alginate promotes the ionization of its carboxyl-negative groups (−COO−) due to its dielectric constant at pH 3.5, facilitating electrostatic interaction with zein. Pectin is another that is negatively charged at relatively high pH values (pKa 4–5), in addition to being soluble in water (Chang, Wang, Hu, and Luo, 2017; Chang, Wang, Hu, Zhou, et al., 2017). Therefore, in zein-polysaccharide interactions, one important factor to consider is the zein isoelectric point (pH 6.2) and the dissociation constant of the polysaccharide. Consequently, and with regard to these two parameters, the following two cases may be mentioned when working with the formation of zein-polysaccharide matrices:

1. Unfavorable case: If the pH of zein is near its isoelectric (non-ionized) point and the carboxyl groups of the polysaccharide with the pH where the dielectric constant co-exists, the results may agglomerate and precipitate the zein, the polysaccharide may remain in solution, and there is no formation of electrostatic interaction.
2. Favorable case: The protein must be below its isoelectric point (acid pH) for it to be protonated, and the polysaccharide must have a pH at which its dielectric constant is promoted. The result will be that there will be electrostatic interaction between the amino group of the protein and the carboxyl group of the polysaccharide.

Then, the formation of zein-polysaccharide nanoparticles consists of two steps: the first step comprises the formation of zein-based nanoparticles as a polymer matrix containing antioxidant compounds, while the second step is, once the zein nanoparticles are formed, a protective layer is added and consists of a polysaccharide that interacts by means of electrostatic deposition.

6. Electrostatic deposition techniques for obtaining antioxidant-zein-polysaccharide nanoparticles

Electrostatic deposition has been employed for several years for the formation of different materials, such as structures with two or three layers for the formation of zein-polysaccharide nanoparticles (Cheng and Jones, 2017; Dai et al., 2018; Wagoner et al., 2016). The advantage of utilizing this technique is that it can be coupled to other particle-forming techniques. The first of these techniques provides the formation of the zein nanoparticle with the bioactive compound to be encapsulated. The second technique is electrostatic deposition, which aids in the formation of the nanoparticle with the polysaccharide-of-interest and which promotes electrostatic interaction.

The electrostatic deposition technique is described in Fig. 6. The principle is based on Coulomb's law, where the magnitude of each of the electrical forces, with which two point charges interact, is directly proportional to the product of the loads and inversely proportional to

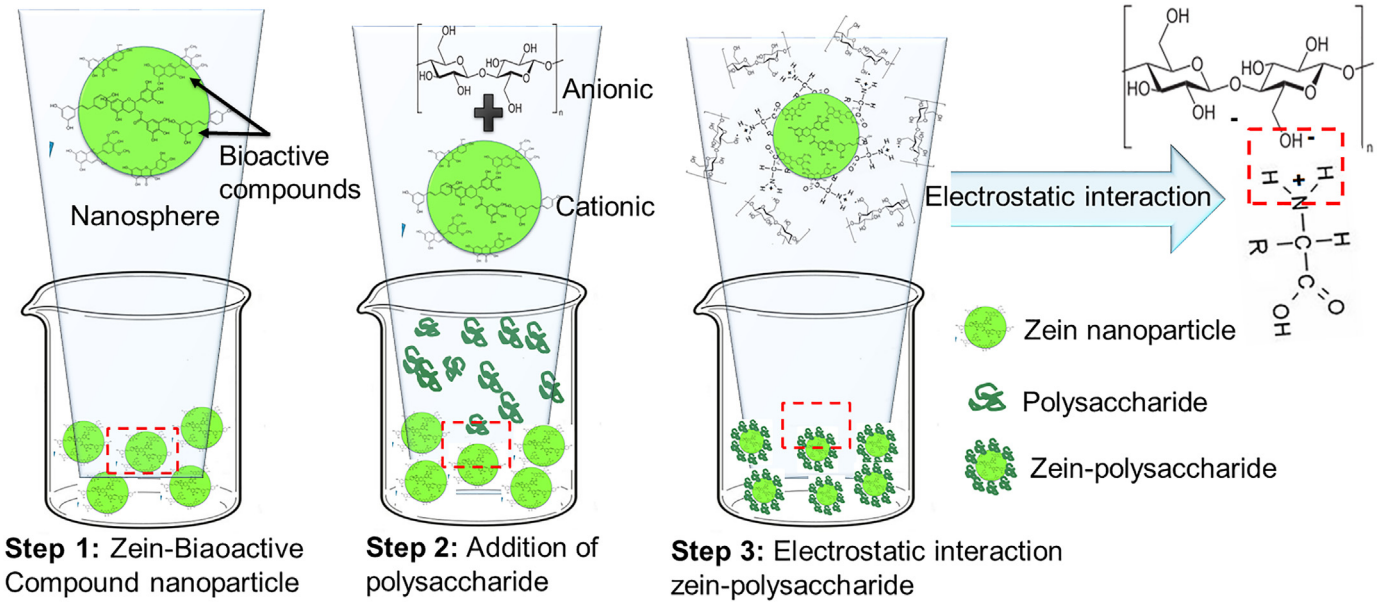

Fig. 6. Electrostatic deposition method for the formation of zein-polysaccharide nanoparticles for the encapsulation of antioxidant compounds.

the square of the distance separating them. In polylectrolytes, polymers that dissociate in charges-in- solution was framed as Coulomb's law (Zeeb et al., 2014; Feng, Lin, et al., 2016; Feng, Zhong, et al., 2016). In charged polymers where the electrostatic forces are different, one of a cationic nature with amine groups and the other, of an anionic nature with carboxyl groups (−COO−), produces electrostatic interaction (Semenova, 2017; Tsai et al., 2018). In contrast, if the polymer charge is the same, electrostatic interaction cannot be produced.

In zein-polysaccharide nanoparticles, some factors must be considered in order to choose the ideal polysaccharide to perform the best electrostatic interaction with zein (Hu and McClements, 2015; Huang, Huang, et al., 2016; Huang, Zhang, and Chen, 2016):

1. The nature of the charge: Zein is protonated in solutions preferably far from its isoelectric point (acid range), and the filler of the polysaccharide must be anionic, preferably in acidic solutions.
2. Dissociation grade: Strong polysaccharides are preferred where they dissociate at a higher pH range, unlike the weak ones within a certain pH range.
3. The location of the charged sites: Ionized polysaccharides interact more easily that have pendant-type ionized groups outside their linear structure, unlike integral-type polysaccharide, where the charge is in the linear structure.
4. The charge density: The average distance between the polysaccharide's charges must be less, where geometry is a factor to consider. Polysaccharides with high-charge density are preferred such as alginate, unlike polysaccharides with low-charge density.
5. The regularity of distribution of the anionic sites: The number of anionic charges of the polysaccharide must be by a certain number of monomer molecules. The more of the charge that exists, the lower the number of monomers preferable for the interaction with zein.

Accordingly, if the polysaccharide fulfills the considerations of providing deficient properties of zein in the GIT in order to protect them from enzymes and pH, in addition to facilitating the interaction for forming the zein-polysaccharide nanoparticles containing the antioxidant compounds, a quality system will be obtained (Lee et al., 2016). There are different techniques that apply the principle of electrostatic deposition of zein-polysaccharide. Advantages and disadvantages of the different techniques can be observed in Table 2.

6.1. *Liquid-liquid dispersion*

The liquid-liquid dispersion technique involves the formation of droplets by the dispersion of a liquid inside another immiscible liquid (Abidin et al., 2015). The technique can be carried out conventionally (Chang, Wang, Hu, and Luo, 2017; Chang, Wang, Hu, Zhou, et al., 2017) or by means of reactors (Lobry et al., 2015; Luo et al., 2017).

This technique consists of two phases. Phase one comprises putting zein in contact with ethanol/water solutions so that it is solubilized. Then the compound-to-be-encapsulated is added and the zein-antioxidant complex is formed, after evaporating the ethanol (Zhong et al., 2009). Phase two consists of placing the nanoparticles in a solution containing the polysaccharide to form the protein-polysaccharide complex by electrostatic deposition. The variables to obtain nanoparticles will depend on the solvents that are used, the concentration of the materials, the capacity of their interaction, and the variables of the technique (Visentini et al., 2017).

Li, Wang, et al. (2016); Li, Dong, et al. (2016) obtained zein-polysaccharide nanoparticles by liquid-liquid dispersion. Zein was solubilized in 85% ethanol (v/v) and homogenized by shaking at 500 rpm for 1 h. Afterward, different concentrations of the active agent were added under agitation for 1 h, and then the solution of ethanol was spiked in water, forming the particles. Finally, 6 mL of zein-active was added to a solution containing the polysaccharide and stirred for 1 h. The results included the formation of zein-polysaccharide nanoparticles with a particle yield of 40.01%, drug loading at 0.12%, and diameters of around 165 nm when the concentration of the polysaccharide was set at 0.2%.

Wang, Yin, et al. (2016); Wang, Ma, et al. (2016) elaborated zein-chitosan particles in order to stabilize emulsions. The procedure in which the particles were made by liquid-liquid dispersion included making a first solution containing 10 g of zein in 100 mL of 70% ethanol. Then a second solution was prepared from 1 g of 100 mL of chitosan at 1% acetic acid with vigorous stirring. Then, solution two was diluted with 1% acetic acid to obtain a concentration of 0.25 and 0.5%. Afterward, 10 mL of the first solution was put into contact with 20 mL at different concentrations of the second solution, under continuous agitation (500 rpm). Subsequently, the ethanol was removed in a rotaevaporator and the pH was adjusted to 3.5 (with 1 M NaOH or 1 M HCl solution). The results revealed the formation of zein-chitosan particles by the method and incorporation into emulsions (water–oil

Table 2
Advantages and disadvantages of techniques for obtaining antioxidant-zein-polysaccharide nanoparticles

Technique	Advantages	Disadvantages
Liquid-liquid dispersion	• Rapid to obtainin nanoparticles • Low cost • Applies to versatile materials • Control of particle size • Coalescence can be limited by purbulence	• Solvent must be removed • Requires two steps to obtain • Generates residual solvents • High energy is necessary • High turbulence for control of particles
Anti-solvent Coprecipitation	• Rapid to obtaining nanoparticles • Useful for low and high molecular weight polymers • Control of particle size • Easy parameter control	• Solvent must be removed • Requires two or more steps to obtain • Two solvents immiscible are necessary • Generates residual solvents • High energy is necessary
Layer-by-layer	• Rapid to obtaining nanoparticles • Low cost • Useful for low and high molecular weight polymers • Easy parameter control	• Solvent must be removed • Requires two or more steps to obtain • Generates residual solvents • High energy is necessary
Electrospraying	• Rapid solvent evaporation • Can be obtained in one step • High molecular weight polymers can be used • Various morphologies can be obtained • Easy control of particle size • Generates little or no residual solvent	• Occupies a specialized equipment • High energy is necessary • Ambient humidity and temperature must be controlled

systems) aided in stabilizing them up to 9 months.

Chen et al. (2017) synthesized nanoparticles of zein-carrageenan by liquid-liquid dispersion for the stabilization of zein-based nanoparticles. First, 1 g zein was solubilized in 40 mL of aqueous ethanol (80% v/v); then, the particles were formed by incorporation of 20 mL of the previous solution (drop-wise) into 60 mL of water with magnetic stirring. The rotavaporation solvent was evaporated and centrifuged at 2,880 *g* for 10 min. Then, the carrageenan solution was formed in 10 mM Sodium Phosphate Buffer (SPB) solution and stirred for 12 h. Finally, 0.1% (w/v) of zein nanoparticles was added different concentrations of carrageenan and stirred vigorously. The pH was adjusted within a range of 5–7 and stored at 4 °C. The zein-carrageenan nanoparticles obtained were more stable with 0.001% carrageenan and in pH ranging from 5.25–6.75.

Hu and McClements (2015) obtained zein-alginate nanoparticles. These authors used 2 g of zein dissolved in 100 mL of 85% ethanol. Then 4 mL of zein was added to 16 mL of Tween 80 followed by 20 mL of sodium alginate. In their results, the authors reported that nanoparticles were stable and without aggregation with Tween 80. Particles of zein without alginate were of 80 nm, while those with 0.01% (w/v) of alginate presented low repulsion among particles forming aggregates and, at 0.01–0.05% (w/v), maintained this diameter without aggregate. Particle yield was 95% and they were stable at pH 3–8. Sein-alginate nanoparticles are feasible for the release of bioactive compounds into the pharmaceutical and food industry.

6.2. Anti-solvent co-precipitation

This technique consists of inducing the co-precipitation of dissolved polymers in an ideal solvent by incorporating an antisolvent, which aids in providing a drive force to precipitate the solute. For this technique, the choice of solvent and anti-solvent is the first step that must be followed and comprises the most critical one for greater efficiency of the results (Joye and McClements, 2013).

In zein-polysaccharide nanoparticles, the co-precipitation anti-solvent technique is performed by the addition of zein in an ideal alcoholic solvent such as 70% ethanol. This is then solubilized with magnetic stirring (Patel and Velikov, 2014). After this, the polysaccharide is subsequently added, which is also solubilized. During the incorporation of the polysaccharide, electrostatic deposition with the zein is conducted by the cationic and anionic functional groups. The solvent is reduced and the solution with zein-polysaccharide nanoparticles is incorporated into a syringe for its latter expulsion into an anti-solvent and precipitate (Sun, Chen, et al. (2017); Sun, Xu, et al. (2017)). The important parameters to consider are type of solvent, which must solubilize zein and the polymer at the same time, this being a disadvantage for polymers that cannot be solubilized in the same solvent as zein, as well as the large amount of solvent that is used.

Sun, Chen, et al. (2017); Sun, Xu, et al. (2017); Sun, Yang, et al. (2017); Sun, Liu, et al. (2017); Sun et al. 2017a, 2017b obtained nanoparticles of zein-propylene-glycol alginate by means of the anti-solvent co-precipitation technique. A stock solution of 0.40 g of zein and 0.08 g of propylene glycol alginate in 40 mL of 70% ethanol was prepared with violent magnetic stirring until it was completely dissolved. The mixture was placed in a syringe and injected at a constant speed of 20 mL min^{-1} in an aqueous solution containing different concentrations of $CaCl_2$. Three quarters of the ethanol were removed in a rotaevaporator at 45 °C for 35 min. The results showed a particle size dependent on the concentration of propylene glycol alginate and calcium from 142 nm at 4.7 μm.

Sun, Chen, et al. (2017); Sun, Xu, et al. (2017); Sun, Yang, et al. (2017); Sun, Liu, et al. (2017); Sun et al. 2017a, 2017b elaborated zein-propylene-glycol alginate nanoparticles containing quercetagetin as a bioactive compound by the anti-solvent co-precipitation method. First, 1 g of zein and 0.2 g of propylene-glycol alginate were solubilized in 70% ethanol and adjusted to pH 4 with 0.1 N of a solution of sodium hydroxide and hydrochloric acid. After a stirring time, 0.1 g of quercetagetin was added to the same glass containing zein-propylene glycol alginate. The suspensions formed were centrifuged at 765 g for 10 min to eliminate quercetagetin without its dissolving. Finally, 120 mL of the stock solution was loaded in a syringe and was sprayed for 2 min into a glass containing 60 mL of aqueous solution with different concentrations of $CaCl_2$. The results demonstrated an average particle size of 774 nm, which decreased with the increase in calcium.

Chen et al. (2018) synthesized zein-shellac nanoparticles by means of the anti-solvent co-precipitation method. First, two polymer solutions were prepared: the first solution contained zein, and the other, second solution contained with shellac, both at a concentration of 10 mg mL^{-1} in 80% ethanol, stirred with a magnetic stirrer at 600 rpm for 2 h at 25 °C, and adjusted to pH 8. The shellac solution was diluted with 80% ethanol to obtain different concentrations. Ten mL of shellac solution was mixed with zein solution at a different radius. Then 20 mL of zein-shellac solution was placed in a syringe and slowly injected into a solution with agitation (600 rpm for 20 min) of 60 mL of PBS (pH 8). Three quarters of ethanol was removed by a rotaevaporator at 45 °C and zein-shellac nanoparticles were obtained with a diameter of less than

100 nm in all preparations with small concentrations of shellac.

6.3. Layer-by-layer deposition

This technique was proposed in 1960 and has undergone several modifications, which consisted of adding different layers of polymers to an already formed rigid structure (substrate) (Ramasamy et al., 2014; Wang, Yin, et al., 2016; Wang, Ma, et al., 2016). Layer-by-layer deposition is similar to liquid-liquid dispersion, but the difference lies in that in the layer-by-layer technique, not necessarily the solvent is not necessarily displaced to form the layers, as in liquid-liquid dispersion. In polymeric nanoparticles, the formation of a substrate such as that of nanospheres is required on which one or two or more layers of polymers are to be deposited (Padua and Wang, 2012). In order for the layer to form on the substrate, an interaction must be formed by which the layers are adhered, forming more complex particles (Borges and Mano, 2014; Wang and Zhao, 2013).

The layer-by-layer technique is carried out from obtaining the zein nanoparticles, for which it adds zein and the compound-to-be-encapsulated to an ideal solvent (aqueous ethanol) and stirred for a certain time, and the excess of bioactive compound is removed. Once the nanoparticle of the zein-bioactive compound is formed, a polymer solution is deposited containing the second polymer (polysaccharide) that will interact with the zein particle, through hydrophobic, covalent, electrostatic, and other weaker interactions, depending on the polysaccharide added (Zhang, Niu, et al., 2014; Zhang, Tong, et al., 2014). Several polysaccharides can be added depending on the needs of the research. The advantage of the technique is that it rapidly obtains nanoparticles with multilayers, in addition to that it occupies little energy for its elaboration (only energy of agitation). Nonetheless, disadvantages include that it occupies several solvents depending on the polysaccharides to be added, these being the solvent residues deriving from the process.

Zhang, Niu, et al. (2014); Zhang, Tong, et al. (2014) obtained nanoparticles of zein-chitosan hydrochloride containing sodium caseinate and thymol as the active compound. The elaboration conditions were, first, zein and thymol were dissolved in two concentrations of aqueous ethanol (80 and 100 mL) to obtain final solutions with 20 and 4 mg mL^{-1}. Then 2 mL of the solutions were added to 10 mL of milli-Q water containing different concentrations of sodium caseinate and stirred with a magnetic stirrer at 750 rpm for 30 min. The aqueous solution of chitosan hydrochloride was made at concentrations ranging from 0.25–1.0 mg mL^{-1}, and this was added slowly to the solution with the same volume and concentration of 0.5 mg mL^{-1} of zein-thymol-sodium caseinate with magnetic stirring at 750 rpm for 30 min. The samples were lyophilized and resuspended. The results revealed zein-chitosan hydrochloride particles containing sodium caseinate and thymol at a final pH of 4.3 with an average particle size of 520 nm and a z potential of +64.45 mV. In addition, good antimicrobial activity was obtained with the complex formed. Therefore, chitosan hydrochloride stabilizes zein nanoparticles on using low energy in the method and being favorable for the maintenance of antimicrobial systems.

6.4. Electrospray

The electrospray technique is based on obtaining nanoparticles by means of the application of an electric field that forms a conductive polymer solution and decreases the surface tension of the polymer and fissions in smaller particles (Liu et al., 2018; Tapia-Hernández et al., 2015). The electrospray technique is currently a novel technique for the formation of zein-polysaccharide nanoparticles, having the advantage of first forming the zein particle, followed by the addition of the polysaccharide (Laelorspoen et al., 2014). The mechanism consists of the ability of an electric field to deform the interface of a liquid drop (Tapia-Hernández, Rodríguez-Félix, Plascencia-Jatomea, et al., 2017; Tapia-Hernández, Rodríguez-Félix, and Katouzian, 2017). The variables to be considered for obtaining nanometer-sized particles are the following: equipment parameters (voltage, flow velocity, and collector distance); polymer-solution parameters (concentration and solvent), and environmental parameters (temperature and relative humidity) (Bhushani et al., 2017; Tapia-Hernández, Rodríguez-Félix, Plascencia-Jatomea, et al., 2017; Tapia-Hernández, Rodríguez-Félix, and Katouzian, 2017).

To our knowledge, few studies of obtaining zein-polysaccharide by electrospray have been carried out, which suggests a field of opportunity for further investigations. Laelorspoen et al. (2014) reported the interaction of zein-polysaccharide particles. The conditions of preparation of the zein solution were as follows: ethanol acidified with 1.5% calcium chloride ($CaCl_2$ 1.5 w/v); 7% (w/v) of zein, and homogenized for 1 h. The polysaccharide solution was made from 1.4% sodium alginate in distilled water, homogenized for 2 h, and 8% glycerol. Then the polysaccharide solution was sterilized and 1 mL of suspension containing *L. acidophilus* was added as active ingredient. Finally, the zein solution was spiked in the polysaccharide solution under the following conditions: voltage of 4–10 kV; flow rate of 10 mL h^{-1}, nd distance of the collector was 6 cm.

Regardless of the technique used for the preparation of zein-polysaccharide nanoparticles, we concluded that these systems are feasible for protection from the pH, temperature, and enzymes present in the GIT and for increasing the bioavailability of bioactive compounds in the bloodstream employed as antioxidants to prevent CDD.

7. Development of antioxidant-zein-polysaccharide nanoparticles for application in chronic degenerative diseases

There are some studies that show the protection of antioxidants in zein-polysaccharide nanoparticles and that render them more bioavailable and aid more efficiently to reduce or eliminate free radicals, which are precursors for the appearance of CDD (Table 1). The most common compounds encapsulated in zein-polysaccharide matrices that are utilized to avoid their degradation and that maintain their bioactivity are antioxidants such as phenolic compounds (curcumin, resveratrol, and epigallocatechin), vitamins D and E, precursor of vitamin A (beta-carotene), among others.

7.1. Phenolic compound-zein-polysaccharide nanoparticles

Phenolic compounds are receiving increasing interest principally for their antioxidant properties that, consequently, can prevent CDD. However, the biological properties of polyphenols depend on their bioavailability, and these types of compounds generally have low bioavailability and are very sensitive to degradation. For these reasons, nanoencapsulation with different matrices as zein-polysaccharide can be a good option to avoid these disadvantages. Despite the fact that there is a great variety of phenols, curcumin, resveratrol, and epigallocatechin have been used as a model of some zein-polysaccharide systems.

7.1.1. Curcumin

The polyphenol curcumin is a molecule with several properties, such as great antioxidant capacity (Guo et al., 2018) and the enhancement of anticancer activity (inhibiting the viability and proliferation of a variety of human cancer-cell lines including skin, gastrointestinal, genitourinary, breast, ovarian, and lung cancer) (Luckanagul et al., 2018), anti-tumor immunity (Momtazi and Sahebkar, 2016), anti-inflammatory (Julie and Jurenka, 2009), preventing atherosclerosis (Sahebkar, 2015), diabetes mellitus (Panahi et al., 2017), pulmonary diseases (Lelli et al., 2017), obesity, and CVD (Mohammadi et al., 2013), among others. Hence, curcumin has been used as a model of some zein-polysaccharide systems. Hu et al. (2015) elaborated zein-pectin nanoparticles for the protection of curcumin during the course of the gastrointestinal system. Zein with

polysaccharides for encapsulating curcumin can protect the latter from the gastrointestinal system until the delivery of curcumin in the intestine. Thus, this antioxidant system could be utilized in the prevention of CDD. (Huang, Huang, et al. (2016); Huang, Zhang, and Chen (2016)) studied the use of zein-pectin/alginate nanoparticles for the encapsulation of curcumin. Antioxidant capacity revealed greater activity for encapsulated curcumin as opposed to curcumin in solution and without encapsulating. Therefore, the zein-pectin/alginate system for curcumin was either efficient for obtaining nanoparticles.

On the other hand, (Chang, Wang, Hu, and Luo, 2017; Chang, Wang, Hu, Zhou, et al., 2017) studied the effect of polysaccharide on the addition of zein-sodium Caseinate (NaCas) systems and curcumin protection as zein-NaCas-pectin, zein-NaCas-carboxymethyl cellulose, and zein-NaCas-gum Arabic. In general, pectin exhibited best chemical stability at pH, while carboxymethyl cellulose possessed least stability, due to its structure. Antioxidant activity was increased 5 times higher with the presence of the polysaccharides specially carboxymethylcellulose. Therefore, this study supports that zein-polysaccharyde systems are useful for the protection of antioxidant compounds in gastrointestinal systems.

Chang, Wang, Hu, and Luo (2017); Chang, Wang, Hu, Zhou, et al. (2017) synthesized zein-NaCas-pectin nanoparticles for the protection of curcumin, in addition to that NaCas-pectin stabilizes zein during passage through the gastrointestinal system. The system was developed from solutions of NaCas, pectin, and zein. Again, zein nanoparticles coated with pectin were more stable during the simulation of physiological conditions, with little variation in particle size and polydispersity. In conclusion, zein-polysaccharide nanoparticles for encapsulating antioxidants can be good systems for use in the prevention of CDD due to their protection of antioxidants until their absortion in the intestine.

There are several mechanisms that curcumin uses to prevent or combat CDD. In cancer disease, curcumin is capable of suppressing tumors in all of their stages, principally inducing apoptosis (Bush et al., 2001; Choudhuri et al., 2002). In lung tumor, curcumin enhanced immune response through the increase of InterFeroN gamma (IFN-γ) secretion and Th1 and TCD8+ cells (Luo, Song, et al., 2011; Luo, Zhang, et al., 2011). In human melanoma cell lines, curcumin induces apoptosis and revealed caspase-3 processing, poly ADP ribose polymerase cleavage, reduced Bcl-2, and decreased basal phosphorylated Signal Transducers and Activators of Transcription 3 (STAT3) (Bill et al., 2009). In addition, curcumin can attenuate the activation and secretion of cytokines of cells that contribute to tumor progression (Th2 and Treg cells) (Abdollahi et al., 2018; Luo, Song, et al., 2011; Luo, Zhang, et al., 2011). However, there is evidence that depends on the dose of curcumin in the response related to antitumor activity. At a high dose (100 mg/kg), curcumin inhibits the expansion and function of immune cells, while low-dose (50 mg/kg) curcumin increased IFN-γ secretion, enhancing the immune response (Bill et al., 2009; Luo, Song, et al., 2011; Luo, Zhang, et al., 2011). In obesity, curcumin can reduce proinflammatory cytokines such as IL-1β, IL-4, and VEGF (Ganjali et al., 2014). In type 1 diabetes, curcumin regulates the gene expression of NO, TNFα, IL-1, and IL-6, ameliorating autoimmune diabetes (Castro et al., 2014). With all of these properties, curcumin must be protected from the environment and gastrointestinal changes until its delivery into the intestine to exercise its action. Thus, on the basis of the studies analyzed regarding this, the nanoencapsulation of curcumin with the zein-polysaccharide system can be a good option.

7.1.2. Resveratrol

Resveratrol is other phenol compound considered at present as one of the most potent antioxidants with multiple applications in health, such as an anti-inflammatory (Penalva et al., 2015), for cardioprotection (Feng et al., 2007), as an anticarcinogenic (Feng, Lin, et al., 2016; Feng, Zhong, et al., 2016), and the prevention of diabetes (Zhao et al., 2018) and obesity (Zhao et al., 2017). However, to maintain or improve water solubility, chemical stability, and bioavailability, several studies have been focusing in the nanoencapsulation of resveratrol in different zein-base matrices. Joye et al. (2015) encapsulated resveratrol with zein and gliadin matrices providing protection to this polyphenol molecule for future use as a delivery system for protection from different CDD, Davidov-Pardo, Joye, Espinal-Ruiz, and McClements, 2015; Davidov-Pardo, Joye, and McClements, 2015 and Davidov-Pardo, Pérez-Ciordia, Marín-Arroyo, and McClements, 2015 obtained nanoparticles of resveratrol in zein and different conjugate polysaccharides (pectin and dextran). Then, zein nanoparticles can be improved by coating them with sodium caseinate and neutral carbohydrates. The molecular mass of the carbohydrates utilized exert a significant impact on particle stabilization, with the stability of the delivery systems increasing with an increasing carbohydrate molecular mass. Penalva et al. (2015) evaluated a resveratrol nanoparticulate (307 nm) formulation based on zein to improve oral bioavailability and its anti-inflammatory effects in a mouse model. The conclusion was that these nanocarriers significantly increase the oral bioavailability of resveratrol and protect the mice from the inflammatory symptoms inhibiting LipoPolySaccharide (LPS)-induced cytokine production, principally by inhibiting transcription factor NF-κB.

(Huang, Panagiotou, et al. (2017); Huang, Dai, et al. (2017)) elaborated zein-pectin nanoparticles for resveratrol protection and application with antioxidant and anticancer activity. In addition, antioxidant activity was measured, indicating that encapsulation promotes greater antioxidant capacity in comparison with samples without encapsulation. On the other hand, in Bel-7402 cells of hepatocarcinoma cancer, the effect of encapsulated resveratrol showed antiproliferative activity. On this context, some mechanisms of resveratrol used to inhibit proliferation in other types of cancer were observed in several studies due to its capacity to suppress the growth of tumor cells by inducing cell-cycle arrest and apoptosis, by the inhibition of free radicals such as those in osteosarcoma cells (Sun et al., 2015), HCA-17 and SW480 carcinoma-cell lines (Feng, Lin, et al., 2016; Feng, Zhong, et al., 2016) and liver cancer-cell line (Zhang, Lakshmanan, et al., 2017; Zhang, Deng, et al., 2017). Resveratrol targets COX, which generate pro-inflammatory molecules that lead to tumor proliferation and down-regulates the AKT, MAPK, and NF-κB signaling pathways, all of which would reduce inflammation and prevent tumorigenesis (Alayev et al., 2015; Berman et al., 2017).

On the other hand, there are studies on resveratrol related with the prevention or treatment of diabetes mellitus. The attenuation of type 1 diabetes-induced testicular OS and apoptosis by resveratrol is mainly related to Akt-mediated Nrf2 activation via p62-dependent Keap1 degradation (Zhao et al., 2018). In addition, resveratrol exhibited protective properties and suppressed the genomic damage mediated by insulin in kidney cells *in vitro* (Awad et al., 2017). Additionally, acetylated Farnesoid X Receptor (FXR) plays a critical role in the regulation of lipid and glucose metabolism; however, disruption of its genes induces diabetes or hypercholesterolemia; thus, there is evidence that resveratrol reduces this receptor in order to regulate this metabolic diseases (Kemper et al., 2009). Otherwise, resveratrol can induce SIRT1 (SIRTuin1) to decrease cellular OS (Yun et al., 2012), mitochondrial superoxide, and ROS (Xu et al., 2012) under hyperglycemic conditions.

Overexpression of endogenous SIRT1 is correlated with cardioprotective effects induced by resveratrol (Yang and Suh, 2013). Additionally, the SIRT1 pathway regulates mitochondrial genes to suppress ROS production in order to protect cardiomyocytes treated with resveratrol (Li et al., 2013; Yang et al., 2013). In atherosclerosis, the decrease in plasma of IFN-γ and the expression of endothelial-cell ICAM (InterCellular Adhesion Molecules), VCAM (Vascular Cell Adhesion Molecules), and IL-8 (InterLeukin 8) is observed when resveratrol is employed as a treatment (Agarwal et al., 2013). With respect to coronary artery disease, resveratrol improves left ventricular systolic and diastolic function as well as FMD (Flow-Mediated Dilation) levels (Magyar et al., 2012). Otherwise, the reduction of diastolic blood

pressure is other effect of resveratrol in hypertension (Biesinger et al., 2016). In addition, resveratrol produces the reduction of LDL cholesterol levels and improves vascular function and mitochondrial number in older adults (Pollack et al., 2017).

The main target for resveratrol as an antiobesity molecule is white adipose tissue, because it is the main triglyceride stored in the body. This phenolic compound inhibits fat accumulation and stimulates lipid mobilization (Fernández-Quintela et al., 2017). In this context, Imamura et al. (2017) studied the effect of resveratrol on the expression of genes regulating triglyceride accumulation and consumption in differentiated 3 T3-L1 preadipocytes. These authors concluded that resveratrol may augment synthesis and oxidation of fatty acid and possibly increases energy- utilization efficiency in adipocytes through the activation of SIRT1. A similar conclusion was reported by Zhao et al. (2017), suggesting that resveratrol may suppress obesity and associated inflammation via the AMPKα1/SIRT1 signaling pathway in rat. Additionally, Rossi et al. (2018) indicated that resveratrol may inhibit obesity-associated inflammation and claudin-low breast cancer growth by inhibiting adipocyte hypertrophy and the associated adipose-tissue dysregulation that typically accompanies obesity.

In conclusion, the mechanism of action of resveratrol in CDD can modify not only biochemical pathways, but also epigenetic mechanisms and, due to the importance of the latter, these topics are the focus of some reviews (Berman et al., 2017; Fernandes, Silva, et al., 2017; Fernandes, Pérez-Gregorio, et al., 2017; Imamura et al., 2017; Marx et al., 2017; Oliveira, Monteiro, et al., 2017; Oliveira, Simão, et al., 2017; Pan et al., 2018).

7.1.3. Epigallocatechin gallate

Catechins are considered polyphenols of the flavan-3-ol family distributed in different food sources, such as in green tea, whichthis polyphenol represents in approximately 30–50% (Ng et al., 2017; Tu et al., 2018). At the biological level, epigallocatechin gallate is attributed to different health benefits, especially its participation in mitigating CDD such as cancer (Fujiki et al., 2017; Rady et al., 2017), diabetes mellitus (Chen et al., 2017; Zhang, Lakshmanan, et al., 2017; Zhang, Deng, et al., 2017), heart disease (Eng et al., 2017; Tu et al., 2018), and obesity (Javaid et al., 2017; Lee et al., 2017), due to its antioxidant property.

The antioxidant activity of epigallocatechin gallate is due to the presence of both the phenolic groups and the galloyl group, which allow electron delocalization (Naponelli et al., 2017). In addition, the mechanisms by which epigallocatechin gallate acts as an antioxidant molecule after its greater bioavailability are diverse and exclusive to each disease type. In cancer, epigallocatechin gallate acts at several levels, such as the induction of apoptosis, modulation of cell proliferation, and inhibition of angiogenesis (Rady et al., 2017). In normal skin cells, epigallocatechin gallate protects against the DNA damage induced by UltraViolet (UV) radiation by means of reducing the phosphorylation of H2AX foci in HaCaT keratinocytes (George et al., 2017). Epigallocatechin gallate induces intracellular apoptosis (mitochondrial pathway) by caspase-9 and by inducing the apoptosome complex, which is composed of cytochrome C, Apoptotic protease activating factor 1 (Apaf-1), and procaspase-9 (Hagen et al., 2013). Epigallocatechin catechin demonstrated the induction of apoptosis through the extrinsic death receptor pathway inMIA-Pa-Ca-2 pancreatic-cancer cells by activating Fas, DR5, and Caspase-8 (Basu and Haldar, 2009). In addition, it can inhibit cell proliferation through inducing G0/G1 cell-cycle arrest (Zhou et al., 2013). In A549 lung-cancer cells, it was observed that epigallocatechin gallate inhibits angiogenesis and reduces tumor growth of the xenograft by inhibiting IGF-1 by means of suppressing the expression of the protein HIF-1α and VEGF (Relat et al., 2012). In addition, there has been an increase in H_2O_2 in cancer cells due to cell activation, which is eliminated by SOD and GPx. When SOD and GPx are diminished, it indicates an alteration in mechanisms of H_2O_2 neutralization. The consumption of epigallocatechin gallate induces the improvement of SOD and GPx activity, functioning as an effective antioxidant (Hussain, 2017).

In diabetes mellitus, hyperglycemia increases OS and decreases antioxidant mechanisms by increasing OS. The OS status can trigger the inflammatory cascade that eventually leads eventually to cell death and apoptosis. In diabetic mice, the administration of epigallocatechin gallate helps to improve the mechanism of ROS elimination, which is mainly produced by the increase of the NADPH oxidase responsible for the generation of superoxide and also promotes downregulation of OS markers such as TAC, Nrf2, HO-1, and HSP 90 (Rasheed et al., 2017). In diabetic nephropathy, one of the factors that propitiates the latter is OS, which is regulated by NRF2 factor, a molecule that activates the signaling of antioxidant mechanisms, such as the activation of the heme oxygenase-1 (*Ho1*) and NAD(P)H dehydrogenase quinone 1 (*Nqo1*) genes. When NRF2 is suppressed, strategies are sought, such as the consumption of epigallocatechin gallate, which aids in promoting its activation. The mechanism by which NRF2 is suppressed comprises the entrapment of the KEAP1 protein, forming a KEAP1-NRF2 complex by means of the inclusion of cysteine residues. It has been stipulated that epigallocatechin gallate interacts directly with the cysteine residues present in KEAP1, thus stimulating the dissociation of NRF2 from KEAP1 (Sun, Chen, et al. (2017); Sun, Xu, et al. (2017); Sun, Yang, et al. (2017); Sun, Liu, et al. (2017); Sun et al. 2017a, 2017b).

In CVD and obesity, epigallocatechin gallate exerts beneficial effects on health (Othman et al., 2017; Rahimi and Falahi, 2017), and specifically in atherosclerosis, a disease of the arteries that is due to endothelial dysfunction, inflammatory vascular cells, and lipid accumulation (Hansson, 2009). Lipid peroxidation is considered a major factor that can lead to atherosclerosis. Diets in rats with epigallocatechin gallate revealed that there was a reduction in Total Cholesterol (TC), TriGlycerides (TG), Low Density Lipoprotein and Very Low Density Lipoprotein (LDL/VLDL) fractions and that there was an increase in High Density Lipoprotein (HDL) cholesterol. Also, it also effectively reduces the production of CRP, Monocyte Chemoattractant Protein 1 (MCP-1), and the oxidized LDL/VLDL cholesterol level in the serum of ApoE −/− mice (Cai et al., 2013; Eng et al., 2017). Epigallocatechin gallate can be utilized to treat atherosclerosis through its anti-inflammatory and antioxidant effects (Eng et al., 2017). In cardiac hypertrophy and fibrosis in aged rats, epigallocatechin gallate demonstrated the inhibition of the ROS-dependent activation of the TGFβ1, TNFα, and NF-κB signaling pathways (Muhammed et al., 2017). In addition, one mechanism is that the cholesterol-lowering effect is due to the decrease in the absorption or reabsorption of cholesterol by epigallocatequin gallate, as well as the decrease in cholesterol synthesis through the inhibition of HMGR (mediated by activation) of AMPK, and nitric oxide synthesze is increased by decreasing blood pressure and myocardial infarction (Yang et al., 2018). In patients with obesity, epigallocatequin gallate inhibits the synthesis of fatty acids, proliferation and differentiation in human primary visceral adipocytes, and suppresses the absorption of triacylglycerols (Saad et al., 2017).

However, its high capacity and health benefits are limited by low absorption and bioavailability (Sanna et al., 2017). A delivery alternative is epigallocatechin- gallate encapsulation to increase its deficiencies in polymeric protein matrices such as zein (Shi et al., 2018). Recent studies report that zein interacts with hydrophilic compounds such as epigallocatechin gallate by means of hydrogen and hydrophobic interactions (Bhushani et al., 2017). Therefore, the majority of studies are focused on the encapsulation of epigallocatechin gallate in zein matrix, providing excellent benefits. For example, Liu et al. (2017) elaborated nanoparticles of zein-epigallocatechin gallate conjugate with smooth sphere morphology compared to the control, observing changes in the secondary structure of the chemical interactions formed. These authors concluded that these systems can function as controlled-release systems in the food and pharmaceutical industry. Bhushani et al. (2017) prepared zein nanoparticles for the encapsulating catechin powder, among which epigallocatechin gallate was found through the

electrospray technique. The results demonstrated that hydrogen bonds and hydrophobic interactions were predominant in this system. On the other hand, Li et al. (2009) prepared zein nanofibers encapsulating epigallocatechin gallate; however, at low concentrations of zein, deformed particles were obtained by means of the electrospinning technique. The interactions between zein and epigallocatechin gallate were studied in the deconvolution of the main bands of the zein, especially changes in the secondary structure of beta sheet and alpha helix, observing significant changes and attributing these to the formation of hydrogen bonding and hydrophobic interactions. In the study of Donsì et al. (2017), the authors elaborated zein nanoparticles with epigallocatechin gallate where the low interaction of epigallocatechin gallate in zein nanoparticles is limited by weak hydrophobic interactions between the aromatic rings of epigallocatechin and the hydrophobic residues of zein. These authors recommended, as a strategy, the addition of a polysaccharide to zein nanoparticles.

Unfortunately, only the study of Liang et al. (2017), to our knowledge, was found to be related to prepared zein-chitosan nanoparticles encapsulating epigallocatechin gallate. This system increased antioxidant activity by up to 95%, being applicable to food systems or therapeutic treatments. Thus, this study suggests that the encapsulation of epigallocatechin gallate in zein-polysaccharide systems provides greater stability and more effective delivery, improving its antioxidant capacity, being useful in reducing the prevalence of CDD. Hence, more studies could be carry out that are related to encapsulating epigallocatequin in zein with other, different polysaccharides.

7.2. Vitamin-zein-polysaccharide nanoparticles

The use of vitamins such as A, D, and E is essential in the organism, since it reduces CDD and their deficiency is susceptible to an attack by free radicals (Luo, Song, et al., 2011; Luo, Zhang, et al., 2011; Luo et al., 2012). This deficiency can be due to environmental factors such as the presence of oxygen, light, and temperature. Therefore, the encapsulation of vitamins in nanoparticles is studied; however, to our knowledge, there is very little information on zein-polysaccharyde matrices.

7.2.1. Precursor of vitamin A

The carotenoid β-Carotene is the primary plant-based source of dietary vitamin A (Novotny et al., 2010). Thus, provitamin A (β-carotene) plays an important role in meeting vitamin A requirements in a diet. Therefore, 12 mg of β-carotene needs to be consumed in order to produce 1 mg of vitamin A, the daily recommended dose, because high doses limit its conversion into vitamin A (Novotny et al., 2010; Strobel et al., 2007). β-Carotene can be converted into retinal, which is essential for vision, and subsequently into retinoic acids, which are essential for pattern recognition during development and cell differentiation (Hickenbottom et al., 2002). β-Carotene acts as an antioxidant by quenching singlet oxygen and scavenging peroxyl radicals; hence, it can prevent CDD. In cancer chemoprevention, β-carotene uses several mechanisms, such as changes in cell signaling pathways, leading to cell growth or cell death, which include immune modulation, growth-factor signaling, and apoptosis (Huang, Panagiotou, et al., 2017; Tanaka et al., 2012). In the study of Shree et al. (2017), β-carotene (1 μM) can inhibit the viability and increase apoptosis of human breast-cancer (MCF-7) cells through increased caspase-3 activity. In addition, it decreases the expression of anti-apoptotic proteins Bcl-2 and PARP and of survival protein NF-kB. It also inhibited the activation of intracellular growth-signaling proteins Akt and ERK1/2. Consequently, it decreased phosphorylation of Bad due to inactivation of Akt. Furthermore, β-carotene downregulated antioxidant enzyme SOD-2 and its transactivation factor (Nrf-2) and Endoplasmic Reticulum (ER) stress marker, XBP-1, at protein levels.

DNA-repair Ku proteins (Ku70 and Ku80) play a crucial role in the repair of DNA double-strand breaks. If these proteins are reduced, they contribute to apoptosis in gastric-cancer cells. Hence, β-carotene-induced alterations increase in caspase-3 activity and decrease in Ku proteins, resulting in the apoptosis of these cancer cells (Park et al., 2015). On the other hand, vitamin A and β-carotene are involved in the methylation of DNA and in DNA damage (Cooper et al., 1999); hence, this could be one of the reasons of why some cancer types increase. For example, the relation of vitamin A and β-carotene in lung cancer is unclear: some studies indicated the decrease of the risk of this cancer type, while others indicated otherwise (Jin et al., 2007; Takata et al., 2013; Yu et al., 2015).

There are several studies in which β-carotene is associated with the prevention of CVD, for example, in stroke (Daviglus et al., 1997; Hak et al., 2004; Hirvonen et al., 2000), coronary artery disease (Osganian et al., 2003), myocardial infarction (Kardinaal et al., 1993; Klipstein-Grobusch et al., 1999; Tavani et al., 1997), coronary mortality (Knekt et al., 1994; Voutilainen et al., 2006), among others. Gopal et al. (2013) showed that dietary supplementation of β-carotene may possess a protective function against angiotensin II-induced abdominal aortic aneurysm by ameliorating macrophage recruitment in mice. Therefore, with all of these properties of β-carotene, several studies are focused on the protection of its bioactivity through encapsulation.

Studies exist in which β-carotene is nanencapsulated in zein matrix to improve stability and enhance antioxidant activity. Chuacharoen and Sabliov (2016) studied the potential of zein nanoparticles to protect entrapped β-carotene in the presence of milk under simulated gastrointestinal conditions, where the authors concluded that zein nanoparticles improved the chemical stability and antioxidant activity of entrapped β-carotene. On the other hand, with the objective of benefiting human health and have novel delivery systems for lipophilic bioactive ingredients, Chen et al. (2016) elaborated zein-based oil-in-glycerol emulgels enriched with β-carotene, which enhanced the UV photostability of beta-carotene, and more than 88% of this antioxidant was retained for 64-h storage under UV exposure, consequently retarding oil oxidation while in storage. In the same manner, López-Rubio and Lagaron (2011) improved the incorporation and stabilization of β-carotene in hydrocolloids such as zein using glycerol, and Fernandez et al. (2009) encapsulated β-carotene in electrospun fibers of zein prolamine. These authors also reported a significant increase in the light stability of β-carotene when the latter was exposed to UV-vis irradiation. However, to our knowledge, solely the recent study of Wang et al. (2017) is focused in the nanoencapsulation of β-carotene in a zein-polysaccharide matrix. The authors elaborated nanoparticles of zein-carboxymethyl chitosan. The stability of β-carotene was higher in zein-carboxymethyl chitosan nanoparticles than in zein nanoparticles. Hence, nanoencapsulation of β-carotene in zein-polysaccharide matrices is not exploited; therefore, it can be considered as an area-of-study for future research.

7.2.2. Vitamin D

Vitamin D, the sunshine vitamin, is a prohormone that has two major physiologically forms, vitamin D2 (ergocalciferol) and vitamin D3 (cholecalciferol) (Luo et al., 2012). Vitamin D is important for calcium absorption, homeostasis regulation and for the prevention of CDD such as hypertension, type 2 diabetes, common cancer and cardiovascular disease (Autier et al., 2014; Picciano, 2010; Pittas et al., 2010). In the estudy of Luo et al. (2012) encapuslated vitamin D3 in zein-carboxymethyl chitosan matrices. The nanoparticles with coatings provided better controlled release of Vitamin D3 and simulated gastrointestinal tract. Hence, this nanoparticules are able to mantain the chemical stability and to controll release property. Until now, this last estudy is the only focused in the nanoencapsulation of Vitamin D in zein-polysaccharide matrices. There is other study using protein-polysaccharides matrices to nanoencapsulate vitamin D3 as the study of Teng et al. (2013), they used soy protein-carboxymethyl chitosan complex nanoparticles. In general, these complex nanoparticles are attractive candidate for the encapsulation and controlled release of hydrophobic nutraceuticals and bioactives, however, more studies need

to be realized in relation to encapsulate vitamin D in zein-polisaccharyde matrices, since some studies indicated a controversial results about its preventing CDD.

There is evidence that supplementation in elderly persons (mainly women) with 20 μg vitamin D per day appeared to slightly reduce all-cause mortality, and high doses of this vitamin can increase the survival of patients with breast, colorectal, and prostate cancer, as well as cutaneous melanoma. However, the results of prospective studies did not suggest a protective effect of high dose of vitamin D in cancer, except colorectal cancer (Autier et al., 2014). On the other hand, the association between the status of vitamin D and cardiometabolic outcomes (type 2 diabetes, hypertension, or CVD) is uncertain. According to Knekt et al. (2008), the association of high doses of vitamin D and a lower risk for incident-type 2 diabetes was significant. Otherwise, in the majority of women's groups studied, no association was found (Knekt et al., 2008; Pittas et al., 2006). Vitamin D affects some mechanisms in type 2 diabetes, including impaired pancreatic β-cell function and insulin resistance, either directly (by vitamin D receptor activation) or indirectly (by calcium homeostasis regulation) (Pittas et al., 2007; Pittas et al., 2010). In hypertension, low doses of vitamin D (< 37 to 51 nmol/L) can generate a higher risk for incident hypertension (Forman et al., 2007; Forman et al., 2008). Similarly, according to Kilkkinen et al. (2009), a low vitamin-D level may be associated with a higher risk of a fatal CVD event, particularly cerebrovascular death. Pilz et al. (2008) concluded that low levels of vitamin D are independently predictive for fatal strokes, suggesting that vitamin D supplementation comprises a promising approach in the prevention of strokes. To prevent or decrease some effects of CVD, vitamin D can inhibit anticoagulant activity (Ohsawa et al., 2000) and myocardial-cell hypertrophy (O'Connell et al., 1997; Simpson et al., 2007), and may modulate cytokine generation as well (Schleithoff et al., 2006) and macrophage activity (Sadeghi et al., 2006). In addition, according with some studies, vitamin D can be associated with OS markers (de Medeiros Cavalcante et al., 2015; Sharifi et al., 2014). However, in some studies, vitamin-D supplementation can reduce OS markers (de Medeiros Cavalcante et al., 2015; Sharifi et al., 2014), but in others, it was not possible to confirm this (Asemi et al., 2013; Eftekhari et al., 2014). In the study of Codoñer-Franch et al. (2012), the authors showed how vitamin-D status is linked to biomarkers of OS, inflammation, and endothelial activation in children with obesity. Similar studies confirm that vitamin D3-deficiency enhances OS (de Almeida et al., 2016; Luo et al., 2014). The results regarding the antioxidant properties are scarce and conflicting due to the different conditions under which the children are exposed. Hence, as mentioned previously, more studies must be performed Oliveira, Monteiro, et al. (2017), Oliveira, Simão, et al. (2017).

7.2.3. Vitamin E

Another vitamin that has been used in encapsulation is vitamin E. Tocopherols and tocotrienols are natural forms of the vitamin E family, which consists of eight distinct isomers denominated α-β-γ-δ-tocopherol and α-β-γ-δ-tocotrienol (Kanchi et al., 2017).

This vitamin plays a key role in protecting cells against oxidative damage; thus, it is an antioxidant molecule that can prevent CDD (Hamdy et al., 2015). Vitamin E possesses the ability to quench the highly reactive lipid-peroxide intermediate by donating hydrogen. This property avoids the extraction of hydrogen from polyunsaturated fatty acids, consequently preventing a lipid-peroxidation chain reaction (Das et al., 2004). Other mechanisms are employed by vitamin E, such as regulation of gene transcription, mRNA stability, protein translation, protein stability, and post-translational events (Jiang, 2017; Li, Wang, et al. (2016), Li, Dong, et al., 2016). Previous studies have demonstrated the potential of vitamin E for cancer chemoprevention. Xu et al. (2017) showed that early-stage supplementation with α-tocopherol significantly prevented esophageal carcinogenesis in an esophageal squamous-cell carcinoma rat model. In this study, it was indicated that α-tocopherol markedly suppressed cell proliferation, promoted G2-phase cell-cycle arrest, and increased apoptosis. Akt signaling was a potential target for α-Tocopherol, increased the expression of PPARγ and its downstream tumor suppressor PTEN. However, in the field of cancer chemotherapy, tocotrienols have shown to display better antitumor activity than α-tocopherol (Catalgol et al., 2011). There are several studies relating tocotrienols to different types of CDD, principally cancer, where they modulate the decrease of cytokines such as IL-1, IL-2, and IL-8 (Hafid et al., 2010; Shibata et al., 2008). In addition, this vitamin reduces transcription factors as c-myc and NF-kB (Ahn et al., 2007), STAT3, and STAT5 (Kashiwagi et al., 2009), HIF-1α (Bi et al., 2010), EBP-α (Uto-Kondo et al., 2009), among others. Some other studies indicated the influence of this vitamin on apoptotic genes, such as in the decrease of cyclin D1, cyclin D3, and cyclin E (Gysin et al., 2002), Ras (Yam et al., 2009), and XIAP, IAP-1, IAP-2, Bcl-2, Bcl-xl, and Survivin (Ahn et al., 2007). On the other hand, Lippman et al. (2009) reported that vitamin E did not prevent prostate cancer, and Njoroge et al. (2017) demonstrated that this vitamin promotes tumorigenesis in the early stages of prostate-cancer evolution in organoid models. Some other studies revealed this contradictory datum of vitamin E in the prevention of different types of cancer (Yang and Suh, 2013).

On the other hand, to reduce the risk of CVD, vitamin E is able to inhibit LDL oxidation, acting as a chain-breaking antioxidant and prevents lipid peroxidation of polyunsaturated fatty acids and the modification of proteins in LDL by ROS (Abdala-Valencia et al., 2012). Consequently, vitamin E reduces the production of chemotactic factors such as IL-8, MCP-1, and CAM-1 (Iuliano et al., 2000), as well as the decrease of the expression of E-Selectin and VCAM-1 and PKC induction (Abdala-Valencia et al., 2012). The development of some CVD, such as infarction and stroke, has been related to diabetes mellitus (Kuusisto and Laakso, 2013). However, there are studies that confirmed the non-effect of vitamin-E supplementation in preventing CVD complications by diabetes (Hodis et al., 2002; Lee et al., 2005). In conclusion, data regarding the beneficial role of vitamin E in protecting against cardiovascular complications in hyperglycemia are contradictory (Mocchegiani et al., 2014). Differences among studies can be due to the doses of vitamin E. Kappus and Diplock (1992) concluded that doses of 100–300 mg/day are well tolerated and do not cause adverse effects; doses of 200–400 mg/day have been recommended for use in food supplements under certain conditions; 400–2,000 mg/day do not exhibit adverse effects in the majority of cases, while > 2,150 mg/day exhibit adverse effects and intolerance has been increasingly noted. Hence, vitamin E continues to be an important molecule to be studied in encapsulated form in terms of conserving its bioactivity; however, its encapsulation in zein-polysaccharide matrices has been, to our knowledge, nearly not studied.

Luo, Song, et al. (2011), Luo, Zhang, et al. (2011) applied zein-polysaccharide electrostatic interaction by adding chitosan (coating) and taking vitamin-E (α-tocopherol) as the model-to-be-encapsulated. Stomach results showed that the release of vitamin E was due to a collapse of zein and chitosan solubility at a low pH. Therefore, the zein-chitosan system functions as a barrier to the degradation of vitamin E under stomach conditions.

There are a few other studies on the encapsulation of vitamin E in zein-polysaccharide matrices, as in zein-beta-cyclodextrin (do Carmo et al., 2017) or zein-chitosan (Wongsasulak et al., 2014); however, in these studies, particle size is on the order of micrometers. There are certain other studies and reviews in which zein was employed to nanoencapsulate vitamin E, such as the scalable and low-cost nanoencapsulation process for use in Nano medicine (Luo and Wang, 2014; Weissmueller et al., 2016). Hence, as mentioned previously, there is little information, to our knowledge, on the nanoencapsulation of vitamin E in zein-polysaccharide matrices for the prevention of CDD. This this can be an area-of-opportunity for study.

8. Conclusion

According with the studies analyzed in this review related to the nanoencapsulation of antioxidants in zein-polysaccharide matrices, all of these are in agreement with regard to that the combination of a protein with a polysaccharide as antioxidant nanoencapsulate offers better nanoparticles, maintains the chemical stability, are able to control the property of release, increase the bioavailability and bioactivity, as well as the capacity to inhibit free radicals. This latter property has been employed to prevent or to interfere at some stage of CDD, such as cancer, diabetes, CVD and obesity, among others, attributed to their properties as free radical scavengers, as antioxidants, and as metal chelators, as well as to their ability to inhibit or reduce different enzymes. However, there are controversial results with respect tothe bioactivity of the antioxidants: different factors affect their action, such as the dose, the genetics, the age, and the metabolism of the person. Additionally, cell receptors and their interaction with signal transduction pathways affect their bioactivity as well. For these reasons, more studies must be conducted in antioxidants with or without encapsulate, specifically targeting free radical production, the OS that limits their production and progression in the body, the concentrations of antioxidants in the circulation after digestion, and the possibility of interaction with other molecules to control CDD.

On the other hand, there are very few studies, to our knowledge, that are associated with the encapsulation of antioxidant compounds in zein-polysaccharide matrices; the majority of these have been studied separately. According to the literature, despite the fact that there is a great variety of phenolic compounds, curcumin, resveratrol, and epigallocatechin have been mostly utilized as a model of some zein-polysaccharide systems focusing on controlling CDD. Vitamins such as E and D, as well as β-carotene (precursor of vitamin A), have also used in the same manner, but scantily. The search for other polysaccharide matrices with zein could be interesting for improving antioxidant nanoparticles. Therefore, this can be an area-of-opportunity to carry out future studies on this topic.

References

Abdala-Valencia, H., Berdnikovs, S., & Cook-Mills, J. M. (2012). Vitamin E isoforms differentially regulate intercellular adhesion molecule-1 activation of PKCα in human microvascular endothelial cells. *PLoS ONE, 7*(7), e41054.

Abdollahi, E., Momtazi, A. A., Johnston, T. P., & Sahebkar, A. (2018). Therapeutic effects of curcumin in inflammatory and immune-mediated diseases: A nature-made jack-of-all-trades? *Journal of Cellular Physiology, 233*(2), 830–848.

Abidin, Z., Izzat, M. I., Raman, A., Aziz, A., Nor, M., & Iskandr, M. (2015). Mean drop size correlations and population balance models for liquid—liquid dispersion. *AICHE Journal, 61*(4), 1129–1145.

Agarwal, B., Campen, M. J., Channell, M. M., Wherry, S. J., Varamini, B., Davis, J. G., & Smoliga, J. M. (2013). Resveratrol for primary prevention of atherosclerosis: clinical trial evidence for improved gene expression in vascular endothelium. *International Journal of Cardiology, 166*(1), 246–248.

Ahmad, W., Ijaz, B., Shabbiri, K., Ahmed, F., & Rehman, S. (2017). Oxidative toxicity in diabetes and Alzheimer's disease: mechanisms behind ROS/RNS generation. *Journal of Biomedical Science, 24*(1), 76.

Ahn, K. S., Sethi, G., Krishnan, K., & Aggarwal, B. B. (2007). γ-Tocotrienol inhibits nuclear factor-κB signaling pathway through inhibition of receptor-interacting protein and TAK1 leading to suppression of antiapoptotic gene products and potentiation of apoptosis. *Journal of Biological Chemistry, 282*(1), 809–820.

Alayev, A., Berger, S. M., & Holz, M. K. (2015). Resveratrol as a novel treatment for diseases with mTOR pathway hyperactivation. *Annals of the New York Academy of Sciences, 1348*(1), 116–123.

Apostolidou, C., Adamopoulos, K., Lymperaki, E., Iliadis, S., Papapreponis, P., & Kourtidou-Papadeli, C. (2015). Cardiovascular risk and benefits from antioxidant dietary intervention with red wine in asymptomatic hypercholesterolemics. *Clinical Nutrition ESPEN, 10*(6), e224–e233.

Argos, P., Pedersen, K., Marks, M. D., & Larkins, B. A. (1982). A structural model for maize zein proteins. *Journal of Biological Chemistry, 257*(17), 9984–9990.

Asemi, Z., Hashemi, T., Karamali, M., Samimi, M., & Esmaillzadeh, A. (2013). Effects of vitamin D supplementation on glucose metabolism, lipid concentrations, inflammation, and oxidative stress in gestational diabetes: a double-blind randomized controlled clinical trial. *The American Journal of Clinical Nutrition, 98*(6), 1425–1432.

Autier, P., Boniol, M., Pizot, C., & Mullie, P. (2014). Vitamin D status and ill health: A systematic review. *The Lancet Diabetes & Endocrinology, 2*(1), 76–89.

Awad, E., Othman, E. M., & Stopper, H. (2017). Effects of resveratrol, lovastatin and the mTOR-Inhibitor RAD-001 on insulin-induced genomic damage In Vitro. *Molecules, 22*(12), 2207.

Bakrania, A. K., Nakka, S., Variya, B. C., Shah, P. V., & Patel, S. S. (2017). *Antitumor potential of herbomineral formulation against breast cancer: Involvement of inflammation and oxidative stress*.

Balaban, R. S., Nemoto, S., & Finkel, T. (2005). Mitochondria, oxidants, and aging. *Cell, 120*(4), 483–495.

Basu, A., & Haldar, S. (2009). Combinatorial effect of epigallocatechin-3-gallate and TRAIL on pancreatic cancer cell death. *International Journal of Oncology, 34*(1), 281–286.

Berman, A. Y., Motechin, R. A., Wiesenfeld, M. Y., & Holz, M. K. (2017). The therapeutic potential of resveratrol: A review of clinical trials. *NPJ Precision Oncology, 1*(1), 35.

Bhushani, J. A., Kurrey, N. K., & Anandharamakrishnan, C. (2017). Nanoencapsulation of green tea catechins by electrospraying technique and its effect on controlled release and in-vitro permeability. *Journal of Food Engineering, 199*, 82–92.

Bi, S., Liu, J. R., Li, Y., Wang, Q., Liu, H. K., Yan, Y. G., & Sun, W. G. (2010). γ-Tocotrienol modulates the paracrine secretion of VEGF induced by cobalt (II) chloride via ERK signaling pathway in gastric adenocarcinoma SGC-7901 cell line. *Toxicology, 274*(1–3), 27–33.

Biesinger, S., Michaels, H. A., Quadros, A. S., Qian, Y., Rabovsky, A. B., Badger, R. S., & Jalili, T. (2016). A combination of isolated phytochemicals and botanical extracts lowers diastolic blood pressure in a randomized controlled trial of hypertensive subjects. *European Journal of Clinical Nutrition, 70*(1), 10.

Bill, M. A., Bakan, C., Benson, D. M., Fuchs, J., Young, G., & Lesinski, G. B. (2009). Curcumin induces proapoptotic effects against human melanoma cells and modulates the cellular response to immunotherapeutic cytokines. *Molecular Cancer Therapeutics, 8*(9), 2726–2735.

Bladé, C., Arola, L., & Salvadó, M. J. (2010). Hypolipidemic effects of proanthocyanidins and their underlying biochemical and molecular mechanisms. *Molecular Nutrition & Food Research, 54*(1), 37–59.

Blomhoff, R. (2005). Dietary antioxidants and cardiovascular disease. *Current Opinion in Lipidology, 16*(1), 47–54.

Blomhoff, R., Carlsen, M. H., Andersen, L. F., & Jacobs, D. R. (2006). Health benefits of nuts: potential role of antioxidants. *British Journal of Nutrition, 96*(S2), S52–S60.

Bohnert, K. R., McMillan, J. D., & Kumar, A. (2018). Emerging roles of ER stress and unfolded protein response pathways in skeletal muscle health and disease. *Journal of Cellular Physiology, 233*, 67–78.

Borges, J., & Mano, J. F. (2014). Molecular interactions driving the layer-by-layer assembly of multilayers. *Chemical Reviews, 114*(18), 8883–8942.

Bothelho, G., Canas, S., & Lameiras, J. (2017). Development of phenolic compounds encapsulation techniques as a major challenge for food industry and for health and nutrition fields. *Nutrient Delivery, 5*, 535–586.

Brown, N. S., & Bicknell, R. (2001). Hypoxia and oxidative stress in breast cancer Oxidative stress-its effects on the growth, metastatic potential and response to therapy of breast cancer. *Breast Cancer Research, 3*(5), 323.

Bush, J. A., Cheung, K. J. J., & Li, G. (2001). Curcumin induces apoptosis in human melanoma cells through a Fas receptor/caspase-8 pathway independent of p53. *Experimental Cell Research, 271*(2), 305–314.

Butterfield, D. A., Di Domenico, F., & Barone, E. (2014). Elevated risk of type 2 diabetes for development of Alzheimer disease: A key role for oxidative stress in brain. *Biochimica et Biophysica Acta (BBA) - Molecular Basis of Disease, 1842*(9), 1693–1706.

Cai, Y., Kurita-Ochiai, T., Hashizume, T., & Yamamoto, M. (2013). Green tea epigallocatechin-3-gallate attenuates Porphyromonas gingivalis-induced atherosclerosis. *Pathogens and Disease, 67*(1), 76–83.

Caimari, A., Del Bas, J. M., Crescenti, A., & Arola, L. (2013). Low doses of grape seed procyanidins reduce adiposity and improve the plasma lipid profile in hamsters. *International Journal of Obesity, 37*(4), 576.

Castro, C. N., Barcala Tabarrozzi, A. E., Winnewisser, J., Gimeno, M. L., Antunica Noguerol, M., Liberman, A. C., & Perone, M. J. (2014). Curcumin ameliorates autoimmune diabetes. Evidence in accelerated murine models of type 1 diabetes. *Clinical and Experimental Immunology, 177*(1), 149–160.

Castro, A. M., Macedo-de la Concha, L. E., & Pantoja-Meléndez, C. A. (2017). Low-grade inflammation and its relation to obesity and chronic degenerative diseases. *Revista Médica del Hospital General de México, 80*(2), 101–105.

Catalgol, B., Batirel, S., & Ozer, N. K. (2011). Cellular protection and therapeutic potential of tocotrienols. *Current Pharmaceutical Design, 17*(21), 2215–2220.

Chang, C., Wang, T., Hu, Q., & Luo, Y. (2017). Caseinate-zein-polysaccharide complex nanoparticles as potential oral delivery vehicles for curcumin: Effect of polysaccharide type and chemical cross-linking. *Food Hydrocolloids, 72*, 254–262.

Chang, C., Wang, T., Hu, Q., Zhou, M., Xue, J., & Luo, Y. (2017). Pectin coating improves physicochemical properties of caseinate/zein nanoparticles as oral delivery vehicles for curcumin. *Food Hydrocolloids, 70*, 143–151.

Chen, X. W., Fu, S. Y., Hou, J. J., Guo, J., Wang, J. M., & Yang, X. Q. (2016). Zein based oil-in-glycerol emulgels enriched with β-carotene as margarine alternatives. *Food Chemistry, 211*, 836–844.

Chen, T. S., Liou, S. Y., Kuo, C. H., Pan, L. F., Yeh, Y. L., Liou, J., & Huang, C. Y. (2017). Green tea epigallocatechin gallate enhances cardiac function restoration through survival signaling expression in diabetes mellitus rats with autologous adipose tissue-derived stem cells. *Journal of Applied Physiology, 123*(5), 1081–1091.

Chen, S., Xu, C., Mao, L., Liu, F., Sun, C., Dai, L., & Gao, Y. (2018). Fabrication and characterization of binary composite nanoparticles between zein and shellac by antisolvent co-precipitation. *Food and Bioproducts Processing, 107*, 88–96.

Cheng, C. J., & Jones, O. G. (2017). Stabilizing zein nanoparticle dispersions with ι-carrageenan. *Food Hydrocolloids, 69*, 28–35.

Cheng, H. T., Hsieh, S. Y., Chen, T. H., Hung, P. F., & Pan, S. H. (2016). Sorafenib-fortified zein–chondroitin sulphate biopolymer nanoparticles as a novel therapeutic system in

gastric cancer treatment. *RSC Advances, 6*(62), 57266–57274.
Choudhuri, T., Pal, S., Agwarwal, M. L., Das, T., & Sa, G. (2002). Curcumin induces apoptosis in human breast cancer cells through p53-dependent Bax induction. *FEBS Letters, 512*(1-3), 334–340.
Chuacharoen, T., & Sabliov, C. M. (2016). The potential of zein nanoparticles to protect entrapped β-carotene in the presence of milk under simulated gastrointestinal (GI) conditions. *LWT- Food Science and Technology, 72*, 302–309.
Chuang, C. C., & McIntosh, M. K. (2011). Potential mechanisms by which polyphenol-rich grapes prevent obesity-mediated inflammation and metabolic diseases. *Annual Review of Nutrition, 31*, 155–176.
Cochemé, H. M., Quin, C., McQuaker, S. J., Cabreiro, F., Logan, A., Prime, T. A., & Porteous, C. M. (2011). Measurement of H2O2 within living Drosophila during aging using a ratiometric mass spectrometry probe targeted to the mitochondrial matrix. *Cell Metabolism, 13*(3), 340–350.
Codoñer-Franch, P., Tavárez-Alonso, S., Simó-Jordá, R., Laporta-Martín, P., Carratalá-Calvo, A., & Alonso-Iglesias, E. (2012). Vitamin D status is linked to biomarkers of oxidative stress, inflammation, and endothelial activation in obese children. *The Journal of Pediatrics, 161*(5), 848–854.
Cooper, D. A., Eldridge, A. L., & Peters, J. C. (1999). Dietary carotenoids and lung cancer: a review of recent research. *Nutrition Reviews, 57*(5), 133–145.
Coyago-Cruz, E., Corell, M., Moriana, A., Hernanz, D., Benítez-González, A. M., Stinco, C. M., & Meléndez-Martínez, A. J. (2018). Antioxidants (carotenoids and phenolics) profile of cherry tomatoes as influenced by deficit irrigation, ripening and cluster. *Food Chemistry, 240*, 870–884.
Dai, L., Sun, C., Wei, Y., Mao, L., & Gao, Y. (2018). Characterization of Pickering emulsion gels stabilized by zein/gum arabic complex colloidal nanoparticles. *Food Hydrocolloids, 74*, 239–248.
Das, N., Chowdhury, T. D., Chattopadhyay, A., & Datta, A. G. (2004). Attenuation of oxidative stress-induced changes in thalassemic erythrocytes by vitamin E. *Polish Journal of Pharmacology, 56*(1), 85–96.
Davidov-Pardo, G., Joye, I. J., Espinal-Ruiz, M., & McClements, D. J. (2015). Effect of maillard conjugates on the physical stability of zein nanoparticles prepared by liquid antisolvent coprecipitation. *Journal of Agricultural and Food Chemistry, 63*(38), 8510–8518.
Davidov-Pardo, G., Joye, I. J., & McClements, D. J. (2015). Encapsulation of resveratrol in biopolymer particles produced using liquid antisolvent precipitation. Part 1: Preparation and characterization. *Food Hydrocolloids, 45*, 309–316.
Davidov-Pardo, G., Pérez-Ciordia, S., Marín-Arroyo, M. R., & McClements, D. J. (2015). Improving resveratrol bioaccessibility using biopolymer nanoparticles and complexes: Impact of protein–carbohydrate maillard conjugation. *Journal of Agricultural and Food Chemistry, 63*(15), 3915–3923.
Davies, K. J. (2000). Oxidative stress, antioxidant defenses, and damage removal, repair, and replacement systems. *IUBMB Life, 50*(4–5), 279–289.
Daviglus, M. L., Orencia, A. J., Dyer, A. R., Liu, K., Morris, D. K., Persky, V., & Stamler, J. (1997). Dietary vitamin C, beta-carotene and 30-year risk of stroke: Results from the Western electric study. *Neuroepidemiology, 16*(2), 69–77.
de Almeida, J. P. S., Liberatti, L. S., Barros, F. E. N., Kallaur, A. P., Lozovoy, M. A. B., Scavuzzi, B. M., & Dichi, I. (2016). Profile of oxidative stress markers is dependent on vitamin D levels in patients with chronic hepatitis C. *Nutrition, 32*(3), 362–367.
de Medeiros Cavalcante, I. G., Silva, A. S., Costa, M. J. C., Persuhn, D. C., Issa, C. I., de Luna Freire, T. L., & Gonçalves, M. D. C. R. (2015). Effect of vitamin D3 supplementation and influence of BsmI polymorphism of the VDR gene of the inflammatory profile and oxidative stress in elderly women with vitamin D insufficiency: Vitamin D3 megadose reduces inflammatory markers. *Experimental Gerontology, 66*, 10–11.
do Carmo, C. C., Maja, C., Poejo, J., Lychko, I., Gamito, P., Nogueira, I., ... Duarte, C. M. M. (2017). Microencapsulation of alpha-tocopherol with zein and beta-cyclodextrin using spray drying for colour stability and shelf-life improvement of fruit beverages. *RSC Advances, 7*(51), 32065–32075.
Dobrynin, A. V., & Rubinstein, M. (2005). Theory of polyelectrolytes in solutions and at surfaces. *Progress in Polymer Science, 30*(11), 1049–1118.
Dong, F., Dong, X., Zhou, L., Xiao, H., Ho, P. Y., Wong, M. S., & Wang, Y. (2016). Doxorubicin-loaded biodegradable self-assembly zein nanoparticle and its anti-cancer effect: Preparation, in vitro evaluation, and cellular uptake. *Colloids and Surfaces B: Biointerfaces, 140*, 324–331.
Donsì, F., Voudouris, P., Veen, S. J., & Velikov, K. P. (2017). Zein-based colloidal particles for encapsulation and delivery of epigallocatechin gallate. *Food Hydrocolloids, 63*, 508–517.
Doo, T., & Maskarinec, G. (2014). Polyphenols and breast cancer prevention: A summary of the epidemiologic evidence. *Polyphenols in human health and disease* (pp. 1331–1340). .
Edeas, M., & Micol, V. (2007). Mitochondrial generation of reactive oxygen species (ROS) and its targeting by antioxidants: a future vision for obesity. *Agro Food Industry Hi-Tech, 18*(5), 16–20.
Eftekhari, M. H., Akbarzadeh, M., Dabbaghmanesh, M. H., & Hassanzadeh, J. (2014). The effect of calcitriol on lipid profile and oxidative stress in hyperlipidemic patients with type 2 diabetes mellitus. *ARYA Atherosclerosis, 10*(2), 82.
Eng, Q. Y., Thanikachalam, P. V., & Ramamurthy, S. (2017). Molecular understanding of Epigallocatechin gallate (EGCG) in cardiovascular and metabolic diseases. *Journal of Ethnopharmacology, 210*, 296–310.
Erejuwa, O. O. (2012). Oxidative stress in diabetes mellitus: Is there a role for hypoglycemic drugs and/or antioxidants. *Oxidative stress and diseases* (pp. 217–246). InTech.
Feng, X., Li, H., Rumbin, A. A., Wang, X., La Cava, A., Brechtelsbauer, K., & Tsao, B. P. (2007). ApoE−/− Fas−/− C57BL/6 mice: a novel murine model simultaneously exhibits lupus nephritis, atherosclerosis, and osteopenia. *Journal of Lipid Research, 48*(4), 794–805.
Feng, J., Lin, C., Wang, H., & Liu, S. (2016). Decoration of gemini alkyl O-glucosides based vesicles by electrostatic deposition of sodium carboxymethyl cellullose: Mechanism, structure and improved stability. *Food Hydrocolloids, 58*, 284–297.
Feng, M., Zhong, L. X., Zhan, Z. Y., Huang, Z. H., & Xiong, J. P. (2016). Resveratrol treatment inhibits proliferation of and induces apoptosis in human colon cancer cells. *Medical Science Monitor: International Medical Journal of Experimental and Clinical Research, 22*, 1101.
Fernandes, G. F. S., Silva, G. D. B., Pavan, A. R., Chiba, D. E., Chin, C. M., & Dos Santos, J. L. (2017). Epigenetic Regulatory Mechanisms Induced by Resveratrol. *Nutrients, 9*(11), 1201.
Fernandes, I., Pérez-Gregorio, R., Soares, S., Mateus, N., & de Freitas, V. (2017). Wine flavonoids in health and disease prevention. *Molecules, 22*(2), 292.
Fernandez, A., Torres-Giner, S., & Lagaron, J. M. (2009). Novel route to stabilization of bioactive antioxidants by encapsulation in electrospun fibers of zein prolamine. *Food Hydrocolloids, 23*(5), 1427–1432.
Fernández-Quintela, A., Milton-Laskibar, I., González, M., & Portillo, M. P. (2017). *Antiobesity effects of resveratrol: Which tissues are involved?* Annals of the New York Academy of Sciences.
Forman, J. P., Giovannucci, E., Holmes, M. D., Bischoff-Ferrari, H. A., Tworoger, S. S., Willett, W. C., & Curhan, G. C. (2007). Plasma 25-hydroxyvitamin D levels and risk of incident hypertension. *Hypertension, 49*(5), 1063–1069.
Forman, J. P., Curhan, G. C., & Taylor, E. N. (2008). Plasma 25-hydroxyvitamin D levels and risk of incident hypertension among young women. *Hypertension, 52*(5), 828–832.
Fujiki, H., Sueoka, E., Rawangkan, A., & Suganuma, M. (2017). Human cancer stem cells are a target for cancer prevention using (−)-epigallocatechin gallate. *Journal of Cancer Research and Clinical Oncology, 143*(12), 2401–2412.
Ganjali, S., Sahebkar, A., Mahdipour, E., Jamialahmadi, K., Torabi, S., Akhlaghi, S., & Ghayour-Mobarhan, M. (2014). Investigation of the effects of curcumin on serum cytokines in obese individuals: A randomized controlled trial. *The Scientific World Journal, 2014*.
George, V. C., Dellaire, G., & Rupasinghe, H. V. (2017). Plant flavonoids in cancer chemoprevention: Role in genome stability. *The Journal of Nutritional Biochemistry, 45*, 1–14.
Göçer, H., & Gülçin, İ. (2011). Caffeic acid phenethyl ester (CAPE): Correlation of structure and antioxidant properties. *International Journal of Food Sciences and Nutrition, 62*(8), 821–825.
Gonçalves, R., Mateus, N., & De Freitas, V. (2010). Study of the interaction of pancreatic lipase with procyanidins by optical and enzymatic methods. *Journal of Agricultural and Food Chemistry, 58*(22), 11901–11906.
Gopal, K., Nagarajan, P., Jedy, J., Raj, A. T., Gnanaselvi, S. K., Jahan, P., & Kumar, J. M. (2013). β-Carotene attenuates angiotensin II-induced aortic aneurysm by alleviating macrophage recruitment in APOE−/− mice. *PLoS ONE, 8*(6), e67098.
Guo, Y., Liu, Z., An, H., Li, M., & Hu, J. (2005). Nano-structure and properties of maize zein studied by atomic force microscopy. *Journal of Cereal Science, 41*(3), 277–281.
Guo, C. J., Yin, J. G., & Chen, D. Q. (2018). Co-encapsulation of curcumin and resveratrol into novel nutraceutical hyalurosomes nano-food delivery system based on oligo-hyaluronic acid-curcumin polymer. *Carbohydrate Polymers, 181*, 1033–1037.
Gysin, R., Azzi, A., & Visarius, T. (2002). γ-Tocopherol inhibits human cancer cell cycle progression and cell proliferation by down-regulation of cyclins. *The FASEB Journal, 16*(14), 1952–1954.
Hafid, S. R. A., Radhakrishnan, A. K., & Nesaretnam, K. (2010). Tocotrienols are good adjuvants for developing cancer vaccines. *BMC Cancer, 10*(1), 5.
Hagen, R. M., Chedea, V. S., Mintoff, C. P., Bowler, E., Morse, H. R., & Ladomery, M. R. (2013). Epigallocatechin-3-gallate promotes apoptosis and expression of the caspase 9a splice variant in PC3 prostate cancer cells. *International Journal of Oncology, 43*(1), 194–200.
Hak, A. E., Ma, J., Powell, C. B., Campos, H., Gaziano, J. M., Willett, W. C., & Stampfer, M. J. (2004). Prospective study of plasma carotenoids and tocopherols in relation to risk of ischemic stroke. *Stroke, 35*(7), 1584–1588.
Hamdy, M. M., Mosallam, D. S., Jamal, A. M., & Rabie, W. A. (2015). Selenium and Vitamin E as antioxidants in chronic hemolytic anemia: Are they deficient? A case-control study in a group of Egyptian children. *Journal of Advanced Research, 6*, 1071–1077.
Hansson, G. K. (2009). Atherosclerosis—an immune disease: The Anitschkov Lecture 2007. *Atherosclerosis, 202*(1), 2–10.
He, F., & Zuo, L. (2015). Redox roles of reactive oxygen species in cardiovascular diseases. *International Journal of Molecular Sciences, 16*(11), 27770–27780.
Hickenbottom, S. J., Follett, J. R., Lin, Y., Dueker, S. R., Burri, B. J., Neidlinger, T. R., & Clifford, A. J. (2002). Variability in conversion of β-carotene to vitamin A in men as measured by using a double-tracer study design. *The American Journal of Clinical Nutrition, 75*(5), 900–907.
Hirvonen, T., Virtamo, J., Korhonen, P., Albanes, D., & Pietinen, P. (2000). Intake of flavonoids, carotenoids, vitamins C and E, and risk of stroke in male smokers. *Stroke, 31*(10), 2301–2306.
Hodis, H. N., Mack, W. J., LaBree, L., Mahrer, P. R., Sevanian, A., Liu, C. R., & Azen, S. P. (2002). Alpha-tocopherol supplementation in healthy individuals reduces low-density lipoprotein oxidation but not atherosclerosis: The vitamin E Atherosclerosis prevention study (VEAPS). *Circulation, 106*(12), 1453–1459.
Hu, K., & McClements, D. J. (2015). Fabrication of biopolymer nanoparticles by antisolvent precipitation and electrostatic deposition: Zein-alginate core/shell nanoparticles. *Food Hydrocolloids, 44*, 101–108.
Hu, K., Huang, X., Gao, Y., Huang, X., Xiao, H., & McClements, D. J. (2015). Core–shell biopolymer nanoparticle delivery systems: Synthesis and characterization of curcumin fortified zein–pectin nanoparticles. *Food Chemistry, 182*, 275–281.
Huang, X., Huang, X., Gong, Y., Xiao, H., McClements, D. J., & Hu, K. (2016). Enhancement of curcumin water dispersibility and antioxidant activity using

core–shell protein–polysaccharide nanoparticles. *Food Research International, 87*, 1–9.
Huang, W. J., Zhang, X. I. A., & Chen, W. W. (2016). Role of oxidative stress in Alzheimer's disease. *Biomedical Reports, 4*(5), 519–522.
Huang, J., Panagiotou, O. A., Anic, G. M., Mondul, A. M., Liao, L. M., Derkach, A., ... Albanes, D. (2017). Metabolomic profiling of serum retinol in the alpha-tocopherol, beta-carotene cancer prevention (ATBC) study. *Scientific Reports, 7*(1), 10601.
Huang, X., Dai, Y., Cai, J., Zhong, N., Xiao, H., McClements, D. J., & Hu, K. (2017). Resveratrol encapsulation in core-shell biopolymer nanoparticles: Impact on antioxidant and anticancer activities. *Food Hydrocolloids, 64*, 157–165.
Hussain, S. (2017). Comparative efficacy of epigallocatechin-3-gallate against H2O2-induced ROS in cervical cancer biopsies and HeLa cell lines. *Contemporary Oncology, 21*(3), 209.
Imamura, H., Nagayama, D., Ishihara, N., Tanaka, S., Watanabe, R., Watanabe, Y., & Ohira, M. (2017). Resveratrol attenuates triglyceride accumulation associated with upregulation of Sirt1 and lipoprotein lipase in 3T3-L1 adipocytes. *Molecular Genetics and Metabolism Reports, 12*, 44–50.
Imlay, J. A., Chin, S. M., & Linn, S. (1988). Toxic DNA damage by hydrogen peroxide through the Fenton reaction in vivo and in vitro. *Science, 240*(4852), 640–642.
Irache, J. M., & González-Navarro, C. J. (2017). *Zein nanoparticles as vehicles for oral delivery purposes*.
Iuliano, L., Mauriello, A., Sbarigia, E., Spagnoli, L. G., & Violi, F. (2000). Radiolabeled native low-density lipoprotein injected into patients with carotid stenosis accumulates in macrophages of atherosclerotic plaque: Effect of vitamin E supplementation. *Circulation, 101*(11), 1249–1254.
Jahangir, Z., Ahmad, W., & Shabbiri, K. (2014). Alternate phosphorylation/O-GlcNAc modification on human insulin IRSs: A road towards impaired insulin signaling in Alzheimer and diabetes. *Advances in Bioinformatics, 2014*.
Javaid, M. S., Latief, N., Ijaz, B., & Ashfaq, U. A. (2017). Epigallocatechin gallate as an anti-obesity therapeutic compound: An in silico approach for structure-based drug designing. *Natural Product Research,* 1–5.
Jiang, Q. (2017). Natural Forms of vitamin e as effective agents for cancer prevention and therapy. *Advances in Nutrition, 8*(6), 850–867.
Jin, Y. R., Lee, M. S., Lee, J. H., Hsu, H. K., Lu, J. Y., Chao, S. S., & Ger, L. P. (2007). Intake of vitamin A-rich foods and lung cancer risk in Taiwan: With special reference to garland chrysanthemum and sweet potato leaf consumption. *Asia Pacific Journal of Clinical Nutrition, 16*(3), 477–488.
Johnston, K., Sharp, P., Clifford, M., & Morgan, L. (2005). Dietary polyphenols decrease glucose uptake by human intestinal Caco-2 cells. *FEBS Letters, 579*(7), 1653–1657.
Jose, R., Sajitha, G. R., & Augusti, K. T. (2014). A review on the role of nutraceuticals as simple as Se 2+ to complex organic molecules such as glycyrrhizin that prevent as well as cure diseases. *Indian Journal of Clinical Biochemistry, 29*(2), 119–132.
Joye, I. J., & McClements, D. J. (2013). Production of nanoparticles by anti-solvent precipitation for use in food systems. *Trends in Food Science & Technology, 34*(2), 109–123.
Joye, I. J., Davidov-Pardo, G., Ludescher, R. D., & McClements, D. J. (2015). Fluorescence quenching study of resveratrol binding to zein and gliadin: Towards a more rational approach to resveratrol encapsulation using water-insoluble proteins. *Food Chemistry, 185*, 261–267.
Julie, S., & Jurenka, M. T. (2009). Anti-inflammatory properties of curcumin, a major constituent. *Alternative Medicine Review, 14*(2), 141–153.
Kalita, J., Kumar, V., Ranjan, A., & Misra, U. K. (2015). Role of oxidative stress in the worsening of neurologic Wilson disease following chelating therapy. *Neuromolecular Medicine, 17*(4), 364–372.
Kanchi, M. M., Shanmugam, M. K., Rane, G., Sethi, G., & Kumar, A. P. (2017). Tocotrienols: the unsaturated sidekick shifting new paradigms in vitamin E therapeutics. *Drug Discovery Today, 22*(12), 1765–1781.
Kansanen, E., Kuosmanen, S. M., Leinonen, H., & Levonen, A. L. (2013). The Keap1-Nrf2 pathway: Mechanisms of activation and dysregulation in cancer. *Redox Biology, 1*(1), 45–49.
Kappus, H., & Diplock, A. T. (1992). Tolerance and safety of vitamin E: A toxicological position report. *Free Radical Biology and Medicine, 13*(1), 55–74.
Kardinaal, A. F., van't Veer, P., Kok, F. J., Ringstad, J., Gómez-Aracena, J., Mazaev, V. P., & Kark, J. D. (1993). Antioxidants in adipose tissue and risk of myocardial infarction: The EURAMIC study. *The Lancet, 342*(8884), 1379–1384.
Kashiwagi, K., Virgona, N., Harada, K., Kido, W., Yano, Y., Ando, A., & Yano, T. (2009). A redox-silent analogue of tocotrienol acts as a potential cytotoxic agent against human mesothelioma cells. *Life Sciences, 84*(19–20), 650–656.
Kelly, F. J., & Fussell, J. C. (2017). Role of oxidative stress in cardiovascular disease outcomes following exposure to ambient air pollution. *Free Radical Biology and Medicine, 110*, 345–367.
Kemper, J. K., Xiao, Z., Ponugoti, B., Miao, J., Fang, S., Kanamaluru, D., & Veenstra, T. D. (2009). FXR acetylation is normally dynamically regulated by p300 and SIRT1 but constitutively elevated in metabolic disease states. *Cell Metabolism, 10*(5), 392–404.
Khan, I., Qureshi, M. S., Akhtar, S., & Ali, I. (2016). Fertility improvement in cross-bred dairy cows through supplementation of vitamin E as antioxidant. *Pakistan Journal of Zoology, 48*(4).
Kilkkinen, A., Knekt, P., Aro, A., Rissanen, H., Marniemi, J., Heliövaara, M., & Reunanen, A. (2009). Vitamin D status and the risk of cardiovascular disease death. *American Journal of Epidemiology, 170*(8), 1032–1039.
Klipstein-Grobusch, K., Geleijnse, J. M., den Breeijen, J. H., Boeing, H., Hofman, A., Grobbee, D. E., & Witteman, J. C. (1999). Dietary antioxidants and risk of myocardial infarction in the elderly: The rotterdam study. *The American Journal of Clinical Nutrition, 69*(2), 261–266.
Knekt, P., Reunanen, A., Jävinen, R., Seppänen, R., Heliövaara, M., & Aromaa, A. (1994). Antioxidant vitamin intake and coronary mortality in a longitudinal population study. *American Journal of Epidemiology, 139*(12), 1180–1189.
Knekt, P., Laaksonen, M., Mattila, C., Härkänen, T., Marniemi, J., Heliövaara, M., & Reunanen, A. (2008). Serum vitamin D and subsequent occurrence of type 2 diabetes. *Epidemiology, 19*(5), 666–671.
Koosha, S., Alshawsh, M. A., Looi, C. Y., Seyedan, A., & Mohamed, Z. (2016). An association map on the effect of flavonoids on the signaling pathways in colorectal cancer. *International Journal of Medical Sciences, 13*(5), 374.
Kundu, N., Zhang, S., & Fulton, A. M. (1995). Sublethal oxidative stress inhibits tumor cell adhesion and enhances experimental metastasis of murine mammary carcinoma. *Clinical & Experimental Metastasis, 13*(1), 16–22.
Kuusisto, J., & Laakso, M. (2013). Update on type 2 diabetes as a cardiovascular disease risk equivalent. *Current Cardiology Reports, 15*(2), 331.
Laelorspoen, N., Wongsasulak, S., Yoovidhya, T., & Devahastin, S. (2014). Microencapsulation of Lactobacillus acidophilus in zein–alginate core–shell microcapsules via electrospraying. *Journal of Functional Foods, 7*, 342–349.
Le, X. T., Rioux, L. E., & Turgeon, S. L. (2017). Formation and functional properties of protein–polysaccharide electrostatic hydrogels in comparison to protein or polysaccharide hydrogels. *Advances in Colloid and Interface Science, 239*, 127–135.
Lee, I. M., Cook, N. R., Gaziano, J. M., Gordon, D., Ridker, P. M., Manson, J. E., ... Buring, J. E. (2005). Vitamin E in the primary prevention of cardiovasculardisease and cancer: the Women's Health Study: A randomized controlled trial. *JAMA, 294*, 56–65.
Lee, H., Lee, Y. J., Choi, H., Ko, E. H., & Kim, J. W. (2009). Reactive oxygen species facilitate adipocyte differentiation by accelerating mitotic clonal expansion. *Journal of Biological Chemistry, 284*(16), 10601–10609.
Lee, S., Kim, Y. C., & Park, J. H. (2016). Zein-alginate based oral drug delivery systems: Protection and release of therapeutic proteins. *International Journal of Pharmaceutics, 515*(1), 300–306.
Lee, M. S., Shin, Y., Jung, S., & Kim, Y. (2017). Effects of epigallocatechin-3-gallate on thermogenesis and mitochondrial biogenesis in brown adipose tissues of diet-induced obese mice. *Food & Nutrition Research, 61*(1), 1325307.
Lelli, D., Sahebkar, A., Johnston, T. P., & Pedone, C. (2017). Curcumin use in pulmonary diseases: State of the art and future perspectives. *Pharmacological Research, 115*, 133–148.
Li, Y., Lim, L. T., & Kakuda, Y. (2009). Electrospun zein fibers as carriers to stabilize (−)-epigallocatechin gallate. *Journal of Food Science, 74*(3).
Li, K. K., Yin, S. W., Yang, X. Q., Tang, C. H., & Wei, Z. H. (2012). Fabrication and characterization of novel antimicrobial films derived from thymol-loaded zein–sodium caseinate (SC) nanoparticles. *Journal of Agricultural and Food Chemistry, 60*(46), 11592–11600.
Li, Y. G., Zhu, W., Tao, J. P., Xin, P., Liu, M. Y., Li, J. B., & Wei, M. (2013). Resveratrol protects cardiomyocytes from oxidative stress through SIRT1 and mitochondrial biogenesis signaling pathways. *Biochemical and Biophysical Research Communications, 438*(2), 270–276.
Li, Z., Jiang, H., Xu, C., & Gu, L. (2015). A review: Using nanoparticles to enhance absorption and bioavailability of phenolic phytochemicals. *Food Hydrocolloids, 43*, 153–164.
Li, S., Wang, X., Li, W., Yuan, G., Pan, Y., & Chen, H. (2016). *Preparation and characterization of a novel conformed bipolymer paclitaxel-nanoparticle using tea*.
Li, X., Dong, Z., Zhang, F., Dong, J., & Zhang, Y. (2016). Vitamin E slows down the progression of osteoarthritis (Review). *Experimental and Therapeutic Medicine, 12*, 18–22.
Li, M., Chong, Y., Fu, P. P., Xia, Q., Croley, T. R., Lo, Y. M., & Yin, J. J. (2017). Effects of P25 TiO2 nanoparticles on the free radical-scavenging ability of antioxidants upon their exposure to simulated sunlight. *Journal of Agricultural and Food Chemistry, 65*(45), 9893–9901.
Liang, H., Huang, Q., Zhou, B., He, L., Lin, L., An, Y., & Li, B. (2015). Self-assembled zein–sodium carboxymethyl cellulose nanoparticles as an effective drug carrier and transporter. *Journal of Materials Chemistry B, 3*(16), 3242–3253.
Liang, H., Zhou, B., He, L., An, Y., Lin, L., Li, Y., & Li, B. (2015). Fabrication of zein/quaternized chitosan nanoparticles for the encapsulation and protection of curcumin. *RSC Advances, 5*(18), 13891–13900.
Liang, J., Yan, H., Wang, X., Zhou, Y., Gao, X., Puligundla, P., & Wan, X. (2017). Encapsulation of epigallocatechin gallate in zein/chitosan nanoparticles for controlled applications in food systems. *Food Chemistry, 231*, 19–24.
Lin, Y., Wang, Y. H., Yang, X. Q., Guo, J., & Wang, J. M. (2016). Corn protein hydrolysate as a novel nano-vehicle: Enhanced physicochemical stability and in vitro bioaccessibility of vitamin D3. *LWT- Food Science and Technology, 72*, 510–517.
Liou, G. Y., & Storz, P. (2010). Reactive oxygen species in cancer. *Free Radical Research, 44*(5), 479–496.
Lippman, S. M., Klein, E. A., Goodman, P. J., Lucia, M. S., Thompson, I. M., Ford, L. G., & Parsons, J. K. (2009). Effect of selenium and vitamin E on risk of prostate cancer and other cancers: The Selenium and Vitamin E Cancer Prevention Trial (SELECT). *JAMA, 301*(1), 39–51.
Liu, G. S., Chan, E. C., Higuchi, M., Dusting, G. J., & Jiang, F. (2012). Redox mechanisms in regulation of adipocyte differentiation: Beyond a general stress response. *Cell, 1*(4), 976–993.
Liu, F., Ma, C., McClements, D. J., & Gao, Y. (2017). A comparative study of covalent and non-covalent interactions between zein and polyphenols in ethanol-water solution. *Food Hydrocolloids, 63*, 625–634.
Liu, Z. P., Zhang, Y. Y., Yu, D. G., Wu, D., & Li, H. L. (2018). Fabrication of sustained-release zein nanoparticles via modified coaxial electrospraying. *Chemical Engineering Journal, 334*, 807–816.
Lobry, E., Lasuye, T., Gourdon, C., & Xuereb, C. (2015). Liquid–liquid dispersion in a continuous oscillatory baffled reactor–application to suspension polymerization. *Chemical Engineering Journal, 259*, 505–518.
López-Rubio, A., & Lagaron, J. M. (2011). Improved incorporation and stabilisation of β-carotene in hydrocolloids using glycerol. *Food Chemistry, 125*(3), 997–1004.

Lü, J. M., Lin, P. H., Yao, Q., & Chen, C. (2010). Chemical and molecular mechanisms of antioxidants: Experimental approaches and model systems. *Journal of Cellular and Molecular Medicine, 14*(4), 840–860.
Lucio, D., Martínez-Ohárriz, M. C., Jaras, G., Aranaz, P., González-Navarro, C. J., Radulescu, A., & Irache, J. M. (2017). Optimization and evaluation of zein nanoparticles to improve the oral delivery of glibenclamide. In vivo study using C. elegans. *European Journal of Pharmaceutics and Biopharmaceutics, 121*, 104–112.
Luckanagul, J. A., Pitakchatwong, C., Bhuket, P. R. N., Muangnoi, C., Rojsitthisak, P., Chirachanchai, S., & Rojsitthisak, P. (2018). Chitosan-based polymer hybrids for thermo-responsive nanogel delivery of curcumin. *Carbohydrate Polymers, 181*, 1119–1127.
Luo, Y., & Wang, Q. (2014). Zein-based micro-and nano-particles for drug and nutrient delivery: A review. *Journal of Applied Polymer Science, 131*(16).
Luo, F., Song, X., Zhang, Y., & Chu, Y. (2011). Low-dose curcumin leads to the inhibition of tumor growth via enhancing CTL-mediated antitumor immunity. *International Immunopharmacology, 11*(9), 1234–1240.
Luo, Y., Zhang, B., Whent, M., Yu, L. L., & Wang, Q. (2011). Preparation and characterization of zein/chitosan complex for encapsulation of α-tocopherol, and its in vitro controlled release study. *Colloids and Surfaces B: Biointerfaces, 85*(2), 145–152.
Luo, Y., Teng, Z., & Wang, Q. (2012). Development of zein nanoparticles coated with carboxymethyl chitosan for encapsulation and controlled release of vitamin D3. *Journal of Agricultural and Food Chemistry, 60*(3), 836–843.
Luo, Y., Wang, T. T., Teng, Z., Chen, P., Sun, J., & Wang, Q. (2013). Encapsulation of indole-3-carbinol and 3, 3′-diindolylmethane in zein/carboxymethyl chitosan nanoparticles with controlled release property and improved stability. *Food Chemistry, 139*(1), 224–230.
Luo, G., Yang, X., Cheng, Y., Wang, X., Wang, X., Xie, T., & Zhong, N. (2014). 25-Hydroxyvitamin D3-deficiency enhances oxidative stress and corticosteroid resistance in severe asthma exacerbation. *PLoS ONE, 9*(11), e111599.
Luo, J. Z., Chu, G. W., Luo, Y., Zou, H. K., Li, G. J., & Chen, J. F. (2017). Experimental investigations of liquid-liquid dispersion in a novel helical tube reactor. *Chemical Engineering and Processing: Process Intensification, 117*, 162–170.
Magrone, T., & Jirillo, E. (2010). Polyphenols from red wine are potent modulators of innate and adaptive immune responsiveness. *Proceedings of the Nutrition Society, 69*(3), 279–285.
Magyar, K., Halmosi, R., Palfi, A., Feher, G., Czopf, L., Fulop, A., & Szabados, E. (2012). Cardioprotection by resveratrol: A human clinical trial in patients with stable coronary artery disease. *Clinical Hemorheology and Microcirculation, 50*(3), 179–187.
Martins, S., Farinha, J. P. S., Baleizão, C., & Berberan-Santos, M. N. (2014). Controlled release of singlet oxygen using diphenylanthracene functionalized polymer nanoparticles. *Chemical Communications, 50*(25), 3317–3320.
Marx, W., Kelly, J., Marshall, S., Nakos, S., Campbell, K., & Itsiopoulos, C. (2017). The Effect of polyphenol-rich interventions on cardiovascular risk factors in haemodialysis: A systematic review and meta-analysis. *Nutrients, 9*(12), 1345.
Matak, S. A., Hashemabadi, D., & Kaviani, B. (2017). Changes in postharvest physiobiochemical characteristics and antioxidant enzymes activity of cut alsteroemeria aurantiaca flower as affected by cycloheximide, coconut water and 6-benzyladenine. *Bioscience Journal, 33*(2).
Maynard, S., Schurman, S. H., Harboe, C., de Souza-Pinto, N. C., & Bohr, V. A. (2009). Base excision repair of oxidative DNA damage and association with cancer and aging. *Carcinogenesis, 30*(1), 2–10.
McEligot, A. J., Yang, S., & Meyskens, F. L., Jr. (2005). Redox regulation by intrinsic species and extrinsic nutrients in normal and cancer cells. *Annual Review of Nutrition, 25*, 261–295.
McMurray, F., Patten, D. A., & Harper, M. E. (2016). Reactive oxygen species and oxidative stress in obesity—recent findings and empirical approaches. *Obesity, 24*(11), 2301–2310.
Mejia, C. D., Mauer, L. J., & Hamaker, B. R. (2007). Similarities and differences in secondary structure of viscoelastic polymers of maize α-zein and wheat gluten proteins. *Journal of Cereal Science, 45*(3), 353–359.
Mocchegiani, E., Costarelli, L., Giacconi, R., Malavolta, M., Basso, A., Piacenza, F., & Monti, D. (2014). Vitamin E–gene interactions in aging and inflammatory age-related diseases: Implications for treatment. A systematic review. *Ageing Research Reviews, 14*, 81–101.
Mohammadi, A., Sahebkar, A., Iranshahi, M., Amini, M., Khojasteh, R., Ghayour-Mobarhan, M., & Ferns, G. A. (2013). Effects of supplementation with curcuminoids on dyslipidemia in obese patients: A randomized crossover trial. *Phytotherapy Research, 27*(3), 374–379.
Mohanty, S. K., Swamy, M. K., Middha, S. K., Prakash, L., Subbanarashiman, B., & Maniyam, A. (2015). Analgesic, anti-inflammatory, anti-lipoxygenase activity and characterization of three bioactive compounds in the most active fraction of Leptadenia reticulata (Retz.) Wight & Arn.–A valuable medicinal plant. *Iranian Journal Of Pharmaceutical Research: IJPR, 14*(3), 933.
Momtazi, A., & Sahebkar, A. (2016). Difluorinated curcumin: A promising curcumin analogue with improved anti-tumor activity and pharmacokinetic profile. *Current Pharmaceutical Design, 22*(28), 4386–4439.
Moussa, S. A. (2008). Oxidative stress in diabetes mellitus. *Romanian Journal of Biophysics, 18*(3), 225–236.
Muhammed, I., Sankar, S., & Govindaraj, S. (2017). Ameliorative effect of Epigallocatechingallate on cardiac hypertrophy and fibrosis in Aged rat. *Journal of Cardiovascular Pharmacology, 71*(2), 65–75.
Naponelli, V., Ramazzina, I., Lenzi, C., Bettuzzi, S., & Rizzi, F. (2017). Green tea Catechins for prostate cancer prevention: present achievements and future challenges. *Antioxidants, 6*(2), 26.
Narra, M. R., Rajender, K., Reddy, R. R., Rao, J. V., & Begum, G. (2015). The role of vitamin C as antioxidant in protection of biochemical and haematological stress induced by chlorpyrifos in freshwater fish Clarias batrachus. *Chemosphere, 132*, 172–178.
Ng, H. L., Premilovac, D., Rattigan, S., Richards, S. M., Muniyappa, R., Quon, M. J., & Keske, M. A. (2017). Acute vascular and metabolic actions of the green tea polyphenol epigallocatechin 3-gallate in rat skeletal muscle. *The Journal of Nutritional Biochemistry, 40*, 23–31.
Nirmala, C., Bisht, M. S., & Laishram, M. (2014). Bioactive compounds in bamboo shoots: Health benefits and prospects for developing functional foods. *International Journal of Food Science and Technology, 49*(6), 1425–1431.
Njoroge, R. N., Unno, K., Zhao, J. C., Naseem, A. F., Anker, J. F., McGee, W. A., & Abdulkadir, S. A. (2017). Organoids model distinct Vitamin E effects at different stages of prostate cancer evolution. *Scientific Reports, 7*(1), 16285.
Nosso, G., Lupoli, R., Saldalamacchia, G., Griffo, E., Cotugno, M., Costabile, G., & Capaldo, B. (2017). Diabetes remission after bariatric surgery is characterized by high glycemic variability and high oxidative stress. *Nutrition, Metabolism, and Cardiovascular Diseases, 27*(11), 949–955.
Novotny, J. A., Harrison, D. J., Pawlosky, R., Flanagan, V. P., Harrison, E. H., & Kurilich, A. C. (2010). β-Carotene conversion to vitamin A decreases as the dietary dose increases in humans. *The Journal of Nutrition, 140*(5), 915–918.
O'Connell, T. D., Berry, J. E., Jarvis, A. K., Somerman, M. J., & Simpson, R. U. (1997). 1, 25-Dihydroxyvitamin D3 regulation of cardiac myocyte proliferation and hypertrophy. *American Journal of Physiology - Heart and Circulatory Physiology, 272*(4), H1751–H1758.
Oguntibeju, O. O., Esterhuyse, A. J., & Truter, E. J. (2010). Possible role of red palm oil supplementation in reducing oxidative stress in HIV/AIDS and TB patients: A Review. *Journal of Medicinal Plant Research, 4*(3), 188–196.
Ohsawa, M., Koyama, T., Yamamoto, K., Hirosawa, S., Kamei, S., & Kamiyama, R. (2000). 1α, 25-dihydroxyvitamin D3 and its potent synthetic analogs downregulate tissue factor and upregulate thrombomodulin expression in monocytic cells, counteracting the effects of tumor necrosis factor and oxidized LDL. *Circulation, 102*(23), 2867–2872.
Oliveira, A. L. D. B., Monteiro, V. V. S., Navegantes-Lima, K. C., Reis, J. F., Gomes, R. D. S., Rodrigues, D. V. S., & Monteiro, M. C. (2017). Resveratrol role in autoimmune disease—a mini-review. *Nutrients, 9*(12), 1306.
Oliveira, S. R., Simão, A. N., Alfieri, D. F., Flauzino, T., Kallaur, A. P., Mezzaroba, L., & Kaimen-Maciel, D. R. (2017). Vitamin D deficiency is associated with disability and disease progression in multiple sclerosis patients independently of oxidative and nitrosative stress. *Journal of the Neurological Sciences, 381*, 213–219.
Ono, K., Condron, M. M., Ho, L., Wang, J., Zhao, W., Pasinetti, G. M., & Teplow, D. B. (2008). Effects of grape seed-derived polyphenols on amyloid β-protein self-assembly and cytotoxicity. *Journal of Biological Chemistry, 283*(47), 32176–32187.
Osganian, S. K., Stampfer, M. J., Rimm, E., Spiegelman, D., Manson, J. E., & Willett, W. C. (2003). Dietary carotenoids and risk of coronary artery disease in women. *The American Journal of Clinical Nutrition, 77*(6), 1390–1399.
Othman, A. I., Elkomy, M. M., El-Missiry, M. A., & Dardor, M. (2017). Epigallocatechin-3-gallate prevents cardiac apoptosis by modulating the intrinsic apoptotic pathway in isoproterenol-induced myocardial infarction. *European Journal of Pharmacology, 794*, 27–36.
Padua, G. W., & Wang, Q. (Eds.). (2012). *Nanotechnology research methods for food and bioproducts*. John Wiley & Sons.
Pan, M. H., Wu, J. C., Ho, C. T., & Lai, C. S. (2018). Antiobesity molecular mechanisms of action: Resveratrol and pterostilbene. *Biofactors, 44*(1), 50–60.
Panahi, Y., Khalili, N., Sahebi, E., Namazi, S., Karimian, M. S., Majeed, M., & Sahebkar, A. (2017). Antioxidant effects of curcuminoids in patients with type 2 diabetes mellitus: a randomized controlled trial. *InflammoPharmacology, 25*(1), 25–31.
Panieri, E., & Santoro, M. M. (2016). ROS homeostasis and metabolism: a dangerous liason in cancer cells. *Cell Death & Disease, 7*(6), e2253.
Park, Y., Choi, J., Lim, J. W., & Kim, H. (2015). β-carotene-induced apoptosis is mediated with loss of Ku proteins in gastric cancer AGS cells. *Genes & Nutrition, 10*(4), 17.
Patel, A. R., & Velikov, K. P. (2014). Zein as a source of functional colloidal nano-and microstructures. *Current Opinion in Colloid & Interface Science, 19*(5), 450–458.
Pelicano, H., Lu, W., Zhou, Y., Zhang, W., Chen, Z., Hu, Y., & Huang, P. (2009). Mitochondrial dysfunction and reactive oxygen species imbalance promote breast cancer cell motility through a CXCL14-mediated mechanism. *Cancer Research, 69*(6), 2375–2383.
Penalva, R., Esparza, I., Larraneta, E., González-Navarro, C. J., Gamazo, C., & Irache, J. M. (2015). Zein-based nanoparticles improve the oral bioavailability of resveratrol and its anti-inflammatory effects in a mouse model of endotoxic shock. *Journal of Agricultural and Food Chemistry, 63*(23), 5603–5611.
Picciano, M. F. (2010). Vitamin D status and health. *Critical Reviews in Food Science and Nutrition, 50*(S1), 24–25.
Pilz, S., Dobnig, H., Fischer, J. E., Wellnitz, B., Seelhorst, U., Boehm, B. O., & März, W. (2008). Low vitamin D levels predict stroke in patients referred to coronary angiography. *Stroke, 39*(9), 2611–2613.
Pittas, A. G., Dawson-Hughes, B., Li, T., Van Dam, R. M., Willett, W. C., Manson, J. E., & Hu, F. B. (2006). Vitamin D and calcium intake in relation to type 2 diabetes in women. *Diabetes Care, 29*(3), 650–656.
Pittas, A. G., Lau, J., Hu, F. B., & Dawson-Hughes, B. (2007). The role of vitamin D and calcium in type 2 diabetes. A systematic review and meta-analysis. *The Journal of Clinical Endocrinology & Metabolism, 92*(6), 2017–2029.
Pittas, A. G., Chung, M., Trikalinos, T., Mitri, J., Brendel, M., Patel, K., & Balk, E. M. (2010). Systematic review: Vitamin D and cardiometabolic outcomes. *Annals of Internal Medicine, 152*(5), 307–314.
Pollack, R. M., Barzilai, N., Anghel, V., Kulkarni, A. S., Golden, A., O'broin, P., & Kim, S. (2017). Resveratrol improves vascular function and mitochondrial number but not glucose metabolism in older adults. *The Journals of Gerontology Series A: Biological*

Sciences and Medical Sciences, 72(12), 1703–1709.
Prior, R. L., Wu, X., & Schaich, K. (2005). Standardized methods for the determination of antioxidant capacity and phenolics in foods and dietary supplements. *Journal of Agricultural and Food Chemistry, 53*(10), 4290–4302.
Quesada, H., Del Bas, J. M., Pajuelo, D., Diaz, S., Fernandez-Larrea, J., Pinent, M., & Bladé, C. (2009). Grape seed proanthocyanidins correct dyslipidemia associated with a high-fat diet in rats and repress genes controlling lipogenesis and VLDL assembling in liver. *International Journal of Obesity, 33*(9), 1007.
Rady, I., Mohamed, H., Rady, M., Siddiqui, I. A., & Mukhtar, H. (2017). *Cancer preventive and therapeutic effects of EGCG, the major polyphenol in green tea.* Egyptian Journal of Basic and Applied Sciences.
Rahimi, R., & Falahi, Z. (2017). Effect of green tea extract on exercise-induced oxidative stress in obese men: A randomized, double-blind, placebo-controlled, crossover study. *Asian Journal of Sports Medicine, 8*(2).
Ramasamy, T., Haidar, Z. S., Tran, T. H., Choi, J. Y., Jeong, J. H., Shin, B. S., & Kim, J. O. (2014). Layer-by-layer assembly of liposomal nanoparticles with PEGylated polyelectrolytes enhances systemic delivery of multiple anticancer drugs. *Acta Biomaterialia, 10*(12), 5116–5127.
Rasheed, N. O. A., Ahmed, L. A., Abdallah, D. M., & El-Sayeh, B. M. (2017). Nephro-toxic effects of intraperitoneally injected EGCG in diabetic mice: involvement of oxidative stress, inflammation and apoptosis. *Scientific Reports, 7*, 40617.
Reddy, K. B., & Glaros, S. (2007). Inhibition of the MAP kinase activity suppresses estrogen-induced breast tumor growth both in vitro and in vivo. *International Journal of Oncology, 30*(4), 971–975.
Relat, J., Blancafort, A., Oliveras, G., Cufí, S., Haro, D., Marrero, P. F., & Puig, T. (2012). Different fatty acid metabolism effects of (−)-epigallocatechin-3-gallate and C75 in adenocarcinoma lung cancer. *BMC Cancer, 12*(1), 280.
Righetti, P. G., Gianazza, E., Viotti, A., & Soave, C. (1977). Heterogeneity of storage proteins in maize. *Planta, 136*(2), 115–123.
Rossi, E. L., Khatib, S. A., Doerstling, S. S., Bowers, L. W., Pruski, M., Ford, N. A., & DiGiovanni, J. (2018). Resveratrol inhibits obesity-associated adipose tissue dysfunction and tumor growth in a mouse model of postmenopausal claudin-low breast cancer. *Molecular Carcinogenesis, 57*(3), 393–407.
Rupasinghe, H. V., Sekhon-Loodu, S., Mantso, T., & Panayiotidis, M. I. (2016). Phytochemicals in regulating fatty acid β-oxidation: Potential underlying mechanisms and their involvement in obesity and weight loss. *Pharmacology & Therapeutics, 165*, 153–163.
Saad, B., Zaid, H., Shanak, S., & Kadan, S. (2017). *Anti-obesity medicinal plants. in anti-diabetes and anti-obesity medicinal plants and phytochemicals.* Cham: Springer59–93.
Sadeghi, K., Wessner, B., Laggner, U., Ploder, M., Tamandl, D., Friedl, J., & Boltz-Nitulescu, G. (2006). Vitamin D3 down-regulates monocyte TLR expression and triggers hyporesponsiveness to pathogen-associated molecular patterns. *European Journal of Immunology, 36*(2), 361–370.
Sahebkar, A. (2015). Dual effect of curcumin in preventing atherosclerosis: The potential role of pro-oxidant–antioxidant mechanisms. *Natural Product Research, 29*(6), 491–492.
Salles, G. N., dos Santos Pereira, F. A., Pacheco-Soares, C., Marciano, F. R., Hölscher, C., Webster, T. J., & Lobo, A. O. (2017). A novel bioresorbable device as a controlled release system for protecting cells from oxidative stress from Alzheimer's Disease. *Molecular Neurobiology, 54*(9), 6827–6838.
Salsali, A., & Nathan, M. (2006). A review of types 1 and 2 diabetes mellitus and their treatment with insulin. *American Journal of Therapeutics, 13*(4), 349–361.
Sanna, V., Singh, C. K., Jashari, R., Adhami, V. M., Chamcheu, J. C., Rady, I., & Siddiqui, I. A. (2017). Targeted nanoparticles encapsulating (−)-epigallocatechin-3-gallate for prostate cancer prevention and therapy. *Scientific Reports, 7*, 41573.
Sarkar, P. K., Halder, A., Adhikari, A., Polley, N., Darbar, S., Lemmens, P., & Pal, S. K. (2018). DNA-based fiber optic sensor for direct in-vivo measurement of oxidative stress. *Sensors and Actuators B: Chemical, 255*, 2194–2202.
Scalbert, A., & Williamson, G. (2000). Dietary intake and bioavailability of polyphenols. *The Journal of Nutrition, 130*(8), 2073–2085.
Schieber, M., & Chandel, N. S. (2014). ROS function in redox signaling and oxidative stress. *Current Biology, 24*(10), R453–R462.
Schleithoff, S. S., Zittermann, A., Tenderich, G., Berthold, H. K., Stehle, P., & Koerfer, R. (2006). Vitamin D supplementation improves cytokine profiles in patients with congestive heart failure: A double-blind, randomized, placebo-controlled trial. *The American Journal of Clinical Nutrition, 83*(4), 754–759.
Semenova, M. (2017). Protein–polysaccharide associative interactions in the design of tailor-made colloidal particles. *Current Opinion in Colloid & Interface Science, 28*, 15–21.
Sharifi, N., Amani, R., Hajiani, E., & Cheraghian, B. (2014). Does vitamin D improve liver enzymes, oxidative stress, and inflammatory biomarkers in adults with non-alcoholic fatty liver disease? A randomized clinical trial. *Endocrine, 47*(1), 70–80.
Shashirekha, M. N., Mallikarjuna, S. E., & Rajarathnam, S. (2015). Status of bioactive compounds in foods, with focus on fruits and vegetables. *Critical Reviews in Food Science and Nutrition, 55*(10), 1324–1339.
Shi, M., Shi, Y. L., Li, X. M., Yang, R., Cai, Z. Y., Li, Q. S., & Zheng, X. Q. (2018). Food-grade encapsulation systems for (−)-epigallocatechin gallate. *Molecules, 23*(2), 445.
Shibata, A., Nakagawa, K., Sookwong, P., Tsuduki, T., Tomita, S., Shirakawa, H., & Miyazawa, T. (2008). Tocotrienol inhibits secretion of angiogenic factors from human colorectal adenocarcinoma cells by suppressing hypoxia-inducible factor-1α. *The Journal of Nutrition, 138*(11), 2136–2142.
Shree, G. S., Prasad, K. Y., Arpitha, H. S., Deepika, U. R., Kumar, K. N., Mondal, P., & Ganesan, P. (2017). β-carotene at physiologically attainable concentration induces apoptosis and down-regulates cell survival and antioxidant markers in human breast cancer (MCF-7) cells. *Molecular and Cellular Biochemistry, 436*(1–2), 1–12.
Sies, H. (1985). Oxidative stress: Introductory remarks. In H. Sies (Ed.). *Oxidative Stress* (pp. 1–8). London: Academic Press.
Simpson, R. U., Hershey, S. H., & Nibbelink, K. A. (2007). Characterization of heart size and blood pressure in the vitamin D receptor knockout mouse. *The Journal of Steroid Biochemistry and Molecular Biology, 103*(3–5), 521–524.
Smid, S. D., Maag, J. L., & Musgrave, I. F. (2012). Dietary polyphenol-derived protection against neurotoxic β-amyloid protein: From molecular to clinical. *Food & Function, 3*(12), 1242–1250.
Soltani, S., & Madadlou, A. (2015). Gelation characteristics of the sugar beet pectin solution charged with fish oil-loaded zein nanoparticles. *Food Hydrocolloids, 43*, 664–669.
Soltani, S., & Madadlou, A. (2016). Two-step sequential cross-linking of sugar beet pectin for transforming zein nanoparticle-based Pickering emulsions to emulgels. *Carbohydrate Polymers, 136*, 738–743.
Song, H., Jung, J. I., Cho, H. J., Her, S., Kwon, S. H., Yu, R., & Park, J. H. Y. (2015). Inhibition of tumor progression by oral piceatannol in mouse 4T1 mammary cancer is associated with decreased angiogenesis and macrophage infiltration. *The Journal of Nutritional Biochemistry, 26*(11), 1368–1378.
Sorriento, D., Pascale, A. V., Finelli, R., Carillo, A. L., Annunziata, R., Trimarco, B., & Iaccarino, G. (2014). Targeting mitochondria as therapeutic strategy for metabolic disorders. *The Scientific World Journal, 2014*.
Steinberg, D., Parthasarathy, S., Carew, T. E., Khoo, J. C., & Witztum, J. L. (1989). Beyond cholesterol. Modifications of low-density lipoprotein that increase its atherogenicity. *The New England Journal of Medicine, 321*(17), 1196–1197.
Storz, P. (2005). Reactive oxygen species in tumor progression. *Frontiers in Bioscience, 10*(1–3), 1881–1896.
Strobel, M., Tinz, J., & Biesalski, H. K. (2007). The importance of β-carotene as a source of vitamin A with special regard to pregnant and breastfeeding women. *European Journal of Nutrition, 46*(9), 1–20.
Sun, Y., Wang, H., Liu, M., Lin, F., & Hua, J. (2015). Resveratrol abrogates the effects of hypoxia on cell proliferation, invasion and EMT in osteosarcoma cells through downregulation of the HIF-1α protein. *Molecular Medicine Reports, 11*(3), 1975–1981.
Sun, C., Chen, S., Dai, L., & Gao, Y. (2017). Structural characterization and formation mechanism of zein-propylene glycol alginate binary complex induced by calcium ions. *Food Research International, 100*, 57–68.
Sun, C., Xu, C., Mao, L., Wang, D., Yang, J., & Gao, Y. (2017). Preparation, characterization and stability of curcumin-loaded zein-shellac composite colloidal particles. *Food Chemistry, 228*, 656–667.
Sun, C., Yang, S., Dai, L., Chen, S., & Gao, Y. (2017). Quercetagetin-loaded zein-propylene glycol alginate composite particles induced by calcium ions: Structural comparison between colloidal dispersions and lyophilized powders after in vitro simulated gastraintestinal digestion. *Journal of Functional Foods, 37*, 25–48.
Sun, W., Liu, X., Zhang, H., Song, Y., Li, T., Liu, X., & Guo, W. (2017). Epigallocatechin gallate upregulates NRF2 to prevent diabetic nephropathy via disabling KEAP1. *Free Radical Biology and Medicine, 108*, 840–857.
Sun, C., Dai, L., & Gao, Y. (2017a). Formation and characterization of the binary complex between zein and propylene glycol alginate at neutral pH. *Food Hydrocolloids, 64*, 36–47.
Sun, C., Dai, L., & Gao, Y. (2017b). Interaction and formation mechanism of binary complex between zein and propylene glycol alginate. *Carbohydrate Polymers, 157*, 1638–1649.
Takata, Y., Xiang, Y. B., Yang, G., Li, H., Gao, J., Cai, H., & Shu, X. O. (2013). Intakes of fruits, vegetables, and related vitamins and lung cancer risk: Results from the Shanghai men's health study (2002–2009). *Nutrition and Cancer, 65*(1), 51–61.
Tan, Y., Chang, S. K., & Zhang, Y. (2017). Comparison of α-amylase, α-glucosidase and lipase inhibitory activity of the phenolic substances in two black legumes of different genera. *Food Chemistry, 214*, 259–268.
Tanaka, T., Shnimizu, M., & Moriwaki, H. (2012). Cancer chemoprevention by carotenoids. *Molecules, 17*(3), 3202–3242.
Tapia-Hernández, J. A., Torres-Chávez, P. I., Ramírez-Wong, B., Rascón-Chu, A., Plascencia-Jatomea, M., Barreras-Urbina, C. G., & Rodríguez-Félix, F. (2015). Micro- and nanoparticles by electrospray: Advances and applications in foods. *Journal of Agricultural and Food Chemistry, 63*(19), 4699–4707.
Tapia-Hernández, J. A., Rodríguez-Félix, D. E., Plascencia-Jatomea, M., Rascón-Chu, A., López-Ahumada, G. A., Ruiz-Cruz, S., & Rodríguez-Félix, F. (2017). Porous wheat gluten microparticles obtained by electrospray: Preparation and characterization. *Advances in Polymer Technology, 00*, 1–11. http://dx.doi.org/10.1002/adv.21907.
Tapia-Hernández, J. A., Rodríguez-Félix, F., & Katouzian, I. (2017). Nanocapsule formation by electrospraying. *Nanoencapsulation technologies for the food and nutraceutical industries* (pp. 320–345). .
Tavani, A., Negri, E., D'avanzo, B., & La Vecchia, C. (1997). Beta-carotene intake and risk of nonfatal acute myocardial infarction in women. *European Journal of Epidemiology, 13*(6), 631–637.
Taverne, Y. J., Bogers, A. J., Duncker, D. J., & Merkus, D. (2013). Reactive oxygen species and the cardiovascular system. *Oxidative Medicine and Cellular Longevity, 2013*.
Teng, Z., Luo, Y., & Wang, Q. (2013). Carboxymethyl chitosan–soy protein complex nanoparticles for the encapsulation and controlled release of vitamin D3. *Food Chemistry, 141*(1), 524–532.
Tsai, Y. H., Yang, Y. N., Ho, Y. C., Tsai, M. L., & Mi, F. L. (2018). Drug release and antioxidant/antibacterial activities of silymarin-zein nanoparticle/bacterial cellulose nanofiber composite films. *Carbohydrate Polymers, 180*, 286–296.
Tsao, R. (2010). Chemistry and biochemistry of dietary polyphenols. *Nutrients, 2*(12), 1231–1246.
Tu, S., Xiao, F., Min, X., Chen, H., Fan, X., & Cao, K. (2018). Catechin Attenuates Coronary Heart Disease in a Rat Model by Inhibiting Inflammation. *Cardiovascular Toxicology*, 1–7.
Uto-Kondo, H., Ohmori, R., Kiyose, C., Kishimoto, Y., Saito, H., Igarashi, O., & Kondo, K.

(2009). Tocotrienol suppresses adipocyte differentiation and Akt phosphorylation in 3T3-L1 preadipocytes. *The Journal of Nutrition, 139*(1), 51–57.
Vandenplas, Y., De Greef, E., Hauser, B., & Paradice Study Group (2014). Safety and tolerance of a new extensively hydrolyzed rice protein-based formula in the management of infants with cow's milk protein allergy. *European Journal of Pediatrics, 173*(9), 1209–1216.
Veneranda, M., Hu, Q., Wang, T., Luo, Y., Castro, K., & Madariaga, J. M. (2018). Formation and characterization of zein-caseinate-pectin complex nanoparticles for encapsulation of eugenol. *LWT- Food Science and Technology, 89*, 596–603.
Visentini, F. F., Sponton, O. E., Perez, A. A., & Santiago, L. G. (2017). Formation and colloidal stability of ovalbumin-retinol nanocomplexes. *Food Hydrocolloids, 67*, 130–138.
Votruba, M., Vecka, M., Prokeš, L., & Jurášková, B. (2009). The natural products in protection agains the most important pathological changes in human metabolism. *Czech Journal of Food Sciences, 27*, S31–S34.
Voutilainen, S., Nurmi, T., Mursu, J., & Rissanen, T. H. (2006). Carotenoids and cardiovascular health. *The American Journal of Clinical Nutrition, 83*(6), 1265–1271.
Wagoner, T., Vardhanabhuti, B., & Foegeding, E. A. (2016). Designing whey protein–polysaccharide particles for colloidal stability. *Annual Review of Food Science and Technology, 7*, 93–116.
Wang, X., & Zhao, J. (2013). Encapsulation of the herbicide picloram by using polyelectrolyte biopolymers as layer-by-layer materials. *Journal of Agricultural and Food Chemistry, 61*(16), 3789–3796.
Wang, L. J., Yin, S. W., Wu, L. Y., Qi, J. R., Guo, J., & Yang, X. Q. (2016). Fabrication and characterization of Pickering emulsions and oil gels stabilized by highly charged zein/chitosan complex particles (ZCCPs). *Food Chemistry, 213*, 462–469.
Wang, T., Ma, X., Lei, Y., & Luo, Y. (2016). Solid lipid nanoparticles coated with cross-linked polymeric double layer for oral delivery of curcumin. *Colloids and Surfaces B: Biointerfaces, 148*, 1–11.
Wang, M., Fu, Y., Chen, G., Shi, Y., Li, X., Zhang, H., & Shen, Y. (2017). Fabrication and characterization of carboxymethyl chitosan and tea polyphenols coating on zein nanoparticles to encapsulate β-carotene by anti-solvent precipitation method. *Food Hydrocolloids, 77*, 577–587.
Weissmueller, N. T., Lu, H. D., Hurley, A., & Prud'homme, R. K. (2016). Nanocarriers from GRAS zein proteins to encapsulate hydrophobic actives. *Biomacromolecules, 17*(11), 3828–3837.
Welsch, C. A., Lachance, P. A., & Wasserman, B. P. (1989). Dietary phenolic compounds: inhibition of Na+-dependent D-glucose uptake in rat intestinal brush border membrane vesicles. *The Journal of Nutrition, 119*(11), 1698–1704.
Wongsasulak, S., Pathumban, S., & Yoovidhya, T. (2014). Effect of entrapped α-tocopherol on mucoadhesivity and evaluation of the release, degradation, and swelling characteristics of zein–chitosan composite electrospun fibers. *Journal of Food Engineering, 120*, 110–117.
Woo, H. D., & Kim, J. (2013). Dietary flavonoid intake and smoking-related cancer risk: a meta-analysis. *PLoS ONE, 8*(9), e75604.
Xia, X., Sun, B., Li, W., Zhang, X., & Zhao, Y. (2017). Anti-diabetic activity phenolic constituents from red wine against α-glucosidase and α-amylase. *Journal of Food Processing and Preservation, 41*(3).
Xu, Y., Nie, L., Yin, Y. G., Tang, J. L., Zhou, J. Y., Li, D. D., & Zhou, S. W. (2012). Resveratrol protects against hyperglycemia-induced oxidative damage to mitochondria by activating SIRT1 in rat mesangial cells. *Toxicology and Applied Pharmacology, 259*(3), 395–401.
Xu, M., Yang, H., Zhang, Q., Lu, P., Feng, Y., Geng, X., ... Jia, J. (2017). Alpha-Tocopherol prevents esophageal squamous cell carcinoma by modulating PPARγ Akt signaling pathway at the early stage of carcinogénesis. *Oncotarget, 8*(56), 95914–95930.
Yam, M. L., Abdul Hafid, S. R., Cheng, H. M., & Nesaretnam, K. (2009). Tocotrienols suppress proinflammatory markers and cyclooxygenase-2 expression in RAW264. 7 macrophages. *Lipids, 44*(9), 787–797.
Yang, C. S., & Suh, N. (2013). Cancer prevention by different forms of tocopherols. *Topics in Current Chemistry, 329*, 21–33.
Yang, Y., Duan, W., Li, Y., Jin, Z., Yan, J., Yu, S., & Yi, D. (2013). Novel role of silent information regulator 1 in myocardial ischemia. *Circulation, 128*(20), 2232–2240.
Yang, C. S., Wang, H., & Sheridan, Z. P. (2018). Studies on prevention of obesity, metabolic syndrome, diabetes, cardiovascular diseases and cancer by tea. *Journal of Food and Drug Analysis, 26*(1), 1–13.
Yu, N., Su, X., Wang, Z., Dai, B., & Kang, J. (2015). Association of dietary vitamin A and β-carotene intake with the risk of lung cancer: A meta-analysis of 19 publications. *Nutrients, 7*(11), 9309–9324.
Yu, X. D., Yang, J. L., Zhang, W. L., & Liu, D. X. (2016). Resveratrol inhibits oral squamous cell carcinoma through induction of apoptosis and G2/M phase cell cycle arrest. *Tumor Biology, 37*(3), 2871–2877.
Yun, J. M., Chien, A., Jialal, I., & Devaraj, S. (2012). Resveratrol up-regulates SIRT1 and inhibits cellular oxidative stress in the diabetic milieu: mechanistic insights. *The Journal of Nutritional Biochemistry, 23*(7), 699–705.
Zeeb, B., Thongkaew, C., & Weiss, J. (2014). Theoretical and practical considerations in electrostatic depositioning of charged polymers. *Journal of Applied Polymer Science, 131*(7).
Zhang, H., & Tsao, R. (2016). Dietary polyphenols, oxidative stress and antioxidant and anti-inflammatory effects. *Current Opinion in Food Science, 8*, 33–42.
Zhang, Y., Niu, Y., Luo, Y., Ge, M., Yang, T., Yu, L. L., & Wang, Q. (2014). Fabrication, characterization and antimicrobial activities of thymol-loaded zein nanoparticles stabilized by sodium caseinate–chitosan hydrochloride double layers. *Food Chemistry, 142*, 269–275.
Zhang, D., Tong, J., Xia, B., & Xue, Q. (2014). Ultrahigh performance humidity sensor based on layer-by-layer self-assembly of graphene oxide/polyelectrolyte nanocomposite film. *Sensors and Actuators B: Chemical, 203*, 263–270.
Zhang, Y., Cui, L., Che, X., Zhang, H., Shi, N., Li, C., ... Kong, W. (2015). Zein-based films and their usage for controlled delivery: Origin, classes and current landscape. *Journal of Controlled Release, 206*, 206–219.
Zhang, B., Lakshmanan, J., Motameni, A., & Harbrecht, B. G. (2017). Resveratrol-mediated repression of a liver cancer cell line. *The FASEB Journal, 31*(1 Suppl) (1067-5).
Zhang, L., Deng, X., Pan, S., Lai, X., Sun, S., & Chen, W. (2017). Research progress on the effect and mechanism of EGCG in the prevention and treatment of diabetes mellitus. *Journal of South China Agricultural University, 38*(5), 50–55.
Zhao, L., Cen, F., Tian, F., Li, M. J., Zhang, Q., Shen, H. Y., & Du, J. (2017). Combination treatment with quercetin and resveratrol attenuates high fat diet-induced obesity and associated inflammation in rats via the AMPKα1/SIRT1 signaling pathway. *Experimental and Therapeutic Medicine, 14*(6), 5942–5948.
Zhao, Y., Song, W., Wang, Z., Wang, Z., Jin, X., Xu, J., & Cai, L. (2018). Resveratrol attenuates testicular apoptosis in type 1 diabetic mice: Role of Akt-mediated Nrf2 activation and p62-dependent Keap1 degradation. *Redox Biology, 14*, 609–617.
Zhong, Q., Tian, H., & Zivanovic, S. (2009). Encapsulation of fish oil in solid zein particles by liquid-liquid dispersion. *Journal of Food Processing and Preservation, 33*(2), 255–270.
Zhou, D. H., Wang, X., Yang, M., Shi, X., Huang, W., & Feng, Q. (2013). Combination of low concentration of (−)-epigallocatechin gallate (EGCG) and curcumin strongly suppresses the growth of non-small cell lung cancer in vitro and in vivo through causing cell cycle arrest. *International Journal of Molecular Sciences, 14*(6), 12023–12036.

CAPÍTULO II

Prolamins from cereal by-products: Classification, extraction, characterization and its applications in micro- and nanofabrication

Trends in Food Science & Technology 90 (2019) 111–132

Contents lists available at ScienceDirect

Trends in Food Science & Technology

journal homepage: www.elsevier.com/locate/tifs

Review

Prolamins from cereal by-products: Classification, extraction, characterization and its applications in micro- and nanofabrication

José Agustín Tapia-Hernández[a], Carmen Lizette Del-Toro-Sánchez[a], Francisco Javier Cinco-Moroyoqui[a], Josué Elías Juárez-Onofre[b], Saúl Ruiz-Cruz[c], Elizabeth Carvajal-Millan[d], Guadalupe Amanda López-Ahumada[a], Daniela Denisse Castro-Enriquez[a], Carlos Gregorio Barreras-Urbina[a], Francisco Rodríguez-Felix[a,*]

[a] Department of Research and Posgraduate in Food (DIPA), University of Sonora, Blvd. Luis Encinas y Rosales, S/N, Colonia Centro, 83000, Hermosillo, Sonora, Mexico
[b] Department of Physics, University of Sonora, Blvd. Luis Encinas y Rosales, S/N, Colonia Centro, 83000, Hermosillo, Sonora, Mexico
[c] Department of Biotechnology and Food Science, Institute Technology of Sonora, 5 de febrero #818 sur, Colonia Centro, 85000, Ciudad Obregón, Sonora, Mexico
[d] Research Center for Food and Development A.C. Carretera a La Victoria KM 0.6, 83304, Hermosillo, Sonora, Mexico

ARTICLE INFO

Keywords:
Prolamins
Cereal by-product
Distillers dried grains with solubles
Gluten meals
Microtechnology
Nanotechnology

ABSTRACT

Background: Prolamins are the endosperm storage proteins of cereal grains. Currently, the agri-food industry generates large quantities of by-products, among which are those generated from wet-milling, such as Gluten Meals (GM), dry-milling, such as the Distillers Dried Grains with Solubles (DDGS) and Brewer's Spent Grain (BSG). These by-products are important biopolymer sources such as prolamins. The prolamins have low nutritional value, however can be are useful for obtaining micro- and nanomaterials

Scope and approach: The main objective of this review was to make known the techniques of obtaining and its main applications in micro- and nanotechnology of prolamins obtained from cereal, and the purpose of this investigation was to promote the use of prolamins obtained from cereal by-products.

Key findings and conclusions: The prolamins can be obtained of by-products cereals and due to their economic importance and high productivity, the main cereals that generate these types of by-products are wheat and corn, in addition to sorghum, which is experiencing an increasing boom. The conformational structure of prolamins render them feasible for producing various micro- and nanomaterials, particles and fibers. These micro- and nanomaterials are of interest in the food industry and medicine for protection of bioactive compounds, pickering emulsions stabilized, drug delivery system and controlled release fertilizer. There is more evidence on nanomaterials that micromaterials that have been obtained from prolamins: from 2014 and up to date, around 247 investigations have been published dealing with the obtention of nanoparticles and nanofibers, of which only 2.0% corresponds to materials obtained from cereals by-products. Therefore, future prolamin research in nanotechnology from the by-products of cereals is necessary, with the purpose of increase added value and decreasing environmental contamination.

1. Introduction

In recent years and up to date, research in agriculture, food, and science in general has focused on finding alternatives that help to mitigate or reduce the environmental impact (Rockström et al., 2017). The areas of agriculture and food are taking into account the drawing on the majority of resources, specifically the efficient use of the by-products generated by agricultural crops or during processing (Stancu, Haugaard, & Lähteenmäki, 2016). Only in the U.S.A., about 35–103 million tons of waste are generated annually (Bellemare, Çakir, Peterson, Novak, & Rudi, 2017), which is currently accumulated or burned generating pollution into the environment and human health. Among the food crops that generate the most waste are cereals (Bessaire et al., 2016; Shahane & Shivay, 2016), since they constitute the basis of the world's diet (Burange, Clark, & Luque, 2016) or are processed for biotechnological uses, such as in the obtaining of biofuels (Singh & Trivedi, 2017).

Cereal grains such as corn, wheat, and rice are in the top of the list of grains with the highest demand worldwide, making a percentage higher than 70% (Guerrieri & Cavaletto, 2018; Luecha & Kokini, 2016;

* Corresponding author.
E-mail address: rodriguez_felix_fco@hotmail.com (F. Rodríguez-Felix).

https://doi.org/10.1016/j.tifs.2019.06.005
Received 30 December 2018; Received in revised form 4 June 2019; Accepted 9 June 2019
Available online 12 June 2019
0924-2244/

Table 1
Prolamins of principal and minority grain cereals.

Cereals	Total protein content (%)	Prolamins (%)	Prolamin Nane	Prolamin sub-groups	Reference
Principal cereals					
Wheat	7–22	70–80	Gliadin and glutenin	α + β-gliadins, ω-gliadins, γ-gliadins, LMW-GS, HMW-GS	Shewry (2007); Scherf, Koehler, and Wieser (2016)
Corn	8–12	44–79	Zein	α-zeins, β-zein, γ-zeins and δ-zeins	Díaz-Gómez, Castorena-Torres, Preciado-Ortiz, and García-Lara (2017)
Rice	6–7	3–6	Prolamin	10-prolamins, 13-prolamins 16-prolamins	Amagliani, O'Regan, Kelly, and O'Mahony (2017)
Minority cereals					
Rye	8–11.3	17–19	Secalin	HMW-secalins, γ-secalins, ω-secalins	Redant, Buggenho, Brijs, & Delcour (2017)
Barley	11.6–15.1	50–80	Hordein	B-hordeins, C-hordeins, D-hordeins, and γ-hordeins	Huang, Dai, Zhong, Xiao, McClemens, & Hu, 2017); Yu et al. (2017)
Oats	15–20	4–15	Avenin	I-avenin, II-avenin, III-avenin, IV-avenin, and V-avenin	Nałęcz, Dziuba, and Szerszunowicz (2017); Zhao et al., (2017)
Sorghum	10–12	70–80	Kafirin	α-kafirin, β-kafirin, and γ-kafirin	Liu, Li, et al. 2017, Liu, Ma, et al, 2017, Liu, Zhu, et al. (2017), Liu, Lamont, et al. (2017), Chaudhary et al. (2018)

Sharma & Wardhan, 2017), followed by sorghum, rye, and barley with lesser demand (Louie, 2017). The most common uses of these cereals are in the preparation of various processed foods, either artisanal or industrial. In several countries of the world, the use of cereal grains comprises the basis for the preparation of various foods (Diao, 2017), but in developed countries, cultivated cereals have been used for biotechnological use as alternative sources of biofuels (Ghosh, Chowdhury, & Bhattacharya, 2017). During the processing of cereals, a large amount of waste is generated that is poorly valued, being the sources of various natural polymers such as lipids, carbohydrates, and proteins (Dhillon, Kaur, Oberoi, Spier, & Brar, 2017; Nuez Ortín & Yu, 2009; Shewry, 2007).

In this context, cereal by-products are in the spotlight of many investigations, such as Gluten Meal (GM) and Distillers Dried Grain with Solubles (DDGS) (Nuez Ortín & Yu, 2009). Among the main uses of cereal by-products is the implementation of balanced feed for animals, due to their high protein content. The protein content of cereal grains ranges from 5.8 to 15% (Shewry, 2007), while the content of protein in cereal by-products ranges from 30 to 85%, due to a reduction of the grain mass attributed at a reduction in carbohydrates, that get used during alcoholic fermentation (Zhou et al., 2015).

In general, cereals contain various proteins and are classified based on their solubility, such as albumins that are soluble in aqueous solutions, globulins soluble in salts, glutenins soluble in alkaline solutions, and prolamins soluble in alcoholic solutions (Shewry, 2002). Albumins and globulins are stored in the germ of the grain and are considered the proteins with the highest nutritional balance, because they contain essential amino acids and are mainly rich in lysine (Guerrieri & Cavaletto, 2018). Prolamins, also called reserve proteins, are found in the endosperm of the grain and are from the nutritional point of view, the poorer proteins, because they lack essential amino acids and are rich in non-essentials (Larkins, Wu, Song, & Messing, 2017). Proteins of the prolamin type are found in the main cereals (corn, wheat, sorghum and barley) and constitute around 80% of the total protein. Prolamin functionalization is required and these are extracted from the by-products of cereals, becoming the center of attention in different areas of knowledge (Landriscina et al., 2017).

Prolamins present different names depending on the type of cereal from which are extracted. In wheat, the prolamins that make up gluten are gliadins and glutenins (Nuttall et al., 2017), in corn these are zeins, in sorghum are kafirins (Giteru, Oey, Ali, Johnson, & Fang, 2017; Luecha & Kokini, 2016) and barley they are denominated hordein (Houde, Khodaei, Benkerroum, & Karboune, 2018). Currently, some applications of prolamins include research, such as obtained the bioactive peptides, that are termed hydrolysates (Hayes & Bleakley, 2018; Orona-Tamayo, Valverde, & Paredes-López, 2018), and their more recent use in nanotechnology takes place in the obtention of polymer matrices for the protection and/or vehicle of many molecules that are labile to environmental conditions in the areas of food, agriculture, and medicine (Peng et al., 2017; Sun, Xu, Mao, Wang, Yang, & Gao, 2017; Xiao, Lu, & Huang, 2017). Micro- and nanotechnology are defined as branchs of the science that studies phenomena at micro- and nanoscale level (Bhushan, 2017; Joye, 2018). In geometry, materials that have been studied in micro- nanotechnology from prolamins include micro-/nanoparticles and micro-/nanofibers.

Therefore, the objective of this review was to present the most recent applications of prolamins in nanotechnology and to study the prolamins obtained from cereal by-products as in wheat, corn, and sorghum generated in agro-industry.

2. Prolamins in cereals: overview

Wheat and corn are considered in the first three places of production worldwide, along with rice (Furtak, Gawryjołek, Gajda, & Gałązka, 2017; Han et al., 2017), where the former two are considered to have a prolamin content that makes around 80% of the total protein, whereas

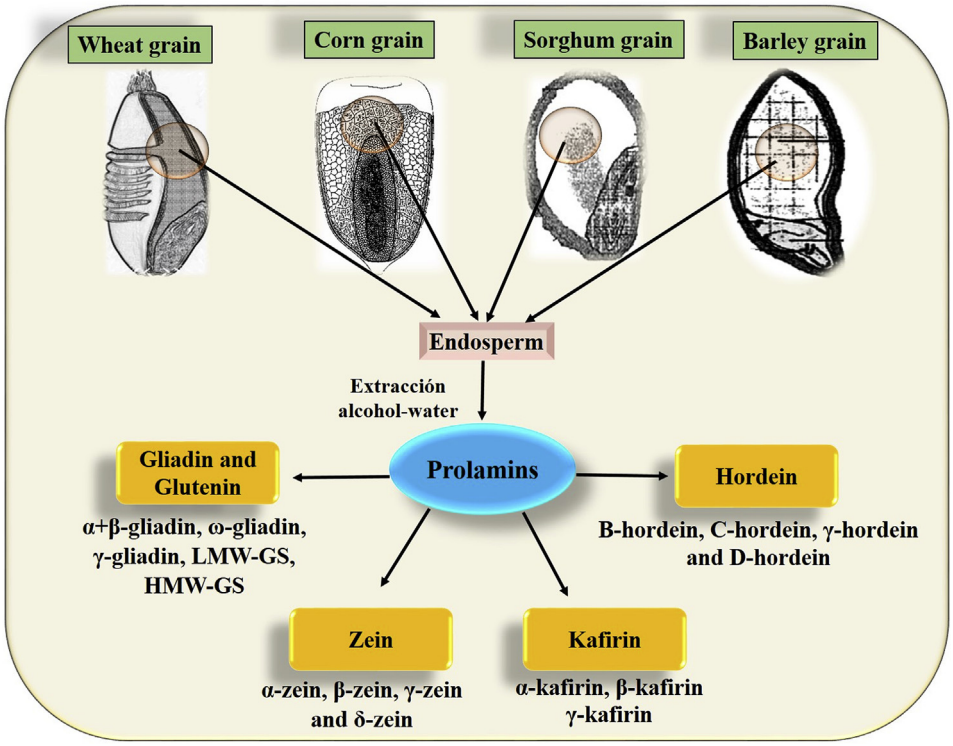

Fig. 1. Location of endosperm in cereal grains to obtain prolamins.

rice contains a less than 10% (Liu, Shao et al., 2018, Liu, Zhang et al., 2018, Liu, Chen et al., 2018). Although sorghum and barley are not considered among the main cereals, there is an increasing number of investigations being conducted on it (de Morais Cardoso, Pinheiro, Martino, & Pinheiro-Sant'Ana, 2017), in addition to the fact that it contains a similar percentage of prolamins as those of wheat and corn (Raza et al., 2017). Table 1 shows the percentage of prolamins found in different cereals, with wheat, corn, sorghum, and barley with the highest prolamin content.

The etymology of the term prolamin is due to that these proteins contain a large amount of proline and glutamine amino acids (Hernández-Espinosa, Reyes-Reyes, González-Jiménez, Núñez-Bretón, & Cooper-Bribiesca, 2015) and are considered the largest storage proteins of cereal grains such as wheat, corn, and sorghum and are mostly synthesized during the development of the seed in the endoplasmic reticulum (Pedrazzini, Mainieri, Marrano, & Vitale, 2016) accumulating in vesicles surrounded by membranes called protein bodies in the grain endosperm (Fig. 1). After germination, they are degraded to serve as nitrogen sources in order to sustain the growth of the shoot and the immediate growth of the seedling at early ages after germination (Pedrazzini & Vitale, 2018).

Prolamins are heterogeneous polypeptides with molecular masses ranging from 10 to greater than 100 kD, depending on the type of cereal (Bunce, White, & Shewry, 1985; Koga et al., 2017). Prolamins can be differentiated into monomers and polymers. The gliadin from wheat is considered as monomeric and glutenin as polymeric (Wang et al., 2014), while corn zein, sorghum kafirin and barley hordein are polymeric and monomeric-type prolamins (Elkonin, Italyanskaya, Panin, & Selivanov, 2017; Izydorczyk & Edney, 2017). Prolamins have different groups based on their mobility in polyacrylamide gels. The generalities of the prolamins of wheat, corn, and sorghum are mentioned later.

2.1. Prolamins in wheat

Wheat-grain prolamins are storage proteins found in the endosperm and are soluble in hydroalcoholic solutions (Fig. 1). They are divided into two types, gliadins and glutenins, both forming wheat gluten, which is a complex protein network that plays a key role in determining the rheology of dough (Biesiekierski, 2017). The covalent structure that makes up gluten is due to non-covalent interactions such as hydrogen bonds, ionic bonds, and hydrophobic interactions, in addition to disulfide-type covalent bonds, although the latter in a smaller proportion around 2% are due to the small amount of cysteine (Gao et al., 2018; Zhou et al., 2014). The disulfide bonds of gluten are of utmost importance for the aggregation of the protein, producing materials with unique characteristics (Tapia-Hernández, Rodríguez-Felix, Juárez-Onofre et al., 2018, Tapia-Hernández, Rodríguez-Félix, Plascencia-Jatomea et al., 2018). The characteristics of wheat gluten will be furnished by the set of individual properties exerted by gliadins (viscous part) and glutenins (elastic part).

Gliadins are monomeric proteins that have molecular weights ranging from 3-8 $\times 10^4$ Da and are classified as α + β-, ω-, and γ-gliadins depending on their molecular weight and amino acid composition (Urade, Sato, & Sugiyama, 2017; Wang, Zou, Liu, Gu, & Yang, 2018). Gliadins contain intrachain disulfide bridges that confer the viscous property to the wheat gluten (Ooms et al., 2018). The functionality of gliadins is based on the percentage of their amino acid content, since it varies depending on the group: ω-gliadin contains a percentage of amino-acid glutamine of between 44 and 56%, while that of proline is 20 and 26%; α + β-gliadin has 37% glutamine and 16% proline, while γ-gliadin has 35% glutamine and 17% proline (Kumar, Kumar, Pandey, & Chauhan, 2017).

Glutenins are polymeric proteins with a molecular weight ranging from 10^5-10^7 Da (Wang, Zou, et al., 2018), being the largest proteins in nature and containing two types of subunits: Low Molecular Weight (LMW-GS) and High Molecular Weight Glutenin Subunits (HMW-GS) (De Santis et al., 2017; Gao et al., 2018). Glutenins, unlike gliadins, contain intra- and interchain disulfide bonds, resulting in a more rigid and compact structure, and in gluten elasticity (Ooms et al., 2018). The amino acids that make up the LMW-GS glutenin subunits are 38% glutamine and 13% proline, while HMW-GS contain 36% glutamine and 11% proline (Kumar et al., 2017). Unlike gliadins, glutenins are

soluble in acidic solutions such as acetic acid.

The molecular interaction between gliadins and glutenin proposed by Wieser (2007) suggests that these two proteins are in gluten based on thiol groups present in cysteines forming disulfide bonds. The model indicates that the cross-linking between HMW and LMW fractions is due to a disulfide bond, where the binding occurs in a cysteine in the B domain of HMW-GS and a cysteine residue in the C domain of LMW-GS. On the other hand, α- and γ-gliadins are also covalently bound to LMW-GS by disulfide bonds, forming a strong interaction between all of the subunits that form gluten.

2.2. Prolamins in corn

Prolamins of corn are storage proteins of the grain endosperm y soluble in 70% ethanol (insoluble in water), and contain 55% of hydrophobic amino acids (Ni, Duquette, & Dumont, 2017; Liang, Chalamaiah, Ren, Ma, & Wu, 2018). Within the endosperm, they are found in clusters called protein bodies that are uniformly distributed throughout the cytoplasm and around the starch granules. Zein was identified in 1987 concerning its solubility in aqueous alcohol solutions and considered a protein with several groups based on its migration in electrophoresis and differentiated by its containing different molecular weights, solubilities, and charges; the first groups found were those of α-zein, β-zein, γ-zein, and δ-zein (Fig. 1) (Shukla & Cheryan, 2001; Tapia-Hernández, Rodríguez-Félix, & Katouzian, 2017). The main amino acids are 10% for proline, 21–26% for glutamine, and 20% for leucine, and the balance of dietary nitrogen being negative due to the absence of lysine and tryptophan (Shukla & Cheryan, 2001).

α-Zein is considered the fraction of zein with greatest presence, soluble in 95% ethanol, representing 75–85% of total zein in the corn grain, depending on variety and culture conditions, and molecular weights are 19 and 22 kD (Tapia-Hernández, Rodríguez-Felix, Juárez-Onofre et al., 2018, Tapia-Hernández, Rodríguez-Félix, Plascencia-Jatomea et al., 2018; Wang, Gotoh, Wang, Kouyama, & Wang, 2017). β-Zein represents 10–15% of total zein, soluble in 30–85% ethanol, and with a molecular weight of 14 kD (Ni & Dumont, 2017; Yin, Wang, Liu, & Yao, 2017). γ-Zein represents less that 10%, is soluble from 0 to 80% (v/v) in 2-propanol, with a reducing agent and molecular weights of 16, 27, and 50 kD (Ni & Dumont, 2017; Tapia-Hernández, Rodríguez-Felix, Juárez-Onofre et al., 2018, Tapia-Hernández, Rodríguez-Félix, Plascencia-Jatomea et al., 2018). Finally, δ-zein represents 1–5% (Larkins et al., 2017) of total zein, its solubility is similar to that of α-zein, and its molecular weights range between 10 and 18 kD (Tapia-Hernández, Rodríguez-Felix, Juárez-Onofre et al., 2018, Tapia-Hernández, Rodríguez-Félix, Plascencia-Jatomea et al., 2018).

Applications of α-zein at the industrial level are based on the study of molecular models that have been proposed to aid in understanding the formation of systems in nanotechnology. The most representative model comprises elongated rectangular prisms with three dimensions including 16, 4.6, and 1.2 nm based on X-ray scattering. The helical units of the tandem model are linearly stacked glutamine spins stabilized by intramolecular hydrogen bonds. Glutamines on the surface provide regions with hydrophilic character, while on the other surfaces the hydrophobic character prevails; therefore, this great hydrophobicity promotes the aggregation of zeins in 70% ethanol (Luo & Wang, 2014).

2.3. Prolamins in sorghum

Prolamins of sorghum grain, called kafirins, are storage proteins soluble in alcohol and are found in the grain endosperm (Fig. 1) (Xiao, Chen, & Huang, 2017). Kafirins are found in protein bodies, as well as in zein in corn (Elhassan, Emmambux, & Taylor, 2017). Kafirins represent 70–80% of the total endosperm protein and are classified based on their solubility, molecular weight, and structure in α-kafirin, β-kafirin, and γ-kafirin (Grootboom et al., 2014). The molecular weights of the three fractions are α-kafirin of 23 and 25 kD, β-kafirin of 20, 18, and 16 kD, and γ-kafirin of 28 kD. α-Kafirin is located within the body proteins, while β-kafirin and γ-kafirin are located within and on the surface (Sullivan, Pangloli, & Dia, 2018). During the development of the grain, the kafirins are synthesized in the rough endoplasmic reticulum, where they are added to and bound to the membrane by means of body proteins (Bean & Ioerger, 2014). The most abundant amino acids in kafirin are proline and glutamine, with 30% of the total amino acids of kafirin (Belton, Delgadillo, Halford, & Shewry, 2006).

α-Kafirin comprises approximately 80–84% of the total fraction in vitreous endosperm and 66–71% in opaque endosperm with two bands by SDS-PAGE with molecular weights of 23 and 25 kD (Belton et al., 2006). α-Kafirin can be found in the form of monomers, dimers, or polymers. β-Kafirin represents approximately 7–8% of total kafirins in the vitreous endosperm and 10–13% in the opaque endosperm. β-Kafirin can be in monomer form by means of intrachain links and as polymer intra- and interchain linkages. γ-Kafirin, in addition to possessing the characteristic band at 28 kD, is mentioned as having another band associated with this subunit at 45 kD, referring to possible dimers (Espinosa-Ramírez & Serna-Saldívar, 2016). The concentration of γ-kafirin ranges from 9 to 12% in vitreous endosperm and from 19 to 21% in the opaque endosperm of total kafirins. Additionally, it can present in the form of oligomers and polymers (Belton et al., 2006). Also, kafirin possesses more hydrophobicity than zein, which makes it attractive for coating materials, being solubilized at a high pH with ionized amino and carboxyl groups (Lal, Tanna, Kale, & Mhaske, 2017). The secondary structure of kafirin is provided by 49% α-helix, 27% β-turn, and 24% β-sheet, respectively (Xiao et al., 2014). The structural model of α-kafirin is similar to that proposed for α-zein, where cylinders are formed from antiparallel helices; these cylinders are joined to other adjacent cylinders from the glutamine residues that are at the ends by hydrogen bonds and that form protein bodies (Raza et al., 2017).

2.4. Prolamins in barley

Barley is considered the fourth most important crop worldwide and more than 60% is produced in Europe (Connolly, Piggott, & FitzGerald, 2013). Barley prolamins are the main storage protein in the grain, and major protein in barley by-product (Bamdad, Wu, & Chen, 2011; Gupta, Abu-Ghannam, & Gallaghar, 2010). The barley prolamins, are called hordeins and constitute approximately 50–80% of total grain proteins (Huang, Kanerva, Salovaara, & Sontag-Strohm, 2016). Hordein is classified in base to their electrophoretic mobility and amino acid composition (Uddin, Nielsen, & Vincze, 2014). Four sub-units are identified, B-hordein of 35–46 kD, C-hordein of 55–75 kD, γ-hordein of < 20 kD and D-hordeins of > 100 kD (Qi, Zhang, & Zhou, 2006; Tanner, Colgrave, Blundell, Howitt, & Bacic, 2019).

B-hordein consists in the major fraction of hordein (70–80%) and are sulfur-rich. C-hordein it is the second most important fraction (10–20%) and are sulfur-poor. D-hordein considered a protein with high molecular weight (HMW) and γ -hordein (1%–5%) with the smallest polypeptides (Guan, Li, Liu, & Li, 2018; Wang, Tian, & Chen, 2011). The amino acid sequence of B-hordein is composed of 5 distinguished domains, including a non-repetitive N-terminal, a repetitive domain, a non-repetitive domain containing 5 cysteine residues, a region high in glutamine residues and a C-terminal (Yang, Huang, Zeng, & Chen, 2015). Some B-hordeins and all C-hordein are found as monomers, also other abundant B-hordein and D-hordeins are linked by interchain disulfide bridges. γ-hordeins are monomers with intrachain disulfide bonds, but some polymeric types may also occur (Celus, Brijs, & Delcour, 2006). On the other hand, hordein structure has excellent surface functional properties, such as foaming and encapsulating (Wang et al., 2011; Yalçın, Çelik, & İbanoğlu, 2008).

The differences among the prolamins of wheat (glutenins and gliadins), corn (zeins), sorghum (kafirins) and barley (hordein) are evident mainly in physicochemical properties such as solubility, molecular

weight, disulfide bonds, and the content of amino acids of proline and glutamine, these exerting an impact on the conformational structure, but all being beneficial for the study and obtaining of diverse materials. Therefore, searching alternative sources for the extraction of these prolamins, such as cereals by-products, is necessary.

3. Sources of prolamins in cereals by-products

At present, researchers in the area of materials focus on using waste material from agro-industry for obtaining natural polymers (Janissen, & , Huynh, 2018; Khedkar & Singh, 2018; Mishra, Zamare, & Manikanta, 2018). Agro-industry waste material is defined as waste generated during the harvest, transfer, processing, or storage of agricultural crops (Yusuf, 2017). These materials, when given an added value, become a by-product synergy that is defined as the waste-production form of a primary process that serves as useful input in another secondary process (Lee & Tongarlak, 2017).

Obtaining prolamins can be performed in two ways; from a primary process that includes agricultural crops, or from a secondary process, which includes agro-industrial waste deriving from the processing of cereals as by-products (Wesołowska-Trojanowska et al., 2017). The source of prolamins from cereal by-products is undergoing a greater boom, especially of cereal by-products such as wheat, corn, sorghum and barley where new extraction processes are being investigated, with higher yields and diverse applications (Santos et al., 2017; Trujillo, Bruni, & Chilibroste, 2017). Cereal by-products are classified based on their process of obtaining wet-milling and dry-milling (Chen, Somavat, Singh, & de Mejia, 2017). Wet-milling is industrially applied in cereals, where the fractionation process included: grain handling, steeping, separation and recovery of germ, fiber, proteins and starch (Wronkowska, 2016), and dry-milling in corn ethanol plant, the ethanol is produced from starch constituent, then liquefaction saccharification and fermentation process (Yu et al., 2019). The difference between both types of milling is the amount of water used in each of them. Dry milling occupies very little water compared to wet milling. Wet-milling has Gluten Meal (GM) as its principal by-product, while that of dry-milling is Distillers Dried Grain with Solubles (DDGS) (Rosentrater & Verbeek, 2017), (Table 2). Other cereal by-product the importance is Brewers' Spent Grain (BSG) of the brewing process (Barrozo, Borel, Lira, & Ataíde, 2019). These by-products can be obtained from the industries of foods, beverages, and from the ethanol-production industry (Stock, Lewis, Klopfenstein, & Milton, 2000; Barrozo, Borel, Lira, & Ataíde, 2019).

3.1. By-products obtained from wet-milling: gluten meal

GM is considered the main by-product of the wet- milling of the cereal industry for obtaining flours (Fig. 2) (Cook, Mallee, & Shulman, 1993; Li, Han, & Chen, 2008). GM has been investigated for obtaining proteins of the prolamin type, considered the majority fraction of this by-product. Proteins of GM are investigated in terms of their energy contribution for animals of fattening, such as beef cows (Geppert, Meyer, Perry, & Gunn, 2017) and as balanced feed for fish (Gerile & Pirhonen, 2017). Current use of GM is the obtained prolamins for applications in materials science and nanotechnology (Shi & Dumont, 2014). The most studied cereals for obtaining GM including wheat (Wheat Gluten Meal, WGM), corn (Corn Gluten Meal, CGM), and sorghum (Sorghum Gluten Meal, SGM), which vary in protein content and prolamin type, as well as in the process of extraction.

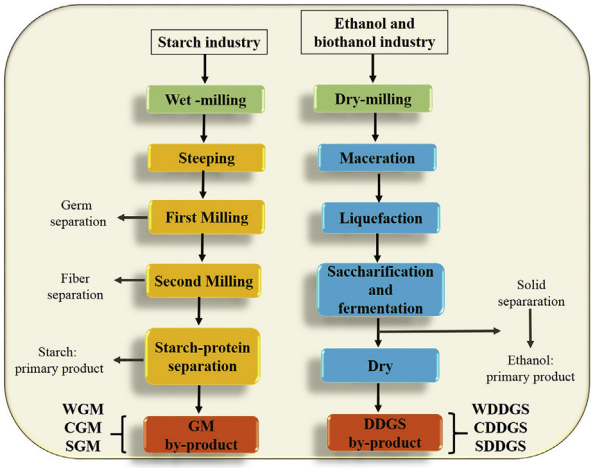

Fig. 2. Primary processes for obtaining GM and DDGS by-products.

3.1.1. Gluten meal from wheat, corn and sorghum cereal

WGM, CGM, and SGM are considered by-products of the starch industry. They are produced in large quantities worldwide and are considered a significant source of dietary protein (Kong, Zhou, & Hua, 2008). WGM is considered a potential functional ingredient in the form of soluble protein hydrolysates, due to its natural origin, availability, low cost, and health-related benefits (Elmalimadi et al., 2017; Qin et al., 2017). The main proteins of WGM are gliadins and glutenins (Liu, Zhu, Guo, Peng, & Zhou, 2017). The protein content of WGM ranges from 72-83% to 75–85%, according to authors in the literature (Fang et al., 2017; Zhang, Li, Li, Ma, & Zhang, 2018); this value is the same for the amount of gliadin and of glutenins. The protein content of CGM is 60–71% and the principal protein is zein, with 68% (Jiang, Zhang, Lin, & Cheng, 2018; Jin et al., 2015). SGM contains a lower percentage of total protein than WGM and CGM, with 35.33–46.51% and prolamin > 92.8%, (Espinosa-Ramírez, Garza-Guajardo, Pérez-Carrillo, & Serna-Saldívar, 2017).

Ortolan and Steel (2017) developed a methodology to obtain WGM from the milling of wheat flour. The process is based on two steps: obtaining the wheat flour, followed by separating the gluten from the starch. First, the wheat grains were ground to separate the main components and to obtain wheat flour (starch + protein) as a result. After this, the flour was mixed with water for form a uniform dough. The dough was washed constantly with water for separate the starch and to obtain the gluten-rich fraction. Finally, this is dried and milled to obtain WGM.

Table 2
Protein composition and content of prolamins in two type of cereal by-products: GM and DDGS.

Cereal by-product	Industry	Obtaining process	Total protein content (%)	Prolamins (%)	Reference
Wet- milling					
WGM	Production of wheat starch	Wheat wet-milling	70–85	75–85	Fang et al. (2017)
CGM	Production of corn starch	Corn wet-milling	60–71	68	Jin et al. (2015)
SGM	Production of sorghum starch	Sorghum wet-milling	35.33–46.51	> 92.8	Espinosa-Ramírez et al. (2017)
Dry- milling					
WDDGS	Ethanol pro-duction	dry-grind distillation	28–38	75	Chatzifragkou et al. (2016)
CDDGS	Ethanol pro-duction	Fermentation	30	12	Gupta et al. (2016)
SDDGS	Ethanol pro-duction	Fermentation	35.5	42.32–98.94	Wang et al. (2009).

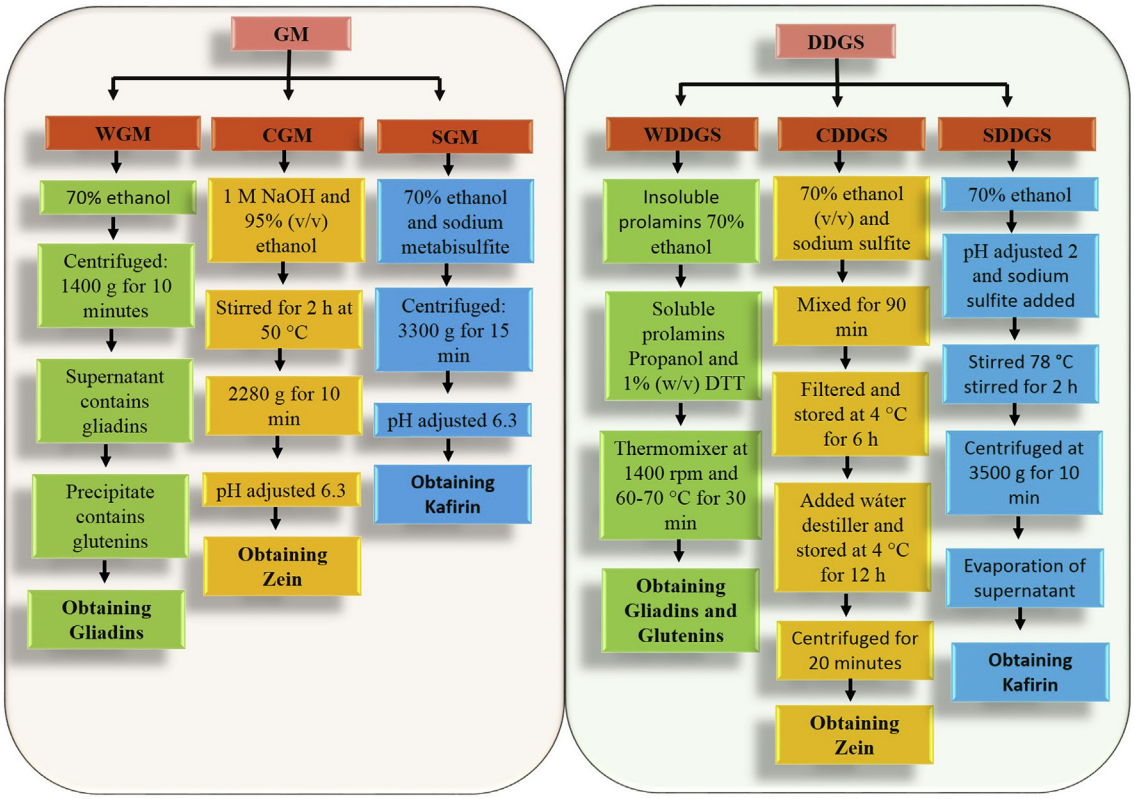

Fig. 3. General procedures for obtaining prolamins from GM and DDGS by-products.

Manochio, Andrade, Rodriguez, and Moraes (2017) proposed a methodology for CGM. The process during which CGM is obtained is through wet-milling (Fig. 2). Once these arrive at the processing plant, they are cleaned of impurities and placed in tanks to be soaked in water and diluted sulfuric acid during 24–36 h at 52 °C. This latter soaking serves to carry out a first separation of the components of the grain, which are the starch, the oil, the gluten, and the fiber. The oil is used for the production of edible corn oil, which is sold to the oil industry, and the fiber is used as animal feed. The starch is separated from the gluten, obtaining CGM. The starch is fermented, distilled, and dehydrated, and the solid residues are removed to obtain the ethanol.

Espinosa-Ramírez et al. (2017) implemented a methodology to obtain SGM by means of the wet- milling process (Fig. 2). First, these authors performed a grinding of the grains (decortication) in order to soak them in water and sodium metabisulfite for 48 h. Then the grain was ground finely at different speeds. Once the flour was obtained, the fractions of fiber and germ were removed by sieving and washing. The starch was recovered from the solid that passed through the sieve. The remaining solids were separated by peristaltic pump, decanted, and centrifuged, and the precipitate was dried to obtain SGM.

3.2. By-products obtaining through dry-milling: Distillers Dried Grain with soluble

Ethanol production worldwide was 88 billion liters in 2013. In the U.S. in 2015, it was over 15 million gallons and it is projected to increase over the next few years (Bhadra, Rosentrater, & Muthukumarappan, 2017; Chatzifragkou et al., 2015). DDGS is considered a by-product of the ethanol industry, with high protein content and a low cost (Biancaniello, Wang, Misra, & Mohanty, 2018). The process in which DDGS is obtained is during the dry-grinding of ethanol-production process (Fig. 2) (Etienne, Trujillo-Barrera, & Hoffman, 2017). The U.S. is the principal generator of DDGS, with about 40.23 million tons of DDGS in 2015, exporting 13.84 million tons representing 82.8% of total world exports, where China and Mexico are the main importers, with 41.5 and 10.4%, respectively (DeOliveira, Brooks, & Nogueira, 2017). The protein content in DDGS is 28–37% (Brancoli, Ferreira, Bolton, & Taherzadeh, 2018; Reddy, Lakshmi, Raju, Kishore, & Anil, 2017). Other important components of DDGS are non-starch polysaccharides such as fiber, containing a high percentage of arabinoxylans and 11.4% of hemicellulose (Abudabos, Al-Atiyat, Stanley, Aljassim, & Albatshan, 2017). The main crops that contribute to producing DDGS are wheat (WDDGS), corn (CDDGS), and sorghum (SDDGS).

3.3. Distillers Dried Grain with soluble from wheat, corn and sorghum cereals

WDDGS, CDDGS, and SDDGS are the principal cereals that contribute to the production of DDGS. The grains of wheat and corn used in ethanol plants for human consumption, are the main source of raw materials, while in biofuel-production plants, they are used as starting materials, in both cases producing WDDGS and CDDGS. WDDGS is composed of polysaccharides, such as cellulose and hemicellulose, and also oils and protein (Villegas-Torres, Ward, & Lye, 2015). WDDGS contains about 28–38% protein with a prolamin content of about 75%, corresponding to gliadins and glutenins (Chatzifragkou et al., 2016). In WDDGS, the major protein content is for glutenins with 42%, while the second is gliadins with 33% (Chatzifragkou et al., 2016). Protein content in CDDGS is similar to that of WDDGS, with around 30%; however, the content of prolamins (zein) is lower with 12% (Gupta, Wilson, & Vadlani, 2016). Adedeji et al. (2017) reported in SDDGS a protein concentration of 28.7–32.9%. However, Wang, Tilley, Bean, Sun, and Wang (2009) reported in SDDGS a 35.5% protein concentration with 42.32–98.94% corresponding to prolamins. Obtaining DDGS from the ethanol industry is reported for WDDGS, CDDGS, and SDDGS.

Joelsson, Galbe, and Wallberg (2014) obtained WDDGS from the process of obtaining ethanol. The general processes to obtain WDDGS

include liquefaction, SSF (Simultaneous Saccharification and Fermentation), distillation, separation of solids, and drying (Fig. 3). During liquefaction, the wheat grains were mixed with fresh water to obtain a mash that was preheated at 60 °C, amylase was added, and the process was carried out at 90 °C. The mixture was cooled (37 °C) and water was added to a temperature of 32 °C. The enzymes were added in a fermenter and SSF was carried out at 32 °C, at which the best yield was obtained. SSF was heated to 91 °C and distilled in a distillation column, and ethanol was obtained. Finally, the solids were separated from the remaining liquid, dried at a temperature of 150 °C, and WDDGS was obtained.

Ou, Brown, Thilakaratne, Hu, and Brown (2014) obtained CDDGS as a by-product of an ethanol plant that employs dry- milled corn. The main processes are depicted in Fig. 3. First the corn is received and cleaned, and then it is introduced into a hammer mill to reduce the size of the grain. Afterward, oligosaccharides are obtained from the starch with water, ammonia, lime, and enzymes at 88 °C. The next step is to convert the oligosaccharides into glucose at 61 °C in order for the glucose is then fermented in ethanol and CO_2 with yeast. After fermentation, the ethanol is centrifuged to obtain the residue, which is dehydrated and concentrated. The final result is the obtaining of CDDGS as by-product.

Appiah-Nkansah, Zhang, Rooney, and Wang (2018) obtained SDDGS as a by-product from the distillation of sorghum grains. The main steps of the process comprised maceration, liquefaction, and scarification (Fig. 3). During maceration, the authors used sorghum flour and sorghum juice at different concentrations to form a final concentration of 33% (w/v) mash. For homogenization of the macerates, each solution was preheated at between 60 and 70 °C and the α-amylase enzyme was added. The flasks were transferred into a shaking bath with a temperature of 70–90 °C and shaking at 180 rpm. The flasks were adjusted to pH 4.2 with HCl. Then the activated yeast was added to carry out the fermentation. Fermentation lasted 72 h at 30 °C under shaking. Afterward, the product obtained was distilled and washed with water. Distillate and SDGS were obtained separately.

3.4. By-products obtaining through brewing industry: Brewers' spent grain

Barley is an important source of by-products generated from the beer industry (Nigam, 2017). Different types of by-products are generated such as barley waste, malt waste, spent grain, spent yeast, trub, conditioning bottom, filter waste and beer waste (Garcia-Garcia, Stone, & Rahimifard, 2019). The most abundant brewing by-product is Brewers' spent grain (BSG) (Klímek, Wimmer, Mishra, & Kúdela, 2017; Mussatto, Dragone, & Roberto, 2006). BSG consisting of the barley malt residue after its separation from work products. Also, this by-product generates around 85% of the all by-products generated (Treimo, Aspmo, Eijsink, & Horn, 2008). Besides the barley, other cereals grain may be in less quantity in BSG as rice, maize, wheat, rye or sorghum depending on the type of beer being produced (Negi & Naik, 2017). The principal proteins present are prolamin and glutelin (Rommi, Niemi, Kemppainen, & Kruus, 2018). Prolamin represent 50% of total protein of BSG (Connolly et al., 2018).

4. Statistics of the by-product generated and its economic implication

The cereals processing mainly is intended to the production of ethanol, generates large quantities of by-products in thousands of tons and continues to increase. The cost of marketing of DDGS is estimated to be valued at USD 10.78 billion in 2018 and is projected to reach 14.95 billion by 2023 (Research and Markets, 2018). In 2012, corn-ethanol industry in US alone generates about 35 Tg of DDGS per year (Gupta et al., 2016) Studies report that from 2011 to 2020, the best producers of grain-based ethanol are USA, Canada and the EU (Chatzifragkou et al., 2015). Estimate that the USA will reach 44 million tonnes DDGS in 2018, whereas EU and Canada contributions are expected to be equal to 9 and 1 million tonnes (Chatzifragkou et al., 2015). Accordingly, crude protein content in DDGS accounts for approximately 300 g kg^{-1} dry matter in maize DDGS and up to 390 g kg^{-1} dry matter in wheat DDGS (Böttger & Südekum, 2018).

From the processing of cereals also generates large amounts of GM. Like DDGS, worldwide from 2010 to 2011 feed consumption of corn gluten meal and corn gluten feed was about 14.9 million tonnes (Heuzé et al., 2018). The biggest consumers were the US (5.6 million tonnes), EU (3 million tonnes), South Korea (1 million tonnes), Japan (0.94 million tonnes) and other Asian countries (1.6 million tonnes) (Heuzé et al., 2018). The USA was the major supplier: they provided 2.1 million t of the 3.5 million t exported worldwide. Main importers were the EU, South Korea, Turkey, China, Japan, Israel, Egypt and Indonesia (Oil World, 2011). USDA of US reported in September 2018 around 83,262 tonnes (NASS-USDA, 2018). Over 840,000 tons of CGM are produced in China every year, mostly being used as feedstuff or discarded (Zhuang, Tang, & Yuan, 2013). From CGM, zein can be recovered at the industrial level (680 g kg^{-1}) (Jin et al., 2015).

In addition, the annual world production of beer is estimated to around 1.8 billion hectoliters, with an average per capita consumption of about 27 L/year (FAOSTAT, 2013). The estimated quantity of spent grain in the beer production process is approx. 20 kg per 100 L of the final product (Łaba, Piegza, & Kawa-Rygielska, 2017). The world production of BSG has been estimated to be on the order of 30–40 million tonnes per year (Fărcaş et al., 2015; Zuorro, Iannone, & Lavecchia, 2019). This is a significant amount considering that BSG is obtained only from the barley husks and that not all the produced barley is used for the production of beer (Mussatto, 2014). According to Eurostat Data, approximately 3.4 million tonnes of BSG are produced annually in the EU (McCarthy et al., 2013) and 2 million tonnes of which are produced in Germany alone (Lynch, Steffen, & Arendt, 2016). Currently the majority of produced BSG is used as a low-value animal feed with a market value of ~€35 per tonne (Lynch et al., 2016). Although rich in polysaccharides, proteins and lignin, which can be used for industrial exploitation, BSG is generally used as animal feed (Ravindran, Jaiswal, Abu-Ghannam, & Jaiswal, 2018). Therefore, its valuation should be promoting.

5. Prolamins from cereal by-products

The extraction of prolamins from GM and DDGS is conducted utilizing aqueous ethanol, according to the solubility of Osborne in cereals (Yazar, Duvarci, Tavman, & Kokini, 2017). The efficiency of obtaining prolamins will depend on the characteristics of the process. Some studies on obtaining prolamins from GM and DDGS are depicted later and in the main steps in Fig. 4.

5.1. Prolamin extraction from wheat by-products

Prolamins in WGM were extracted according to the AACC method and to Osborne solubility and from of the methodology proposed by Yazar et al. (2017). Gluten is washed with 70% ethanol to separate the two fractions: gliadins soluble in 70% ethanol, and insoluble glutenin. The samples were centrifuged at 1,400 *g* for 10 min. Afterward, the ethanol present in the supernatant containing gliadins was evaporated for 6 h at 40 °C and the gliadin concentrate was lyophilized. The glutenin-rich precipitate was also lyophilized. Gliadin and glutenin powders were stored at −20 °C. The identification of gliadin and glutenin were by SDS-PAGE electrophoresis, where bands in glutenin fraction were around 30–75 kDa for LMW-GS and 130.180 kDa for HMW-GS. In the gliadin-rich fraction, bands 5–12 kDa, 25 kDa, 30–40 kDa, and 55–180 kDa were shown for α-, β-, γ-, and ω-gliadin subunits, respectively.

Prolamins of WDDGS were extracted similarly at WGM using the solubility of Osborne, where 100 mg of sample was used and from of the

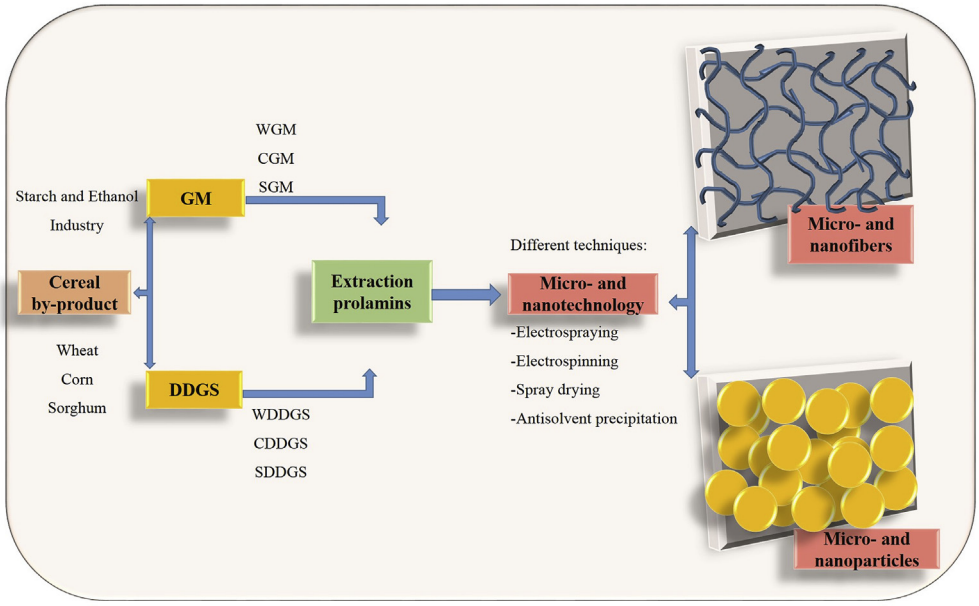

Fig. 4. Prolamins for the development of nanospheres and nanofibers.

methodology proposed by Chatzifragkou et al. (2016). For aqueous ethanol soluble-prolamins, 70% of ethanol was employed, and for aqueous ethanol insoluble-prolamins, 1-propanol was used with 1% (w/v) of DTT (DiThioThreitol). In both cases, the 1:10 (w/v) ratio of solid-liquid was utilized. Then the samples were placed in a thermomixer at 1,400 rpm at temperature of 60–70 °C for 30 min. In the extracts, characteristic bands were revealed by SDS-PAGE electrophoresis for subunits of gliadins, LMW-GS, and HMG-GS and prolamins with reduced disulfide bonds. The percentage of gliadin was 33% (w/v) and that of glutenin was 42% (w/v).

5.2. Prolamin extraction of corn by-products

Prolamins from CGM with a 60% protein content were extracted using the methodology proposed by Tang and Zhuang (2014). The solvets used were 1 M NaOH solution and 95% (v/v) ethanol at 45:55 ratio. The solvent was added to the CGM powder at a ratio of 1:15 (w/v). The system was stirred for 2 h at 50 °C and centrifuged at 2,280 *g* for 10 min. After that, the supernatant was added to distilled water, the pH was adjusted to 6.3, and 2% NaCl (w/v) was added at a ratio of 1:5 (v/v) and stirred during 1 h at 25 °C. Finally, this was centrifuged at 2,280 *g* for 10 min and the precipitate was dried at 37 °C and sieved through #100 mesh. The protein content was referred as the content of prolamins (zein).

Prolamins from CDDGS were extracted following the methodology proposed by Gupta et al. (2016). Firtly, 2 g of CDDGS was mixed with 20 mL of ethanol 70% (v/v) and 0.005 g of sodium sulfite and mixed for 90 min with vigorous shaking. After the mixture was filtered, it was stored at 4 °C for 6 h, an equal volume of distilled water was added, and this was stored at 4 °C for 12 h. A precipitate formed that is attributed to zein. The solution was centrifuged for 20 min and the supernatant was discarded to obtain the extracted zein. The extraction efficiency of prolamin (zein) was 80.8%.

5.3. Prolamin extraction of sorghum by-products

Prolamins from SGM were extracted by adding proteases and methodology proposed by Espinosa-Ramírez et al. (2017). First, SGM was placed in contact with ethanol 70% (v/v) and sodium metabisulfite at 65 °C with a ratio of 1:5 and 1:20, respectively. Then, it was centrifuged at 3,300 *g* for 15 min and the prolamins were sedimented. The pH was measured and adjusted to 6.3 with 0.1 N NaOH. All of the extractions were performed in triplicate. The extraction yield of prolamin was greater than 92%.

Prolamins from SDDGS were extracted following the methodology proposed by Lau et al. (2015). Firstly, five to six volumes of water at 50 °C to remove most of the water-soluble substances. The result was dried in hot air oven at 50 °C overnight, ground with a pin mill, passed through a 1 mm sieve, and stored at room temperature in airtight bags. Later 100 g was agitated with three volumes of petroleum ether for 5 min and decanted to remove the lipid-containing solvent. The sample was then incubated in a water bath for 1 h with five volumes of a mixture of 70% (w/v) ethanol, 0.35% (w/w) sodium hydroxide, and 0.5% (w/w) sodium metabisulfite at 70 °C. Then the material was cooled to room temperature and centrifuged (3500 × *g* at 4 °C) and the prolamins-rich supernatant was obtained. Finally, the concentration of ethanol was reduced to 40% with deionized water and it was placed at −20 °C overnight for the precipitation and collection of prolamines by centrifugation. The prolamins were washed, lyophilized, milled and stored at 4 °C until use.

5.4. Prolamins extraction of barley by-product

Prolamins from BSG were extracted by alkaline treatment and methodology proposed by Connolly et al. (2013). Firstly, as pretreatment, a suspension 1:20 (dw/v) was prepared with distilled water and wet agitation for 60 s at 24000 rpm. Then, the suspension was subjected to extraction with continuous agitation for 1 h at room temperature and centrifuged at 2700 g for 20 min at 10 °C. Then the precipitate was subjected to two sequential extractions with NaOH (1:20, original dw/v) for 1 h at 50 °C. The two extracts were centrifuged and the precipitates mixed to perform a second extraction with gentle stirring and addition of 1 N NaOH (1:14, original dw/v) at room temperature for 16 h. Finally, the supernatant after the centrifugation was adjusted to pH 3.8 with 2 N HCl and gentle stirring for 15 min at room temperature and centrifuged. The precipitated protein was resuspended with distilled water and pH 3.8 and neutralized using pH 7 with 1 N NaOH. The prolamin-rich extract was lyophilized and stored at −20 °C until use.

In general, the obtaining of prolamins from cereal by-products can have several applications, such as the obtaining of micro- and nanometer-scale materials.

Table 3
Some investigations of nanoparticles and nanofibers from prolamins from 2014 to May 2018.

Prolamin	Year	Morphology	Size (nm)	Objective of the study	Reference
Gliadin	2015	Nanoparticle	115–248	Focused on establishing the main factors affecting the formation and stability of gliadin nanoparticles fabricated using antisolvent precipitation	Joye, Nelis, and McClements (2015a,b)
Gliadin	2015	Nanoparticle	150–900	Gliadin n nanoparticles was produced using antisolvent precipitation, and then coated with a polysaccharide layer to improve their aggregation stability	Joye et al. (2015a,b)
Gliadin	2016	Nanoparticle	160–190	Design and develop gliadin nanoparticles of curcumin for oral delivery of drug for targeting colon cancer cells	Sonekar et al. (2016)
Gliadin	2017	Nanoparticle	76.7–77.5	Influences of changing pH and heating on the physical properties of gliadin nanoparticles were investigated in terms of particle size, zeta potential, and morphology	Peng et al. (2018)
Gliadin	2017	Nanoparticle	105.3	Fabricated Gliadin nanoparticles dispersion and investigated the influence of the particle concentration on foaming properties and interfacial behaviors	Peng et al. (2017)
Gliadin	2017	Nanoparticle	200	Investigate the potential of a combination of thermally denatured OVAlbumin (OVA) with Gemini-C12 as stabilizers for gliadin nanoparticle	Feng, Wu, Wang, and Liu (2017)
Gliadin	2017	Nanofiber	720–1760	Single-fluid electrospinning was first conducted to determine the electrospinnable- concentration window of gliadin	Xu et al. (2017)
Gliadin	2018	Nanoparticle	570–890	Coaxial electrospraying process, in which an additional shell solvent was used to modify the working interfaces of the traditional blending electrospraying	Yang, Zhang, et al. (2018).
Glutenin	2015	Nanoparticle	65–145	Wheat glutenin can be made into biocompatible nanoparticles that have the ability to biodistribute into the various organs in mice	Reddy, Shi, Xu, and Yang (2015)
Zein	2014	Nanoparticle	249–462	Examined the possibility of using zein nanoparticles to encapsulate tangeretin	Chen, Zheng, McClements, and Xiao (2014)
Zein	2014	Nanoparticle	176.85–204.75	Investigate the possible Application Antimicrobial and physicochemical properties of SC stabilized thymol-loaded zein nanoparticles	Zhang et al. (2014)
Zein	2014	Nanoparticle	122–136	Preparation of zein nanoparticles by liquid–liquid dispersion	Chen and Zhong (2014)
Zein	2015	Nanoparticle	44–349	Characterize zein nanoparticles formation and stability as impacted by GA	Chen and Zhong (2015)
Zein	2015	Nanoparticle	160	Possibility of forming protein-polysaccharide nanoparticles from zein and alginate using a combined antisolvent precipitation/ electrostatic deposition method	Hu and McClements (2015)
Zein	2015	Nanoparticle	244–252.9	Investigated the ability of citrus pectin to form and stabilize curcumin-loaded zein nanoparticles that might be suitable for use as delivery systems in the food and pharmaceutical industries	Hu et al. (2015)
Zein	2016	Nanoparticle	120	Investigate the possibility of using mixed colloidal dispersions containing two different types of nanoparticles to increase curcumin bioaccessibility	Zou et al. (2016)
Zein	2017	Nanoparticle	100	Determine the relative stabilization of ZNP at different pH values by addition of carrageenan	Cheng and ones (2017)
Zein	2017	Nanoparticle	< 200	Compared the properties of the protein nanoparticles produced using the microfluidization and simple batch injection method	Ebert, Koo, Weiss, and McClements (2017)
Zein	2017	Nanoparticle	224.6–237.6	Fabricate resveratrol-loaded core-shell nanoparticles, and then compared their in vitro antioxidant and anticancer activity with free resveratrol	Huang et al. (2017)
Zein	2017	Nanoparticle	130–150	Prepare Vor and Bor combination (VB)-loaded zein nanoparticles for effective delivery of combination chemotherapeutics to prostate cancer cells with enhanced biocompatibility	Thapa et al. (2017)
Zein	2017	Nanoparticle	222–294	Evaluate the capability of zein nanoparticles, when combined with HP-β-CD in promoting the oral absorption and bioavailability of quercetin	Penalva, González-Navarro, Gamazo, Esparza, and Irache (2017)
Zein	2017	Nanoparticle	98.1–172.1	Investigate the effect of pectin coating on the physicochemical stability of two types of zein/NaCas nanoparticles	Chang, Wang, Hu, Zhou, Xue, & Luo (2017)
Zein	2017	Nanoparticle	50–230	Synthesize ZNPs via the emulsion-diffusion method using didodecyldimethylammonium bromide (ddMab)	Prasad et al. (2017)
Zein	2017	Nanoparticle	184–196	Evaluate the capability of zein nanoparticles as nanocarriers for the oral delivery of glibenclamide	Lucio et al. (2017)
Zein	2017	Nanoparticle	DNS [a]	Study both covalent and non-covalent interactions of zein with three type of polyphenols	Liu, Ma, McClements, and Gao (2017)
Zein	2017	Nanoparticle	260	Evaluate quercetin-loaded in zein nanoparticles containing HP-β-CD as potential treatment for AD.	Puerta, Suárez-Santiago, Santos-Magalhães, & Ramirez, Irache (2017)
Zein	2017	Nanoparticle	> 134.6	Explore the effect of PGA addition with different concentrations on the physical, conformational, thermal, and morphological characteristics of zein colloidal particles	Sun,Dai, & Gao (2017)
Zein	2017	Nanoparticle	130–759.3	Fabricate liquid and solid samples including individual zein nanoparticles and Zein-PGA composite particles in the presence and absence of Q	Sun, Yang, Dai, Chen, and Gao (2017)
Zein	2018	Nanoparticle	198.5–2898.5	Evaluated for the first time the development of silymarin-zein nanoparticle/BC nanocomposite films for active food packaging application	Tsai, Yang, Ho, Tsai, and Mi (2018)
Zein	2018	Nanoparticle	110–225	Zein and GA complex colloidal nanoparticles (ZGAP) were fabricated by anti-solvent precipitation method as novel renewable natural particle-stabilizers of Pickering emulsion gels	Dai, Sun, Wei, Mao, and Gao (2018)
Zein	2018	Nanoparticle	140–297	Study the feasibility of zein-caseinate-pectin complex nanoparticles to encapsulate eugenol	Veneranda et al. (2018)
Zein	2018	Nanoparticle	278.3–482.2	Increase the water solubility and stability of lutein using zein and its derived peptides nanoencapsulation	Jiao et al. (2018)
Zein	2018	Nanoparticle	250–500	Zein biopolymeric nanoparticle-based DSPE was used for the detection of nitrite ions in environmental samples	Hatamie, Nassiri, Alivand, and Bhatnagar (2018)
Zein	2018	Nanoparticle	152.3–260.8	Enhance the dissolution rate of FD and simplify preparation processes by preparing FD-zein complexes using a dual shift technique	Ren et al. (2018)
Zein	2018	Nanoparticle	469.47–764.42	Investigate the effects of ultrasound treatment on the preparation of resveratrol-loaded zein nanoparticles	Liang, Chalamaiah, et al. (2018) and Liang, Ren, et al. (2018)

(*continued on next page*)

Table 3 (*continued*)

Prolamin	Year	Morphology	Size (nm)	Objective of the study	Reference
Zein	2014	Nanofiber	141–882	Reports on the development of novel protein- based scaffold	Ali, Khatri, Oh, Kim, and Kim (2014)
Zein	2014	Nanofiber	400–700	Demonstrates the process, stability, and the characterization of the composite nanofibrous scaffolds	Unnithan, Gnanasekaran, Sathishkumar, Lee, and Kim (2014)
Zein	2014	Nanofiber	86–146	Investigate the effect of adding bark tannin obtained from barbatimão (*S. adstringens*) in the properties of bio-nanostructured zein membranes	de Oliveira et al. (2014)
Zein	2015	Nanofiber	80–250	Fabricate zein nanofibers for siRNA delivery	Karthikeyan, Krishnaswamy, Lakra,. Kiran, & Korrapati (2015)
Zein	2015	Nanofiber	300–350	Fabricate a novel enzyme biosensor based on natural polymer composite nanomaterials	Chen et al. (2015)
Zein	2016	Nanofiber	310–504	Prepare and characterize PLLA/zein-RCSPs nanofiber mats by blend and coaxial electrospinning techniques	Zhang, Li, Li, Liu, and Hao (2016)
Zein	2016	Nanofiber	DNS [a]	Prepare curcumin-loaded zein nanofibers and to use as a coating material to coat apple surface to understand to what extent postharvest decay on apples would be limited	Yilmaz et al. (2016)
Zein	2016	Nanofiber	150–342	New material combination suitable to fabricate composite fibers using PGS and zein	Dippold, Tallawi, Tansaz, Roether, and Boccaccini (2016)
Zein	2016	Nanofiber	636–776	Investigate the kinetics and antioxidant capacity of PA encapsulated in zein (zein-PA) fibers by CV	Wang, Hao,Niu, Jiang, Cheng, & Jiang (2016)
Zein	2017	Nanofiber	600–790	Provide valuable information for the development of anti-infective GTR membranes	He, Jiang, Wang, Xie, and Zhao (2017)
Zein	2017	Nanofiber	58.34–76.63	Determine the effect of quercetin-loaded nanofibers on functional recovery in STreptoZotocin- (STZ)-induced diabetes in rats	Thipkaew, Wattanathorn, and Muchimapura (2017)
Zein	2017	Nanofiber	615–785	Investigation of the kinetics and antioxidant capacity of CUR in zein-CUR electrospun fibers by cyclic voltammetry and the evaluation of antibacterial activities of the fibers	Wang, Hao, Wang, Chen, Jiang, & Jiang (2017)
Zein	2017	Nanofiber	325	First experimental investigation focusing on application of zein nanofibers as an inexpensive, rapid-acting, and sustainable adsorbent for RB5 attenuation	Qureshi, Khatri, Ahmed, Khatri, and Kim (2017)
Zein	2017	Nanofiber	310–348	Process of fabricating cross-linked zein nanofibers by reactive electrospinning with immobilized antibacterial function	Zhang, Wang, Liao, Lallier, Wen, & Xu (2017)
Zein	2017	Nanofiber	444–510	Ultrafine fibers sensitive to pH variation were developed by the incorporation of red cabbage anthocyanin to zein ultrafine fibers by electrospinning	Prietto et al. (2018)
Zein	2018	Nanofiber	74.8	Hypothesize that zein might be uniformly dispersed in gelatin network to improve the water resistance of gelatin nanofibers by hybrid electrospinning	Deng et al. (2018)
Kafirin	2015	Nanoparticle	200–236	Kafirin-based nanoparticles containing CURcumin (CUR) was first prepared (cc-kaf). Then, CM-chitosan was introduced by acid-induced aggregation (cc-kaf/CMC	Xiao, Nian, and Huang (2015)
Kafirin	2015	Nanoparticle	DNS [a]	The physical stability of Kafirin particle-stabilized Pickering Emulsions (KPE) was investigated	Xiao, Li, and Huang (2015).
Kafin	2016	Nanoparticle	90–340	Kafirin nanoparticles were formed through the anti-solvent precipitation method and then characterized in terms of their particle sizes, morphology, and wettability	Xiao, Wang, et al. (2016)
Kafirin	2017	Nanoparticle	DNS [a]	Investigate the feasibility of utilizing protein-based nanoparticles as the outer interface stabilizer for double emulsion	Xiao, Lu, and Huang (2017).

[a] DNS: Data Not Shown.

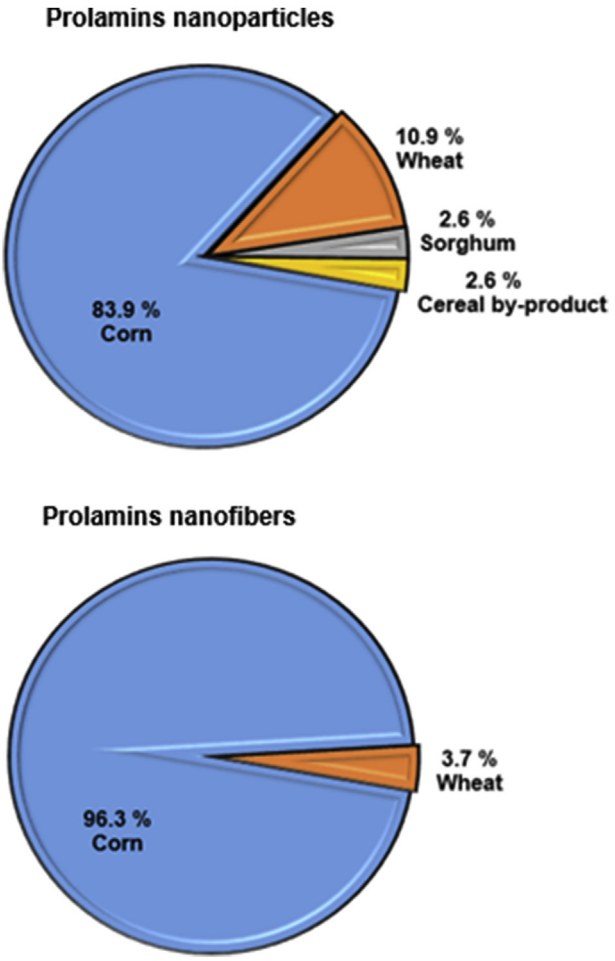

Fig. 5. Prolamin investigation statistics in nanotechnology from 2014 to May 2018.

6. Prolamins in micro- and nanotechnology

Micro- and nanotechnology are the understanding and control of matter at dimensions between approximately > 1 μm (micrometer scale) and 1–100 nm (nanometer scale), where unique phenomena enable novel applications (Kreyling, Semmler-Behnke, & Chaudhry, 2010; Tapia-Hernández et al., 2015). In this context, prolamins from cereal by-products are being investigated for conversion into various micro-nanomaterials with applications mainly in health and food. The studies are focused on obtaining micro- and nanomaterials with two different morphologies from prolamins such as particle and fiber (Fig. 4). These structures are used for the protection and release systems of drugs, bioactive compounds, dyes, etc. Some recent studies (between the years 2014 and 2018) of prolamins nanomaterials are shown later and in Table 3. The term prolamin micro- and nanomaterials refers to the elaboration of micro-/nanofibers and micro-/nanoparticles from wheat, corn, and sorghum (Fig. 5).

From 2014 to date, around 247 investigations have been published for obtaining nanoparticles and nanofibers, of which only 2.0% corresponds at materials obtained from cereal by-products. There have been more investigations of prolamin nanoparticles from corn with 83.9% (162 researches), followed by wheat with 10.9% (21 researches with 20 with gliadin and 1 with glutenin), leaving ample space for the investigation of nanoparticles of sorghum prolamins with 2.6% (five researches) (Table 3). On the other hand, prolamin nanofibers are polymer fibers obtained from cereal prolamins or by-products as a base. The main cereals, as well as the principal nanofibers, are those of wheat, corn, and sorghum (Fig. 5). Prolamin nanofibers of corn are mostly used with 96.3% (52 researches) followed by wheat 3.7% (gliadin, two researches) from 2014 to 2018. Glutenin, sorghum prolamins, and prolamin cereal by-products did not present, to our knowledge, nanofiber research (Table 3). Also, only 7 researches have been reported for obtaining hordein particles (1 microparticles and 6 nanoparticles). There are no reported studies for obtaining hordein micro- and nanofiber, so it is a window of opportunity for future research.

6.1. Techniques for obtaining micro- and nanomaterials of prolamins

Micro-/nanoparticles and micro-/nanofibers from prolamins have been obtained through different techniques such as electrospraying, electrospinning, spray drying, nano spray drying and antisolvent precipitation. The techniques and their fundament, as well as some studies from prolamins are mentioned below.

6.1.1. Electrospraying/electrospinning techniques

Electrospraying and electrospinning, commonly known as electrohydrodynamic atomization (EHDA) process, is one of the tools that is included as a novel method for application in the field of micro- and nanotechnology (Fig. 6) (Tapia-Hernández et al., 2015; Bhushani, Kurrey, & Anandharamakrishnan, 2017; Vogt, Liverani, Roether, & Boccaccini, 2018). Advantages of the electrospraying and electrospinning technique is that micro- and nanoencapsulated are obtained in one step, low cost, the process parameters are simple to manipulate, the synthesis can be produced at industrial level, reproducibility characteristic, obtaining of lower and more uniform fiber and particles size, higher encapsulation efficiency and is feasible for fabrication of protein as prolamins (Zhang, Feng, & Zhang, 2018; Yilmaz et al., 2019). Unlike electrospinning, the electrospraying technique uses diluted solutions for particle formation. Basically, the electrospraying/electrospinning apparatus is made of the following three major parts: a high-voltage power supply, a capillary tube containing polymer solution connected to a needle, and a collector plate (Zhu et al., 2017).

Electrospraying is a technique, which produces fine particle through exerting electrostatic forces on conductive liquid flow that comes out from a capillary (Esmaili et al., 2018). This technique is based in the application of an electric field, due to which the polymeric solution jet at the end of the needle stretches and when the electrostatic force is sufficiently high, the solution forms a jet-cone (called Taylor-cone) which is broken into smaller drops. When the droplet is displacing towards the collector plate, the solvent is evaporated and solid particles are deposited on the plate collector (Prabhakaran, Zamani, Felice, & Ramakrishna, 2015; Zhang, Campagne, & Salaün, 2019). On the other hand, electrospinning is recognized as the most versatile, convenient, and facile process to generate ultrathin nanofibers (Lv et al., 2018). This technique consists is a polymer solution spinning process driven by electrical force where involves the application of an electrical field, induced by a high-voltage power supply, between the polymer solution in a spinneret and a collector plate (Wang & Hsiao, 2016). Accordingly, the solvent evaporates while the jet grows longer and thinner until it is collected on the collector plate in the form of micro- and nanofibers (Drosou, Krokida, & Biliaderis, 2018). Also, prolamin nanofiber membranes can be obtained by electrospinning with high surface-to-volume ratio, large porosity, controllability of nanofiber properties (chemical composition, structure, morphology, diameter, etc.), and easiness of functionalization (Qiao et al., 2019; Zhang, Wang, et al., 2017, Zhang, Qiao, et al., 2017). Fig. 6a and b show the structure of electrospraying and electrospinning equipment respectively. Several studies to obtain micro-/nanofibers and micro-/nanoparticles from prolamines by these methods have been reported.

Xiao, Li, et al. (2016), Xiao, Shi, et al. (2016), Xiao, Wang, et al. (2016) reported nanofibers from sorghum prolamins (kafirin) of and PolyCaproLactone (PCL) with mechanical properties, wettability, and release profile. Development of the nanofibers was from the

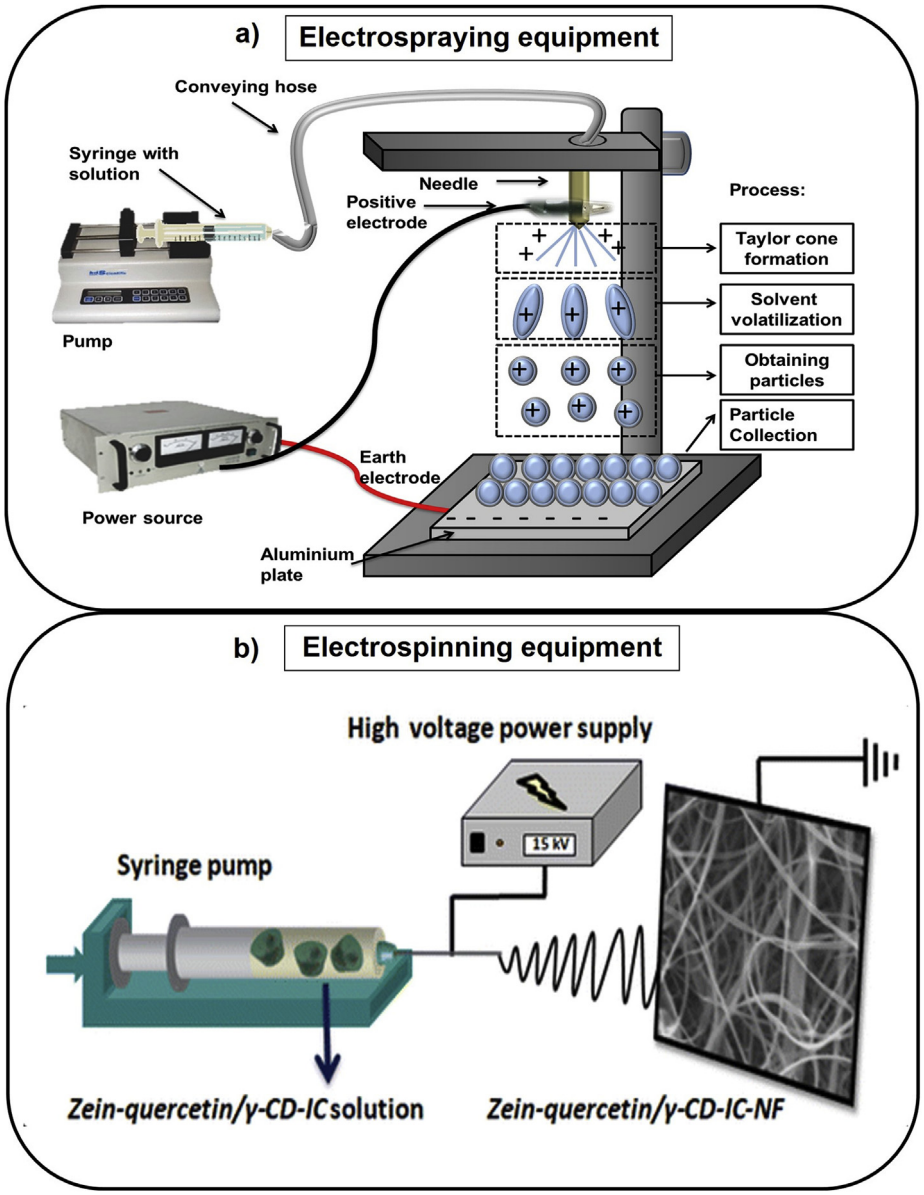

Fig. 6. Electrohydrodynamic atomization techniques for obtaining nanospheres and nanofibers from prolamins. a) electrospraying technique (Tapia-Hernández et al., 2017), b) electrospinning technique (Aytac, Ipek, Durgun, & Uyar, 2018).

electrospinning process. First, the primary solutions were made: 20% (w/v) of kafirin and 10% (w/v) of PCL were dissolved in acetic acid/dichloromethane with a ratio of 4:1 (v/v), separately. Then, different ratios of solvents containing kafirin to PCL were obtained. The conditions of the electrospinning equipment were 17.5 kV, 0.8 mL h^{-1}, and an 8-cm distance. The results demonstrated kafirin/PCL nanofibers from 300 to 500 nm for all treatments.

Xu et al. (2017) employed wheat prolamin (gliadin) as base material, and these authors elaborated nanofibers to study the effect of drug distribution in nanofibers. The technique for obtaining nanofibers was electrospinning. First, different solutions containing different concentrations of gliadin between 5 and 25% (w/v) were obtained using 1,1,1,3,3,3-HexaFluoro-2-Propanol (HFIP) as solvent. Electrospinning conditions included room temperature with 58% humidity, a voltage of 15 kV, a flow rate of 2.5 mL h^{-1}, and a collector distance of 15 cm. Ibuprofen was placed by means of a coaxial electrospray modification. The average diameter of the nanofibers was around 500 nm; in addition, distribution of the drug in the fiber was observed to be throughout the nanofiber and in the center, depending on the treatment.

Yang, Zhang, Liu, Wang, and Yu (2018) elaborated wheat prolamin (gliadin) nanoparticles to encapsulate meletin (a flavonoid used against diabetes). The method these authors used was that of electrospraying as a solution containing 6% (w/v) of gliadin and 1% (w/v) of meletin with a 50:50 mixture of trifluoroacetic acid and trifluoroethanol. Equipment conditions were 21 kV, 1 mL h^{-1}, and a 15 cm distance. The results revealed the obtaining of nanospheres, and all of the meletin was homogeneous in the zein nanospheres Tapia-Hernández et al. (2019) related the parameters of the polymer solution such as viscosity, density, surface tension and equipment parameters such as, applied voltage, flow rate and collector distance in the morphology and particle size of nanoparticles from corn prolamin (zein, polymer matrix) and gallic acid (bioactive compounds) as starting materials. The results were that at a low concentration of gallic acid (1% (w/v), low viscosity (0.00464 ± 0.00001 Pa s), low density (0.886 ± 0.00002 g cm^{-3}) and high electrical conductivity (69 ± 4.3 μs cm^{-1}) promote the formation of a stable Taylor-cone. In addition to high voltage (15 kV), low speed flow (0.1 mL^{-1}) and short distance (10 cm), spherical, compact, and smaller diameter nanoparticles were produced.

Sharif, Golmakani, Niakousari, Ghorani, and Lopez-Rubio (2019) elaborated nanostructures from wheat prolamin (gliadin). They evaluated the parameters of the polymer solution such as concentration, viscosity, surface tension and electrical conductivity and equipment parameters such as applied voltage and flow rate. The results showed that as the prolamin concentration increased from 5 to 35% (w/v), the viscosity increased from 61.73 ± 1.06 to 7880.1 ± 2.16 mPa s, the surface tension from 28.03 ± 0.11 to 29.73 ± 0.46 mN.m^{-1} and electrical conductivity from 19.68 ± 0.16 to 119.10 ± 0.14 μs cm^{-1}. These changes were evident in the morphology where 5% (w/v) not show a material due to the lack of entanglement of wheat prolamin, while at 10% (w/v) particles were obtained and 15, 20 and 25% (w/v) fibers with beads were obtained, while at 30 and 35% (w/v) fibers were obtained. The formation of fibers is due to the increase in molecular entanglements that prevented the breakage of the polymer. The voltage of 15–18 kV decreased the particle size and the flow rate had no impact (from 1 to 0.5 mL h^{-1}).

6.1.2. Antisolvent-precipitation technique

Antisolvent precipitation is a widely used technique for obtain micro- and nanosuspensions and easily scaled for industrial production (Shariare, Sharmin, Jahan, Reza, & Mohsin, 2018). Its based in a solution of a hydrophobic compound (prolamins) dissolved in an organic solvent (organic phase) is added to an aqueous solvent (aqueous phase) containing one or more hydrophilic biopolymers which induces supersaturation process and thereby the driving force for nucleation, growth processes and formation of particles (Doost, Muhammad, Stevens, Dewettinck, & Van der Meeren, 2018; Ozkan, Franco, De Marco, Xiao, & Capanoglu, 2019). Fig. 7 shows schematically the production of prolamin nanoparticles by antisolvent-precipitation and some studies are shown below.

Xiao, Wang, Gonzalez, and Huang (2016) obtained nanoparticles of sorghum prolamin (kafirin) by antisolvent-precipitation. Firtly, the organic phase was performing from 0.4 g sorghum prolamin and dissolved in 3 mL acetic acid to form stock solution. After the organic phase was added drop by drop to 17 mL of aqueous phase. The acetic acid was removed by dialysis and NaCl was added for the dispersion by ionic strength. The results showed two populations of particle size 90 and 340 nm and AFM confirmed the formation of roughly spherical particles.

Yang, Dai, Sun, and Gao (2018) elaborated nanoparticles by antisolvent-precipitation of wheat prolamin (gliadin) -lecithin for the encapsulation of curcumin. The method was based on mixing in an organic phase of ethanol-water (70-30% v/v) with wheat prolamin, followed by lecithin and curcumin. After, 20 mL of organic phase was added to 100 mL of aqueous phase (distilled water) and the pH was adjusted to 4 with 1 M HCl. The suspension was centrifuged to eliminate aggregates or free curcumin. The results showed nanoparticles with spherical morphology and size of 122.1 ± 1.6 nm.

Ren et al. (2018) employed corn prolamin (zein) to encapsulate felodipine (a drug for hypertension). For preparation of nanoparticles, different concentrations of zein were studied at alkaline pH (11.5). The zein solutions were stirred at 800 rpm and Felodipine was added at different concentrations. For the formation of the zein-Felodipine solution, 3 mL of Felodipine solution in 100 mL of zein solution was added. Then, hydrochloric acid was added to precipitate zein and to form the complex. Then, the suspension was stirred and passed through a millipore membrane (0.45-μm), and the samples were dried. The results demonstrated particle sizes ranging from 150 to 300 nm.

Boostani et al., 2019 reported the fabrication of barley prolamins (hordein) nanoparticles by antisolvent precipitation method. Firtly, one part of heat-treated or non-treated prolamin dispersions was gradually added to three parts of deionized water within 2 min under vigorous shaking. A turbid dispersion was immediately formed with an ethanol content of about 18% (v/v). After, the pH was adjusted to 4 and the solvent was evaporated in a rotary-evaporated to almost reach the particle concentration required for the emulsification (about 1% w/v). The final dispersion was stored at 4 °C until analysis. The results showed that the heating reduced the particle size, from 402 to 338 nm. Also, heat treatment might induce an increase in the hydrophobicity of individual prolamin molecules, facilitating the formation of particles by increase in the hydrophobicity of individual prolamin molecules.

6.1.3. Spray drying/nano spray drying techniques

Spray drying and nano spray drying are mechanical techniques, simple, fast, reproducible, and scalable drying technology (Arpagaus, Collenberg, Rütti, Assadpour, & Jafari, 2018), which can be used to prepare powders or submicron particles from a solution, nanoemulsion, or nanosuspension in dry forms with high yields (Arpagaus, John, Collenberg, & Rütti, 2017; Faheem & Haggag, 2015). Spray drying and nano spray drying are a suitable one-step process and its defined as the transformation of a fluid from a liquid state into a dried particulate form by spraying the fluid into a hot drying médium (Arpagaus et al., 2017). The dried powder form by these techniques has higher stability, better protection from the environment as oxidation, light, and temperature, easier handling and storage, and redispersibility in aqueous solutions (Arpagaus et al., 2017). Specifically, nano spray drying is an emerging technology recently invented by Büchi® in 2010 and utilizes a vibration mesh spray technology to create millions of tiny droplets that are quickly dried by a laminar heating flow, which is designed to provide gentle heating with inlet temperature ranging from 0 °C to 120 °C (Wang, Hu, Zhou, Xue, & Luo, 2016). Fig. 8 shows the principle of the nano spray dryer B-90 and some studies from prolamins are discussed below.

Chang, Wang, Hu, and Luo (2017) prepared nanoparticles of corn prolamin (zein)-caseinate-polysaccharide complex by nano spray drying. First nanoemulsion by liquid-liquid dispersion was carried out

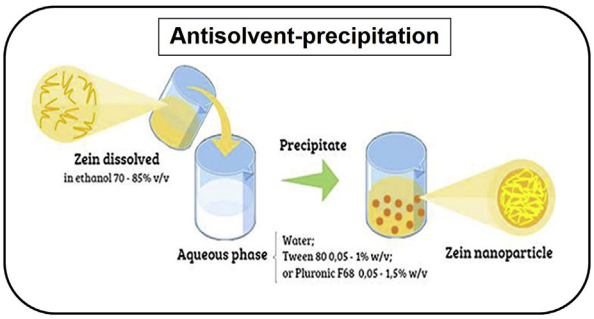

Fig. 7. Antisolven-precipitation technique for obtaining of nanospheres from prolamins (Pascoli, de Lima, & Fraceto, 2018).

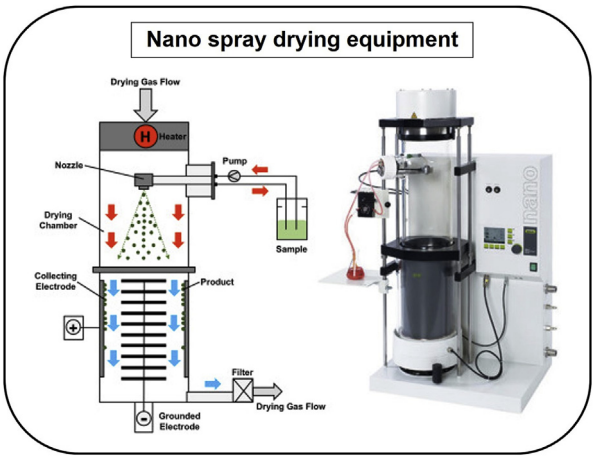

Fig. 8. Nano spray drying technique for obtaining of nanospheres from prolamins by Nano Spray Dryer B-90 (Wang, Hu, et al., 2016).

with adjusted pH, heating and cross-linking. Three polysaccharides were evaluated for complexation, pectin, carboxymethyl cellulose and gum arabic. After the nanoemulsions were subjected to a nano spray drying equipment and the morphology was evaluated. Corn prolamin-caseinate-pectin formed a powder with spherical and resdispersible particles, on the other hand, corn prolamin-caseinate-carboxymethyl cellulose formed a powder with collapsed but redispersible particles and corn prolamin-caseinate-gum arabic formed large aggregates, collapsed dust and not were redispersible. The morphology of the particle was more attributed to the type of polysaccharide than to the corn prolamin. The morphology of the complexation with gum arabic is mainly due to the small molecular weight and the flexible structure of the gum arabic that contains glycoproteins and polysaccharides.

6.2. Fabrication of micro- and nanomaterials from prolamins cereal by-product

Currently, to our knowledge, there has been no research reporting the use of prolamines from the by-products of cereals to obtain nanofibers, and only about 2% of the total researches conducted in nanotechnology employ prolamins to obtain nanospheres from cereal by-products. However, the use of these by-products in nanotechnology would supply added value and help to mitigate environmental pollution. Therefore, it is important to conduct research in this regard. The few studies used sorghum prolamin, are reported below.

Lau et al. (2015) extracted sorghum prolamins (kafirin) from DDGS and performed their functionalization by forming microspheres with prednisolone. The extraction methodology was presented in section 5.3. The formation of nanoparticles was from the addition of prolamins extract in an ethanolic solution (70% v/v) with prednisolone and after added NaCl 0.1 M. The results showed that the extraction of prolamins was from 6 ± 0.2 g/100 g db and the SEM micrographs demonstrated the presence of spherical particles with a textured surface that were varied in size. Similarly, Lau et al., 2017 reported the obtaining of microspheres from sorghum prolamin extracted of DDGS for encapsulation of prednisolone. The loading efficiency ranged from 5.26% to 36.92% and SEM micrographs showed spherical particles with different size. The surface structure of the microspheres without prednisolone was irregular and crinkled, while with prednisolone were generally more crenated.

6.3. Applications of micro- and nanomaterials from cereal prolamins

Particles and fiber from prolamins have application in the food and pharmaceutical industry as protection of bioactive compounds, pickering emulsions stabilized, drug delivery system, antibacterial, antioxidant and anticancer carrier. The different applications of prolamins are due to their easy interaction to trap other molecules mainly of hydrophobic type such as drugs, phenolic compounds, carotenoids, nitrogen fertilizers (Liu, Shao, Luo, Bian, & Yu, 2018; Dehcheshmeh & Fathi, 2019; Horuz & Belibağlı, 2019; Castro-Enríquez et al., 2019).

6.3.1. Protection of bioactive compounds

Bioactive compounds are abundantly found in fruits, vegetables, cereals, pulses, roots and other plant sources (Shishir, Xie, Sun, Zheng, & Chen, 2018). These commonly called phytochemicals obtained from plants are classifieds in polyphenols terpenoids, alkaloids, betalains, nitrogen containing compounds (sinigrin, alliin), lipids (fatty acids, triglycerides) and essential oils (Labuschagne, 2018). Bioactive compounds have emerged as a health-beneficial therapeutic agent, potentiating the design of novel supplements and functional food products (Đorđević et al., 2015). However, have low bioavailability and are very susceptible to degradation by environmental factors such as photosensistive and thermolabile, or body factors such as pH and enzymes (Tapia-Hernández, Rodríguez-Felix, Juárez-Onofre et al., 2018, Tapia-Hernández, Rodríguez-Félix, Plascencia-Jatomea et al., 2018).

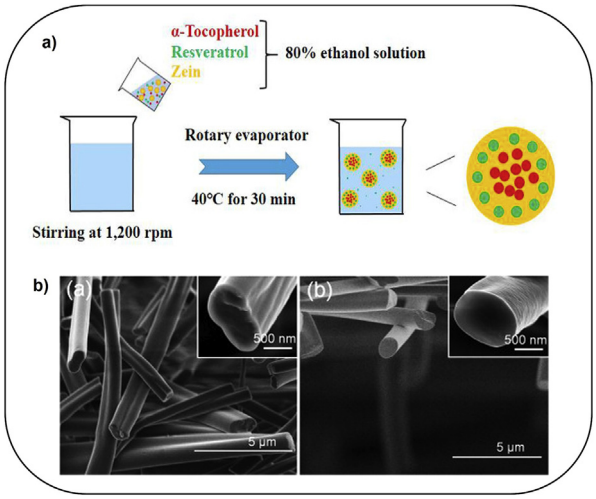

Fig. 9. Prolamins in protection of bioactive compounds. a) Process of obtaining corn prolamin nanoparticles for co-encapsulation of α-tocopherol and resveratrol (Zhang, Khan, Cheng, & Liang, 2019). b) SEM micrographs of corn prolamin fibers-gallic acid for protection of gallic acid (Yang, Zha, Yu, & Liu, 2013).

Therefore, nanoencapsulation in prolamin matrices could be a good option to avoid these disadvantages. Fig. 9a show the obtain of corn prolamin nanoparticles for co-encapsulation of α-tocopherol and resveratrol and Fig. 9b show the morphology of zein and ferulic acid nanofiber.

Cheng, Ferruzzi, and Jones (2019) mention that nanoencapsulation of bioactive compounds in corn prolamin (zein) offer unique advantages of low ingredient cost and potentially reduced accessibility to digestive enzymes. Also, have great potential to improve the stability and bioaccessibility of other bioactives such as the carotenoid compound lutein. Liu, Li, Yang, Xiong, and Sun (2017) developed wheat prolamin (gliadin) nanospheres for the nanoencapsulation of proanthocyanidins, which are potent antioxidants and preventing chronic diseases. These nanospheres with size of 114 nm–212 nm, decreases the capture free radicals by donation of phenolic hydrogen atoms (antioxidant activity) due to binding to protein within the particles. The in vitro release study showed that nanoencapsulated proanthocyanidins are more sustained release than non-encapsulated at philological pH evaluated. Liu, Zhou, and Chen (2019) synthesized barley prolamins (hordein)/glutelins nanospheres for the nanoencapsulation of β-carotene prepared using a high pressure homogenizing method. β-carotene has numerous biological functions. The synthesis was completed by breaking microparticles into nanoparticles by pepsin digestion. β-hordein was the major fraction stabilizing liberated nanoparticles (200–300 nm) after pepsin digestion. Also, pressure treatment can enhance the intermolecular β-sheets in β-hordein, resulting in solid interfacial network that could better stabilize nanoparticles in gastric environment than other proteins. This changes make B-hordein less vulnerable under the enzymatic hydrolysis from pepsin, which prefers to attack a hydrophobic or aromatic residue of protein. This is because hordein has very low lysine (~0%) and arginine (~2.7%) content which are the exclusive target amino acids for trypsin promoting greater protection during digestion to β-carotene.

6.3.2. Pickering emulsions stabilized

Emulsions have research interest in the food, dietary supplement, pharmaceutical, and cosmetic industries, why a wide range of products function through emulsion-based formulations (Xiao, Li, & Huang, 2015). However, emulsion can easily be destabilized, therefore strategies for their stabilization must be proposed (Xiao, Li, & Huang, 2016). Three mechanisms have been proposed to pickering emulsions stabilize:

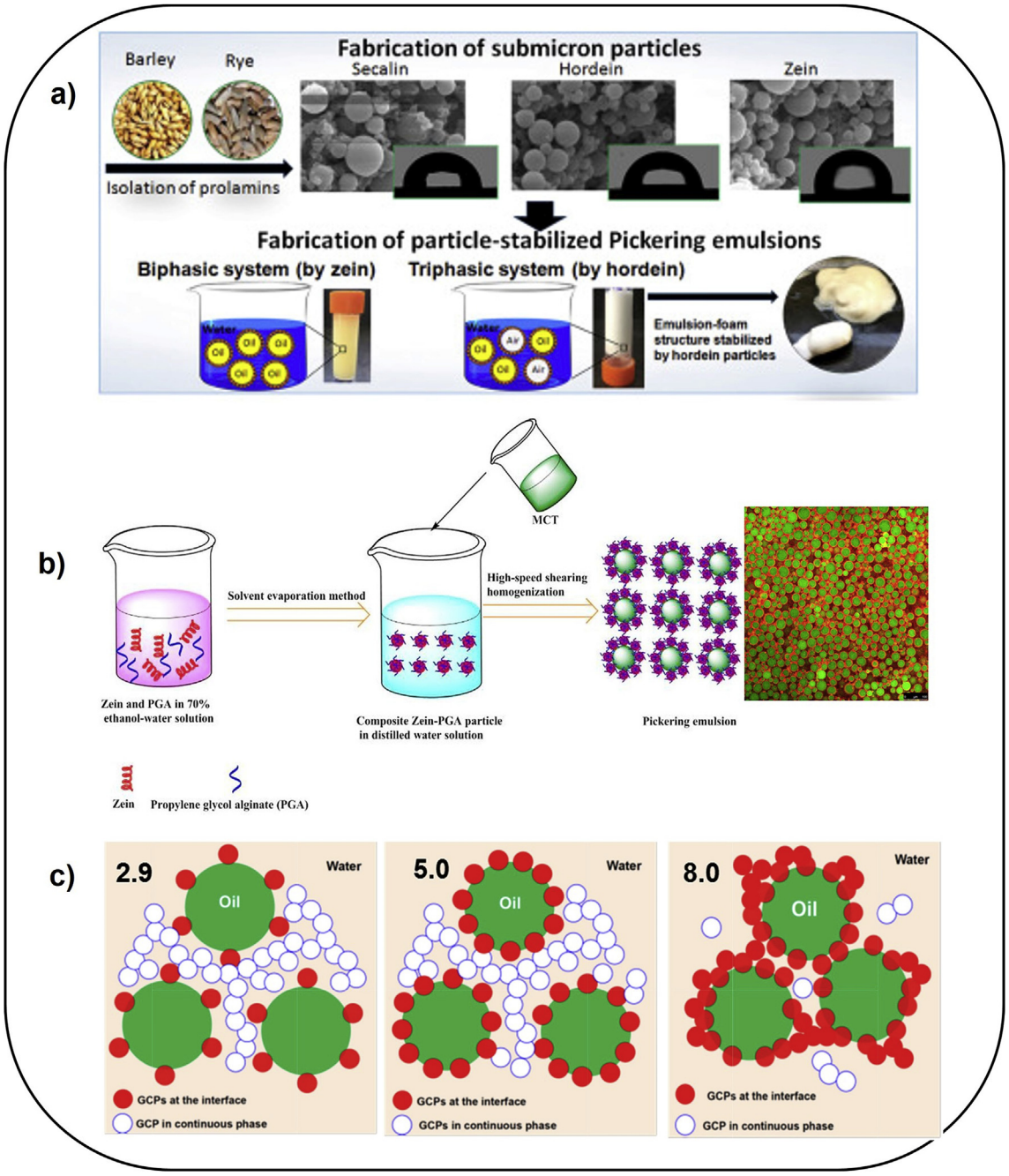

Fig. 10. Prolamins in pickering emulsion stabilizers. a) SEM micrographs of prolamins nanoparticles for applications as pickering emulsion stabilizers (Boostani et al., 2019). b) Method of emulsion stabilization from corn prolamin/PGA nanoparticles (Dai, Sun, et al., 2018). c) Mechanism of pickering emulsions and pickering high internal emulsions stabilized from wheat prolamins (Hu et al., 2016).

1. either reducing interfacial tension through small molecular weight surfactants, 2. forming steric interfacial films via water-soluble proteins and hydrocolloids and 3. forming physical barrier through surface-active colloidal particles (Xiao, Wang, Gonzalez, & Huang, 2016). For food applications by using particles fabricated from food-grade proteins polysaccharides, and polyphenols (Dai, Zhan, Wei, Sun, Mao, McClements, & Gao, 2018). Specifically, prolamins have good properties to Pickering emulsions stabilize when are produced in the form of nanoparticles and can be obtained from of an emulsion or double emulsion (Xiao, Lu, et al., 2017; Zou, Guo, Yin, Wang, & Yang, 2015). Fig. 10a shows obtaining prolamin nanoparticles with application in Pickering emulsions stabilizer. Fig. 10b shows the obtaining of Pickering emulsions stabilizer with corn prolamin/zein-propylene glycol alginate and Fig. 10c show the stabilization mechanism of pickering emulsions.

Prolamin nanoparticles have a number of potential advantages as Pickering emulsion stabilizers because of their ease of preparation. Prolamin such as zein, gliadin, and kafirin, which are by-products of the cereal starch isolation process, are insoluble in water but soluble in concentrated aqueous ethanol solutions (Dai et al., 2019). Liu, Huang, Chen, Deng, and Yang (2019) report that the ease of Pickering emulsions stabilized by corn prolamins nanoparticles is due to the amphiphilic character they possess, that is, around 50% of hydrobic and hydrophilic amino acids. However, pure prolamin nanoparticles can not typically be utilized as particulate emulsifiers due to their unfavorable wettability characteristics (Dai et al., 2019; Zhu, Lu, Zhu, Zhang, & Yin,

2019). Zou, Yang, and Scholten (2019) studied the effect of Pickering emulsions stabilized from corn prolamin and tannic acid complex nanoparticles as a strategy to decrease the hydrophobicity of prolamin nanoparticle. This complex with average diameter of 67.67 ± 1.57 nm at pH 3, then able to stabilize oil-water interfaces. Li et al. (2019) mention that prolamin-polysaccharide complexes nanoparticles have pickering emulsions stabilized via strengthening the interfacial architecture. They studied the effect of wheat prolamin-chitosan complex. The results showed that wheat prolamin–chitosan interactions reduced the surface charges of the particles and improved the wettability of the particles to absorb at the oil–water interface, producing the percolating network structure against coalescence.

However, despite the many studies on prolamins such as Pickering emulsions stabilized, still lack research on prolamins such as hordein in Pickering emulsions stabilized, also still lack research on the addition of other polysaccharides.

6.3.3. Drug delivery system

From prolamins, different systems (nanoparticle, electrospun multilayer nanofibers, nanodepots, and electrosprayed microspheres) have been designed as drug release systems, mainly for oral administration and a slower drug dosing (Fig. 11) (Liu, Zhang, Yu, D. Wu, & Li, 2018). Recent studies of prolamins (alone or with another polymer) for encapsulate drugs have been designed as drug delivery system: corn prolamin nanoparticles with antibiotic (Franco, Reverchon, & De Marco, 2019), corn prolamin nanofibers with triamcinolone acetonide (Mirzaeei, Berenjian, & Khazaei, 2018), wheat prolamin nanoparticles with follic acid and curcumin (Sonekar et al., 2016), wheat prolamin nanofibers with ibuprofen (Xu et al., 2017). These authors, also agree that the drug release system from prolamines promotes a better dosage of the drug and decreases the burst effect.

Wang, Zhang, Zhu, Jiang, and Zhang (2018) designed a drug delivery system as therapy of inflammatory bowel disease. Encapsulated indomethacin in corn prolamin/polydopamine with average size of 9.0 ± 0.8 μm. They mention that this type of microparticles with good physical stability, especially under complex biological conditions, are strongly desired to realice the surface-mediated interaction and controllable drug release behavior. Also, Drug delivery system for dermal application, have also been designed. Sallam and Elzoghby (2018), used corn prolamin for the release of flutamide, a recognized drug to control acne and androgenic alopecia that are due to excess local activity of androgens. This dermal system improved drug penetration and localization in the skin while minimizing permeation.

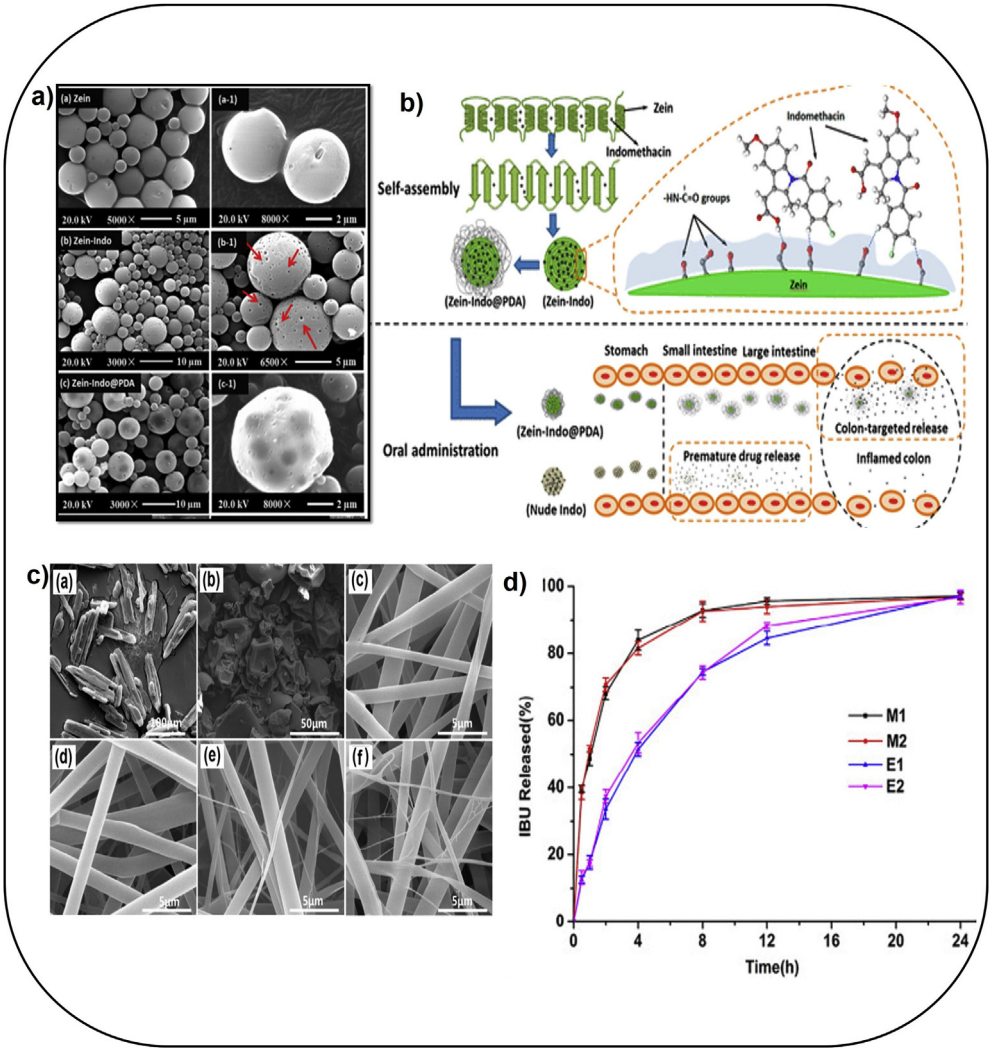

Fig. 11. Prolamins in drug delivery system. a) SEM micrographs of corn prolamin microparticles, corn prolamin-indomethacin microparticles and corn prolamin-indomethacin-PDA microparticles and b) drug delivery system mechanism of zein-indomethacin-PDA in colon (Wang, Zhang, Zhu, Jiang, & Zhang, 2018). c) SEM micrographs of wheat prolamins fibers at different concentrations of ibuprofen (1, 2 and 5%) and two eletrospinning methods (coaxial and tradicional), and d) electrospun wheat prolamins fibers on drug-release as a function of time (Xu et al., 2017).

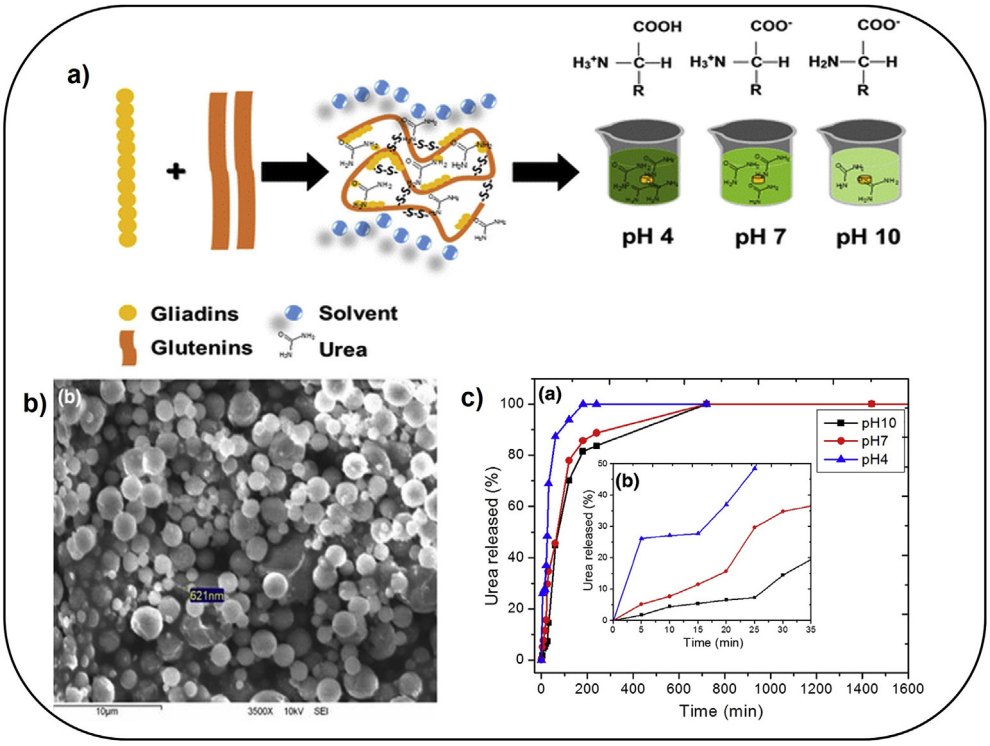

Fig. 12. Prolamins as controlled release fertilizer. a) fiber membrane from wheat gluten and its evaluation at different pH (Dorame-miranda et al., 2018). b) SEM micrograph and c) urea release from glutenin microparticles (Castro-Enríquez, 2019).

6.3.4. Controlled release fertilizer

Fertilisers are agrochemical materials added to soil to supply required nutrients for plant growth (Noruzi et al., 2016). Nowadays, the main problematic in agriculture is the loss of fertilizers to the environment by different mechanisms producing environmental pollution (Barreras-Urbina et al., 2018). Therefore, is important improve fertilizers efficacy and the use of controlled release fertilizers has been suggested. Controlled release fertilizer (CRF) is a purposely designed manure that releases fertilizing nutrients in a controlled and delayed manner in synchrony with the sequential needs of plants for nutrients, thus, they provide enhanced nutrient use efficiency along with enhanced yields (Azeem, KuShaari, Man, Basit, & Thanh, 2014). Castro-Enríquez et al. (2012) mention that for the proposed application requires a material that 100% natural, biodegradable, inexpensive and highly available. Prolamins cereals fulfill with these characteristics.

Urea is the main fertilizer worldwide due to its low cost, however is lost to the environment up to 90% by processes such as leaching (Rodríguez-Félix et al., 2014). Dórame-Miranda et al. (2018) reported the effect of pH and temperature on the release kinetics of urea release fertilizer from fiber membrane from wheat gluten (glutenins + gliadin prolamins). Fiber membrane (150 mg) contain urea (60.06 mg) was placed at three pH (4, 7 and 10) and two temperatures (25 and 40 °C) (Fig. 12a). The use of fiber membrane was in pastille form. The results showed at pH 4 and 40 °C, highest release rate of urea was obtained. In contrast, at pH 10 and 25 °C, the release rate of urea was the slowest. The release system studied revealed a potential application of fiber membranes in containing urea in soils mainly at pH 7 and two temperatures. Castro-Enríquez et al. (2019) propose in their study the encapsulation of urea in wheat prolamins microparticles (glutenin) as urea controlled-release system to avoid these losses to the environment. The results demonstrate that 12% of wheat glutenin shows spherical morphology and size of 600 nm to 3 µm with load capacity of 52.9 mg and maximal release kinetics of urea at 12 h (Fig. 12b and c). Therefore, this material has potential use as a controlled-release fertilizer in agricultural.

7. Conclusions

Prolamins can be obtained from the by-products of cereals such as wheat, corn, and sorghum. The industries that generate these by-products are producers starch, edible ethanol, and bioethanol. The main by-products are derived from wet-milling, such as Gluten Meals (GM), and from dry-milling, such as Distillers Dried Grains with Soluble (DDGS). The advantages of obtaining these from by-products is to provide added value and aid in mitigating environmental pollution. In addition, the conformational structure of prolamins render them feasible for producing various micro- and nanomaterials with application in protection of bioactive compounds, pickering emulsions stabilized, drug delivery system and controlled release fertilizer. Future prolamin research in micro- and nanotechnology from the by-products of cereals is necessary.

Acknowledgments

José Agustín Tapia-Hernández, M.Sc., thanks CONACYT for the scholarship granted.

References

Abudabos, A. M., Al-Atiyat, R. M., Stanley, D., Aljassim, R., & Albatshan, H. A. (2017). The effect of corn distiller's dried grains with solubles (DDGS) fortified with enzyme on growth performance of broiler. *Environmental Science and Pollution Research, 24*(26), 21412–21421.

Adedeji, A. A., Zhou, Y., Fang, X., Davis, D. A., Fahrenholz, A., & Alavi, S. (2017). Utilization of sorghum distillers dried grains in extruded and steam pelleted shrimp diets. *Aquaculture Research, 48*(3), 883–898.

Ali, S., Khatri, Z., Oh, K. W., Kim, I. S., & Kim, S. H. (2014). Zein/cellulose acetate hybrid nanofibers: Electrospinning and characterization. *Macromolecular Research, 22*(9), 971–977.

Amagliani, L., O'Regan, J., Kelly, A. L., & O'Mahony, J. A. (2017). Composition and protein profile analysis of rice protein ingredients. *Journal of Food Composition and Analysis, 59*, 18–26.

Appiah-Nkansah, N. B., Zhang, K., Rooney, W., & Wang, D. (2018). Ethanol production from mixtures of sweet sorghum juice and sorghum starch using very high gravity fermentation with urea supplementation. *Industrial Crops and Products, 111*, 247–253.

Arpagaus, C., Collenberg, A., Rütti, D., Assadpour, E., & Jafari, S. M. (2018). Nano spray drying for encapsulation of pharmaceuticals. *International Journal of Pharmaceutics, 546*(1-2), 194–214.
Arpagaus, C., John, P., Collenberg, A., & Rütti, D. (2017). Nanocapsules formation by nano spray drying. *Nanoencapsulation technologies for the food and nutraceutical industries Elsevier* (pp. 346–401). Gorgan, Iran: Academic Press.
Aytac, Z., Ipek, S., Durgun, E., & Uyar, T. (2018). Antioxidant electrospun zein nanofibrous web encapsulating quercetin/cyclodextrin inclusion complex. *Journal of Materials Science, 53*(2), 1527–1539.
Azeem, B., KuShaari, K., Man, Z. B., Basit, A., & Thanh, T. H. (2014). Review on materials & methods to produce controlled release coated urea fertilizer. *Journal of Controlled Release, 181*, 11–21.
Bamdad, F., Wu, J., & Chen, L. (2011). Effects of enzymatic hydrolysis on molecular structure and antioxidant activity of barley hordein. *Journal of Cereal Science, 54*(1), 20–28.
Barreras-Urbina, C. G., Rodríguez-Félix, F., López-Ahumada, G. A., Burruel-Ibarra, S. E., Tapia-Hernández, J. A., Castro-Enríquez, D. D., et al. (2018). Microparticles from wheat-gluten proteins soluble in ethanol by nanoprecipitation: Preparation, characterization, and their study as a prolonged-release fertilizer. *International Journal of Polymer Science, 2018*.
Bean, S., & Ioerger, B. P. (2014). Sorghum and millet proteins. *Applied Food Protein Chemistry,* 323–359.
Bellemare, M. F., Çakir, M., Peterson, H. H., Novak, L., & Rudi, J. (2017). On the measurement of food waste. *American Journal of Agricultural Economics, 99*(5), 1148–1158.
Belton, P. S., Delgadillo, I., Halford, N. G., & Shewry, P. R. (2006). Kafirin structure and functionality. *Journal of Cereal Science, 44*(3), 272–286.
Bessaire, T., Tarres, A., Stadler, R. H., Wermann, S., Hofmann, J., Theurillat, V., et al. (2016). Mepiquat: A process-induced byproduct in roasted cereal-based foodstuffs. *Journal of Agricultural and Food Chemistry, 64*(5), 1185–1190.
Bhadra, R., Rosentrater, K., & Muthukumarappan, K. (2017). Modeling distillers dried grains with solubles (DDGS) mass flow rate as affected by drying and storage conditions. *Cereal Chemistry, 94*(2), 298–309.
Bhushan, B. (2017). Introduction to nanotechnology. *Springer handbook of nanotechnology* (pp. 1–19). (4th ed.). Berlin, Heidelberg: Springer.
Bhushani, J. A., Kurrey, N. K., & Anandharamakrishnan, C. (2017). Nanoencapsulation of green tea catechins by electrospraying technique and its effect on controlled release and in-vitro permeability. *Journal of Food Engineering, 199*, 82–92.
Biancaniello, M., Wang, T., Misra, M., & Mohanty, A. K. (2018). Plywood adhesives derived from distillers' dried grains with solubles (DDGS) incorporating 2-hydroxyethyl acrylate. *Journal of Applied Polymer Science, 135*(6).
Biesiekierski, J. R. (2017). What is gluten? *Journal of Gastroenterology and Hepatology, 32*(S1), 78–81.
Boostani, S., Hosseini, S. M. H., Yousefi, G., Riazi, M., Tamaddon, A. M., & Van der Meeren, P. (2019). The stability of triphasic oil-in-water Pickering emulsions can be improved by physical modification of hordein-and secalin-based submicron particles. *Food Hydrocolloids, 89*, 649–660.
Böttger, C., & Südekum, K. H. (2018). Review: protein value of distillers dried grains with solubles (DDGS) in animal nutrition as affected by the ethanol production process. *Animal Feed Science and Technology, 244*, 11–17.
Brancoli, P., Ferreira, J. A., Bolton, K., & Taherzadeh, M. J. (2018). Changes in carbon footprint when integrating production of filamentous fungi in 1st generation ethanol plants. *Bioresource Technology, 249*, 1069–1073.
Bunce, N. A. C., White, R. P., & Shewry, P. R. (1985). Variation in estimates of molecular weights of cereal prolamins by SDS-PAGE. *Journal of Cereal Science, 3*(2), 131–142.
Burange, A., Clark, J. H., & Luque, R. (2016). Trends in food and agricultural waste valorization. *EIBC,* 1–10.
Castro-Enríquez, D. D., Castillo-Ortega, M. M., Romero-García, J., Rodríguez-Félix, D. E., Dórame-Miranda, R. F., Torres-Arreola, W., et al. (2019). Development of microparticles from wheat glutenins by electrospray and potential application as controlled-release fertilizers. *Bulletin of Materials Science, 42*(1), 41.
Castro-Enríquez, D., Rodríguez-Félix, F., Ramírez-Wong, B., Torres-Chávez, P., Castillo-Ortega, M., Rodríguez-Félix, D., et al. (2012). Preparation, characterization and release of urea from wheat gluten electrospun membranes. *Materials, 5*(12), 2903–2916.
Celus, I., Brijs, K., & Delcour, J. A. (2006). The effects of malting and mashing on barley protein extractability. *Journal of Cereal Science, 44*(2), 203–211.
Chang, C., Wang, T., Hu, Q., & Luo, Y. (2017). Caseinate-zein-polysaccharide complex nanoparticles as potential oral delivery vehicles for curcumin: Effect of polysaccharide type and chemical cross-linking. *Food Hydrocolloids, 72*, 254–262.
Chang, C., Wang, T., Hu, Q., Zhou, M., Xue, J., & Luo, Y. (2017). Pectin coating improves physicochemical properties of caseinate/zein nanoparticles as oral delivery vehicles for curcumin. *Food Hydrocolloids, 70*, 143–151.
Chatzifragkou, A., Kosik, O., Prabhakumari, P. C., Lovegrove, A., Frazier, R. A., Shewry, P. R., et al. (2015). Biorefinery strategies for upgrading distillers' dried grains with solubles (DDGS). *Process Biochemistry, 50*(12), 2194–2207.
Chatzifragkou, A., Prabhakumari, P. C., Kosik, O., Lovegrove, A., Shewry, P. R., & Charalampopoulos, D. (2016). Extractability and characteristics of proteins deriving from wheat DDGS. *Food Chemistry, 198*, 12–19.
Chaudhary, J. D., Pavaya, R. P., Malav, J. K., Dipika, G., Chaudhary, N., Kuniya, N. K., et al. (2018). Effect of nitrogen and potassium on yield, nutrient content and uptake by forage sorghum (Sorghum bicolor (L.) Moench) on loamy sand. *International Journal of Communication Systems, 6*(2), 761–765.
Cheng, C. J., Ferruzzi, M., & Jones, O. G. (2019). Fate of lutein-containing zein nanoparticles following simulated gastric and intestinal digestion. *Food Hydrocolloids, 87*, 229–236.
Cheng, C. J., & ones, O. G. (2017). Stabilizing zein nanoparticle dispersions with ι-carrageenan. *Food Hydrocolloids, 69*, 28–35.
Chen, X., Li, D., Li, G., Luo, L., Ullah, N., Wei, Q., et al. (2015). Facile fabrication of gold nanoparticle on zein ultrafine fibers and their application for catechol biosensor. *Applied Surface Science, 328*, 444–452.
Chen, C., Somavat, P., Singh, V., & de Mejia, E. G. (2017). Chemical characterization of proanthocyanidins in purple, blue, and red maize coproducts from different milling processes and their anti-inflammatory properties. *Industrial Crops and Products, 109*, 464–475.
Chen, J., Zheng, J., McClements, D. J., & Xiao, H. (2014). Tangeretin-loaded protein nanoparticles fabricated from zein/β-lactoglobulin: Preparation, characterization, and functional performance. *Food Chemistry, 158*, 466–472.
Chen, H., & Zhong, Q. (2014). Processes improving the dispersibility of spray-dried zein nanoparticles using sodium caseinate. *Food Hydrocolloids, 35*, 358–366.
Chen, H., & Zhong, Q. (2015). A novel method of preparing stable zein nanoparticle dispersions for encapsulation of peppermint oil. *Food Hydrocolloids, 43*, 593–602.
Connolly, A., Cermeño, M., Crowley, D., O'Callaghan, Y., O'Brien, N. M., & FitzGerald, R. J. (2018). Characterisation of the in vitro bioactive properties of alkaline and enzyme extracted brewers' spent grain protein hydrolysates. *Food Research International, 121*, 524–532.
Connolly, A., Piggott, C. O., & FitzGerald, R. J. (2013). Characterisation of protein-rich isolates and antioxidative phenolic extracts from pale and black brewers' spent grain. *International Journal of Food Science & Technology, 48*(8), 1670–1681.
Cook, R. B., Mallee, F. M., & Shulman, M. L., (1993). U.S. Patent No. 5,254,673. Washington, DC: U.S. Patent and Trademark Office.
Dai, L., Sun, C., Wei, Y., Mao, L., & Gao, Y. (2018a). Characterization of Pickering emulsion gels stabilized by zein/gum Arabic complex colloidal nanoparticles. *Food Hydrocolloids, 74*, 239–248.
Dai, L., Yang, S., Wei, Y., Sun, C., McClements, D. J., Mao, L., et al. (2019). Development of stable high internal phase emulsions by pickering stabilization: Utilization of zein-propylene glycol alginate-rhamnolipid complex particles as colloidal emulsifiers. *Food Chemistry, 275*, 246–254.
Dai, L., Zhan, X., Wei, Y., Sun, C., Mao, L., McClements, D. J., et al. (2018b). Composite zein-propylene glycol alginate particles prepared using solvent evaporation: Characterization and application as Pickering emulsion stabilizers. *Food Hydrocolloids, 85*, 281–290.
De Santis, M. A., Giuliani, M. M., Giuzio, L., De Vita, P., Lovegrove, A., Shewry, P. R., et al. (2017). Differences in gluten protein composition between old and modern durum wheat genotypes in relation to 20th century breeding in Italy. *European Journal of Agronomy, 87*, 19–29.
Dehcheshmeh, M. A., & Fathi, M. (2019). Production of core-shell nanofibers from zein and tragacanth for encapsulation of saffron extract. *International Journal of Biological Macromolecules, 122*, 272–279.
Deng, L., Zhang, X., Li, Y., Que, F., Kang, X., Liu, Y., et al. (2018). Characterization of gelatin/zein nanofibers by hybrid electrospinning. *Food Hydrocolloids, 75*, 72–80.
DeOliveira, V., Brooks, K., & Nogueira, L. (2017). *A short introduction to the Distillers' dried grains export market*.
Dhillon, G. S., Kaur, S., Oberoi, H. S., Spier, M. R., & Brar, S. K. (2017). Agricultural-based protein by-products: Characterization and applications. In G. S. Dhillon (Ed.). *In protein byprodcts* (pp. 21–36). Edmonton AB, Canada: Academic Press, Elsevier.
Diao, X. (2017). Production and genetic improvement of minor cereals in China. *Crop Journal, 5*(2), 103–114.
Díaz-Gómez, J. L., Castorena-Torres, F., Preciado-Ortiz, R. E., & García-Lara, S. (2017). Anti-Cancer activity of maize bioactive peptides. *Frontiers in Chemistry, 5*, 44.
Dippold, D., Tallawi, M., Tansaz, S., Roether, J. A., & Boccaccini, A. R. (2016). Novel electrospun poly (glycerol sebacate)–zein fiber mats as candidate materials for cardiac tissue engineering. *European Polymer Journal, 75*, 504–513.
Doost, A. S., Muhammad, D. R. A., Stevens, C. V., Dewettinck, K., & Van der Meeren, P. (2018). Fabrication and characterization of quercetin loaded almond gum-shellac nanoparticles prepared by antisolvent precipitation. *Food Hydrocolloids, 83*, 190–201.
Dórame-Miranda, R. F., Rodríguez-Félix, D. E., López-Ahumada, G. A., Castro-Enriquez, D. D., Quiroz-Castillo, J. M., Márquez-Ríos, E., et al. (2018). Effect of pH and temperature on the release kinetics of urea from wheat-gluten membranes obtained by electrospinning. *Polymer Bulletin, 75*(11), 5305–5319.
Drosou, C., Krokida, M., & Biliaderis, C. G. (2018). Composite pullulan-whey protein nanofibers made by electrospinning: Impact of process parameters on fiber morphology and physical properties. *Food Hydrocolloids, 77*, 726–735.
Ebert, S., Koo, C. K., Weiss, J., & McClements, D. J. (2017). Continuous production of core-shell protein nanoparticles by antisolvent precipitation using dual-channel microfluidization: Caseinate-coated zein nanoparticles. *Food Research International, 92*, 48–55.
Elhassan, M. S., Emmambux, M. N., & Taylor, J. R. (2017). Transgenic sorghum with suppressed synthesis of kafirin subclasses: Effects on flour and dough rheological characteristics. *Journal of Cereal Science, 75*, 69–76.
Elkonin, L. A., Italyanskaya, J. V., Panin, V. M., & Selivanov, N. Y. (2017). Development of transgenic sorghum plants with improved in vitro kafirin digestibility. In Snježana Jurić (Ed.). *Plant engineering* (pp. 91–112). InTech.
Elmalimadi, M. B., Jovanović, J. R., Stefanović, A. B., Tanasković, S. J., Djurović, S. B., Bugarski, B. M., et al. (2017). Controlled enzymatic hydrolysis for improved exploitation of the antioxidant potential of wheat gluten. *Industrial Crops and Products, 109*, 548–557.
Esmaili, Z., Bayrami, S., Dorkoosh, F. A., Akbari Javar, H., Seyedjafari, E., Zargarian, S. S., et al. (2018). Development and characterization of electrosprayed nanoparticles for encapsulation of C urcumin. *Journal of Biomedical Materials Research Part A, 106*(1), 285–292.
Espinosa-Ramírez, J., Garza-Guajardo, I., Pérez-Carrillo, E., & Serna-Saldívar, S. O.

(2017). Differences in the functionality and characterization of kafirins extracted from decorticated sorghum flour or gluten meal treated with protease. *Journal of Cereal Science, 73*, 174–182.
Espinosa-Ramírez, J., & Serna-Saldívar, S. O. (2016). Functionality and characterization of kafirin-rich protein extracts from different whole and decorticated sorghum genotypes. *Journal of Cereal Science, 70*, 57–65.
Etienne, X. L., Trujillo-Barrera, A., & Hoffman, L. A. (2017). Volatility spillover and time-varying conditional correlation between DDGS, corn, and soybean meal markets. *Agricultural and Resource Economics Review, 46*(3), 529–554.
Faheem, A., & Haggag, Y. (2015). Evaluation of nano spray drying as a method for drying and formulation of therapeutic peptides and proteins. *Frontiers in Pharmacology, 6*, 140.
Fang, J., Martínez, Y., Deng, C., Zhu, D., Peng, H., Jiang, H., et al. (2017). Effects of dietary enzymolysis products of wheat gluten on the growth performance, serum biochemical, immune, and antioxidant status of broilers. *Food and Agricultural Immunology,* 1–13.
FAOSTAT (2013). *Food and agricultural commodities production. Final.* Data http://faostat3.fao.org/, Accessed date: 17 April 2019.
Feng, J., Wu, S., Wang, H., & Liu, S. (2017). Gliadin nanoparticles stabilized by a combination of thermally denatured ovalbumin with gemini dodecyl O-glucoside: The modulating effect of cosurfactant. *Colloids and Surfaces A: Physicochemical and Engineering Aspects, 516*, 94–105.
Franco, P., Reverchon, E., & De Marco, I. (2019). Production of zein/antibiotic microparticles by supercritical antisolvent coprecipitation. *The Journal of Supercritical Fluids, 145*, 31–38.
Furtak, K., Gawryjołek, K., Gajda, A. M., & Gałązka, A. (2017). Effects of maize and winter wheat grown under different cultivation techniques on biological activity of soil. *Plant Soil and Environment, 63*(10), 449–454.
Fărcaş, A. C., Socaci, S. A., Dulf, F. V., Tofană, M., Mudura, E., & Diaconeasa, Z. (2015). Volatile profile, fatty acids composition and total phenolics content of brewers' spent grain by-product with potential use in the development of new functional foods. *Journal of Cereal Science, 64*, 34–42.
Gao, X., Liu, T., Ding, M., Wang, J., Li, C., Wang, Z., et al. (2018). Effects of HMW-GS Ax1 or Dx2 absence on the glutenin polymerization and gluten micro structure of wheat (Triticum aestivum L.). *Food Chemistry, 240*, 626–633.
Garcia-Garcia, G., Stone, J., & Rahimifard, S. (2019). Opportunities for waste valorisation in the food industry–A case study with four UK food manufacturers. *Journal of Cleaner Production, 211*, 1339–1356.
Geppert, T. C., Meyer, A. M., Perry, G. A., & Gunn, P. J. (2017). Effects of excess metabolizable protein on ovarian function and circulating amino acids of beef cows: 1. Excessive supply from corn gluten meal or soybean meal. *Animal, 11*(4), 625–633.
Gerile, S., & Pirhonen, J. (2017). Replacement of fishmeal with corn gluten meal in feeds for juvenile rainbow trout (Oncorhynchus mykiss) does not affect oxygen consumption during forced swimming. *Aquaculture, 479*, 616–618.
Ghosh, S., Chowdhury, R., & Bhattacharya, P. (2017). Sustainability of cereal straws for the fermentative production of second generation biofuels: A review of the efficiency and economics of biochemical pretreatment processes. *Applied Energy, 198*, 284–298.
Giteru, S. G., Oey, I., Ali, M. A., Johnson, S. K., & Fang, Z. (2017). Effect of kafirin-based films incorporating citral and quercetin on storage of fresh chicken fillets. *Food Control, 80*, 37–44.
Grootboom, A. W., Mkhonza, N. L., Mbambo, Z., O'Kennedy, M. M., Da Silva, L. S., Taylor, J., et al. (2014). Co-suppression of synthesis of major α-kafirin sub-class together with γ-kafirin-1 and γ-kafirin-2 required for substantially improved protein digestibility in transgenic sorghum. *Plant Cell Reports, 33*(3), 521–537.
Guan, X., Li, L., Liu, J., & Li, S. (2018). Effects of ultrasonic-microwave-assisted technology on hordein extraction from barley and optimization of process parameters using response surface methodology. *Journal of Food Quality, 2018*.
Guerrieri, N., & Cavaletto, M. (2018). Cereals proteins. In R. Y. Yada (Ed.). *Proteins in food processing* (pp. 223–244). (2nd ed.). United Kingdom: Elsevier.
Gupta, M., Abu-Ghannam, N., & Gallaghar, E. (2010). Barley for brewing: Characteristic changes during malting, brewing and applications of its by-products. *Comprehensive Reviews in Food Science and Food Safety, 9*(3), 318–328.
Gupta, J., Wilson, B. W., & Vadlani, P. V. (2016). Evaluation of green solvents for a sustainable zein extraction from ethanol industry DDGS. *Biomass and Bioenergy, 85*, 313–319.
Han, Y., Song, L., Zou, N., Qin, Y., Li, X., & Pan, C. (2017). Rapid multiplug filtration cleanup method for the determination of 124 pesticide residues in rice, wheat, and corn. *Journal of Separation Science, 40*(4), 878–884.
Hatamie, A., Nassiri, M., Alivand, M. D., & Bhatnagar, A. (2018). Trace analysis of nitrite ions in environmental samples by using in-situ synthesized Zein biopolymeric nanoparticles as the novel green solid phase extractor. *Talanta, 176*, 156–164.
Hayes, M., & Bleakley, S. (2018). Peptides from plants and their applications. In S. Koutsopoulos (Ed.). *Peptide applications in biomedicine, biotechnology and bioengineering* (pp. 603–622). United Kingdom: Elsevier.
He, M., Jiang, H., Wang, R., Xie, Y., & Zhao, C. (2017). Fabrication of metronidazole loaded poly (ε-caprolactone)/zein core/shell nanofiber membranes via coaxial electrospinning for guided tissue regeneration. *Journal of Colloid and Interface Science, 490*, 270–278.
Hernández-Espinosa, N., Reyes-Reyes, M., González-Jiménez, F. E., Núñez-Bretón, L. C., & Cooper-Bribiesca, B. L. (2015). The importance of the storage proteins in cereals (prolamins). *Vertientes Revista Especializada en Ciencias de la Salud, 18*(1), 3–7.
Heuzé, V., Tran, G., Sauvant, D., Renaudeau, D., Lessire, M., & Lebas, F. (2018). *Corn gluten meal. Feedipedia, a programme by INRA, CIRAD, AFZ and FAO.* https://www.feedipedia.org/node/715/, Accessed date: 17 April 2019.
Horuz, T.İ., & Belibağlı, K. B. (2019). Nanoencapsulation of carotenoids extracted from tomato peels into zein fibers by electrospinning. *Journal of the Science of Food and Agriculture, 99*(2), 759–766.
Houde, M., Khodaei, N., Benkerroum, N., & Karboune, S. (2018). Barley protein concentrates: Extraction, structural and functional properties. *Food Chemistry, 254*, 367–376.
Huang, X., Dai, Y., Cai, J., Zhong, N., Xiao, H., McClements, D. J., et al. (2017). Resveratrol encapsulation in core-shell biopolymer nanoparticles: Impact on antioxidant and anticancer activities. *Food Hydrocolloids, 64*, 157–165.
Huang, Kanerva, Salovaara, & Sontag-Strohm (2016). Degradation of C-hordein by metal-catalysed oxidation. *Food Chemistry, 196*, 1256–1263.
Hu, K., Huang, X., Gao, Y., Huang, X., Xiao, H., & McClements, D. J. (2015). Core–shell biopolymer nanoparticle delivery systems: Synthesis and characterization of curcumin fortified zein–pectin nanoparticles. *Food Chemistry, 182*, 275–281.
Hu, K., & McClements, D. J. (2015). Fabrication of biopolymer nanoparticles by antisolvent precipitation and electrostatic deposition: Zein-alginate core/shell nanoparticles. *Food Hydrocolloids, 44*, 101–108.
Hu, Y. Q., Yin, S. W., Zhu, J. H., Qi, J. R., Guo, J., Wu, L. Y., et al. (2016). Fabrication and characterization of novel Pickering emulsions and Pickering high internal emulsions stabilized by gliadin colloidal particles. *Food Hydrocolloids, 61*, 300–310.
Izydorczyk, M. S., & Edney, M. (2017). Barley: Grain-Quality characteristics and management of quality requirements. *Cereal grains* (pp. 195–234). Woodhead Publishing.
Janissen, B., & Huynh, T. (2018). Chemical composition and value-adding applications of coffee industry by-products: A review. *Resources, Conservation and Recycling, 128*, 110–117.
Jiang, Y., Zhang, M., Lin, S., & Cheng, S. (2018). Contribution of specific amino acid and secondary structure to the antioxidant property of corn gluten proteins. *Food Research International, 105*, 836–844.
Jiao, Y., Zheng, X., Chang, Y., Li, D., Sun, X., & Liu, X. (2018). Zein-derived peptides as nanocarriers to increase the water solubility and stability of lutein. *Food & Function, 9*(1), 117–123.
Jin, J., Ma, H., Wang, K., Yagoub, A. E. G. A., Owusu, J., Qu, W., et al. (2015). Effects of multi-frequency power ultrasound on the enzymolysis and structural characteristics of corn gluten meal. *Ultrasonics Sonochemistry, 24*, 55–64.
Joelsson, E., Galbe, M., & Wallberg, O. (2014). Heat integration of combined 1st and 2nd generation ethanol production from wheat kernels and wheat straw. *Sustainable Chemical Processes, 2*(1), 20.
Joye, I. J. (2018). Cereal biopolymers for nano-and microtechnology: A myriad of opportunities for novel (functional) food applications. *Trends in Food Science & Technology, 83*, 1–11.
Joye, I. J., Nelis, V. A., & McClements, D. J. (2015a). Gliadin-based nanoparticles: Fabrication and stability of food-grade colloidal delivery systems. *Food Hydrocolloids, 44*, 86–93.
Joye, I. J., Nelis, V. A., & McClements, D. J. (2015b). Gliadin-based nanoparticles: Stabilization by post-production polysaccharide coating. *Food Hydrocolloids, 43*, 236–242.
Karthikeyan, K., Krishnaswamy, V. R., Lakra, R., Kiran, M. S., & Korrapati, P. S. (2015). Fabrication of electrospun zein nanofibers for the sustained delivery of siRNA. *Journal of Materials Science: Materials in Medicine, 26*(2), 101.
Khedkar, R., & Singh, K. (2018). Food industry waste: A panacea or pollution hazard? In T. Jindal (Ed.). *In paradigms in pollution prevention* (pp. 35–47). Cham, India: Springer.
Klímek, P., Wimmer, R., Mishra, P. K., & Kúdela, J. (2017). Utilizing brewer's-spent-grain in wood-based particleboard manufacturing. *Journal of Cleaner Production, 141*, 812–817.
Koga, S., Böcker, U., Wieser, H., Koehler, P., Uhlen, A. K., & Moldestad, A. (2017). Polymerisation of gluten proteins in developing wheat grain as affected by desiccation. *Journal of Cereal Science, 73*, 122–129.
Kong, X., Zhou, H., & Hua, Y. (2008). Preparation and antioxidant activity of wheat gluten hydrol107ysates (WGHs) using ultrafiltration membranes. *Journal of the Science of Food and Agriculture, 88*(5), 920–926.
Kreyling, W. G., Semmler-Behnke, M., & Chaudhry, Q. (2010). A complementary definition of nanomaterial. *Nano Today, 5*(3), 165–168.
Kumar, J., Kumar, M., Pandey, R., & Chauhan, N. S. (2017). Physiopathology and management of gluten-induced celiac disease. *Journal of Food Science, 82*(2), 270–277.
Labuschagne, P. (2018). Impact of wall material physicochemical characteristics on the stability of encapsulated phytochemicals: A review. *Food Research International, 107*, 227–247.
Lal, S. S., Tanna, P., Kale, S., & Mhaske, S. T. (2017). Kafirin polymer film for enteric coating on HPMC and Gelatin capsules. *Journal of Materials Science, 52*(7), 3806–3820.
Landriscina, L., D'Agnello, P., Bevilacqua, A., Corbo, M. R., Sinigaglia, M., & Lamacchia, C. (2017). Impact of gluten-friendly™ technology on wheat kernel endosperm and gluten protein structure in seeds by light and electron microscopy. *Food Chemistry, 221*, 1258–1268.
Larkins, B. A., Wu, Y., Song, R., & Messing, J. (2017). 14 maize seed storage proteins. In B. A. Larkins (Ed.). *Maize Kernel development* (pp. 175–189). Boston: CABI.
Lau, E. T., Johnson, S. K., Stanley, R. A., Mereddy, R., Mikkelsen, D., Halley, P. J., et al. (2015). Formulation and characterization of drug-loaded microparticles using distillers dried grain kafirin. *Cereal Chemistry, 92*(3), 246–252.
Lau, E. T., Johnson, S. K., Williams, B. A., Mikkelsen, D., McCourt, E., Stanley, R. A., et al. (2017). Optimizing prednisolone loading into distiller's dried grain kafirin microparticles, and in vitro release for oral delivery. *Pharmaceutics, 9*(2), 17.
Lee, D., & Tongarlak, M. H. (2017). Converting retail food waste into by-product. *European Journal of Operational Research, 257*(3), 944–956.
Liang, Q., Chalamaiah, M., Ren, X., Ma, H., & Wu, J. (2018). Identification of new anti-inflammatory peptides from zein hydrolysate after simulated gastrointestinal digestion and transport in caco-2 cells. *Journal of Agricultural and Food Chemistry, 66*(5), 1114–1120.

Liang, Q., Ren, X., Zhang, X., Hou, T., Chalamaiah, M., Ma, H., et al. (2018). Effect of ultrasound on the preparation of resveratrol-loaded zein particles. *Journal of Food Engineering, 221*, 88–94.
Li, X. X., Han, L. J., & Chen, L. J. (2008). In vitro antioxidant activity of protein hydrolysates prepared from corn gluten meal. *Journal of the Science of Food and Agriculture, 88*(9), 1660–1666.
Li, M. F., He, Z. Y., Li, G. Y., Zeng, Q. Z., Su, D. X., Zhang, J. L.,., & He, S. (2019). The formation and characterization of antioxidant pickering emulsions: Effect of the interactions between gliadin and chitosan. *Food Hydrocolloids, 90*, 482–489.
Liu, C. K., Chen, C. A., Lee, T. Y., Chang, H. H., Liao, H. F., & Chen, Y. J. (2018c). Rice protein prolamin promotes anti-leukemia immunity and inhibits leukemia growth in vivo. *Food and Chemical Toxicology, 112*, 435–440.
Liu, X., Huang, Y. Q., Chen, X. W., Deng, Z. Y., & Yang, X. Q. (2019a). Whole cereal protein-based Pickering emulsions prepared by zein-gliadin complex particles. *Journal of Cereal Science, 87*, 46–51.
Liu, G., Lamont, K. C., Ahmad, N., Tomkins, A., Mudge, S. R., Gilding, E. K., et al. (2017d). The functionality of α-kafirin promoter and α-kafirin signal peptide. *Plant Cell, Tissue and Organ Culture, 128*(1), 133–143.
Liu, C., Li, M., Yang, J., Xiong, L., & Sun, Q. (2017a). Fabrication and characterization of biocompatible hybrid nanoparticles from spontaneous co-assembly of casein/gliadin and proanthocyanidin. *Food Hydrocolloids, 73*, 74–89.
Liu, F., Ma, C., McClements, D. J., & Gao, Y. (2017b). A comparative study of covalent and non-covalent interactions between zein and polyphenols in ethanol-water solution. *Food Hydrocolloids, 63*, 625–634.
Liu, X., Shao, W., Luo, M., Bian, J., & Yu, D. G. (2018a). Electrospun blank nanocoating for improved sustained release profiles from medicated gliadin nanofibers. *Nanomaterials, 8*(4), 184.
Liu, Z. P., Zhang, Y. Y., Yu, D. G., Wu, D., & Li, H. L. (2018b). Fabrication of sustained-release zein nanoparticles via modified coaxial electrospraying. *Chemical Engineering Journal, 334*, 807–816.
Liu, G., Zhou, Y., & Chen, L. (2019b). Intestinal uptake of barley protein-based nanoparticles for β-carotene delivery. *Acta Pharmaceutica Sinica B, 9*(1), 87–96.
Liu, B. Y., Zhu, K. X., Guo, X. N., Peng, W., & Zhou, H. M. (2017c). Effect of deamidation-induced modification on umami and bitter taste of wheat gluten hydrolysates. *Journal of the Science of Food and Agriculture, 97*(10), 3181–3188.
Louie, J. (2017). Food groups. In J. Mann, & A. S. Truswell (Eds.). *Essentials of human nutrition* (pp. 273–305). (Fourt ed). United Kingdom: Oxford.
Lucio, D., Martínez-Ohárriz, M. C., Jaras, G., Aranaz, P., González-Navarro, C. J., Radulescu, A., et al. (2017). Optimization and evaluation of zein nanoparticles to improve the oral delivery of glibenclamide. In vivo study using C. elegans. *European Journal of Pharmaceutics and Biopharmaceutics, 121*, 104–112.
Luecha, J., & Kokini, J. L. (2016). Molecular organization and topography of prolamin protein films. In N. Sozer (Ed.). *Imaging technologies and Data processing for food engineers* (pp. 243–267). Switzerland: Springer International Publishing.
Luo, Y., & Wang, Q. (2014). Zein-based micro-and nano-particles for drug and nutrient delivery: A review. *Journal of Applied Polymer Science, 131*(16).
Lv, D., Zhu, M., Jiang, Z., Jiang, S., Zhang, Q., Xiong, R., et al. (2018). Green electrospun nanofibers and their application in air filtration. *Macromolecular Materials and Engineering, 303*(12), 1800336.
Lynch, K. M., Steffen, E. J., & Arendt, E. K. (2016). Brewers' spent grain: A review with an emphasis on food and health. *Journal of the Institute of Brewing, 122*(4), 553–568.
Manochio, C., Andrade, B. R., Rodriguez, R. P., & Moraes, B. S. (2017). Ethanol from biomass: A comparative overview. *Renewable & Sustainable Energy Reviews, 80*, 743–755.
McCarthy, A. L., O'Callaghan, Y. C., Neugart, S., Piggott, C. O., Connolly, A., Jansen, M. A., et al. (2013). The hydroxycinnamic acid content of barley and brewers' spent grain (BSG) and the potential to incorporate phenolic extracts of BSG as antioxidants into fruit beverages. *Food Chemistry, 141*(3), 2567–2574.
Mirzaeei, S., Berenjian, K., & Khazaei, R. (2018). Preparation of the potential ocular inserts by electrospinning method to achieve the prolong release profile of triamcinolone acetonide. *Advanced Pharmaceutical Bulletin, 8*(1), 21.
Mishra, B., Zamare, D., & Manikanta, A. (2018). Selection and utilization of agro-industrial waste for biosynthesis and hyper-production of pullulan: A review. In S. J. Varjani, B. Parameswaran, S. Kumar, & S. K. Khare (Eds.). *Biosynthetic technology and environmental challenges* (pp. 89–103). Singapore: Springer.
de Morais Cardoso, L., Pinheiro, S. S., Martino, H. S. D., & Pinheiro-Sant'Ana, H. M. (2017). Sorghum (Sorghum bicolor L.): Nutrients, bioactive compounds, and potential impact on human health. *Critical Reviews in Food Science and Nutrition, 57*(2), 372–390.
Mussatto, S. I. (2014). Brewer's spent grain: A valuable feedstock for industrial applications. *Journal of the Science of Food and Agriculture, 94*(7), 1264–1275.
Mussatto, S. I., Dragone, G., & Roberto, I. C. (2006). Brewers' spent grain: Generation, characteristics and potential applications. *Journal of Cereal Science, 43*(1), 1–14.
NASS-USDA (2018). *National agricultural statistics service, agricultural statistics board, United States department of agricultural, grain crushings and Co-products production.* https://www.nass.usda.gov/Publications/Todays_Reports/reports/cagc1118.pdf/, Accessed date: 17 April 2019.
Nałęcz, D., Dziuba, M., & Szerszunowicz, I. (2017). Isolation of oat (avena sativa L.) total proteins and their prolamin fractions for 2D electrophoresis. In S. Gasparis (Ed.). *Oat: Methods and protocols* (pp. 225–234). New York, NY: Springer, Humana Press.
Negi, R., & Naik, A. (2017). Non-prolamin fraction from brewer's spent grain: A novel plant-based emulsifier. *Journal of Food Measurement and Characterization, 11*(2), 887–893.
Ni, N., & Dumont, M. J. (2017). Protein-based hydrogels derived from industrial by-products containing collagen, keratin, zein and soy. *Waste and Biomass Valorization, 8*(2), 285–300.
Ni, N., Duquette, D., & Dumont, M. J. (2017). Synthesis and characterization of zein-based cryogels and their potential as diesel fuel absorbent. *European Polymer Journal, 91*, 420–428.
Nigam, P. S. (2017). An overview: Recycling of solid barley waste generated as a by-product in distillery and brewery. *Waste Management, 62*, 255–261.
Noruzi, M. (2016). Electrospun nanofibres in agriculture and the food industry: A review. *Journal of the Science of Food and Agriculture, 96*(14), 4663–4678.
Nuez Ortín, W. G., & Yu, P. (2009). Nutrient variation and availability of wheat DDGS, corn DDGS and blend DDGS from bioethanol plants. *Journal of the Science of Food and Agriculture, 89*(10), 1754–1761.
Nuttall, J. G., O'Leary, G. J., Panozzo, J. F., Walker, C. K., Barlow, K. M., & Fitzgerald, G. J. (2017). Models of grain quality in wheat—a review. *Field Crops Research, 202*, 136–145.
Oil World (24 June 2011). 2011. World supply, demand and price forecasts for oilseeds, oils and meals. *Oil World Weekly, 54*(25), 297–308.
de Oliveira Mori, C. L., dos Passos, N. A., Oliveira, J. E., Mattoso, L. H. C., Mori, F. A., Carvalho, A. G., et al. (2014). Electrospinning of zein/tannin bio-nanofibers. *Industrial Crops and Products, 52*, 298–304.
Ooms, N., Jansens, K. J., Pareyt, B., Reyniers, S., Brijs, K., & Delcour, J. A. (2018). The impact of disulfide bond dynamics in wheat gluten protein on the development of fermented pastry crumb. *Food Chemistry, 242*, 68–74.
Orona-Tamayo, D., Valverde, M. E., & Paredes-López, O. (2018). Bioactive peptides from selected Latin american food crops–A nutraceutical and molecular approach. *Critical Reviews in Food Science and Nutrition,* 1–27.
Ortolan, F., & Steel, C. J. (2017). Protein characteristics that affect the quality of vital wheat gluten to be used in baking: A review. *Comprehensive Reviews in Food Science and Food Safety, 16*(3), 369–381.
Ou, L., Brown, T. R., Thilakaratne, R., Hu, G., & Brown, R. C. (2014). Techno-economic analysis of co-located corn grain and corn stover ethanol plants. *Biofuels, Bioproducts and Biorefining, 8*(3), 412–422.
Ozkan, G., Franco, P., De Marco, I., Xiao, J., & Capanoglu, E. (2019). A review of microencapsulation methods for food antioxidants: Principles, advantages, drawbacks and applications. *Food Chemistry, 272*, 494–506.
Pascoli, M., de Lima, R., & Fraceto, L. F. (2018). Zein nanoparticles and strategies to improve colloidal stability: A mini-review. *Frontiers in Chemistry, 6*, 6.
Pedrazzini, E., Mainieri, D., Marrano, C. A., & Vitale, A. (2016). Where do protein bodies of cereal seeds come from? *Frontiers of Plant Science, 7*, 1139.
Pedrazzini, E., & Vitale, A. (2018). Protein biosynthesis and maturation in the ER. In C. Hawes, & V. Kriechbaumer (Eds.). *The plant endoplasmic reticulum* (pp. 179–189). New York, NY: Springer, Humana Press.
Penalva, R., González-Navarro, C. J., Gamazo, C., Esparza, I., & Irache, J. M. (2017). Zein nanoparticles for oral delivery of quercetin: Pharmacokinetic studies and preventive anti-inflammatory effects in a mouse model of endotoxemia. *Nanomedicine, 13*(1), 103–110.
Peng, D., Jin, W., Li, J., Xiong, W., Pei, Y., Wang, Y., et al. (2017). Adsorption and distribution of edible gliadin nanoparticles at the air/water interface. *Journal of Agricultural and Food Chemistry, 65*(11), 2454–2460.
Peng, D., Jin, W., Tang, C., Lu, Y., Wang, W., Li, J., et al. (2018). Foaming and surface properties of gliadin nanoparticles: Influence of pH and heating temperature. *Food Hydrocolloids, 77*, 107–116.
Prabhakaran, M. P., Zamani, M., Felice, B., & Ramakrishna, S. (2015). Electrospraying technique for the fabrication of metronidazole contained PLGA particles and their release profile. *Materials Science and Engineering: C, 56*, 66–73.
Prasad, A., Astete, C. E., Bodoki, A. E., Windham, M., Bodoki, E., & Sabliov, C. M. (2017). Zein nanoparticles uptake and translocation in hydroponically grown sugar cane plants. *Journal of Agricultural and Food Chemistry, 66*, 6544–6551.
Prietto, L., Pinto, V. Z., Halal, E., Mello, S. L., de Morais, M. G., Costa, J. A. V., et al. (2018). Ultrafine fibers of zein and anthocyanins as natural pH indicator. *Journal of the Science of Food and Agriculture, 98*(7), 2735–2741.
Puerta, E., Suárez-Santiago, J. E., Santos-Magalhães, N. S., Ramirez, M. J., & Irache, J. M. (2017). Effect of the oral administration of nanoencapsulated quercetin on a mouse model of Alzheimer's disease. *International Journal of Pharmaceutics, 517*(1), 50–57.
Qiao, Y., Shi, C., Wang, X., Wang, P., Zhang, Y., Wang, D., & Zhong, J. (2019). Electrospun nanobelt-shaped polymer membranes for fast and high-sensitivity detection of metal ions. *ACS Applied Materials & Interfaces, 11*(5), 5401–5413.
Qin, X. S., Sun, Q. Q., Zhao, Y. Y., Zhong, X. Y., Mu, D. D., Jiang, S. T., et al. (2017). Transglutaminase-set colloidal properties of wheat gluten with ultrasound pretreatments. *Ultrasonics Sonochemistry, 39*, 137–143.
Qi, J. C., Zhang, G. P., & Zhou, M. X. (2006). Protein and hordein content in barley seeds as affected by nitrogen level and their relationship to beta-amylase activity. *Journal of Cereal Science, 43*(1), 102–107.
Qureshi, U. A., Khatri, Z., Ahmed, F., Khatri, M., & Kim, I. S. (2017). Electrospun zein nanofiber as a green and recyclable adsorbent for the removal of reactive black 5 from the aqueous phase. *ACS Sustainable Chemistry & Engineering, 5*(5), 4340–4351.
Ravindran, R., Jaiswal, S., Abu-Ghannam, N., & Jaiswal, A. K. (2018). A comparative analysis of pretreatment strategies on the properties and hydrolysis of brewers' spent grain. *Bioresource Technology, 248*, 272–279.
Raza, H., Pasha, I., Shoaib, M., Zaaboul, F., Niazi, S., & Aboshora, W. (2017). Review on functional and rheological attributes of kafirin for utilization in gluten free baking industry. *American Journal of Food Science and Nutrition Research, 4*(5), 150–157.
Redant, L., Buggenhout, J., Brijs, K., & Delcour, J. A. (2017). Extractability and chromatographic separation of rye (Secale cereale L.) flour proteins. *Journal of Cereal Science, 73*, 68–75.
Reddy, P. R. K., Lakshmi, R. S., Raju, J., Kishore, K. R., & Anil, C. (2017). Cornell net carbohydrate and protein system (CNCPS) fractionations and in-vitro nutrient digestibility of corn dried distiller grains with solubles (DDGS) from various ethanol

plants in Andhra Pradesh. *International Journal of Livestock Research, 7*(2), 164–171.
Reddy, N., Shi, Z., Xu, H., & Yang, Y. (2015). Development of wheat glutenin nanoparticles and their biodistribution in mice. *Journal of Biomedical Materials Research Part A, 103*(5), 1653–1658.
Ren, F., Fu, J., Xiong, H., Cui, L., Ren, G., Guan, H., et al. (2018). Complexes of felodipine nanoparticles with zein prepared using a dual shift technique. *Journal of Pharmaceutical Sciences, 107*(1), 239–249.
Research and Markets (2018). *Global Distillers grains market 2018-2023 - analysis by type, source, and livestock.* https://www.prnewswire.com/news-releases/global-distillers-grains-market-2018-2023—analysis-by-type-source-and-livestock-300634326.html/, Accessed date: 17 April 2019.
Rockström, J., Williams, J., Daily, G., Noble, A., Matthews, N., Gordon, L., et al. (2017). Sustainable intensification of agriculture for human prosperity and global sustainability. *Ambio, 46*(1), 4–17.
Rodríguez-Félix, F., Ramirez-Wong, B., Isabel Torres-Chavez, P., Álvarez-Avilés, A., Moreno-Salazar, S., Eugenia Renteria-Martinez, M., et al. (2014). Yellow berry, protein and agronomic characteristics in bread wheat under different conditions of nitrogen and irrigation in Northest Mexico. *Pakistan Journal of Botany, 46*(1), 221–226.
Rommi, K., Niemi, P., Kemppainen, K., & Kruus, K. (2018). Impact of thermochemical pre-treatment and carbohydrate and protein hydrolyzing enzyme treatment on fractionation of protein and lignin from brewer's spent grain. *Journal of Cereal Science, 79*, 168–173.
Rosentrater, K. A., & Verbeek, C. J. R. (2017). Water adsorption characteristics of extruded blends of corn gluten meal and distillers dried grains with solubles. *Food and Bioproducts Processing, 101*, 110–117.
Sallam, M. A., & Elzoghby, A. O. (2018). Flutamide-Loaded zein nanocapsule hydrogel, a promising dermal delivery system for pilosebaceous unit disorders. *AAPS PharmSciTech, 19*(5), 2370–2382.
Santos, T. M., Souza Filho, M. D. S. M., Muniz, C. R., Morais, J. P. S., Kotzebue, L. R. V., Pereira, A. L. S., et al. (2017). Zein films with unoxidized or oxidized tannic acid. *Journal of the Science of Food and Agriculture, 97*(13), 4580–4587.
Scherf, K. A., Koehler, P., & Wieser, H. (2016). Gluten and wheat sensitivities–an overview. *Journal of Cereal Science, 67*, 2–11.
Shahane, A. A., & Shivay, Y. S. (2016). Cereal residues-not a waste until we waste it: A review. *International Journal of Bio-Resource & Stress Management, 7*(1).
Shariare, M. H., Sharmin, S., Jahan, I., Reza, H. M., & Mohsin, K. (2018). The impact of process parameters on carrier free paracetamol nanosuspension prepared using different stabilizers by antisolvent precipitation method. *Journal of Drug Delivery Science and Technology, 43*, 122–128.
Sharif, N., Golmakani, M. T., Niakousari, M., Ghorani, B., & Lopez-Rubio, A. (2019). Food-grade gliadin microstructures obtained by electrohydrodynamic processing. *Food Research International, 116*, 1366–1373.
Sharma, V. P., & Wardhan, H. (2017). Overview of maize economy: Production, procurement, and marketed surplus. In V. P. Sharma, & H. Wardhan (Eds.). *Marketed and marketable surplus of major food grains in India* (pp. 77–100). Springer India.
Shewry, P. R. (2002). The major seed storage proteins of spelt wheat, sorghum, millets and pseudocereals. In P. S. Belton, & J. R. N. Taylor (Eds.). *Pseudocereals and less common cereals* (pp. 1–24). Springer Berlin Heidelberg.
Shewry, P. R. (2007). Improving the protein content and composition of cereal grain. *Journal of Cereal Science, 46*(3), 239–250.
Shi, W., & Dumont, M. J. (2014). bio-based films from zein, keratin, pea, and rapeseed protein feedstocks. *Journal of Materials Science, 49*(5), 1915–1930.
Shishir, M. R. I., Xie, L., Sun, C., Zheng, X., & Chen, W. (2018). Advances in micro and nano-encapsulation of bioactive compounds using biopolymer and lipid-based transporters. *Trends in Food Science & Technology, 78*, 34–60.
Shukla, R., & Cheryan, M. (2001). Zein: The industrial protein from corn. *Industrial Crops and Products, 13*(3), 171–192.
Singh, J., & Trivedi, J. (2017). Raw materials for biofuels production. In M. R. Riazi, & D. Chiaramonti (Eds.). *Biofuels production and processing technology*Boca Raton, Fl: Taylor & Francis, group, CRC Press.
Sonekar, S., Mishra, M. K., Patel, A. K., Nair, S. K., Singh, C. S., & Singh, A. K. (2016). Formulation and evaluation of folic acid conjugated gliadin nanoparticles of curcumin for targeting colon cancer cells. *Journal of Applied Pharmaceutical Science, 6*(10), 068–074.
Stancu, V., Haugaard, P., & Lähteenmäki, L. (2016). Determinants of consumer food waste behaviour: Two routes to food waste. *Appetite, 96*, 7–17.
Stock, R. A., Lewis, J. M., Klopfenstein, T. J., & Milton, C. T. (2000). Review of new information on the use of wet and dry milling feed by-products in feedlot diets. *Journal of Animal Science, 77*, 1–12.
Sullivan, A. C., Pangloli, P., & Dia, V. P. (2018). Impact of ultrasonication on the physicochemical properties of sorghum kafirin and in vitro pepsin-pancreatin digestibility of sorghum gluten-like flour. *Food Chemistry, 240*, 1121–1130.
Sun, C., Dai, L., & Gao, Y. (2017a). Formation and characterization of the binary complex between zein and propylene glycol alginate at neutral pH. *Food Hydrocolloids, 64*, 36–47.
Sun, C., Xu, C., Mao, L., Wang, D., Yang, J., & Gao, Y. (2017b). Preparation, characterization and stability of curcumin-loaded zein-shellac composite colloidal particles. *Food Chemistry, 228*, 656–667.
Sun, C., Yang, S., Dai, L., Chen, S., & Gao, Y. (2017c). Quercetagetin-loaded zein-propylene glycol alginate composite particles induced by calcium ions: Structural comparison between colloidal dispersions and lyophilized powders after in vitro simulated gastraintestinal digestion. *Journal of Functional Foods, 37*, 25–48.
Tang, N., & Zhuang, H. (2014). Evaluation of antioxidant activities of zein protein fractions. *Journal of Food Science, 79*(11).
Tanner, G. J., Colgrave, M. L., Blundell, M. J., Howitt, C. A., & Bacic, A. (2019). Hordein accumulation in developing barley grains. *Frontiers of Plant Science, 10*, 649.
Tapia-Hernández, J. A., Rodríguez-Felix, F., Juárez-Onofre, J. E., Ruiz-Cruz, S., Robles-García, M. A., Borboa-Flores, J., et al. (2018a). Zein-polysaccharide nanoparticles as matrices for antioxidant compounds: A strategy for prevention of chronic degenerative diseases. *Food Research International, 111*, 451–471.
Tapia-Hernández, J. A., Rodríguez-Félix, F., & Katouzian, I. (2017). Nanocapsule formation by electrospraying. In S. M. Jafari (Ed.). *Nanoencapsulation technologies for the food and nutraceutical industries* (pp. 320–345). Gorgan, Iran: Elsevier, Academic Press.
Tapia-Hernández, J. A., Torres-Chávez, P. I., Ramírez-Wong, B., Rascón-Chu, A., Plascencia-Jatomea, M., Barreras-Urbina, C. G., et al. (2015). Micro-and nanoparticles by electrospray: Advances and applications in foods. *Journal of Agricultural and Food Chemistry, 63*(19), 4699–4707.
Tapia-Hernández, J. A., Del-Toro-Sánchez, C. L., Cinco-Moroyoqui, F. J., Ruiz-Cruz, S., Juárez, J., Castro-Enríquez, D. D., et al. (2019). Gallic acid-loaded zein nanoparticles by electrospraying process. *Journal of Food Science, 84*(4), 818–831.
Tapia-Hernández, J. A., Rodríguez-Félix, D. E., Plascencia-Jatomea, M., Rascón-Chu, A., López-Ahumada, G. A., Ruiz-Cruz, S., et al. (2018b). Porous wheat gluten microparticles obtained by electrospray: Preparation and characterization. *Advances in Polymer Technology, 37*(6), 2314–2324.
Thapa, R. K., Nguyen, H. T., Jeong, J. H., Shin, B. S., Ku, S. K., Choi, H. G., et al. (2017). Synergistic anticancer activity of combined histone deacetylase and proteasomal inhibitor-loaded zein nanoparticles in metastatic prostate cancers. *Nanomedicine: Nanotechnology, Biology and Medicine, 13*(3), 885–896.
Thipkaew, C., Wattanathorn, J., & Muchimapura, S. (2017). Electrospun nanofibers loaded with quercetin promote the recovery of focal entrapment neuropathy in a rat model of streptozotocin-induced diabetes. *BioMed Research International*. https://doi.org/10.1155/2017/2017493.
Treimo, J., Aspmo, S. I., Eijsink, V. G., & Horn, S. J. (2008). Enzymatic solubilization of proteins in brewer's spent grain. *Journal of Agricultural and Food Chemistry, 56*(13), 5359–5365.
Trujillo, A. I., Bruni, M., & Chilibroste, P. (2017). Nutrient content and nutrient availability of sorghum wet distiller's grain in comparison with the parental grain for ruminants. *Journal of the Science of Food and Agriculture, 97*(8), 2353–2357.
Tsai, Y. H., Yang, Y. N., Ho, Y. C., Tsai, M. L., & Mi, F. L. (2018). Drug release and antioxidant/antibacterial activities of silymarin-zein nanoparticle/bacterial cellulose nanofiber composite films. *Carbohydrate Polymers, 180*, 286–296.
Uddin, M. N., Nielsen, A. L. L., & Vincze, E. (2014). Zinc blotting assay for detection of zinc-binding prolamin in barley (hordeum vulgare) grain. *Cereal Chemistry, 91*(3), 228–232.
Unnithan, A. R., Gnanasekaran, G., Sathishkumar, Y., Lee, Y. S., & Kim, C. S. (2014). Electrospun antibacterial polyurethane–cellulose acetate–zein composite mats for wound dressing. *Carbohydrate Polymers, 102*, 884–892.
Urade, R., Sato, N., & Sugiyama, M. (2017). Gliadins from wheat grain: An overview, from primary structure to nanostructures of aggregates. *Biophysical Reviews*, 1–9.
Veneranda, M., Hu, Q., Wang, T., Luo, Y., Castro, K., & Madariaga, J. M. (2018). Formation and characterization of zein-caseinate-pectin complex nanoparticles for encapsulation of eugenol. *LWT- Food Science and Technology, 89*, 596–603.
Villegas-Torres, M. F., Ward, J. M., & Lye, G. J. (2015). The protein fraction from wheat-based dried distiller's grain with solubles (DDGS): Extraction and valorization. *New Biotechnology, 32*(6), 606–611.
Vogt, L., Liverani, L., Roether, J., & Boccaccini, A. (2018). Electrospun zein fibers incorporating poly (glycerol sebacate) for soft tissue engineering. *Nanomaterials, 8*(3), 150.
Wang, L., Gotoh, T., Wang, Y., Kouyama, T., & Wang, J. Y. (2017a). formation of a mimetic biomembrane from the hydrophobic protein zein and phospholipids: Structure and application. *The Journal of Physical Chemistry C, 121*(36), 19999–20006.
Wang, H., Hao, L., Niu, B., Jiang, S., Cheng, J., & Jiang, S. (2016). Kinetics and antioxidant capacity of proanthocyanidins encapsulated in zein electrospun fibers by cyclic voltammetry. *Journal of Agricultural and Food Chemistry, 64*(15), 3083–3090.
Wang, H., Hao, L., Wang, P., Chen, M., Jiang, S., & Jiang, S. (2017b). Release kinetics and antibacterial activity of curcumin loaded zein fibers. *Food Hydrocolloids, 63*, 437–446.
Wang, X., & Hsiao, B. S. (2016). Electrospun nanofiber membranes. *Current Opinion in Chemical Engineering, 12*, 62–81.
Wang, T., Hu, Q., Zhou, M., Xue, J., & Luo, Y. (2016). Preparation of ultra-fine powders from polysaccharide-coated solid lipid nanoparticles and nanostructured lipid carriers by innovative nano spray drying technology. *International Journal of Pharmaceutics, 511*(1), 219–222.
Wang, R., Tian, Z., & Chen, L. (2011). A novel process for microencapsulation of fish oil with barley protein. *Food Research International, 44*(9), 2735–2741.
Wang, Y., Tilley, M., Bean, S., Sun, X. S., & Wang, D. (2009). Comparison of methods for extracting kafirin proteins from sorghum distillers dried grains with solubles. *Journal of Agricultural and Food Chemistry, 57*(18), 8366–8372.
Wang, P., Xu, L., Nikoo, M., Ocen, D., Wu, F., Yang, N., et al. (2014). Effect of frozen storage on the conformational, thermal and microscopic properties of gluten: Comparative studies on gluten-, glutenin-and gliadin-rich fractions. *Food Hydrocolloids, 35*, 238–246.
Wang, H., Zhang, X., Zhu, W., Jiang, Y., & Zhang, Z. (2018a). Self-assembly of Zein-based microcarrier system for colon-targeted oral drug delivery. *Industrial & Engineering Chemistry Research, 57*(38), 12689–12699.
Wang, P., Zou, M., Liu, K., Gu, Z., & Yang, R. (2018b). Effect of mild thermal treatment on the polymerization behavior, conformation and viscoelasticity of wheat gliadin. *Food Chemistry, 239*, 984–992.
Wesołowska-Trojanowska, M., Tomczyńska-Mleko, M., Terpiłowski, K., Sołowiej, B., Nastaj, M., & Mleko, S. (2017). Effect of gluten on the properties of ternary biopolymers based on gluten, whey protein concentrate, and kaolinite. *European Food*

Research and Technology, 1–11.
Wieser, H. (2007). Chemistry of gluten proteins. *Food Microbiology, 24*(2), 115–119.
Wronkowska, M. (2016). Wet-milling of cereals. *Journal of Food Processing and Preservation, 40*(3), 572–580.
Xiao, J., Chen, Y., & Huang, Q. (2017a). Physicochemical properties of kafirin protein and its applications as building blocks of functional delivery systems. *Food &Function, 8*(4), 1402–1413.
Xiao, J., Li, C., & Huang, Q. (2015a). Kafirin nanoparticle-stabilized pickering emulsions as oral delivery vehicles: Physicochemical stability and in vitro digestion profile. *Journal of Agricultural and Food Chemistry, 63*(47), 10263–10270.
Xiao, J., Li, Y., & Huang, Q. (2016a). Recent advances on food-grade particles stabilized Pickering emulsions: Fabrication, characterization and research trends. *Trends in Food Science & Technology, 55*, 48–60.
Xiao, J., Li, Y., Li, J., Gonzalez, A. P., Xia, Q., & Huang, Q. (2014). Structure, morphology, and assembly behavior of kafirin. *Journal of Agricultural and Food Chemistry, 63*(1), 216–224.
Xiao, J., Lu, X., & Huang, Q. (2017b). Double emulsion derived from kafirin nanoparticles stabilized Pickering emulsion: Fabrication, microstructure, stability and in vitro digestion profile. *Food Hydrocolloids, 62*, 230–238.
Xiao, J., Nian, S., & Huang, Q. (2015b). Assembly of kafirin/carboxymethyl chitosan nanoparticles to enhance the cellular uptake of curcumin. *Food Hydrocolloids, 51*, 166–175.
Xiao, J., Shi, C., Zheng, H., Shi, Z., Jiang, D., Li, Y., et al. (2016b). Kafirin protein based electrospun fibers with tunable mechanical property, wettability, and release profile. *Journal of Agricultural and Food Chemistry, 64*(16), 3226–3233.
Xiao, J., Wang, X. A., Gonzalez, A. J. P., & Huang, Q. (2016c). Kafirin nanoparticles-stabilized Pickering emulsions: Microstructure and rheological behavior. *Food Hydrocolloids, 54*, 30–39.
Xu, Y., Li, J. J., Yu, D. G., Williams, G. R., Yang, J. H., & Wang, X. (2017). Influence of the drug distribution in electrospun gliadin fibers on drug-release behavior. *European Journal of Pharmaceutical Sciences, 106*, 422–430.
Yalçın, E., Çelik, S., & İbanoğlu, E. (2008). Foaming properties of barley protein isolates and hydrolysates. *European Food Research and Technology, 226*(5), 967.
Yang, S., Dai, L., Sun, C., & Gao, Y. (2018). Characterization of curcumin loaded gliadin-lecithin composite nanoparticles fabricated by antisolvent precipitation in different blending sequences. *Food Hydrocolloids, 85*, 185–194.
Yang, J., Huang, J., Zeng, H., & Chen, L. (2015). Surface pressure affects B-hordein network formation at the air–water interface in relation to gastric digestibility. *Colloids and Surfaces B: Biointerfaces, 135*, 784–792.
Yang, Y. Y., Zhang, M., Liu, Z. P., Wang, K., & Yu, D. G. (2018). Meletin sustained-release gliadin nanoparticles prepared via solvent surface modification on blending electrospraying. *Applied Surface Science, 434*, 1040–1047.
Yang, J. M., Zha, L. S., Yu, D. G., & Liu, J. (2013). Coaxial electrospinning with acetic acid for preparing ferulic acid/zein composite fibers with improved drug release profiles. *Colloids and Surfaces B: Biointerfaces, 102*, 737–743.
Yazar, G., Duvarci, O. C., Tavman, S., & Kokini, J. L. (2017). LAOS behavior of the two main gluten fractions: Gliadin and glutenin. *Journal of Cereal Science, 77*, 201–210.
Yilmaz, A., Bozkurt, F., Cicek, P. K., Dertli, E., Durak, M. Z., & Yilmaz, M. T. (2016). A novel antifungal surface-coating application to limit postharvest decay on coated apples: Molecular, thermal and morphological properties of electrospun zein–nano-fiber mats loaded with curcumin. *Innovative Food Science and Emerging Technologies, 37*, 74–83.
Yilmaz, M. T., Yilmaz, A., Akman, P. K., Bozkurt, F., Dertli, E., Basahel, A.,., & Sagdic, O. (2019). Electrospraying method for fabrication of essential oil loaded-chitosan nanoparticle delivery systems characterized by molecular, thermal, morphological and antifungal properties. *Innovative Food Science & Emerging Technologies, 52*, 166–178.
Yin, B., Wang, C., Liu, Z., & Yao, P. (2017). Peptide-polysaccharide conjugates with adjustable hydrophilicity/hydrophobicity as green and pH sensitive emulsifiers. *Food Hydrocolloids, 63*, 120–129.
Yusuf, M. (2017). Agro-industrial waste materials and their recycled value-added applications. *Handbook of Ecomaterials,* 1–11.
Yu, W., Tan, X., Zou, W., Hu, Z., Fox, G. P., Gidley, M. J., et al. (2017). Relationships between protein content, starch molecular structure and grain size in barley. *Carbohydrate Polymers, 155*, 271–279.
Yu, J., Xu, Z., Liu, L., Chen, S., Wang, S., & Jin, M. (2019). Process integration for ethanol production from corn and corn stover as mixed substrates. *Bioresource Technology, 279*, 10–26.
Zhang, S., Campagne, C., & Salaün, F. (2019a). Influence of solvent selection in the electrospraying process of polycaprolactone. *Applied Sciences, 9*(3), 402.
Zhang, C., Feng, F., & Zhang, H. (2018a). Emulsion electrospinning: Fundamentals, food applications and prospects. *Trends in Food Science & Technology, 80*, 175–186.
Zhang, F., Khan, M. A., Cheng, H., & Liang, L. (2019b). Co-encapsulation of α-tocopherol and resveratrol within zein nanoparticles: Impact on antioxidant activity and stability. *Journal of Food Engineering, 247*, 9–18.
Zhang, M., Li, X., Li, S., Liu, Y., & Hao, L. (2016). Electrospun poly (L-lactide)/zein nanofiber mats loaded with Rana chensinensis. *Journal of Materials Science: Materials in Medicine, 27*(9), 1–12.
Zhang, Y., Li, J., Li, S., Ma, H., & Zhang, H. (2018b). Mechanism study of multimode ultrasound pretreatment on the enzymolysis of wheat gluten. *Journal of the Science of Food and Agriculture, 98*(4), 1530–1538.
Zhang, Y., Niu, Y., Luo, Y., Ge, M., Yang, T., Yu, L. L., et al. (2014). Fabrication, characterization and antimicrobial activities of thymol-loaded zein nanoparticles stabilized by sodium caseinate–chitosan hydrochloride double layers. *Food Chemistry, 142*, 269–275.
Zhang, N., Qiao, R., Su, J., Yan, J., Xie, Z., Qiao, Y., et al. (2017a). Recent advances of electrospun nanofibrous membranes in the development of chemosensors for heavy metal detection. *Small, 13*(16), 1604293.
Zhang, J. F., Wang, Y., Liao, S., Lallier, T., Wen, Z. T., & Xu, X. (2017b). Photo-cross-linked antibacterial zein nanofibers fabricated by reactive electrospinning and its effects against Streptococcus mutans. *Oral Health and Dental Studies, 1*(1), 1.
Zhao, C. B., Zhang, H., Xu, X. Y., Cao, Y., Zheng, M. Z., Liu, J. S., et al. (2017). Effect of acetylation and succinylation on physicochemical properties and structural characteristics of oat protein isolate. *Process Biochemistry, 57*, 117–123.
Zhou, C., Hu, J., Ma, H., Yagoub, A. E. A., Yu, X., Owusu, J., et al. (2015). Antioxidant peptides from corn gluten meal: Orthogonal design evaluation. *Food Chemistry, 187*, 270–278 7.
Zhou, Y., Zhao, D., Foster, T. J., Liu, Y., Wang, Y., Nirasawa, S., et al. (2014). Konjac glucomannan-induced changes in thiol/disulphide exchange and gluten conformation upon dough mixing. *Food Chemistry, 143*, 163–169.
Zhuang, H., Tang, N., & Yuan, Y. (2013). Purification and identification of antioxidant peptides from corn gluten meal. *Journal of Functional Foods, 5*(4), 1810–1821.
Zhu, M., Han, J., Wang, F., Shao, W., Xiong, R., Zhang, Q., et al. (2017). Electrospun nanofibers membranes for effective air filtration. *Macromolecular Materials and Engineering, 302*(1), 1600353.
Zhu, Q., Lu, H., Zhu, J., Zhang, M., & Yin, L. (2019). Development and characterization of pickering emulsion stabilized by zein/corn fiber gum (CFG) complex colloidal particles. *Food Hydrocolloids, 91*, 204–213.
Zou, Y., Guo, J., Yin, S. W., Wang, J. M., & Yang, X. Q. (2015). Pickering emulsion gels prepared by hydrogen-bonded zein/tannic acid complex colloidal particles. *Journal of Agricultural and Food Chemistry, 63*(33), 7405–7414.
Zou, Y., Yang, X., & Scholten, E. (2019). Tuning particle properties to control rheological behavior of high internal phase emulsion gels stabilized by zein/tannic acid complex particles. *Food Hydrocolloids, 89*, 163–170.
Zou, L., Zheng, B., Zhang, R., Zhang, Z., Liu, W., Liu, C., et al. (2016). Enhancing the bioaccessibility of hydrophobic bioactive agents using mixed colloidal dispersions: Curcumin-loaded zein nanoparticles plus digestible lipid nanoparticles. *Food Research International, 81*, 74–82.
Zuorro, A., Iannone, A., & Lavecchia, R. (2019). Water–organic solvent extraction of phenolic antioxidants from brewers' spent grain. *Processes, 7*(3), 126.
Đorđević, V., Balanč, B., Belščak-Cvitanović, A., Lević, S., Trifković, K., Kalušević, A.,., & Nedović, V. (2015). Trends in encapsulation technologies for delivery of food bioactive compounds. *Food Engineering Reviews, 7*(4), 452–490.
Łaba, W., Piegza, M., & Kawa-Rygielska, J. (2017). Evaluation of brewer's spent grain as a substrate for production of hydrolytic enzymes by keratinolytic bacteria. *Journal of Chemical Technology & Biotechnology, 92*(6), 1389–1396.

CAPÍTULO III

Identification by UPLC-DAD-MS and antioxidant activity of phenolic compounds from safflower (*Carthamus tinctorius* L.) by-product

Evaluation of Antioxidant Activity, Protective Effect on Human Erythrocytes and Phenolic Compound Identification in Safflower (*Carthamus tinctorius L.*) by-product by UPLC-DAD-MS

Tapia-Hernández J. A.[1], Rodríguez-Felix F. [1], Cinco-Moroyoqui F. J. [1], Juárez-Onofre J. E.[2], Ruiz-Cruz S.[3], Wong-Corral F. J. [1], Castro-Enríquez D. D.[1] Barreras-Urbina C. G.[1] and Del Toro-Sánchez C. L.[1]*

[1]Department of Research and Posgraduate in Food (DIPA). University of Sonora. Blvd. Luis Encinas y Rosales, S/N, Colonia Centro, 83000. Hermosillo, Sonora, México.

[2]Department of Physics, University of Sonora, Blvd. Luis Encinas y Rosales, S/N, Colonia Centro, 83000. Hermosillo, Sonora, México.

[3]Department of Biotechnology and Food Science. Institute Technology of Sonora. 5 de febrero #818 sur, Colonia Centro, 85000, Ciudad Obregón, Sonora, México

*Corresponding author: carmen.deltoro@unison.mx

Tapia-Hernández J. A.: tapia_hernandez_agustin@hotmail.com

Rodríguez-Felix F.: rodriguez_felix_fco@hotmail.com

Cinco-Moroyoqui F. J.: fcinco@guayacan.uson.mx

Juárez-Onofre J. E.: josue.juarez@unison.mx

Ruiz-Cruz S.: saul.ruiz.cruz@itson.edu.mx

Wong-Corral F. J.: francisco.wong@unison.mx

Castro-Enriquez D. D: daniela.castro.e@hotmail.com

Barreras-Urbina C.G.: carlosgbarrerasu@gmail.com

Del Toro-Sánchez C. L: carmen.deltoro@unison.mx

Abstract

Nowadays, agro-industrial by-products are an important source of obtaining phenolic compounds with application in reduce the prevalence of chronic degenerative diseases. The objective of this study was to identify the phenolic compounds present in methanolic and ethanolic extracts of leaf-stem by-product of Safflower (*Carthamus tinctorius L.*) by UPLC-DAD-MS and evaluate their antioxidant capacity. The determinations for each extract were antioxidant capacity, IC50, total phenols and flavonoids. The highest antioxidant activity and IC50 was for leaf methanolic extract by DPPH● and ABTS●+ methods (9.65 amd 8.46 µg mL^{-1}). Antioxidant activity by protective effect in human erythrocytes was stem methanolic extract (91.86 ± 0.72 %) and stem ethanolic extract (87.55 ± 0.61 %). Total phenols and flavonoids were also higher in leaf followed by mixture and stem. The major compounds identified and that contribute the antioxidant capacity in both extracts were two phenolic compounds of flavonoid type (luteolin 7-O-β-D-glucoside and Quercetin-3-galactoside) and a pigment (hydroxysafflor yellow A) in both solvents. Therefore, the agroindustrial residues of safflower are an alternative source of obtaining antioxidant phenolic compounds being a sustainable alternative with application in chronic degenerative diseases.

Keywords: safflower by-product, phenolic compounds, UPLC-DAD-MS, antioxidant, protective effect on human erythrocytes,

1. INTRODUCTION

Currently the trend is to reduce global warming through novel strategies. In the area of agriculture and food research is aimed at taking advantage of agroindustrial waste to give them an added value, thus avoiding burning or excessive accumulation, reducing pollution to the environment and damage to human health (Yusuf, 2017; de los Ángeles Fernández *et al.*, 2018). In addition, agroindustrial waste is a source of numerous compounds that can be extracted for different applications such as food (Arun *et al*., 2017; Marin *et al.*, 2018), health (Vodnar *et al*, 2017; de Francisco *et al.*, 2018) and cosmetics (Medina *et al.*, 217; Vuong, 2017; Squillaci *et al.*, 2018).

Safflower (*Carthamus tinctorius L*.) is a crop of Northwest of Mexico, that grows and achieves high production by arid and semiarid conditions (Ulloa *et al*, 2011; Avila *et al*., 2017). It is an attractive crop for the farmers of the region mainly to obtain edible oil from the seed and for the obtaining of different processed foods (Buitimea-Cantúa *et al.,* 2017). In other countries as China is used as a medicinal plant mainly flower petals and oil, (Liu *et al.*, 2017; Yan *et al.*, 2017; Wang *et al.*, 2017). In India flower pigments are used as food colorant (Bhogaita *et al*. 2016). In Alemania oil of seed is used as active principle of cosmetic formulations (Bielfeldt *et al.,* 2017). However, in Mexico and other countries leaf and stem are considered by-products of the oil industry (> 80% of the total plant).

Safflower research has focused on identifying bioactive compounds in flower, seed and oil, elucidating more than 200 structures. Phenolic compounds are the majority in safflower and are secondary metabolites found in plants, whose function is provide good development and growth and, in turn, be a defense mechanism (Perez-Perez et al., 2018). Safflower bioactive

compounds are classified into five groups. Group 1 (pigments): carthamine, hydroxysafflor yellow A, safflor yellow B, safflomin A, safflomin C and cartormin and derivates (Ibrahim *et al*., 2016; Ohama *et al.*, 2016; Li *et al.*, 2017; Liao *et al.*, 2018). Group 2 (flavonoids) as quercetin, naringenin, kaemperol, lutein, catechins, acacetin and derivatives (Hiramatsu *et al*., 2017; Kim et al., 2017; Yao *et al.*, 2017). Group 3 (lignans): matairesinol and its derivatives (Park *et al.*, 2017; Solyomváry *et al*., 2017). Group 4 (phenolic acids): gallic acid, trans-ferulic acid, chlorogenic acid, syringic acid, p-coumaric acid, Vanillic acid, synapicm acid and Salicylic acid (Khalid *et al.*, 2017; Namdjoyan *et al.,* 2017). Group 5: phenolic acids bound to serotonin (Karimkhani *et al*., 2016; Lazari *et al.*, 2017; Peng *et al*., 2017).

In spite of this wide range of molecules, there is no research in the literature identifying the profile of molecules and used of safflower by-products (leaf-stem) and their relationship to antioxidant activity and protective effect on human erythrocytes. Therefore, the present study establishes the bases for the identification of the phenolic compounds of safflower by-product (*Carthamus tinctorius L*.) by UPLC-DAD-MS and their relation with the antioxidant activity.

2. MATERIALS AND METHODS

Plant Material

Safflower (*Carthamus Tintorious* L.) by-product was used for the present investigation. The by-product consists in leaf-stem mixture (Aprox. 1:3 w/w) after the process of obtaining oil from the seed. The sample was collected at 150 days of growth in the northwest region of Mexico in 2018. The location was Ejido San Miguel of Horcasitas, Hermosillo, Sonora, Mexico with coordinates: 29° 29' 00" N 110° 45' 00" W.

Chemicals

2,2′-Azino-bis(3-ethylbenzothiazoline-6-sulfonic acid) diammonium salt (ABTS), 2,2-Diphenyl-1-picrylhydrazyl (DPPH), 6-hydroxy-2,5,7,8-tetramethylchroman-2-carboxylic acid (Trolox), 2,2′-azobis (2-amidinopropane) dihydrochloride (AAPH), Folin ciocalteu's phenol 2 N, Quercetin, Gallic Acid and all HPLC grade standars were from Sigma-Aldrich (St. Louis, MO, United States). All other chemicals and solvents were of the highest commercial grade.

Preparation of Raw Material

Samples of dry safflower were cleaned to remove weeds from crops zone. Then seeds, flowers, and damaged parts were removed. The by-product of safflower was divided into three samples as leaf, stem and leaf-stem mixture (1:3 w/w). The samples obtained were reduced in particle size in a mill (Krups Gris mark model GX410011). Then they were placed in a sieveof mesh #40 (Newark mark, model TS8323S77) for obtaing uniform particles (425 μm). The samples were collected in airtight bags and stored at -20 °C until its use.

Extraction

Methodology described by Morales-Del Rio et al. (2015) was followed. Methanol and ethanol were evaluated as extraction solvents. Firstly, 3 g of each sample were weighed on an OHAUS Pioneer analytical balance and 20 mL of solvents were added. The sample were mixed for 1 min at 25 °C in a VWR Vortex 2, G-560. Then they were sonicated for 15 minutes (Branson sonicator, M3800H, frequency of 40 kHz). Finally, thye were centrifuged at 7000 rpm, 4 °C for 15 min (Eppendorf centrifuge 5804 R). The supernatants were obtained and filtered on Whatman #4 paper. Extractions were made by triplicate. The supernatants were evaporated to dryness using a rotavapor (Heidolph Rotava- por, 4003 VAC Senso T) at 45–50 °C. The dry extracts were weighed to obtain the yield of the extracts. Later, all samples were adjusted to a final concentration of 0.4 mg/mL using methanol and ethanol respectively to determine all the assays.

Quantifiction of Total Phenols

Folin-Ciocalteu technique was used according to del Pilar Garcia-Mendoza *et al.,* (2017) with some modifications. The determination was performing for methanolic and ethanolic extract. Firstly, 10 μL of extract and 25 μL of Folin 1 N solution were added in a 96-well microplate. Then, the samples were reposed during 5 minutes at 25 °C in dark. Subsequently, 25 μL of 20% Na_2CO_3 and 140 μL of distilled water were added. These samples were incubated for 30 minutes in the dark. The absorbance was measured at 760 nm using a microplate reader (Multiskan GO, Thermo Scientific, Waltham, MA, USA). Measurements were made by triplicate. A standard curve of gallic acid (0.02-2 mg mL^{-1}) was otained and the results were expressed as mg of galic acid equivalent (GAE)/g dry sample.

Quantifiction of Total Flavonoids

This colorimetric method was determined in triplicate according to Jiménez-Aguilar *et al*., (2017) with modifications. The reaction was made mixing 80 µL of extract and 80 µL of ethanolic solution of aluminum trichloride (20 g L^{-1}). The samples were reposed 10 min in the dark at 25 °C. The absorbance was measured at 415 nm using a microplate reader (Multiskan GO, Thermo Scientific, Waltham, MA, USA). A standard curve was constructed using quercetin (0.02-3 mg mL^{-1}). The results were expressed as mg of quercentin eqivalent (QE)/ g dry sample.

Radical Scavenging Capacity Using the DPPH Method

Free radical-scavenging capacity of each sample was determined using the DPPH assay as described by Yahia *et al.,* (2017). An aliquot of 20 µL of sample solutions were mixed with 200 µL of a free radical DPPH methanolic solution (6×10^{-5} mol/L). The mixture reactions were incubated for 30 minutes in the darkness and measured at a wavelength of 515 nm using a microplate reader (Multiskan GO, Thermo Scientific, Waltham, MA, USA) against controls prepared with each solvent (methanol or ethanol). Standar curve Trolox from 0.005 to 1 mg mL^{-1} was obtained and results were reported as µmol of Trolox equivalents (TE)/g dry sample, % inhibition (Eq. 1), and by inhibitory concentration at 50 % (IC_{50}).

$$\%\ inhibition = \frac{\text{absorbance control} - \text{absorbance sample}}{\text{absorbance control}}\ x\ 100 \qquad (Eq.1)$$

ABTS Radical Scavenging Assay

The ABTS assay was performed using the procedure of Valdez-Carmona et al., (2017) with modifications. First the radical formation ($ABTS^{\bullet+}$) was preparing from a stock solution of ABTS (7.4 mM) and potassium persulfate (2.6 mM) in water. The solution reacted overnight (12-16 h) at room temeperature in the dark. The $ABTS^{\bullet+}$ radical solution was diluted with ethanol to reach an absorbance of 0.7 ± 0.02 at 734 nm using a microplate reader (Multiskan GO, Thermo Scientific, Waltham, MA, USA). The measurements were assessed placing 270 µL of the prepared cationic radical solution and 20 µL of sample in a 96-well microplate. The free radical scavenging activity was evaluated by measuring the aborbance at 734 nm after 30 min. Calibration curve of Trolox from 0.005 to 1 mg mL^{-1} was prepared and the results were reported as µmol of Trolox equivalents (TE)/g dry simple, % inhibition (Eq. 1) and as inhibitory concentration at 50 % (IC_{50}).

Ferric reducing antioxidant power (FRAP) assay

The antioxidant power by reduction of the ferric ion was determined using the methodology described by Parit et al., (2018) with modifications. FRAP reagent was formed by assimilation of the acetate buffer (300 mmol/L, pH 3.6), 10 mM 2,4,6-tripyridyl-s- triazine (TPTZ) in HCL (40 mM) and $FeCl_3,6H_2O$ (20 mM) in 10:1:1 ratio. To determine the antioxidant power, 20 µL of extract was added in 280 µL of working solution. The samples were read at 638 nm in a microplate reader (Thermo Fisher Scientific Inc. Multiskan GO, NY, USA) at 10, 20 and 30 min. A standard Trolox curve from 0.008 to 2 mg mL^{-1} was performed and the results were expressed as µmol of Trolox equivalents (TE)/g dry sample. The determinations were made in triplicate.

Evaluation of the Protective Effect on Human Erythrocytes

To evaluate the protective effect on human erythrocytes, hemolysis was induced by AAPH radical as described by Hernández-Ruiz *et al.,* (2018). Human erythrocytes were washed three times with phosphate-buffered saline solution (PBS) at pH 7, and then a suspension of erythrocytes was prepared with PBS (5:95 v/v). An erythrocyte control (300 µL erythrocyte suspension), hemolysis control (150 µL erythrocyte suspension + 150 µL AAPH) and work solution (100 µL erythrocyte suspension + 100 µL extract + 100 µL AAPH) were prepared. Controls and samples were incubated with shaking (100 rpm) for 3 hours at 37 °C. After this time, 1 mL of PBS was added and centrifuged at 1500 rpm for 10 minutes. Finally, 300 µL of the supernatant was taken and the absorbance was measured at 540 nm using a microplate reader (Thermo Fisher Scientific Inc. Multiskan GO, NY, USA). The percentage of haemolysis inhibition (PHI) and the inhibitory concentration at 50 % (IC_{50}) was calculated by equation 2.

$$\text{PHI}(\%) = \frac{\text{AHI} - \text{ASE}}{\text{AHI}} \text{ x } 100 \qquad (\text{eq. } 2)$$

Where AHI= absorbance of hemolysis induced by AAPH; ASE = absorbance of the safflower by-product extracts.

Identification of Phenolic Compounds by UPLC-DAD-MS

The identification of phenolic compounds was carried out at 280 nm in an Ultra Performance Liquid Chromatography (UPLC) (Waters, ACQUITY LC, IRL), using a diode array detector (DAD) coupled to a mass spectrometer (MS). For the analysis a C18 column (2.1 x 50 mm, 1.7 µm particle size; ACQUITY, UPLC BEH) was used. The phenolic compounds were identified according to the method proposed by Huang and Liaw, (2017) with slight

modifications. In this study, three mobile phases were used to achieve compound separation: (A) 0.1% acetic acid, (B) methanol and (C) HPLC-grade acetonitrile. The flow rate for analysis was 0.3 mL/min; the column and sample temperatures were maintained at 35 °C and 20 °C, respectively; the injection volume was 5 µL; and the absorbance was monitored at 280 nm. The following gradient was used during the 14 min of run: 5 min, 90% A, 5% B and 5% C; 5 min, 78% A, 11% B and 11% C; 11 min, 36% A, 31% B and 31% C; and 12 min, 90% A, 5% B and 5% C. The initial conditions were held for 15 min before each analysis.

The electrospray ionization (ESI) was operated in positive and negative mode, and spectra were acquired over a mass range of 100–750 m/z using a capillary voltage of of 0.08 to 3 kV and a cone voltage of 1 to 20 V. The other optimum values of ESI-MS parameters were a desolvation temperature of 53 to 400 °C and a desolvation gas flow of 650 L/h.

Statistic analysis

The experimental data were subjected to analysis of variance (ANOVA) for each analysis. All determinations were performed for triplicate. Tukey´s test was used with a confidence level of 95% with the software Infostat 2008 to analayze significant differences. The results are expressed as the mean value ± standard deviation (SD).

3. RESULTS AND DISCUSSIONS

Safflower by-product extract yield

With the addition of methanol and ethanol as solvents, different extract yields were obtained from safflower byproduct (Table 1). All the extracts presented significant differences (p <0.5). Leaf extract obtained the highest yield, followed by mixture and stem. These results were similar for both solvents. However, leaf extract in methanol was approximately 2 times

greater than leaf extract in ethanol. This suggests that the extracted compounds are more related to methanol than to ethanol because of the polar character. The main compounds that have been isolated from different anatomical parts of safflower are phenolic compounds this reported by Cho et al., (2004), Golkar et al., (2018).

Table 1. Extracts yield of safflower (*Carthamus tinctorius* L.*)* by-product

Extract	Initial dry weight (g)**	Extract weight (g)**	Extract yield (g/g dry weight)**	Extract yield (%)**
Methanol				
Leaf	3 ± 0.04	0.52 ± 0.015	0.17 ± 0.005	17.22 ± 0.51[a]
Stem	3 ± 0.04	0.06 ± 0.021	0.02 ± 0.007	02.03 ± 0.72 [f]
Mixture*	3 ± 0.04	0.21 ± 0.007	0.07 ± 0.002	07.08 ± 0.24[c]
Ethanol				
Leaf	3 ± 0.04	0.28 ± 0.040	0.09 ± 0.013	09.30 ± 1.34[b]
Stem	3 ± 0.04	0.07 ± 0.006	0.02 ± 0.002	02.30 ± 0.20[e]
Mixture*	3 ± 0.04	0.11 ± 0.008	0.04 ± 0.003	03.74 ± 0.27[d]

*Mixture = leaf + stem. **Meands ± standard deviation (SD) of three independient experiments. Different letters in the last column indicate significant differences ($p < 0.05$) between leaf, stem and mixture from two solvents metanol and ethanol.

Total Phenols

The total phenolic compounds present in safflower by-products are shown in Figure 1. Significant differences were presented in methanol leaf with respect to ethanol leaf. However, stem and mixture not show significant differences between both solvents. In methanolic extract the concentration was higher in leaf with 6.44 ± 0.18 mg GAE/g dry sample, followed by mixture extract with a difference of half of leaf extract. In addition, stem extract was lower in 74.2 % compared to leaf extract. Similarly, in ethanolic extract the concentration was higher in leaf 5.85 ± 0.01 mg GAE /g dry sample and a difference 77.4% with respect to stem. There are studies that show that in leaf of plants is where most of the

phenolic compounds are concentrated, is the aerial part that is more in contact with the environment and that produces them in defense to factors such as microorganisms, insects and climatic conditions (Shikamo *et al.*, 2017).

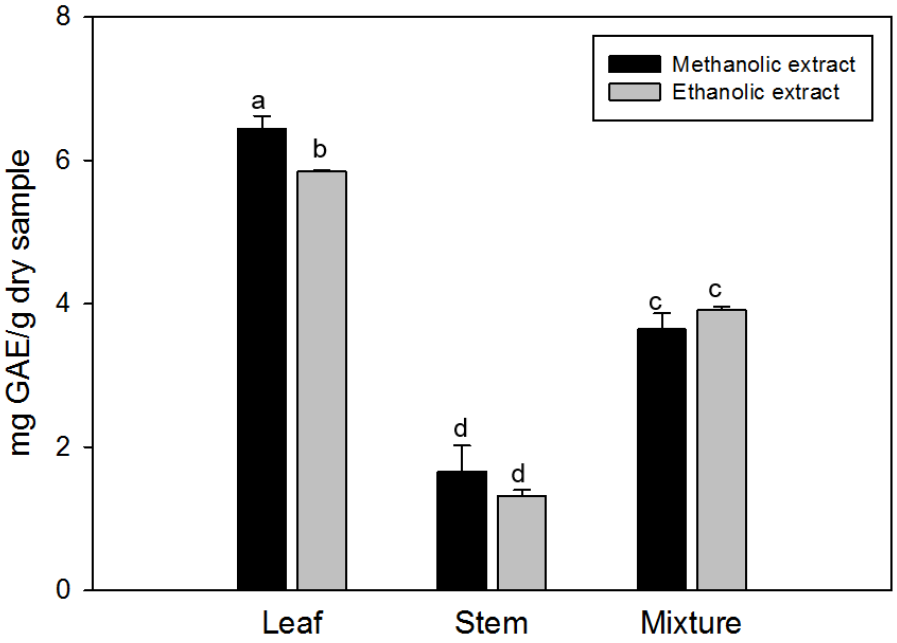

Figure 1. Total phenols of safflower (*Carthamus tinctorius* L.) by-products. The values represent the means with significant differences by Tukey (ANOVA, $p < 0.05$), means of 3 repetitions ($n = 3$). The different letters mark statistically significant differences.

The difference of phenols compared to other studies is due to the climatological conditions of the region where they are cultivated. In northwest Mexico, safflower cultivation is favorable due to the prevailing arid and semi-arid climate. The total phenols and flavonoids of safflower leaf samples were similar to reported by Abdallah *et al.* (2013). They reported Total Phenols of 3 geographic regions in Tunisia: Northeast: 2.1 ± 0.29, center: 7.4 ± 0.31 and southeast: 3.6 ± 0.11 mg GAE/g dry sample. The samples from the center were closer to

those obtained in this study with 6.16 mg GAE/g dry simple. Ivanova, (2017) reported the content of flavonoids in safflower leaves obtaining a result of 0.2 to 0.25 mg mL^{-1} for two different seasons, being much smaller than what was reported for safflower by-product. Taha and Matthaus, (2018) reported the content of phenols in methanol-water extract (60% v / v) of flowers and seeds for different varieties of safflower from Egypt obtaining between 6.4 and 13 mg GAE/g for flowers and between 3.17 mg g^{-1} and 4.89 mg g^{-1} for seed, similar to that reported in methanolic and ethanolic extract of safflower b-product, due to the similar semi-arid regions between India and northwestern Mexico.

Total flavonoids

The total flavonoids determined by the $AlCl_3$ method for the different safflower by-products are shown in Figure 2. Significant differences were presented in methanol leaf with respect to ethanol leaf. However, stem and mixture not show significant differences between both solvents. Total flavonoids present in methanolic extract were higher in leaf extract with a concentration of 11.22 ± 0.023 mg QE/g dry sample. Mixture extract presented 1.41 mg QE/g dry sample less than leaf extract, while stem extract was reduced up to 66%, obtaining the lowest concentration of flavonoids. The mixture can vary depending on the leaf concentration present, which is the one that contributes the highest concentration of flavonoids. On the other hand, ethanolic extract of safflower presented lower concentration of flavonoids than methanolic extract, being in the same way majority for leaf with a 10.83 ± 0.12 mg QE /g dry sample, followed by mixing with 1.26 mg QE/g dry sample minor and stem with 67.13% lower with respect to the concentration of total flavonoids present in the leaf.

Other studies that have reported the flavonoid content in different anatomical parts of safflower have been reported. Abdallah *et al.*, (2013) reproted the flavonoid content in young

(green) and old (dry) leaves of safflower, observing significant variations between both phenological stages and different regions of Tunisia. Cultivation of the Kairouan region with 2.0 ± 0.02 for old leaf and 3.9 ± 0.06 mg CE g^{-1} DW for young leaf, in the Gabes region with 6.1 ± 0.08 for old leaf and 6.9 ± 0.24 mg CE g^{-1} DW for young leaf, in the Tazarka region 6.1 ± 0.18 for Old leaf and 3.1 ± 0.07 mg CE g^{-1} DW for young leaf. Karimkhani, *et al.*, (2016) reported the content of flavonoids in methanol extract of safflower, obtaining a content of 46.2 to 62.3 mg gallic acid equivalent/g dry sample. Shaki *et al.*, (2018) reported the content of flavonoids for samples of safflower leaf at different salt concentrations, noting that at 0 mM NaCl the flavonoid content is around 150 µg mL^{-1} and as the salt content increases, the flavonoid content increases, this due to the oxidative stress which the plant is subjected. Also, the leaf methanolic extract of our study presented a similar flavonoid content to those reported for extract of Plumbago auriculata LAM with 11.35 mg QE/g dry sample (Rivera *et al.*, 2018).

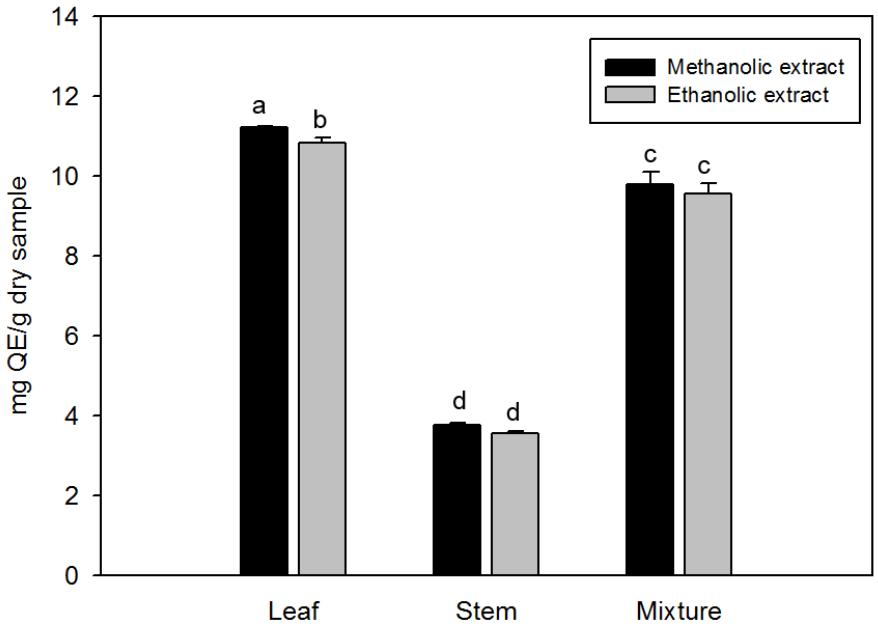

Figure 2. Total flavonoids of safflower (*Carthamus tinctorius* L.) by-products. The values represent the means with significant differences by Tukey (ANOVA, $p < 0.05$), means of 3 repetitions ($n = 3$). The different letters mark statistically significant differences.

Total Antioxdant Activity

Inhibition of DPPH• radical.

The total antioxidant activity was measured for the three safflower samples in methanolic and ethanolic extracts and reported in % inhibition and μmol TE/g dry sample. To inhibit the DPPH• radical (Table 2) with 0.2 mg mL^{-1} of extract. The antioxidant activity was different in all the samples varying from a inhibition (%) of 72.47 ± 0.29 to 91.24 ± 0.95 and inhibitión (μmol TE/g dry sample) of 15.02 ± 0.05 to 17.95 ± 0.16 being in both cases greater in leaf and smaller in stem. The difference in antioxidant activity (μmol TE/g dry sample) between methanolic and ethanolic extract were of 0.29 for leaf, 0.5 for stem and 0.07 for mixture. The variation of the antioxidant activity in micromol that were needed was minimal, however, that difference makes the antioxidant activity in percentage of inhibition is observed with more amplitude, concluding that the micromoles per minimo that vary they influence significantly. In the mixture extract (leaf-stem) the concentration will depend on the ratio of leaf and stem present, since the collection of this by-product varies in proportion.

In a previous study by Yu *et al*., (2013) evaluated antioxidant activity of safflower seeds by DPPH methods, they reported that at a concentration of 1 mg mL^{-1} an inhibition percentage of 36.2 ± 0.5 was obtained. These results are different from those reported in this study, where an inhibition percentage of 72.47 ± 0.29 to 91.24 ± 0.95 was obtained in leaf, stem and mixture. Although the dietary matrices are different, it suggests that safflower agroindustrial residue (leaf-stem) is an alternative to obtaining compounds with good antioxidant activity.

Studies of antioxidant activity of leaf and stem were similar trend to those reported by other researchers, where the leaf has a higher antioxidant capacity than stem. Kubola *et al.*, 2008 evaluated the total antioxidant capacity at the same concentration (0.2 mg mL^{-1}) of this study by the DPPH method. The results shown by Kubola were that leaf inhibited the DPPH radical was 56.8 ± 2.18 % and stem was 28.9 ± 2.43 %.

Table 2. Antioxidant activity by inhibition of $ABTS^{\bullet}$ and $DPPH^{\bullet+}$ radicals of safflower (*Carthamus tinctorius L*) by-product.

Sample	DPPH•		ABTS•+	
	% Inhibition	µmol TE/g dry sample	% Inhibition	µmol TE/g dry sample
Methanolic extract				
Leaf	91.24 ± 0.95[a]	18.02 ± 0.16[a]	93.16 ± 1.17[a]	18.20 ± 0.19[a]
Stem	83.60 ± 1.11[d]	15.52 ± 0.11[d]	86.70 ± 0.50[d]	16.30 ± 0.07[c]
Mixture*	88.86 ± 1.17[ab]	17.18 ± 0.20[ab]	91.77 ± 0.44[b]	17.88 ± 0.11[b]
Ethanolic extract				
Leaf	88.16 ± 0.60[bc]	17.66 ± 0.10[bc]	90.00 ± 0.22[bc]	18.16 ± 0.04[ab]
Stem	72.47 ± 0.29[e]	15.02 ± 0.05[e]	78.33 ± 0.86[e]	16.24 ± 0.14[c]
Mixture*	86.95 ± 0.45[c]	17.11 ± 0.20[c]	87.95 ± 0.34[cd]	17.92 ± 0.10[ab]

*Mixture = leaf and stem of safflower (*Carthamus tinctorius* L.) by-product. **Meands ± standard deviation (SD) of three independient experiments. Different letters in each column indicate significant differences ($p < 0.05$) in antioxidant activity by DPPH and ABTS between leaf, stem and mixture from two solvents metanol and ethanol.

Inhibition of ABTS$^{\bullet+}$ radical

The antioxidant activity by radical ABTS$^{\bullet+}$ was similar to the trend between the 3 samples in methanolic and ethanolic extracts and reported in % inhibition and μmol TE/g dry sample (Table 2). The antioxidant activity was different in all the samples varying for inhibition (%) of 78.33 ± 0.86 to 93.16 ± 1.17 and inhibitión (μmol TE/g dry sample) of 16.24 ± 0.14 to 18.20 ± 0.19 being in both cases greater in leaf and smaller in stem. The difference in antioxidant activity (μmol TE/g dry sample) between methanolic and ethanolic extract were of 0.04 for leaf, 0.06 for stem and 0.04 for mixture. In the mixture extract (leaf-stem) the concentration will depend on the ratio of leaf and stem present, since the collection of this by-product varies in proportion. The same way as in the DPPH$^{\bullet}$ radical inhibition, the variation of the antioxidant activity in micromol that were needed was minimal and even less than the DPPH$^{\bullet}$ radical.

The difference between the DPPH$^{\bullet}$ and ABTS$^{\bullet+}$ methods is due to the specificity that each one has to be inhibited, since being chemical reactions that happen between the antioxidant and the radical. It will depend on the chemical structure of each one to be able to interact, as well as the hydrophobic and hydrophilic character that show. In the case of the DPPH$^{\bullet}$ method, it interacts more feasibly with hydrophobic entities, whereas ABTS$^{\bullet+}$ method with hydrophobic and hydrophilic (de Camargo *et al.,* 2017). Due to the chemical structure of phenolic compounds, mainly of type flavonoids, they tend to be more hydrophobic due to the aromatic A and B rings present, although they also have a hydrophilic part by the hydroxyl groups (-OH) (Masek *et al.,* 2017). Although is demonstrated that not all the hydroxyl molecules present in the estructure interact with ease to donate the electron or hydrogen atom,

this due to the masking that occurs in the molecule (Farhoosh *et al.,* 2016). In alcoholic extracts, the donation of hydrogen atoms predominates (Tohama *et al.,* 2017).

Determinación of IC_{50}

The IC50 refers to the concentration of antioxidant to inhibit 50% free radicals. The IC50 is considered a parameter to determine the efficacy of the extracts of inhibiting 50% of the $DPPH^{\bullet}$ and $ABTS^{\bullet+}$ radicals. For methanolic and ethanolic safflower by-products different IC50 were obtained. Both solvents presented the same tendency as the total antioxidant activity, but showed significant differences between them (Table 3). In methanol solvent, the leaf extract presented lower IC50, followed by mixture extract and stem extract with 9.65, 12.45 and 64.88 μg mL^{-1} for $DPPH^{\bullet}$ and 8.46, 18.63 and 46.01 μg mL^{-1} for the $ABTS^{\bullet+}$ radical. When the IC50 is calculated in the extracts it is expected to be lower, since it is predicted that less concentration of the extract is taken to inhibit 50% of the radical. Comparing the radicals evaluated, $ABTS^{\bullet+}$ presented lower IC50 in all three samples than $DPPH^{\bullet}$.

Souri *et al.,* (2008) obtained a classification based on his research on different plant extracts, where he related the IC50 concentration. Its Classification mentions that an IC50 <20 μg mL^{-1} is considered High Antioxidant Capacity (HAC), 20 μg mL^{-1}> IC50 <75 μg mL^{-1} is Moderate Antioxidant Capacity (MAC) and IC50> 75 μg mL^{-1} is Low Antioxidant Capacity (LAC). Comparing the classification of Souri with the IC50 of this study, moderate (stem) to high antioxidant capacity (leaf and mixture) was obtained, being the agroindustrial residues of safflower an alternative compound with high antioxidant capacity.

Table 3. Estimation of the IC_{50} by DPPH● and ABTS●+ and their classification according to Souri *et al*. (2008) of safflower (*Carthamus tinctorius* L.) by-product.

Sample	DPPH•		ABTS•+	
	IC_{50} µg mL^{-1}	Classification	IC_{50} µg mL^{-1}	Classification
Methanolic extract				
Leaf	9.65	HAC	8.46	HAC
Stem	64.88	MAC	46.01	MAC
Mixture*	12.45	HAC	18.63	HAC
Ethanolic extract				
Leaf	13.61	HAC	12.03	HAC
Stem	73.04	MAC	56.46	MAC
Mixture*	25.35	MAC	14.06	HAC

*Mixture = leaf and stem of safflower (*Carthamus tinctorius* L.) by-product. IC_{50} < 20 µg mL^{-1} = High Antioxidant Capacity (HAC); 20 µg mL^{-1} > IC_{50} < 75 µg mL^{-1} = Moderate Antioxidant Capacity (MAC); IC_{50} > 75 µg mL^{-1} = Low Antioxidant Capacity (LAC)

FRAP assay

FRAP assay was realized for methanolic and ethanolic extracts of leaf, stem and mixture (leaf-stem) of safflower (*Carthamus tinctorius L.*) by-product at different reaction times and it is shown in Table 4. First, significant differences ($p < 0.5$) were observed for all the extracts at 10, 20 and 30 minutes of reaction. After of 30 minutes, the extracts not show changes in reducing power by FRAP assay. Likewise, all the extracts at the same time of reaction not show significant differences ($p < 0.5$) in the three times studied. The leaf was the anatomical part that presented the greatest reducing power, followed by the mixture and stem, both for methanolic and ethanolic extracts, observing that the phenolic compounds present in leaf of safflower (*Carthamus tinctorius L.*) by-product have greater reducing power to reduce the

ferric ion. This tendencies were similar to that reported by the radicals $ABTS^{\bullet+}$ and $DPPH^{\bullet}$, where the leaf was the one with the highest total antioxidant activity.

Table 4. Ferric reducing antioxidant power (FRAP) assay of safflower (*Carthamus tinctorius* L.) by-product.

Sample	**FRAP (µmol TE/g dry sample)**		
	Value at different times (min)		
	10	**20**	**30**
Methanolic extract			
Leaf	1.76 ± 0.036^{Af}	2.29 ± 0.330^{Bf}	2.67 ± 0.715^{Cf}
Stem	0.33 ± 0.060^{Ab}	0.42 ± 0.052^{Bb}	0.50 ± 0.080^{Cb}
Mixture*	0.88 ± 0.246^{Ad}	1.29 ± 0.050^{Bd}	1.35 ± 0.023^{Cd}
Ethanolic extract			
Leaf	1.67 ± 0.315^{Ae}	1.91 ± 0.132^{Be}	2.32 ± 0.056^{Ce}
Stem	0.26 ± 0.036^{Aa}	0.31 ± 0.045^{Ba}	0.38 ± 0.112^{Ca}
Mixture*	0.67 ± 0.247^{Ac}	1.12 ± 0.117^{Bc}	1.25 ± 0.027^{Cc}

*Mixture = leaf and stem of safflower (*Carthamus tinctorius* L.) by-product. The values represent the means ± DS with significant differences by Tukey (ANOVA, $p < 0.05$), means of 3 repetitions (n = 3). The different majuscule letters mark statistically significant differences between the three reaction times for methanolioc and ethanolic extracts of leaf, stem and mixture of safflower (*Carthamus tinctorius* L.) by porduct. The different minuscule letters mark statistically significant differences between all the extracts in a same reaction time.

FRAP assay is based on the reducing power of an antioxidant as phenplic compounds. A potential antioxidant will reduce the ferric ion (Fe^{3+}) to the ferrous ion (Fe^{2+}); the latter forms a blue complex (Fe^{2+}/TPTZ) (Wojdyło et al., 2007; Benzie & Devaki 2018). For phenolic compounds, the reducing power may depend on the degree of hydroxylation and degree of conjugation of the compounds (Pulido et al., 2000). In addition, the reducing power will depend on the type of extract and the concentration of the same. Yao et al., (2016) reported the FRAP assay for petal safflower (*Carthamus tinctorius L.)* extract at three concentrations

(5, 2.5 y 1.25 mg mL^{-1}), observing that the reducing power was less than 35 mMol. On the other hand, Qu et al., 2017 evaluated by FRAP assay 11 different individual compounds extracted from 300 mg mL^{-1} of petals safflower (*Carthamus tinctorius L.)* extract and reported that all presented reducing power less than 25 mMol and that the most influential were hydroxysafflor yellow A, 6-hydroxykaempferol 3-O-β-rutinoside and anhydrosafflor yellow B. Therefore, concluded that unlike the two previously described studies, the current study reported the FRAP assay at a concentration of 0.2 mg mL^{-1} of safflower (*Carthamus tinctorius L.)* by-products.

Protective effect on human erythrocyte

The protective effect of leaf extracts, stem and mixture in human erythrocytes and induced hemolysis by radical AAPH were evaluated and shown in the Figure 3. The three samples showed high inhibition in methanolic and ethanolic extract. Unlike the antioxidant activity by $DPPH^{\bullet}$ and $ABTS^{\bullet+}$, where the leaf presented greater antioxidant activity, while in the protective effect of human heritrocytes the stem was the one that presented the highest % inhibition of hemolysis in methanolic and ethanolic extract. In methanolic extract the percentage of inhibition of hemolysis were 91.9, 90 and 88.3% for stem, mixture and leaf, respectively. On the other hand, the percentage of inhibition of hemolysis for ethanolic extract was lower than methanolic with 87.5, 85.8 and 84.2 for leaf, stem and mixture, respectively. All samples were at a maximum concentration of 0.40 mg mL^{-1}. The difference between the two solvents was a variation of 4 to 5% with respect to each sample. La IC50 Para las muestras fue alrededor de 0.01 mg mL^{-1}.

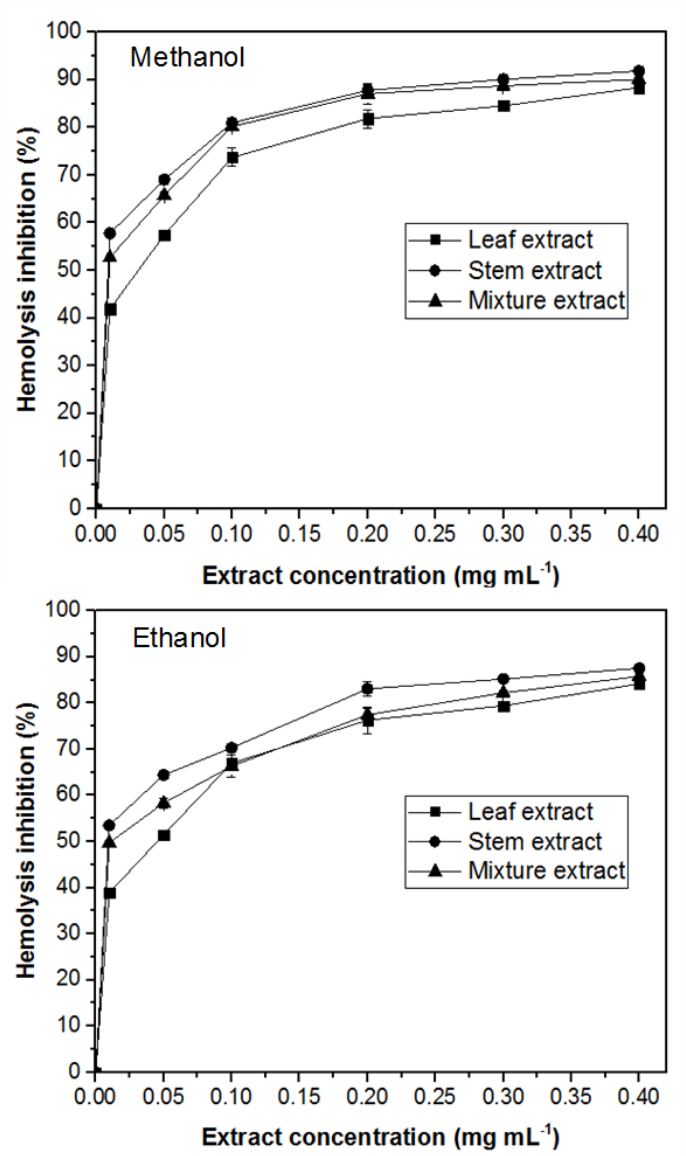

Figure 3. Antioxidant activity by protective effect in human erythrocytes of safflower (*Carthamus tinctorius* L.) by-product. a) methanolic extract and b) ethanolic extract.

Currently there is no evidence to measure the protective effect in human erythrocytes of safflower extracts. Therefore, this research is the first article to report this technique with safflower samples from northwestern Mexico. Other studies that report the % of hemolysis in the protective effect of human erythrocytes from methanolic and ethanolic extracts of

different plants containing phenolic compounds are reported in the literature. García-Becerra *et al*, 2016 reported the protective effect of methanolic extracts of grape pomace Mexican. They obtained a percentage of inhibition of hemolysis of 85 to 95% and an IC50 of 0.1 μg mL^{-1}. In conclusion, methanol extracts obtained by maceration present a higher total phenolic content and antioxidant capacity against damage induced by AAPH. Bento *et al.*, (2018) reported the protective effect of ethanolic extract of peaches. In thus study, the peach extract inhibited hemolysis in a concentration-dependent manner with an IC50 value at 109.9 ± 4.5 μg mL^{-1}. In conclusión, phenolic compound of ethanolic extract of peaches induce the protective effect in human erythrocytes. Comparing these two studies with that reported for safflower by-product extract, grape pomace Mexican presents lower IC50 while peach extract presents higher IC50.

The principle of the technique of protective effect of human erythrocytes, is that the radical AAPH, first undergoes a chemical decomposition at physiological temperature in aqueous solution to generate alkyl radicals, which in the presence of oxygen are converted into the corresponding peroxyl radicals; then these peroxyl radicals induce the oxidation of polyunsaturated lipids in the erythrocyte membrane, which causes a spread known as lipid peroxidation (Baccarin *et al.*, 2015). This lipid peroxidation can be reduced or not occur in the erythrocyte by the protection of antioxidants such as phenolic compounds. Suwalsky *et al.*, (2015) demonstrated from of micrographs of SEM, that erythrocytes in the presence of 0.5 mM to 2 mM resveratrol promotes the formation of echinocytosis. In addition, erythrocytes incubated with 0.5 mM HClO induce the formation of stomatocytes, therefore, when erythrocytes incubate with HClO and resveratrol the formation of stomatocytes decreases and the formation of normocytes and echinocytosis increases.

Correlation of phenolic compounds and flavonoids with antioxidant activity

To observe if the antioxidant activity is given by the phenolic compounds and flavonoids, the correlation coefficient (R^2) was obtained. Researchers have reported that there is a strong correlation of phenolic compounds with the antioxidant activity of extracts (Montaño-Leyva et al., 2019). In this study the correlation was determined for the three samples for methanolic and ethanolic extract and resume in the Table 5. The correlations from R^2 were obtained for antioxidant activity in percentage inhibition and μmol TE/g dry sample. For phenolic compounds, all samples presented an R^2 since 0.896 to 0.999 in percentage, being the lowest for stem ethanolic extract by $DPPH^{\bullet}$ radical inhibition, while the highest R^2 was for leaf methanolic extract with 0.999 by means of $ABTS^{\bullet+}$ radical inhibition. The same tendency was for the inhibition expressed in μmol TE/g dry sample. Moreover, Table 6 shows the correlation of flavonoids and antioxidant activity. High correlation was observed for leaf, stem and mixture in both solvents. In $DPPH^{\bullet}$ the R^2 varied from 0.783 to 0.97 in percent inhibition and from 0.828 to 0.97 in μmol TE/g dry simple. For $ABTS^{\bullet+}$ the R^2 varied from 0.904 to 0.991 in percent inhibition and from 0.8 to 0.991 in μmol TE/g dry simple. Being stem in methanol the one that presented the lowest correlation of the flavonoids and antioxidant activity in both solvents.

Some comparative studies between the correlation of antioxidant activity and phenolic compounds have been published. The different authors mention that phenolic compounds are responsible for the highest antioxidant activity in methanolic extracts. Karimi *et al.,* (2015) obtained crude methanolic extracts of *Quercus brantii* L. acorn and mentioned with a R^2 of 0.768 that the phenolic compounds are the main responsible for the total antioxidant activity. Teixeira *et al.,* (2017) reported a correlation coefficient of R^2 of 0.912 for the radical $ABTS^{\bullet+}$

and R^2 = 0.848 for the DDPH$^{\bullet}$ for different methanolic extracts. Bujor *et al*., (2018) determined the correlation coefficient for antioxidant activity and phenolic compounds of methanol extracts of lingonberry (*Vaccinium vitis-idaea* L.) leaf and determined R^2 of 0.91. Hamdi *et al*., (2018) obtained a correlation coefficient of R^2 of 0.563 for the DPPH$^{\bullet}$ radical and R^2 of 0.256 for the ABTS$^{\bullet+}$ radical of of *Haplophyllum tuberculatum A*. Juss leaves, observing a correlation between phenolic compounds and activity antioxidant by DPPH$^{\bullet}$ but not by ABTS$^{\bullet+}$. Therefore, comparing previous studies with safflower extracts, it can be mentioned that the phenolic compounds of safflower (*Carthamus tinctorius* L.) by-product present a higher correlation with the antioxidant activity.

Table 5. Correlation of phenolic compounds and antioxidant activity of methanolic and ethanolic extract of safflower (*Carthamus tinctorius* L.) by-product.

Sample	DPPH$^{\bullet}$		ABTS$^{\bullet+}$	
	% Inhibition R^2	µmol TE/g dry simple R^2	% Inhibition R^2	µmol TE/g dry simple R^2
Methanolic extract				
Leaf	0.973	0.976	0.999	0.999
Stem	0.949	0.974	0.986	0.996
Mixture*	0.958	0.988	0.99	0.986
Ethanolic extract				
Leaf	0.951	0.980	0.976	0.976
Stem	0.896	0.896	0.950	0.968
Mixture*	0.99	0.99	0.985	0.985

Table 6. Correlation of flavonoids and antioxidant activity of methanolic and ethanolic extract of safflower (*Carthamus tinctorius* L.) by-product.

Sample	DPPH●		ABTS●+	
	% Inhibition R^2	µmol TE/g dry simple R^2	% Inhibition R^2	µmol TE/g dry simple R^2
Methanolic extract				
Leaf	0.954	0.923	0.991	0.991
Stem	0.783	0.828	0.938	0.80
Mixture*	0.961	0.94	0.986	0.957
Ethanolic extract				
Leaf	0.97	0.97	0.969	0.969
Stem	0.925	0.926	0.904	0.935
Mixture*	0.952	0.926	0.977	0.961

Identification of phenolic compounds

For identify the molecules responsible of the antioxidant activity, a UPLC-DAD-MS equipment was used, besides an investigation in the literature. Also, 25 peaks were shown of which 22 were identified corresponding compounds identifid in methanolic and ethanolic extracts of leaf, stem and mixture of safflower (*Carthamus tinctorius* L.) by-product are shown in Table 7 and principal compounds of respective chromatograms are shown in Figure 4. The compounds were identified as phenolic compounds of flavonoid type and pigments. There were no differences in the peaks identified in methanolic and ethanolic extract of the three anatomical parts. The safflower leaf extract presented a principal peak at retention time of 6.93 minutes which was identified as a glycosylated flavonoid named luteolin 7-O-β-D-

glucoside, and with a common name of Cinaroside. Other studies that have identified this compound in different anatomical parts of safflower were Kim *et al.*, (2006) in ethanolic seed extract, Peirreti *et al*., in extract methanolic-water (80 % v/v), Han *et al*., (2010) in extract of safflowers.

Table 7. Identification of phenolic compounds by UPLC-DAD-MS of methanolic and ethanolic extract safflower (*Carthamus tinctorius* L) by-product**.**

	Methanol (Rt)			Ethanol(Rt)			[M-H]+	[M-H]-	Compounds
Peak	L	S	M	L	S	M			
1	0.36	0.38	0.38	0.36	0.37	0.38	111	NP	Resorcinol
2	0.38	0.36	0.36	0.37	0.36	0.36	181	NP	Caffeic acid
3	0.57	0.57	0.57	NP	NP	NP	171	NP	Gallic acid
4	0.76	0.77	0.76	0.78	0.77	0.77	166	NP	NI
5	1.05	1.04	1.04	1.03	10.02	1.04	155	153	Protocatechuic acid
6	NP	NP	NP	NP	NP	NP	NP	445	acatecin-7-O-B-D-glucoside (tilianin)
7	4.33	4.37	4.34	4.33	NP	4.35	209	NP	T-chalcone
8	4.46	4.50	4.49	4.45	4.49	4.48	642	NP	4, 4 "-bis (N-p-coumaroyl) serotonin
9	5.09	NP	5.10	5.10	NP	5.09	195	NP	T-ferulic acid
10	6.08	6.10	6.12	NP	NP	NP	461	NP	Acacetin 7-O-β-glucuronide
11	6.47	6.50	6.54	6.46	6.49	6.49	465	463	Quercetin-3-galactoside (Hyperoside)
12	6.76	6.78	6.76	6.75	6.78	6.77	611	NP	Kaempferol 3-sophoroside
13	6.93	7.01	6.99	6.96	6.99	7.01	449	447	Luteolin 7-O-β-D-glucoside (Cynaroside)
14	7.2	7.22	7.23	7.19	7.19	7.23	581	579	Naringenin

15	8.14	8.05	8.06	8.12	8.16	8.15	613	NP	Hydroxysafflor yellow A
16	8.58	8.58	8.60	NP	NP	NP	702	NP	4, 4 "-bis (N-feruloyl) serotonin
17	8.74	NP	8.76	8.76	NP	8.74	459	457	NI
18	NP	NP	NP	NP	NP	NP	NP	305	Gallocatechin
19	9.21	9.22	9.22	9.23	9.21	9.24	359	NP	Matairesinol
20	9.25	9.26	9.24	9.25	9.25	9.25	339	337	Quercetin dehydrate
21	9.29	9.28	9.29	9.25	9.29	930	303	301	Quercetin
22	9.37	9.37	9.37	9.30	9.37	9.38	287	285	Kaempferol
23	NP	NP	NP	NP	NP	NP	NP	457	Epigallocatechin gallate
24	10.98	NP	11.01	11.0	NP	10.99	285	NP	NI
25	12.28	12.27	12.27	12.27	12.28	12.26	285	NP	Acacetin

L= leaf; S= stem; M= mixture; NI = not identified; NP= not present

In safflower stems extracts, two maximum peaks corresponding to a glycosylated flavonoid and a pigment were identified. The first identified peak was a retention time of 6.47 minutes and named as Quercetin-3-galactoside and with a common name of Hyperoside. Other studies in the literature that have identified this compound in safflower (*Carthamus tinctorius* L.) were Salem *et al*., (2011) in flower extracts with three solvents (methanol, ethanol and acetone) and three stages of the plant, Salem *et al.,* (2014) in methanolic extract of flowers of in two flowering stages safflowers cultivated in Tunisian. The second peak identified in stem corresponds to a pigment with a retention time of 8.15 minutes and named hydroxysafflor yellow A, being one of the principals compounds that gives the color to the petals of safflower. Several studies have identified this compound as Yoon *et al*., (2003) extracted this compound from dried safflower petals, Wei *et al*., (2005) and Chu et al., (2006) extracted this pigment of safflowers petals as a neuroprotective agent in rats. Feng *et al.*, (2013) identified and studied the structure of this pigment from safflower by NMR. He *et al.*,

(2018) identified hydroxysafflor yellow A form methanol extract of safflower by high-performance thin-layer chromatography (HPTLC) method.

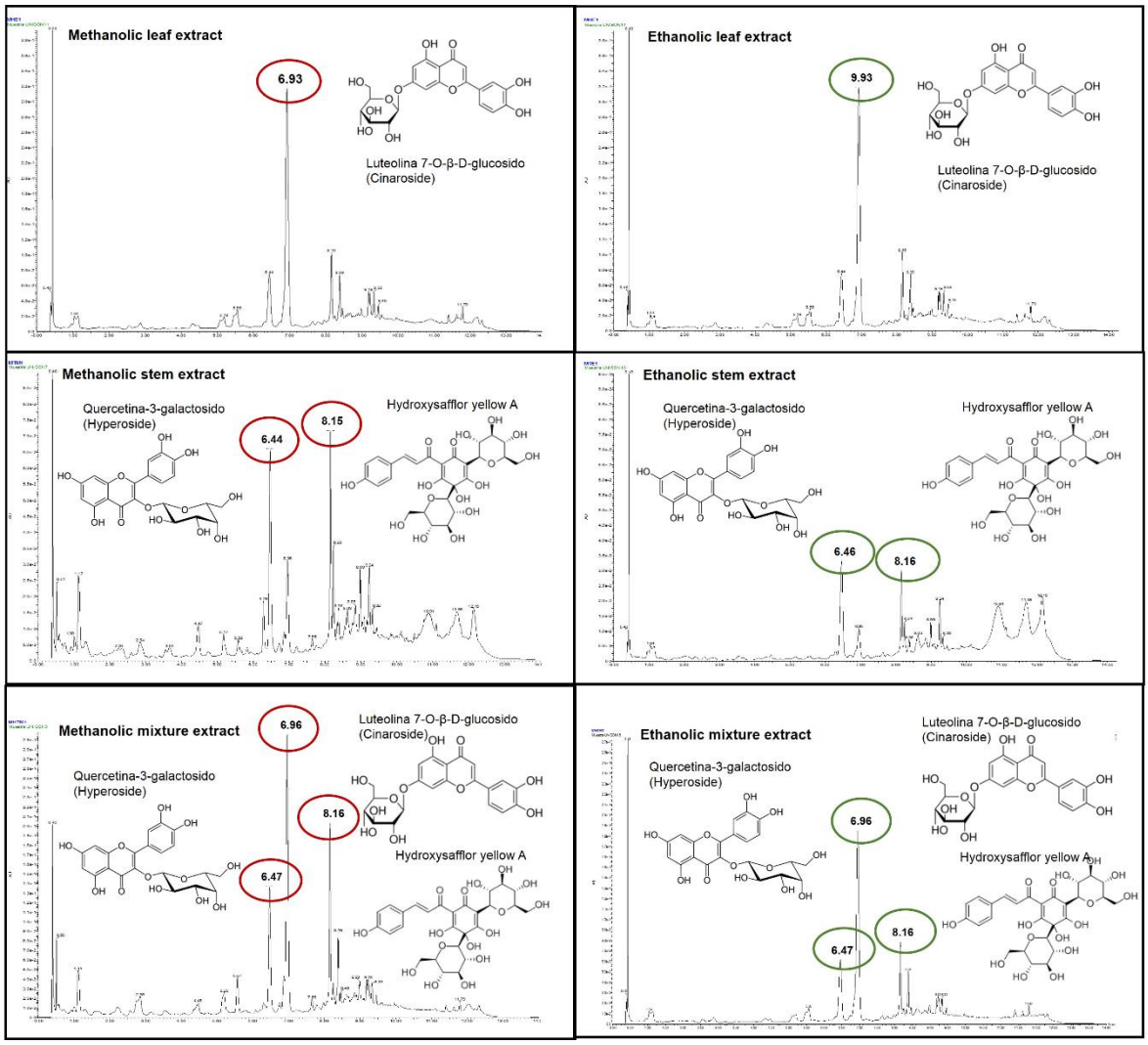

Figure 4. UPLC-DAD-MS of safflower (*Carthamus tinctorius* L.) by-products. The principal compounds are shown for leaf, stem and mixture.

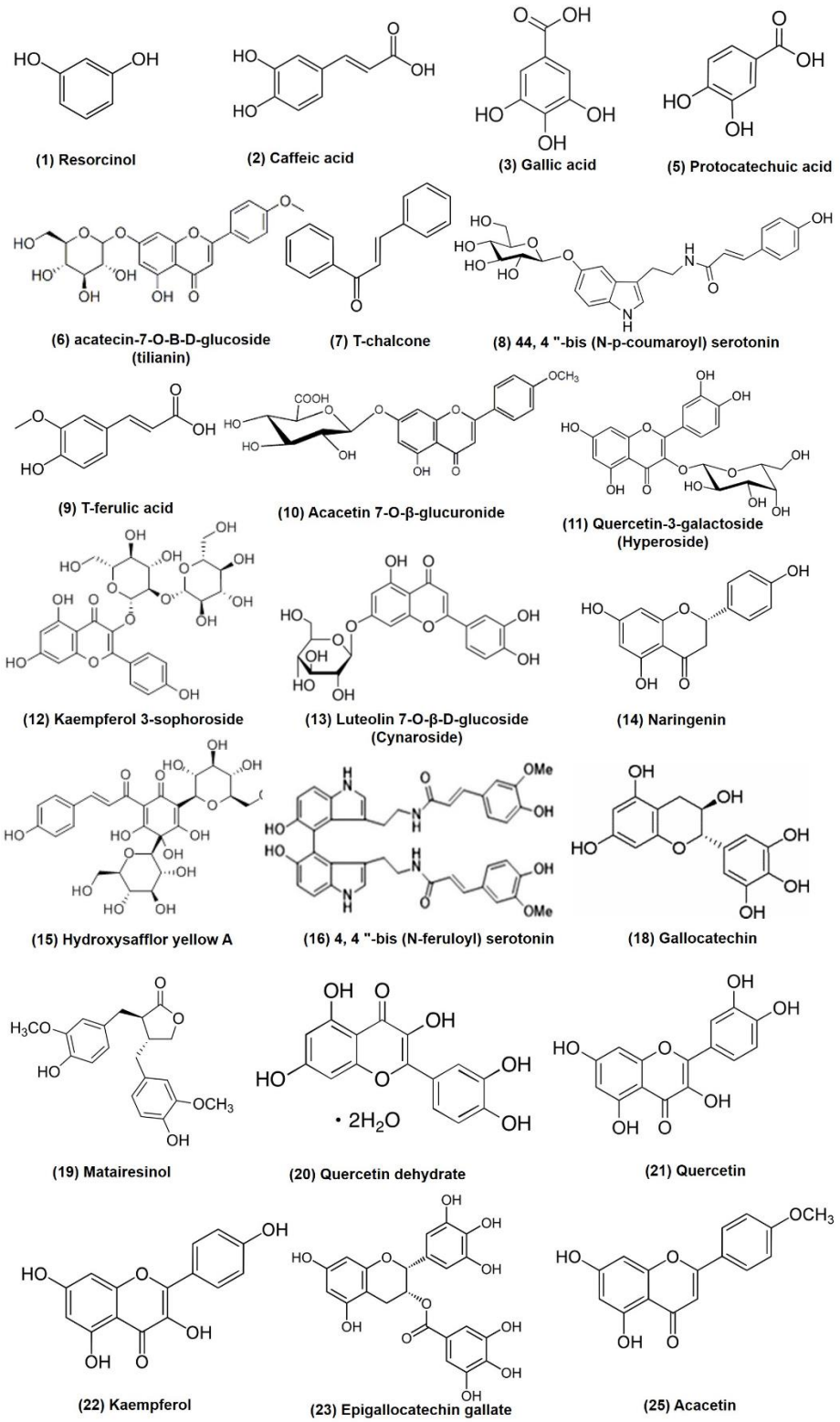

Figure 5. Structures of phenolic compounds identified in safflower (*Carthamus tinctorius* L.) by-products.

In the leaf-stem mixture were identified both the principal leaf compound (luteolin 7-O-β-D-glucoside), as well as, the two principal stem compounds (Quercetin-3-galactoside and hydroxysafflor yellow A). In addition, Table 7 shows all peaks identified by order in retention time in safflower by-products and for each extract obtained. These compounds are classified into 5 groups as mentioned in the introduction and their structures are shown in Figure 6. Group 1 (pigments): (15) Hydroxysafflor yellow A. Group 2 (flavonoids): (6) acatecin-7-O-B-D-glucoside, (7) T-chalcone, (10) acacetin-7-O-β-glucuronide, (11) quercetin-3-galactoside, (12) Kaempferol 3-soforoside, (13) Luteolin 7-O-β-D-glucoside, (14) Naringenin, (18) gallocatechin, (20) quercetin dehydrate, (21) quercetin, (22) kaempferol, (23) epigallocatechin gallate, (259) acacetin. Group 3 (lignans): (19) matairesinol. Group 4 (phenolic acids): (2) caffeic acid, (3) gallic acid, (5) protocatechuic acid, (9) acid T-ferulic. Group 5 (phenolic acids bound to serotonin): (8) 4, 4 "-bis (N-p-coumaroyl) serotonin, (16) 4, 4 "-bis (N-feruloyl) serotonin. (1) resorcinol was also identified. In addition, three compounds were (4, 17 and 24). All these compounds were previously identified in safflowers by other authors as Zhang et al., (1996), Kang et al., (1999), Takki et al., (1999), Kazuma et al., (2000), Wei et al., (2005), Han et al., (2010), Salem et al., (2011), Yu et al., (2013), Asgarpanah et al., (2013), Sakamura et al, (2014), Yao, (2016).

Therefore, different compounds can be isolated from methanolic and ethanolic extracts of safflower (*Carthamus tinctorius* L.) by-products, where the principals compounds are phenolic compounds of flavonoid type.

4. CONCLUSION

The present study showe the basis for the harnessed of phenolic compounds extracted from safflower by-products (mixture leaf-stem) using towo solvents (methanol and ethanol). Was observed that safflower has high antioxidant capacity by the DPPH, ABTS and Protective effect on human erythrocyte (AAPH) methods. In addition, the phenolic compounds present in leaf and mixture have high IC50 compared to stem with moderate IC50 in both solvents. In addition, phenolic compounds showed to be the responsible of the antioxidant activity in both extracts obtained. The phenolic compounds identified of type flavonoids which luteolin 7-O-β-D-glucoside and Quercetin-3-galactoside, highlighting as the principal. Therefore agroindustrial residues of safflower are an alternative the phenolic compounds and to be harnessed to prevent the occurrence of cardiovascular diseases, eliminating or reducing free radicals in later studies.

ACKNOWLEDGMENTS

M.C. José Agustín Tapia-Hernández is grateful to CONACYT for the scholarship granted.

REFERENCES

Perez-Perez, L. M., García-Borbón, L. L., González-Vega, R. I., Rodríguez-Figueroa, J. C., Rosas-Burgos, E. C., Huerta-Ocampo, J. Á., ... & Del-Toro-Sánchez, C. L. (2018). Liberación de compuestos fenólicos ligados en el garbanzo (Cicer arietinum L.) utilizando microbiota humana intestinal. Biotecnia, 20(3), 146-154.

Rivera, G. I., Lomelí, M. G., & García, M. Á. R. (2018). Análisis fitoquímico y actividad antibacteriana del extracto metanólico de hojas de Plumbago auriculata LAM. Biotecnia, 20(1), 53-60.

Montaño-Leyva, B., Quintero-Vargas, J. T., Ortega-García, J., Lugo-Sepúlveda, R. E., González, R. R., & Valencia-Rivera, D. E. (2018). Actividad antioxidante y antiproliferativa del extracto metanólico de Asparagus officinalis. Biotecnia, 21(1), 148-153.

Hernández-Ruiz, K. L., Ruiz-Cruz, S. , Cira-Chávez, L. A., Gassos-Ortega L. E., Ornelas-Paz J. J., Del-Toro-Sánchez, C.L., Márquez-Ríos, E. López-Mata, M. A., & Rodríguez-Félix, F. (2018). Evaluation of Antioxidant Capacity, Protective Effect on Human Erythrocytes and Phenolic Compound Identification in Two Varieties of Plum Fruit (Spondias spp.) by UPLC-MS. Molecules. 23, 3200.

Yusuf, M. (2017). Agro-Industrial Waste Materials and their Recycled Value-Added Applications. Handbook of Ecomaterials, 1-11.

de los Ángeles Fernández, M., Espino, M., Gomez, F. J., & Silva, M. F. (2018). Novel approaches mediated by tailor-made green solvents for the extraction of phenolic compounds from agro-food industrial by-products. Food Chemistry, 239, 671-678.

Arun, K. B., Chandran, J., Venugopal, V. V., Madhavankutty, T. S., & Nisha, P. (2017). Spent cumin seeds generated from ayurvedic industry as a source of bioactive compounds for nutraceutical/functional food applications. Journal of Food Processing and Preservation.

Marín, D., Alemán, A., Sánchez-Faure, A., Montero, P., & Gómez-Guillén, M. C. (2018). Freeze-dried phosphatidylcholine liposomes encapsulating various antioxidant extracts from natural waste as functional ingredients in surimi gels. *Food chemistry*, *245*, 525-535.

Vodnar, D. C., Călinoiu, L. F., Dulf, F. V., Ştefănescu, B. E., Crişan, G., & Socaciu, C. (2017). Identification of the bioactive compounds and antioxidant, antimutagenic and antimicrobial activities of thermally processed agro-industrial waste. Food Chemistry, 231, 131-140.

de Francisco, L., Pinto, D., Rosseto, H., Toledo, L., Santos, R., Tobaldini-Valério, F., ... & Rodrigues, F. (2018). Evaluation of radical scavenging activity, intestinal cell viability and antifungal activity of Brazilian propolis by-product. Food Research International, 105, 537-547.

Medina, S., Collado-González, J., Ferreres, F., Londoño-Londoño, J., Jiménez-Cartagena, C., Guy, A., .& Gil-Izquierdo, A. (2017). Valorization Strategy of Banana Passion Fruit Shell

Wastes: An Innovative Source of Phytoprostanes and Phenolic Compounds and Their Potential Use in Pharmaceutical and Cosmetic Industries. Journal of Food and Nutrition Research, 5(11), 801-808.

Vuong, Q. V. (2017). Utilisation of Bioactive Compounds from Agricultural and Food Production Waste. CRC Press.

Squillaci, G., Apone, F., Sena, L. M., Carola, A., Tito, A., Bimonte, M., & Morana, A. (2018). Chestnut (Castanea sativa Mill.) industrial wastes as a valued bioresource for the production of active ingredients. Process Biochemistry, 64, 228-236.

Ulloa, J. A., Rosas-Ulloa, P., & Ulloa-Rangel, B. E. (2011). Physicochemical and functional properties of a protein isolate produced from safflower (Carthamus tinctorius L.) meal by ultrafiltration. Journal of the Science of Food and Agriculture, 91(3), 572-577.

Ávila Casillas, E., Ocho Espinoza, X. M., Montoya Coronado, L., Aguilera Molina, N. A., Borbón Gracia, A., & Alvarado Padilla, J. I. (2017). Chey-ol: new variety of oleic safflowerfor northwest Mexico. *Revista Mexicana de Ciencias Agrícolas*, *8*(5).

Buitimea-Cantúa, N. E., Salazar-García, M. G., Vidal-Quintanar, R. L., Serna-Saldívar, S. O., Ortega-Ramirez, R., & Buitimea-Cantúa, G. V. (2017). Formulation of Zero-Trans Crystalized Fats Produced from Palm Stearin and High Oleic Safflower Oil Blends. Journal of Food Quality, 2017.

Yan, Z., Wang, Y., & Huang, X. (2017). Studies on the chemical constituents of Safflower (Carthamus tinctorius L.) and their tyrosinase inhibitory activity. Asian Journal of Traditional Medicines, 12(3).

Wang, F., Miao, M., Xia, H., Yang, L. G., Wang, S. K., & Sun, G. J. (2017). Antioxidant activities of aqueous extracts from 12 Chinese edible flowers in vitro and in vivo. Food & nutrition research, 61(1), 1-9.

Bielfeldt, S., Blaak, J., Wohlfart, R., Manger, C., & Wilhelm, K. P. (2017). Observer-Blind Randomized Controlled Study of a Cosmetic Blend of Safflower, Olive and Other Plant Oils in the Improvement of Scar and Striae Appearance. International Journal of Cosmetic Science.

Ibrahim, O. H. M., Abdul-Hafeez, E. Y., & Abdel-Kader, A. A. S. (2016). Impact of climatic changes on safflower (Carthamus tinctorius L.) productivity: improving growth and carthamin pigment content by sowing date adaptation and micronutrients foliar application. J. Plant Production, Mansoura Univ, 7(1), 77-84.

Ohama, P., Namwong, S., & Kumpun, S. (2016). Pigment Extraction of Safflower, Dyeing Properties and Antimicrobial Study of Dyed Silk. In Key Engineering Materials (Vol. 675, pp. 19-22). Trans Tech Publications.

Li, F., He, Z., & Ye, Y. (2017). Isocartormin, a novel quinochalcone C-glycoside from Carthamus tinctorius. Acta Pharmaceutica Sinica B, 7(4), 527-531.

Liao, Y., Liang, F., Liu, H., Zheng, Y., Li, P., Peng, W., & Su, W. (2018). Safflower yellow extract inhibits thrombus formation in mouse brain arteriole and exerts protective effects against hemorheology disorders in a rat model of blood stasis syndrome. Biotechnology & Biotechnological Equipment, 32(2), 487-497.

Hiramatsu, M., Igarashi, K., Suzuki, J., Murakami, A., Oikawa, A., & Takahashi, T. (2017). Composition and radical scavenging activity of polyphenols present in petals and young leaves of mogami-benibana (safflower, Carthamus tinctrius LINNE). Current Topics in Nutraceutical Research, 15(1).

Kim, S. M., Park, Y. J., Shin, M. S., Kim, H. R., Kim, M. J., Lee, S. H., & Kwon, S. H. (2017). Acacetin inhibits neuronal cell death induced by 6-hydroxydopamine in cellular Parkinson's disease model. Bioorganic & Medicinal Chemistry Letters, 27(23), 5207-5212.

Yao, C. L., Yang, W. Z., Si, W., Shen, Y., Zhang, N. X., Chen, H. L., & Guo, D. A. (2017). An enhanced targeted identification strategy for the selective identification of flavonoid O-glycosides from Carthamus tinctorius by integrating offline two-dimensional liquid chromatography/linear ion-trap-Orbitrap mass spectrometry, high-resolution diagnostic product ions/neutral loss filtering and liquid chromatography-solid phase extraction-nuclear magnetic resonance. Journal of Chromatography A, 1491, 87-97.

Park, S. H., Park, H. J., Kim, J. Y., Lee, S. H., Jang, J. S., & Lee, M. H. (2017). Mixed seeds juice with high antioxidant capacity and digestive enzyme activity and its application. Food Science and Biotechnology, 26(1), 237-244.

Solyomváry, A., Beni, S., & Boldizsar, I. (2017). Dibenzylbutyrolactone Lignans–A Review of Their Structural Diversity, Biosynthesis, Occurrence, Identification and Importance. Mini reviews in medicinal chemistry, 17(12), 1053-1074.

Khalid, N., Khan, R. S., Hussain, M. I., Farooq, M., Ahmad, A., & Ahmed, I. (2017). A comprehensive characterisation of safflower oil for its potential applications as a bioactive food ingredient-a review. Trends in Food Science & Technolog.

Namdjoyan, S., Kermanian, H., Soorki, A. A., Tabatabaei, S. M., & Elyasi, N. (2017). Interactive effects of Salicylic acid and nitric oxide in alleviating zinc toxicity of Safflower (Carthamus tinctorius L.). Ecotoxicology, 1-10.

Karimkhani, M. M., Shaddel, R., Khodaparast, M. H. H., Vazirian, M., & Piri-Gheshlaghi, S. (2016). Antioxidant and antibacterial activity of safflower (Carthamus tinctorius L.) extract from four different cultivars. Quality Assurance and Safety of Crops & Foods, 8(4), 565-574.

Lazari, D., Alexiou, G. A., Markopoulos, G. S., Vartholomatos, E., Hodaj, E., Chousidis, I., & Kyritsis, A. P. (2017). N-(p-coumaroyl) serotonin inhibits glioblastoma cells growth through triggering S-phase arrest and apoptosis. Journal of Neuro-Oncology, 1-9.

Peng, X. R., Wang, X., Dong, J. R., Qin, X. J., Li, Z. R., Yang, H., ... & Qiu, M. H. (2017). Rare Hybrid Dimers with Anti-Acetylcholinesterase Activities from a Safflower (Carthamus

tinctorius L.) Seed Oil Cake. Journal of Agricultural and Food Chemistry, 65(43), 9453-9459.

Yu, S. Y., Lee, Y. J., Kim, J. D., Kang, S. N., Lee, S. K., Jang, J. Y., .& Lee, O. H. (2013). Phenolic composition, antioxidant activity and anti-adipogenic effect of hot water extract from safflower (Carthamus tinctorius L.) seed. Nutrients, 5(12), 4894-4907.

Yahia, E. M., Gutiérrez-Orozco, F., & Moreno-Pérez, M. A. (2017). Identification of phenolic compounds by liquid chromatography-mass spectrometry in seventeen species of wild mushrooms in Central Mexico and determination of their antioxidant activity and bioactive compounds. Food Chemistry, 226, 14-22.

Valadez-Carmona, L., Plazola-Jacinto, C. P., Hernández-Ortega, M., Hernández-Navarro, M. D., Villarreal, F., Necoechea-Mondragón, H., ... & Ceballos-Reyes, G. (2017). Effects of microwaves, hot air and freeze-drying on the phenolic compounds, antioxidant capacity, enzyme activity and microstructure of cacao pod husks (Theobroma cacao L.). Innovative Food Science & Emerging Technologies, 41, 378-386

Parit, S. B., Dawkar, V. V., Tanpure, R. S., Pai, S. R., & Chougale, A. D. (2018). Nutritional quality and antioxidant activity of wheatgrass (Triticum aestivum) unwrap by proteome profiling and DPPH and FRAP assays. Journal of food science, 83(8), 2127-2139.

del Pilar Garcia-Mendoza, M., Espinosa-Pardo, F. A., Baseggio, A. M., Barbero, G. F., Junior, M. R. M., Rostagno, M. A., & Martínez, J. (2017). Extraction of phenolic compounds and anthocyanins from juçara (Euterpe edulis Mart.) residues using pressurized liquids and supercritical fluids. The Journal of Supercritical Fluids, 119, 9-16.

Jiménez-Aguilar, D. M., & Grusak, M. A. (2017). Minerals, vitamin C, phenolics, flavonoids and antioxidant activity of Amaranthus leafy vegetables. Journal of Food Composition and Analysis, 58, 33-39.

Huang, H. S., & Liaw, E. T. (2017). HPLC-DAD-MS method for Simultaneous quantitation of flavonoids in Hypericum formosanum and antiglycation activity. Journal of Pharmacognosy and Phytochemistry, 6(5), 854-858.

Cho, S. H., Lee, H. R., KIM, T. B., Choi, S. W., Lee, W. J., & Choi, Y. (2004). Effects of defatted safflower seed extract and phenolic compounds in diet on plasma and liver lipid in ovariectomized rats fed high-cholesterol diets. Journal of nutritional science and vitaminology, *50*(1), 32-37.

Golkar, P., & Taghizadeh, M. (2018). In vitro evaluation of phenolic and osmolite compounds, ionic content, and antioxidant activity in safflower (Carthamus tinctorius L.) under salinity stress. Plant Cell, Tissue and Organ Culture (PCTOC), 1-12.

Kubola, J., & Siriamornpun, S. (2008). Phenolic contents and antioxidant activities of bitter gourd (Momordica charantia L.) leaf, stem and fruit fraction extracts in vitro. Food chemistry, 110(4), 881-890.

de Camargo, A. C., Regitano-d'Arce, M. A. B., Rasera, G. B., Canniatti-Brazaca, S. G., do Prado Silva, L., Alvarenga, V. O., ... & Shahidi, F. (2017). Phenolic acids and flavonoids of peanut by-products: Antioxidant capacity and antimicrobial effects. Food Chemistry.

Masek, A., Chrzescijanska, E., Latos, M., & Zaborski, M. (2017). Influence of hydroxyl substitution on flavanone antioxidants properties. Food chemistry, 215, 501-507.

Farhoosh, R., Johnny, S., Asnaashari, M., Molaahmadibahraseman, N., & Sharif, A. (2016). Structure–antioxidant activity relationships of o-hydroxyl, o-methoxy, and alkyl ester derivatives of p-hydroxybenzoic acid. Food chemistry, 194, 128-134.

Tohma, H., Gülçin, İ., Bursal, E., Gören, A. C., Alwasel, S. H., & Köksal, E. (2017). Antioxidant activity and phenolic compounds of ginger (Zingiber officinale Rosc.) determined by HPLC-MS/MS. Journal of Food Measurement and Characterization, 11(2), 556-566.

García-Becerra, L., Mitjans, M., Rivas-Morales, C., Verde-Star, J., Oranday-Cárdenas, A., & María, P. V. (2016). Antioxidant comparative effects of two grape pomace Mexican extracts from vineyards on erythrocytes. Food chemistry, 194, 1081-1088

Bento, C., Gonçalves, A. C., Silva, B., & Silva, L. R. (2018). Assessing the phenolic profile, antioxidant, antidiabetic and protective effects against oxidative damage in human erythrocytes of peaches from Fundão. Journal of Functional Foods, 43, 224-233.

Baccarin, T., Mitjans, M., Lemos-Senna, E., & Vinardell, M. P. (2015). Protection against oxidative damage in human erythrocytes and preliminary photosafety assessment of Punica granatum seed oil nanoemulsions entrapping polyphenol-rich ethyl acetate fraction. Toxicology in Vitro, 30(1), 421-428.

Suwalsky, M., Villena, F., & Gallardo, M. J. (2015). In vitro protective effects of resveratrol against oxidative damage in human erythrocytes. Biochimica et Biophysica Acta (BBA)-Biomembranes, 1848(1), 76-82.

Benzie, I. F., & Devaki, M. (2018). The 5 ferric reducing/antioxidant power (FRAP) assay for non-enzymatic antioxidant capacity: concepts, procedures, limitations and applications. Measurement of Antioxidant Activity and Capacity: Recent Trends and Applications, 77.

Pulido, R., Bravo, L., & Saura-Calixto, F. (2000). Antioxidant activity of dietary polyphenols as determined by a modified ferric reducing/antioxidant power assay. Journal of agricultural and food chemistry, 48(8), 3396-3402.

Qu, C., Wang, L. Y., Lin, H., Shang, E. X., Tang, Y. P., Yue, S. J., ... & Liu, P. (2017). Hierarchical identification of bioactive components in a medicinal herb by preparative high-performance liquid chromatography and selective knock-out strategy. Journal of pharmaceutical and biomedical analysis, 135, 206-216.

Yao, D., Wang, Z., Miao, L., & Wang, L. (2016). Effects of extracts and isolated compounds from safflower on some index of promoting blood circulation and regulating menstruation. Journal of ethnopharmacology, 191, 264-272.

Wojdyło, A., Oszmiański, J., & Czemerys, R. (2007). Antioxidant activity and phenolic compounds in 32 selected herbs. Food chemistry, 105(3), 940-949.

Souri, E., Amin, G., & Farsam, H. (2008). Screening of antioxidant activity and phenolic content of 24 medicinal plant extracts. DARU Journal of Pharmaceutical Sciences, 16(2), 83-87.

Karimi, A., & Moradi, M. T. (2015). Total phenolic compounds and in vitro antioxidant potential of crude methanol extract and the correspond fractions of Quercus brantii L. acorn. Journal of HerbMed Pharmacology, 4.

Teixeira, T. S., Vale, R. C., Almeida, R. R., Ferreira, T. P. S., & Guimarães, L. (2017). Antioxidant Potential and its Correlation with the Contents of Phenolic Compounds and Flavonoids of Methanolic Extracts from Different Medicinal Plants. Revista Virtual de Química, 9, 1546-1559

Bujor, O. C., Giniès, C., Popa, V. I., & Dufour, C. (2018). Phenolic compounds and antioxidant activity of lingonberry (Vaccinium vitis-idaea L.) leaf, stem and fruit at different harvest periods. Food Chemistry.

Shikano, I., Shumaker, K. L., Peiffer, M., Felton, G. W., & Hoover, K. (2017). Plant-mediated effects on an insect–pathogen interaction vary with intraspecific genetic variation in plant defences. Oecologia, 183(4), 1121-1134.

Abdallah, S. B., Rabhi, M., Harbaoui, F., Zar-kalai, F., Lachâal, M., & Karray-Bouraoui, N. (2013). Distribution of phenolic compounds and antioxidant activity between young and old leaves of Carthamus tinctorius L. and their induction by salt stress. Acta physiologiae plantarum, 35(4), 1161-1169.

Ivanova, R. (2017). Antioxidant activity of safflower leaves and its modification by abiotic factors. Agronomy Series of Scientific Research/Lucrari Stiintifice Seria Agronomie, 60(2).

Taha, E., & Matthaus, B. (2018). Study of Safflower Varieties Cultivated Under Southern Egypt Conditions for Seeds and Flowers. Journal of Biological Sciences, 18(2), 74-83.

Karimkhani, M. M., Shaddel, R., Khodaparast, M. H. H., Vazirian, M., & Piri-Gheshlaghi, S. (2016). Antioxidant and antibacterial activity of safflower (Carthamus tinctorius L.) extract from four different cultivars. Quality Assurance and Safety of Crops & Foods, 8(4), 565-574.

Kim, E. O., Lee, J. Y., & Choi, S. W. (2006). Quantitative changes in phenolic compounds of safflower (Carthamus tinctorius L.) seeds during growth and processing. Preventive Nutrition and Food Science, 11(4), 311-317.

HAN, W., YANG, Y. L., & KANG, T. G. (2010). Determination of Luteolin-7-O-glucoside and Luteolin in Overground Portiono of Carthamus tinctorius L. by HPLC. Chinese Archives of Traditional Chinese Medicine, 6, 080.

Peiretti, P. G., Gai, F., Karamać, M., & Amarowicz, R. ANTIOXIDANT ACTIVITIES AND PHENOLIC COMPOSITION OF THE SAFFLOWER (CARTHAMUS TINCTORIUS L.) PLANT DURING ITS GROWTH CYCLE.

Salem, N., Msaada, K., Hamdaoui, G., Limam, F., & Marzouk, B. (2011). Variation in phenolic composition and antioxidant activity during flower development of safflower (Carthamus tinctorius L.). Journal of agricultural and food chemistry, 59(9), 4455-4463.

Salem, N., Msaada, K., Dhifi, W., Limam, F., & Marzouk, B. (2014). Effect of salinity on plant growth and biological activities of Carthamus tinctorius L. extracts at two flowering stages. Acta physiologiae plantarum, 36(2), 433-445.

Yoon, J. M., Cho, M. H., Park, J. E., Kim, Y. H., Hahn, T. R., & Paik, Y. S. (2003). Thermal stability of the pigments hydroxysafflor yellow A, safflor yellow B, and precarthamin from safflower (Carthamus tinctorius). Journal of food science, 68(3), 839-843.

Wei, X., Liu, H., Sun, X., Fu, F., Zhang, X., Wang, J., & Ding, H. (2005). Hydroxysafflor yellow A protects rat brains against ischemia-reperfusion injury by antioxidant action. Neuroscience letters, 386(1), 58-62.

Chu, D., Liu, W., Huang, Z., Liu, S., Fu, X., & Liu, K. (2006). Pharmacokinetics and excretion of hydroxysafflor yellow A, a potent neuroprotective agent from safflower, in rats and dogs. Planta medica, 72(05), 418-423.

Yoon, J. M., Cho, M. H., Park, J. E., Kim, Y. H., Hahn, T. R., & Paik, Y. S. (2003). Thermal stability of the pigments hydroxysafflor yellow A, safflor yellow B, and precarthamin from safflower (Carthamus tinctorius). Journal of food science, 68(3), 839-843.

Feng, Z. M., He, J., Jiang, J. S., Chen, Z., Yang, Y. N., & Zhang, P. C. (2013). NMR solution structure study of the representative component hydroxysafflor yellow A and other quinochalcone C-glycosides from Carthamus tinctorius. Journal of natural products, 76(2), 270-274.

He, T., Zeng, Y., & Zhou, X. (2018). Qualitative and quantitative analysis of hydroxysafflor yellow A in safflower by using high-performance thin-layer chromatography. JPC-Journal of Planar Chromatography-Modern TLC, 31(2), 129-134.

Zhang, H. L., Nagatsu, A., & SAKAKIBARA, J. (1996). Novel antioxidants from safflower (Carthamus tinctorius L.) oil cake. Chemical and pharmaceutical bulletin, 44(4), 874-876.

Takii, T., Hayashi, M., Hiroma, H., Chiba, T., Kawashima, S., Zhang, H. L., & Onozaki, K. (1999). Serotonin derivative, N-(p-coumaroyl) serotonin, isolated from safflower (Carthamus tinctorius L.) oil cake augments the proliferation of normal human and mouse

fibroblasts in synergy with basic fibroblast growth factor (bFGF) or epidermal growth factor (EGF). The Journal of Biochemistry, 125(5), 910-915.

Kang, G. H., Chang, E. J., & Park, S. W. (1999). Antioxidative activity of phenolic compounds in roasted safflower (Carthamus tinctorius L.) seeds. Preventive Nutrition and Food Science, 4(4), 221-225.

Asgarpanah, J., & Kazemivash, N. (2013). Phytochemistry, pharmacology and medicinal properties of Carthamus tinctorius L. Chinese journal of integrative medicine, 19(2), 153-159.

Han, S. Y., Li, H. X., Bai, C. C., Wang, L., & Tu, P. F. (2010). Component Analysis and Free Radical-Scavenging Potential of Panax notoginseng and Carthamus tinctorius Extracts. Chemistry & biodiversity, 7(2), 383-391.

Sakamura, S., Terayama, Y., Kawakatsu, S., Ichihara, A., & Saito, H. (1980). Conjugated serotonins and phenolic constituents in safflower seed (Carthamus tinctorius L.). Agricultural and Biological Chemistry, 44(12), 2951-2954.

Kazuma, K., Takahashi, T., Sato, K., Takeuchi, H., Matsumoto, T., & Okuno, T. (2000). Quinochalcones and flavonoids from fresh florets in different cultivars of Carthamus tinctorius L. Bioscience, biotechnology, and biochemistry, 64(8), 1588-1599.

Yao, D., Wang, Z., Miao, L., & Wang, L. (2016). Effects of extracts and isolated compounds from safflower on some index of promoting blood circulation and regulating menstruation. Journal of ethnopharmacology, 191, 264-272.

CAPÍTULO IV

Preparation and Characterization of Quercetin-Loaded Zein Nanoparticles by Electrospraying and Study of *In Vitro* Bioavailability

Preparation and Characterization of Quercetin-Loaded Zein Nanoparticles by Electrospraying and Study of *In Vitro* Bioavailability

Francisco Rodríguez-Félix[a], Carmen Lizette Del-Toro-Sánchez[a], Francisco Javier Cinco-Moroyoqui[a], Josué Juárez[b], Saúl Ruiz-Cruz[c], Guadalupe Amanda López-Ahumada[a], Elizabeth Carvajal-Millan[d], Daniela Denisse Castro-Enríquez[a], Carlos Gregorio Barreras-Urbina[a], José Agustín Tapia-Hernández[a]

[a]Department of Research and Posgraduate in Food (DIPA). University of Sonora. Blvd. Luis Encinas y Rosales, S/N, Colonia Centro, 83000. Hermosillo, Sonora, Mexico.

[b]Department of Physics, University of Sonora, Blvd. Luis Encinas y Rosales, S/N, Colonia Centro, 83000. Hermosillo, Sonora, Mexico.

[c]Department of Biotechnology and Food Science. Institute Technology of Sonora. 5 de febrero #818 sur, Colonia Centro, 85000, Ciudad Obregón, Sonora, Mexico.

[d]Research Center for Food and Development A.C. Carretera a La Victoria KM 0.6, 83304, Hermosillo, Sonora, México.

*Corresponding author: José Agustín Tapia-Hernández

E-mail: joseagustin.tapia@unison.mx

Telephone number: +52-662-259-2208. Fax: +52-662-259-2209.

Orcid: https://orcid.org/0000-0003-1124-7001

Short version of title: Quercetin-Loaded Zein Nanoparticles

Choice of journal/section: Food Engineering, Materials Science, and Nanotechnology

Abstract

Quercetin is a hydrophobic flavonoid with high antioxidant activity. However, for biological applications, the bioavailability of quercetin is low due to physiological barriers. For this reason, an alternative is the protection of quercetin in matrices of biopolymers as zein. The objective of this work was to prepare and characterize quercetin-loaded zein nanoparticles by electrospraying and its study of in vitro bioavailability. The physicochemical parameters such as viscosity, density and electrical conductivity of zein solutions showed a dependence of the ethanol concentration. In addition, rheological parameters demonstrated that solutions of zein in aqueous ethanol present Newtonian behavior, rebounding in the formation of nanoparticles by electrospraying, providing spherical, homogeneous, and compact morphologies, mainly at a concentration of 80% (v/v) of ethanol and of 5% (w/v) of zein. The size and shape of quercetin-loaded zein nanoparticles were studied by Transmission Electron Microscopy (TEM), observing that it was entrapped, distributed throughout the nanoparticle of zein. Analysis by Fourier Transform-Infrared (FT-IR) of zein nanoparticles loaded with quercetin revealed interactions via hydrogen bonds. The efficacy of zein nanoparticles to entrap quercetin was particularly high for all quercetin concentration evaluated in this work (87.9 ± 1.5 to 93.0 ± 2.6%). The *in vitro* gastrointestinal release of trapped quercetin after 240 min was 79.1%, while that for free quercetin was 99.2%. The *in vitro* bioavailability was higher for trapped quercetin (5.9%) compared to free quercetin (1.9%), then of gastrointestinal digestion. It is concluded, that the electrospraying technique made possible the obtention of quercitin-loaded zein nanoparticles increasing their bioavailability.

Keywords: zein, quercetin, nanoparticles, electrospraying, entrapment, bioavailability.

Practical Application:

This type of nanosystems can be used in the food and pharmaceutical industry. Quercetin-loaded zein nanoparticles for its improvement compared to free quercetin can be used to decrease the prevalence of chronic degenerative diseases by increasing of the bioavailability of quercetin in the bloodstream. Other application can be as an antioxidant system in functional foods or oils to increase shelf life.

1. Introduction

Quercetin is a hydrophobic polyphenol from the subfamily of flavonols that is mainly present in the human diet (Sharma, Kashyap, Sak, Tuli, & Sharma, 2018). The chemical structure of quercetin consists of 15 carbon atoms with two aromatic rings connected by three-carbon bridges and three hydroxyl groups (-OH) in the position 3, 5 and 7 in hydroxychromen structure (ring A and C) and two in the position 3 and 4 in hydroxyphenyl structure (ring B) (Lin and Zhou, 2018). At the biological level, health benefits have been attributed to quercetin (Kumar, Vijayalakshmi, & Nadanasabapathi, 2017), mainly to reduce the prevalence of chronic degenerative diseases such as cardiovascular diseases (Terao, 2017; Porcu et al., 2018), cancer (Granato et al., 2017; Wu et al., 2018), diabetes (Dhanya, Arya, Nisha, & Jayamurthy, 2017; Peng et al., 2017), and obesity (Nabavi, Russo, Daglia, & Nabavi, 2015; Ting et al., 2017).

However, the biological properties of quercetin could be affected by physical, chemical and physiological factors such as temperature, pH, O_2, and enzymatic activity affecting its potential therapeutic activity (Huang et al., 2018). Other disadvantages comprise chemical instability and high degradability when it is consumed and during its path through the stomach due to its low pH (Nathiya, Durga, & Devasena, 2014), which affects its potential health benefit. To preserve the biological activity of quercetin, the use of hydrophobic matrices in form of nanoparticles has been suggested (Mirpoor, Hosseini, & Nekoei, 2017; Ni, Hu, Sun, Zhao, & Xia, 2017). At this regard, protein matrices, such as kafirin and zein, play an important role in the construction of nanoparticles to entrap hydrophobic compounds (Xiao, Nian, & Huang, 2015; Yao, Chen, Song, McClements, & Hu, 2017; Tapia-Hernández et al., 2019). The difference between zein and kafirin is that the native zein structure has

fewer disulfide bonds and a higher proportion of α-helix in its secondary structure (Taylor, Anyango, Muhiwa, Oguntoyinbo, & Taylor, 2018). Zein is soluble in 70% ethanol, and it is a biodegradable and biocompatible biopolymer. Furthermore, it has been cataloged by the Food and Drug Administration (FDA) as a Generally Recognized As Safe (GRAS) product (Paliwal, & Palakurthi, 2014; Cheng, & Jones, 2017; Tapia-Hernández et al., 2018). Therefore, zein currently represents an ideal matrix for the formation of nanoparticles.

Recently, zein nanoparticles have been loaded with different compounds such as resveratrol (Liang et al., 2018), curcumin (Zou et al., 2016); epigallocatechin gallate (Donsì, Voudouris, Veen, & Velikov, 2017), rutin (Zhang and Zhao, 2017), and β-carotene (Chuacharoen & Sabliov, 2016); these studies showed that this protein matrix possesses a high capability to encapsulate these nutraceutical compounds. Furthermore, antioxidant activity and bioaccessibility increases and chemical degradation decrease in the gastrointestinal tract; therefore, its high bioactivity may be compared with unencapsulated compounds. There are several techniques to obtain zein nanoparticles, such as liquid antisolvent precipitation, spray-drying, and electrohydrodynamic atomization (EHDA) (Chen, Zhang, & Zhong, 2015; Davidov-Pardo, Joye, Espinal-Ruiz, & McClements, 2015; Liu, Zhang, Yu, Wu, & Li, 2018).

EHDA processes include electrospraying, electrospinning and e-jet printing (Tapia-Hernández et al., 2019). Electrospraying is a very simple technique that it is used to prepare nanoparticles, requires low-cost equipment, and generates little residues (Tapia-Hernández et al., 2015). This technique allows higher encapsulation efficiency with respect to other techniques (Gómez-Mascaraque, Tordera, Fabra, Martínez-Sánz, & López-Rubio, 2018). The principle is based on that an electrostatic force generates by applied high voltage inside the liquid, breaking the surface tension of the liquid. Then, the liquid entering in the needle forms

a cone ending in a jet through its apex. Finally, the highly charged liquid droplets disperse radially on the collector plate, due to Coulomb's repulsion of charges (Jayaraman et al., 2015; Alehosseini, Ghorani, Sarabi-Jamab, & Tucker, 2017). The parameters that exert an influence on the control of particle size are equipment parameters (applied voltage, flow rate, and distance of the collector), parameters of the polymer solution (concentration, viscosity, density, conductivity and surface tension), and environmental parameters (humidity and temperature) (Tapia-Hernández et al., 2017; Jaworek, Sobczyk, & Krupa, 2018). For instance, Liu et al., (2018) elaborated nanoparticles by coaxial electrospray using 12% zein and 3% (w/v) tamoxifen citrate and concluded that this technique produces particles with better quality in terms of particle size, distribution of size, and morphology. Other studies have developed zein nanoparticles by the electrospraying technique (Gómez-Estaca, Balaguer, Gavara, & Hernández-Muñoz, 2012, Bhushani, Kurrey, & Anandharamakrishnan, 2017, Baspinar, Üstündas, Bayraktar, & Sezgin, 2018; Tapia-Hernández et al., 2019), and coincide that at 5% zein, nanoparticles are obtained with a spherical, monodispersed, compact structure, with size ranging between 157 and 500 nm, and encapsulation efficiency ranging from 80 up to 97.44% for curcumin and catechins.

Different arrays have been used by electrospraying for the formation of nanoparticles as coaxial electrospraying for core-shell nanoparticles (Wang, Wen, Yu, Yang, & Zhang, 2018; Yang, Zhang, Wang, & Yu, 2018; Yu, Zheng, Yang, Li, Williams, & Zhao, 2019), coaxial electrospraying to creating high quality monolithic particles (Li, Zheng, Yu, Liu, Qu, & Li, 2017; Liu, Z. P., Zhang, L. L., Yang, Y. Y., Wu, D., Jiang, G., & Yu, D. G. 2018; Yang, Zhang, Liu, Wang, & Yu, 2018), and to study the influences of experimental parameters and process characteristics on working processes (Huang et al., 2019). However, few publications

can be found to investigate the relationships between the working fluids' properties and their adaptability for electrospraying, which is a significant merit of the present work. Therefore, the objective was to prepare and characterize quercetin-loaded zein nanoparticles by the electrospraying technique and assess their *in vitro* bioavailability.

2. Materials and methods

2.1. Chemical reagents

Zein with 86.06% (w/w) protein content, quercetin with ≥95% purity, gallic acid with ≥97.5% purity, Folin & Ciocalteu's phenol reagent, hydrochloric acid with 36.5-38% purity, sodium carbonate, and sodium bicarbonate were purchased from Sigma-Aldrich (St. Louis, MO, USA).

2.2 Preparation of solutions

2.2.1 Zein and zein-quercetin solutions.

Zein solutions were prepared at different concentrations of aqueous ethanol (60, 70, 80 and 90% v/v) and zein (1, 5, and 10%, w/v) under stirring for 1 h at 25 ºC.

Zein at 5% (w/v) in 80% (v/v) of aqueous ethanol were made. After different levels of quercetin, (20, 10, 15, 5, and 1 mg mL^{-1}) was added in zein solution. All the solutions were homogenized using magnetic stirring by 1 h at 25 ºC.

2.2.2 Solvent evaluation

Evaluation by the solvent effect was determined following the methodology described by Gómez-Estaca et al. (2012) with modifications. Aqueous ethanol was utilized as a solvent at 60, 70, 80, and 90% (v/v). The zein concentration was kept constant 5% (w/v) for all solutions

obtained. The nanoparticles contained in all solutions were evaluated in morphology by Scanning Electron Microscopy (SEM), as well as in their physicochemical properties (viscosity, density, conductivity) and rheological parameters (shear stress and viscosity with respect to shear rate, and viscosity with respect to time).

2.3 Physicochemical characterization of solutions of zein

2.3.1 Viscosity

The viscosity of all solutions was analyzed on a Modular Compact Rheometer (MCR-102; Anton Paar, Germany), using concentric cylinder geometry at a constant shear rate of 50 (s^{-1}) at 25 °C (Tapia-Hernández et al., 2018). Measurements were performed in three independent assays.

2.3.2 Density

Density was determined by the pycnometer method as described by Chevalier, Assezat, Prochazka, & Oulahal (2018). First, the empty pycnometer was brought to a constant weight (M1). A reference pattern was generated consisting of a pycnometer containing distilled water (M2). Then, solutions of 5% (w/v) of zein containing different concentrations of aqueous ethanol (60-90% v/v) were placed into a pycnometer (M3). Measurements were performed in three independent assays. The density of the prepared zein solutions was determined based on Equation 1:

$$\rho = \frac{M3 - M1}{M2 - M1}\ 1g/cm^3 \qquad \text{Equation 1}$$

2.3.3 Electrical conductivity

Electrical conductivity was determined as described by Smeets, Clasen, & Van den Mooter (2017). Zein solutions at different concentration ranges of aqueous ethanol (60-90% v/v) were tested using a HANNA Instrument Conductometer, Model HI 2550 (pH, ORP, & EC/TDS/NaCl meter). Measurements were performed in three independent assays.

2.3.4 Surface tension

Surface tension was determined by the Wilhelmy plate method (Wilhelmy sensor, NIMA England) as described by Juárez, Taboada, Valdez, & Mosquera (2008). Zein solutions were prepared at different concentration ranges (60-90% v/v) in ethanol-water. The surface tension was recorded using water as a blank. Measurements were performed in three independent assays.

2.4 Rheology behaviour of zein solution at different ethanol concentration

The rheological behavior was studied using MCR-102 equipment (Anton Paar, Germany) with concentric cylinder geometry. For the measurements, a distance between the base and the cylinder of 1 mm was used according to Ni et al., (2018) with modifications. The effect of shear rate vs shear stress was performed with a continuous ramp from 0.1 to 100 s^{-1} at 25°C., with 100 points and interval of 2 s per point, with a duration of 200 s per measurement. The data obtained were adjusted to the Power Law model to deduce the behavior of zein solutions (Newtonian or non-Newtonian). Values equal to 1 are considered Newtonian fluids, those of <1 are considered non-Newtonian fluids, and those of >1 are fluids with a tendency to thicken. For determination of the type of fluid Equation 2 was used:

$$\tau = K\,\dot{Y}^{n} \qquad \text{Equation 2}$$

Where τ is the shear stress (Pa), $\dot{Y}$ is the shear rate (s^{-1}), n is the Power Law index, and K is the consistency parameter (Pa s^n).

The effect of time vs viscosity was performed using a continuous ramp from 1 to 360 s and constant shear rate of 50 s^{-1} at 25°C. For each measurement, 60 points were used with time interval of 6 s per point.

2.5 Electrospray equipment parameters

The zein and zein-quercetin solutions were transferred into a plastic syringe with a needle of 20G (outside diameter of 0.9 mm and inside diameter of 0.6 mm). A pump for the syringe (KD Scientific, USA) was used to regulate the flow of the polymer solution. The voltage applied to the polymer solution was conducted using a high-voltage power source (CZE 1000R model; Spellman, USA). An aluminum plate of 10 cm × 10 cm was used for the collection of nanoparticles. The conditions of the equipment were as follows: an electrical potential of 15 kV; flow rate of 0.1 mL h^{-1}, and a distance from the needle to the collector of 15 cm. Figure 1 shows the schematic representation of obtaining quercetin-loaded zein nanoparticles by electrospraying technique.

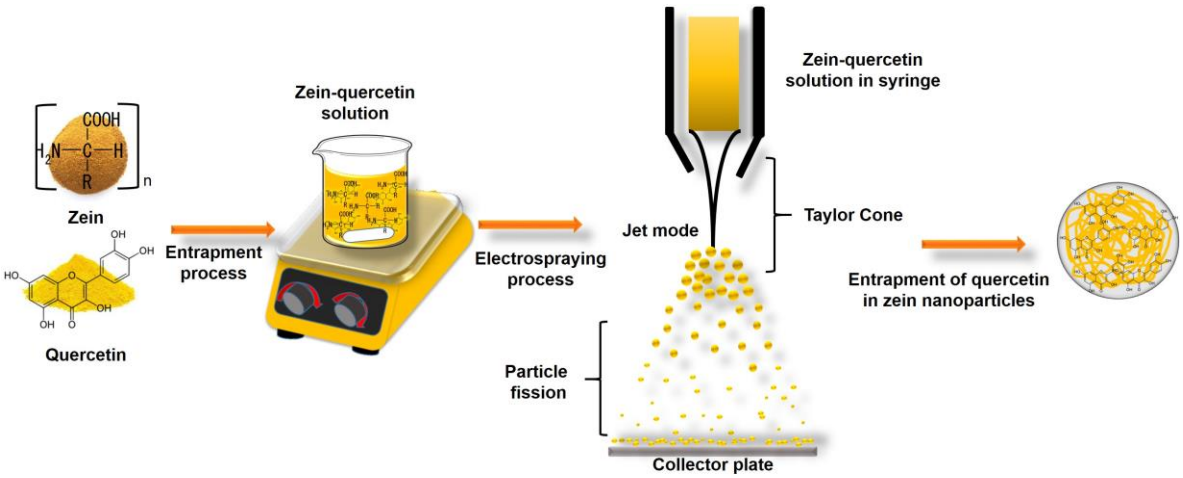

Figure 1 Schematic representation of electrospraying technique utilized for obtaining of quercetin-loadeded zein nanoparticles.

2.6 Characterization of nanoparticles

2.6.1 Scanning electron microscopy

The morphology of the commercial zein, zein nanoparticles, and zein-quercetin nanoparticles was analyzed by Scanning Electron Microscopy (SEM) using a JEOL Model JSM-7800F equipment (JEOL, Pleasanton, CA, USA). Powder nanoparticles were prepared through their immobilization on carbon-coated 400-mesh copper grids (Ted Pella, Inc., Redding, CA, USA). An acceleration voltage of 10 kV was used.

Additionally, all quercetin concentrations in zein nanoparticles were analyzed in particle-size distribution and average diameter employing the ImageJ software program (NIH, Maryland, USA). Also, the polydispersity index (PDI) was obtained from the following equation:

$$PDI = \frac{\sigma}{\dot{X}} \qquad \text{Equation 3}$$

Where σ represents the standard deviation and $\dot{X}$ represents the average diameter of the nanoparticles. PDI closer to 0 are monodispersed particles and PDI close to 1 are polydispersed particles.

2.6.2 Transmission electronic microscopy

The shape of quercetin-loaded zein nanoparticles was studied by Transmission Electron Microscopy using a JEOL equipment (JEOL, Ltd., Tokyo, Japan) at 200 kV operating voltage

and a field emission filament. An aliquot of 100 μL of a nanoparticle suspension (100 μg in 500 μL of distilled water) was placed in a copper grid and allowed to dry before its analysis.

2.6.3 Fourier Transform-Infrared spectroscopy

To observe the physical interaction between quercetin and zein Fourier Transform-Infrared spectroscopy (FT-IR) was employed. A Spectrum GX FT-IR (Perkin-Elmer. USA) Infrared Spectrometer equipment was used and spectrum scans were performed in the range 4,000 to 500 cm^{-1}. A small amount of the sample (1 mg) was taken and mixed with KBr (19 mg) to form a pastille. Measurements were performed in transmittance mode. Samples were run in triplicate.

2.7 *In vitro* gastrointestinal release and bioavailability

For the *in vitro* gastrointestinal release of free quercetin and trapped quercetin, the methodology described by Bhushani et al., (2017) was followed to perform a gastrointestinal simulation (SGI). SGI was divided into gastric digestion and intestinal digestion depending on the pH and enzymes used. The quantification of the released quercetin was carried out using the Folin-Ciocalteu reagent at 760 nm and reported as a percentage. A curve of gallic acid was used as the reference. The measurements were made in triplicate.

For the preparation of the simulated gastric fluid (SGF) 4 mg of sample was diluted with 5 mL of distilled water. The pH was adjusted to 2 with 6 M HCl and constant agitation. Alternatively, a solution containing 160 mg mL^{-1} of porcine pepsin (315 U/mL) in 0.6 mL of 0.1 M HCl was prepared and added to the SGF. The volume was adjusted 10 mL with distilled water. Gastric digestion was initiated and the samples were incubated at 37 °C and agitated at 80 rpm for 2 h in a water bath. Aliquots of 300 μL were taken every 30 min and centrifuged

at 10,000 rpm for 15 min. The supernatants were recovered to measure the concentration of quercetin.

Once the simulated gastric digestion was performed, enough 0.045 M $NaHCO_3$ was added to the digest to adjust the pH to 5. Then, a solution containing 4 mg mL^{-1} of pancreatin in 2.5 mL of 0.1 M $NaHCO_3$ was added. The pH was increased to 7 with 0.005 M $NaHCO_3$ to obtain the simulated intestinal fluid (SIF). The samples were incubated at 37 °C and stirred at 80 rpm for 2 h in a water bath. Aliquots of 300 µL were taken every 30 min and centrifuged at 10,000 rpm for 15 min. The supernatants were recovered to measure the concentration of released quercetin.

To measure the bioavailability of the released quercetin, the digests obtained from the intestinal digestion were placed in dialysis bags with a pore size of 12 kD. The dialysis bags were then placed in a recipient containing 150 mL phosphate buffer, pH 7.4. The bioavailability was initiated and incubated at 37 °C and 80 rpm for 2 h in a water bath. The concentration of quercetin that passed through the dialysis bag was calculated as indicated before.

2.8 Experimental design and statistical analysis

For determination of particle size and morphology, a factorial design was used of 4 x 3 x 5. Independent variables included an aqueous-ethanol concentration with four levels (60, 70, 80, and 90% v/v), a zein concentration with three levels (1, 5, and 10 w/v), and a quercetin concentration with five levels (1, 5, 10, 15, and 20 mg mL^{-1}). Descriptive statistic was used for all analyses. For comparison of means of the physicochemical properties, particle

diameter, entrapment efficiency, and bioavailability, the Tukey test was employed at a 95% confidence level (p <0.05) were performed using Infostat 2008 software.

3. Results and discussion

3.1 Physicochemical characterization of solutions of zein

3.1.1 Effect of ethanol

In this study, we observed that the best ethanol concentration for obtaining nanoparticles was 80% (v/v), followed by 70% (v/v) and 60% (v/v). The concentration that exhibited very different nanoparticle characteristics was 90% (v/v). These results were corroborated by analysis of viscosity, density, electrical conductivity, surface tension and morphology by SEM. Zein is a water-insoluble protein, but soluble in binary solutions of alcohol and water due to its amphiphilic characteristics predicted by the amino acid sequence, which contains more than 50% of hydrophobic residues (leucine, proline, and alanine) (Wang & Padua, 2010; Chen, Yen & Liu, 2013). It has been known that, due to these amphiphilic characteristics, zein tends to form micellar-like structures that are dependent on the ethanol concentration. In the zein micelle structure, the hydrophilic part is aligned to the outside in each aggregate when the ethanol concentration is lower than 90% (v/v), but the hydrophobic domain is exposed to the surface of each aggregate at an ethanol concentration higher than 90% (v/v) (Chen, Ye, Liu, 2014; Ni et al., 2018). Also, Bisharat et al., (2018) studied the effect of ethanol concentration (70, 80, and 90% v/v) and temperature (10-70 °C) on aggregation state in a zein solution (5%, w/v). These researchers observed that, at concentrations of 70 and 80% of zein, the values of transmittance decrease, while at 90% the

values of transmittance were high. For this reason, the effect of zein at different ethanol-water solutions must be studied.

Table 1. Physicochemical properties of zein solutions at different concentrations of aqueous ethanol

Sample	Zein (% p/v)	Ethanol (% v/v)	Viscosity (Pa · s)	Density (g cm^{-3})	Conductivity (μs cm^{-1})	Surface tension (mN cm^{-1})
1	5	60	0.0056 ± 0.0001^a	0.916 ± 0.0008^a	531 ± 3.6^a	26.0 ± 0.7^a
2	5	70	0.0054 ± 0.0000^b	0.895 ± 0.0004^b	457 ± 1.1^b	23.3 ± 0.6^b
3	5	80	0.0049 ± 0.0000^c	0.867 ± 0.001^c	397 ± 2.0^c	22.1 ± 0.4^c
4	5	90	0.0040 ± 0.0001^d	0.856 ± 0.005^d	327 ± 1.5^d	21.2 ± 0.1^d

Different letters (a, b, c, d) represent significant statistically differences by Tukey test ($p<0.05$)

Figure 2 shows the SEM micrographs of zein nanoparticles prepared by the electrospraying technique at different concentrations of aqueous ethanol and 5% (w/v) of zein. The 60, 70 and 80% (v/v) ethanol revealed the formation of spherical particles, attributed to the physicochemical properties of the solutions (Table 1). However, 60 and 70% (v/v) of ethanol presented particles of different size (Figures 2a and 2b) and 80% (v/v) of ethanol with homogeneous size (Figure 2c). The solution of 90% (v/v) was that which presented irregular morphology (non-spherical) (Figure 2d), this being observed in the polymer solution formed, which was different from the other three. Therefore, comparing the polymer solution formed and the micrographs by SEM, the best concentration of aqueous ethanol was that of 80% (v/v). In the electrospraying technique, one of the conditions for its use is that the polymer matrix forms a solution or, in this case, a homogeneous suspension with the ideal solvent for the formation of nanoparticles with desirable sphere morphology and nanometric size.

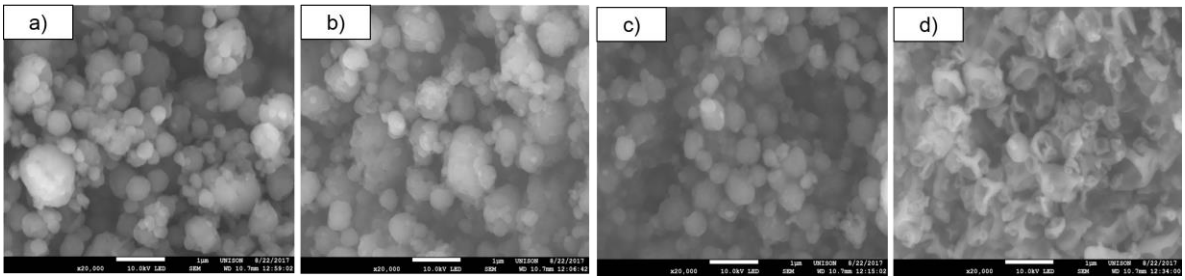

Figure 2 Micrography by SEM of zein nanoparticles at different concentrations of ethanol (60-90% v/v) and zein 5% (w/v). Conditions: voltage of 15 kV, flow rate of 0.1 mL h^{-1} and collector distance of 15 cm. Magnification, 10, 000X.

Similar results were reported by Zhong & Jin (2009) when studied the effect of an aqueous ethanol concentration on the formation of nanoparticles. Concentrations from 55 to 90% (v/v) aqueous ethanol were used. It was observed, by DLS and SEM, that the particle size varied as the ethanol concentration varied, where the smallest diameters were 70% and 80% by DLS. Also, the highest ethanol concentration allowed obtaining the smallest particle diameter by SEM, and similar results were obtained in this study. Other studies demonstrated the formation of spherical zein nanoparticles at a concentration of 80% aqueous ethanol (Wang, Su, Schulmerich, & Padua, 2013; Xue et al, 2018). Gómez-Estaca et al., (2012) studied the formation of nanoparticles by electrospraying technique in aqueous ethanol. The results showed that spherical nanoparticles were formed at a concentration of 80% (v/v) ethanol and 5% zein (w/v). In contrast, Olenskyj, Feng, & Lee, (2017) reported the effect of the ethanol concentration in obtaining zein nanoparticles. The results demonstrated that the nanoparticle diameter produced was significantly lower with an ethanol concentration of 65% (v/v) and higher nanoparticle diameter was yielded with higher ethanol concentrations, with a significance value of p <0.01. The results obtained by Olenskyj et al., (2017) (65% v/v of ethanol) are different from those reported by Zhong & Jin (2009) and by Gómez-Estaca et

al., (2012) (80% v/v of ethanol). This may be due to the type of processing employed for obtaining zein nanopartícles or to the type of zein used.

3.1.2 Effect of the viscosity

Table 1 lists the physicochemical properties (viscosity, density, electrical conductivity, and surface tension) of the zein solutions at different concentrations of aqueous ethanol and 5% (w/v) of zein. In terms of viscosity, all the solutions exhibited significant differences (p <0.05), decreasing as the ethanol concentration increased. Viscosity is a parameter that is dependent on the concentration and molecular weight of the polymer, as well as on the solvent used. For nanoparticle formation, the adequate viscosity of protein solution is necessary to obtain more spherical, smaller, and monodispersed particles. In this study, the solution with the highest viscosity was 60% ethanol (v/v) followed by 70% (v/v) zein solution, with a difference of 0.0002 Pa·s with respect to 60% (v/v). Although there was a significant difference between the 60% and 70% (v/v) zein solutions, SEM micrographs revealed nanoparticles obtained by electrospraying that were very similar in morphology and size (Figures 2a and 2b), because the viscosity values were very close to each other. The solution of 80% (v/v) zein solution showed lower viscosity than the 70% (v/v) zein solution, representing the optimal viscosity for the formation of spherical aggregates with few polydispersed particles. That was corroborated by micrography by SEM (Figures 2b and 2c). The 90% (v/v) ethanol solution showed the lowest value of viscosity (Table 1) being not adequated for the formation of nanoparticles (Figure 2d).

This effect of the viscosity with respect to the ethanol concentration is mainly due to apparent molecular weight, which decreases at higher ethanol contents (Kim & Xu, 2008). Furhermore, the viscosity is a parameter to consider in the formation of the Taylor cone

where high viscosity unstable cone-jet mode is obtained, however, a low viscosity is related to stable cone-jet mode. Gómez-Estaca et al., (2012) reported that the viscosity plays a significant role during the break-up and atomization of the liquid jet, and thus influencing the droplet size. Also, report that at a viscosity of 0.0050 Pa s smaller particle size is obtained. This result is similar to that reported in this investigation with a viscosity of 0.0049 Pa s deducting a stable cone-jet mode. Similarly, Neo et al., (2012) reported that, at 80% (v/v) ethanol and 5% (w/v) zein, the viscosity obtained was 0.0043 Pa s.

3.1.3 Effect of the density

In terms of density, this parameter showed a behavior similar to that of the viscosity in which, as the ethanol concentration increases, the density decreases (Table 1). Statistical analysis showed significant differences (p <0.05) in the density among zein solutions at different concentrations of aqueous ethanol. Density comprises a parameter that is related to the formation of the Taylor cone. An optimal density can form a Taylor cone of the jet-cone type, resulting in the formation of nanoparticles that are smaller in diameter, more spherical, and monodispersed, whereas an unsuitable density can form a Taylor cone of the dripping-cone type, forming nanoparticles that are irregular, very polydispersed, and with very large diameters. First, the 60% (v/v) zein solution showed the highest density followed by 70, 80 and 90% (v/v), respectively. Although there were no significant differences, the density difference among solutions was evident, where the difference between the zein solutions of 60 and 70% (v/v) was 0.021 g cm^{-3}. That situation can be attributed to a Taylor-cone formation of the jet-cone type, but with one not so finely sprayed, forming more polydispersed particles as observed in the SEM micrographs (Figures 2a and 2b). The 70% (v/v) zein solution showed a density difference of 0.028 g cm^{-3} greater than the 80% (v/v)

zein solution, giving as a results particle size disparity (Figure 2c). Density at 90% (v/v) was the least adequate as that the SEM micrograph (Figure 2d) suggests that the Taylor cone was not in jet-cone mode.

However, the Taylor-cone form determines the morphology and particle diameter. Light density tends to form drops (60% and 70% and 90% v/v) while, at a lower density (80% v/v), Taylor jetting or the multijet mode is formed. This behavior is due to the relationship between the mass and the inertial force (Fρ) of zein solutions. The concept of inertial force is defined as the fluid resistance to changes in conditions either at rest or in motion (Jaworek & Sobczyk, 2008; Tapia-Hernández et al., 2018).

3.1.4 Effect of the electrical conductivity

Electrical conductivity, as well as the viscosity and the density, was a parameter that was measured at different solutions of aqueous ethanol (Table 1). Electrical conductivity is a parameter that measures the capacity of a polymer to pass through the electrical current. In electrospraying equipment, this parameter is important since it is related to the electrical potential applied to the polymer solution. That is, if the polymers used in the electrospraying equipment have high electrical conductivity, a low electric potential is necessary, but if the polymer has low electrical conductivity, a high electrical potential is required. In solutions of zein at different concentrations of aqueous ethanol, significant differences were demonstrated (p <0.05). Electrical conductivity decreased as the concentration of ethanol increased. In point of fact, the 60% (v/v) zein solution was the one with the highest conductivity followed by 70, 80 y 90 (v/v), with lower density respectively. The difference between solutions from 60% to 70% (v/v) was 74 μs cm^{-1} and from 70 to 80% (v/v) was 60 μs cm^{-1}, revealing that these differences did not influence the formation of nanoparticles, in

that both concentrations of aqueous ethanol formed similar nanoparticles, as observed in micrographs by SEM (Figure 2a and 2b). Optimal electrical conductivity, together with the electrical power applied to the formation of nanoparticles, was reached at 80% ethanol (v/v), as illustrated in the micrograph by SEM (Figure 2c), while electrical conductivity at 90% (v/v) was not necessary, along with the electrical potential for the formation of nanoparticles (Figure 2d).

For nanoparticle formation, high electrical conductivity of polymeric solutions is required while, at low electrical conductivity, low yields are obtained, because correct electrical conductivity forms a stable cone-jet mode (Smeets et. al., 2017). Zhang & Kawakami (2010) elaborated chitosan solutions for the formation of nanoparticles by the electrospraying technique. These authors reported that as the ethanol concentration increases, the electrical conductivity decreases. Bhushani et al., (2017) developed zein solutions at different concentrations of this protein and 80% (v/v) ethanol was used. The results showed that 5% of zein showed an electrical conductivity of 700.05 ± 0.21 μs cm^{-1}, a value higher than that reported in the present study of 397 ± 2.0 μs cm^{-1}.

3.1.5 Effect of the Surface tension

Table 1 shows the surface tension values at different concentrations of aqueous ethanol. This parameter corresponds to the force necessary to fissure a drop and form smaller drops. In zein solutions at different concentrations of ethanol, the surface tension decreased as the concentration of ethanol is increased and were statistically different ($p < 0.05$). The surface tension varied of 26.0 ± 0.7 mN cm^{-3} for 60% (v/v) to 21.2 ± 0.1 mN cm^{-3} for 90% (v/v) of zein solution. The surface tension plays an important role together with viscosity to form

particles with the morphology of spheres or fibers, in consequence, lower surface tension tend to form spherical particles of smaller diameter (Neo et al., 2012).

3.2 Rheological behavior of zein solution at different ethanol concentrations

The result obtained of shear rate vs shear stress was inversely proportional to the concentration of ethanol, that is, as the ethanol concentration increased, maximal shear stress decreased at 100 s^{-1} (Figure 3a). For ethanol concentrations at 60, 70, 80, and 90% (v/v), maximal shear stress was 0.532, 0.491, 0.469, and 0.373 Pa, respectively, at 100 s^{-1}. The shear rate ramp from 0.1 to 100 s^{-1} showed that, as the shear rate ramp increased in all zein solutions, shear stress increased. The 60% (v/v) zein solution demonstrated the greatest increase in shear stress from 0.00038 Pa at 0.1 s^{-1} to 0.532 Pa at 100 s^{-1}. The 70% (v/v) zein solution showed a shear stress of 0.00296 Pa at 0.1 s^{-1} until reaching 0.491 Pa at 100 s^{-1}. The 80% (v/v) zein solution showed a range very near to that of 70% (v/v), with 0.00332 Pa at 0.1 s^{-1} and from 0.0469 Pa at 100 s^{-1}. Finally, the solution that showed the greatest change was that of 90% (v/v), especially at 100 s^{-1} in comparison to the remaining three solutions, showing shear stress of 0.00173 at 0.1 s^{-1} up to 0.373 Pa at 100 s^{-1}. These results suggest that there is a dependency on the concentration of ethanol in the rheology of zein solutions.

Fu & Weller (1999) studied the effect of shear rate vs shear stress of 60, 70, 80, and 90% (v/v) of ethanol at different concentrations of zein. The results showed that there was no change in viscosity as shear stress increased. Therefore, the solutions were classified as Newtonian fluids due to their constant viscosity. Soltani & Madadlou (2015) prepared zein nanoparticles for the stabilization of pectin gels. Zein nanoparticles prepared from a 80% (v/v) ethanol solution and 0.2 % w/v zein concentration of were used as a control. Afterward, the rheological behavior of shear stress, with respect to the shear rate, was measured in terms

of zein-nanoparticle dispersity. The results revealed that the dispersity showed a linear upward trend in shear stress as the shear rate increased. This rheological behavior includes Newtonian fluids, which the authors confirmed by means of the flow behavior index (n) of 1.0. Although in the current study there were differences among the samples due to the concentration of ethanol, all exhibited Newtonian behavior and were in agreement with previously described studies.

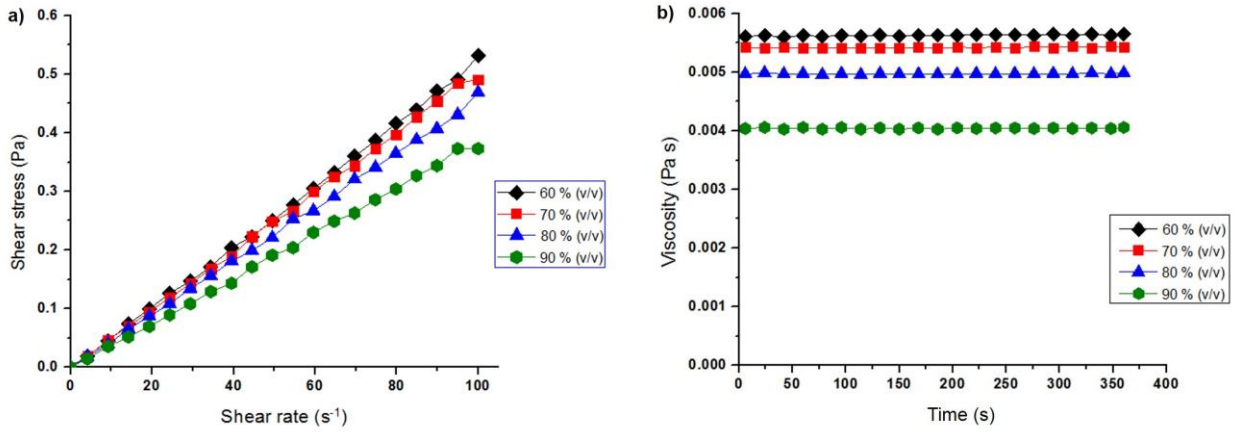

Figure 3 Rheograms of a) effect of shear rate *vs* shear stress and b) effect of time *vs* viscosity of zein solutions at different concentrations of ethanol (60-90%); 5% (w/v) of zein was used.

To observe the rheological behavior of the solutions, the corresponding fluid type was calculated by means of the Power Law model (Table 2). This model predicts whether a fluid is considered Newtonian, not Newtonian, or viscous, depending on the parameter n. Newtonian fluids are preferable for the formation of nanoparticles with more similar morphologies and more monodispersed particles by the electrospraying technique, than viscous or non-Newtonian fluids. Zein solutions of 60, 70, 80, and 90% (v/v) showed a value of parameter n of around 1, revealing a Newtonian behavior. Also, a variable K value, defined as the consistency parameter (Pa s^n), showed a decreasing behavior as the ethanol

concentration increased, with a K of 0.1002 ± 0.0030 for a 60% (v/v) zein solution to 0.0886 ± 0.0020 for a 90% (v/v) zein solution. All of the solutions presented an $R^2 = 0.99$, with data n and K showing a good fit. Although all of the zein solutions showed a Newtonian behavior, there were differences among them depending on their viscosity, observing different scenarios in morphology and particle dispersity as depicted in Figure 2, and verified by the parameters of shear stress with respect to shear rate and of viscosity with respect to shear-rate parameters.

Table 2. Power-Law parameters of zein solution at different concentrations of aqueous ethanol.

Smple	Ethanol (% v/v)	Zein (% p/v)	Power law parameters		
			***K* (Pa s^n)**	**n**	***R*^{2}**
1	60	5	0.1002 ± 0.0030	1.037 ± 0.012	0.99
2	70	5	0.1019 ± 0.0005	0.992 ± 0.001	0.99
3	80	5	0.0898 ± 0.0026	1.026 ± 0.005	0.99
4	90	5	0.0886 ± 0.0020	0.994 ± 0.003	0.99

Nonthanum, Lee & Padua, (2013) prepared zein solutions (1 mg mL^{-1} and 5 mg mL^{-1}) at different ratios of ethanol-water (65-90% v/v). Results showed that all of the samples by means of Power Law model behaved as a Newtonian fluid and obtained indices of K consistency between 0.08 and 0.14 Pa s^n at different pH (2, 6, and 12). These K results are similar to those reported in the present investigation for zein solutions with different ethanol concentrations. Soltani & Madadlou (2016) reported the behavior of zein with a concentration of 2 mg mL^{-1} in 80% (v/v) aqueous ethanol solution. The results showed

Newtonian behavior with a flow behavior index of n = 1 and a consistent index K = 0.03 at a 99% confidence interval of fit. These results agree with those reported in this study for the 80% (v/v) ethanol solution. Uzun, Ilavsky, Padua (2017) reported the flow-behavior-index median of the Power Law model for solutions with high concentrations of zein and for ethanol concentrations of 70, 80, and 90% (v/v). The results showed that for 30% zein, the flow behavior indexes were 0.93, 0.97, and 0.64 for 70, 80, and 90% (v/v), respectively, concluding that solutions of zein with 30% (w/v) and with solvents of 70% and 80% (v/v) behave as Newtonian fluids.

Viscosity vs time was also measured for all zein solutions (Figure 3a). This parameter determines the variation of the zein solutions at different periods of time, which is important for the formation of stable or unstable nanoparticles during the electrospraying technique. The stability measurement was performed at a time ramp from 1 to 360 s and at a constant shear rate of 50 s^{-1}. The solutions showed a behavior dependent on the ethanol concentration. It was observed that the higher ethanol concentration, the lower the viscosity with respect to time. However, all solutions were stable with respect to time with very small SD among the 60 points taken with values of 0.000013, 0.00001, 0.000009, and 0.00001 Pa s for 60, 70, 80, and 90% (v/v), respectively. Therefore, these small variations in viscosity of zein solutions indicated a Newtonian behavior, thus confirming the results obtained by means of the Power Law model.

3.3 Characterization of nanoparticles

3.3.1 Nanoparticle morphology by SEM

3.3.1.1 Effect of zein concentration

The SEM micrographs are presented in Figure 4 and, for the three evaluated concentrations, we can observe significant differences in the physical characteristics in particle size and morphology. For instance, zein solution at 10% (w/v) formed non-spherical zein nanoparticles. The morphology of nanoparticle formed at this concentration of zein was biconcave discs due to collapse and shrinkage of the nanoparticle. On the other hand, zein solutions at the concentrations of 5% and 1% (w/v) formed spherical nanoparticles (Figures 4b and 4c). These results suggest that there is a relationship between the increase in the concentration and its physicochemical properties (viscosity, density, and electrical conductivity) in the morphology of the nanoparticles obtained by means of electrospraying equipment.

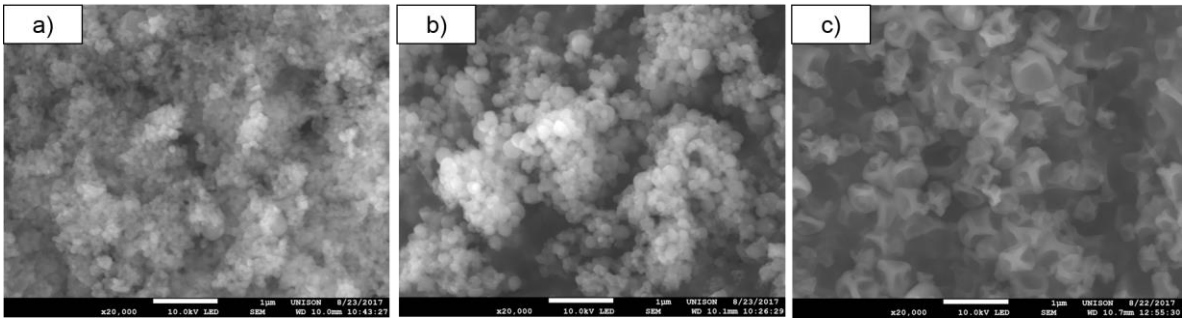

Figure 4 Micrography by SEM of nanoparticles at different concentrations of zein (1-10 % w/v) and ethanol at 80% (v/v). Conditions: voltage of 15 kV, flow rate of 0.1 mL h^{-1} and collector distance of 15 cm. Magnification, 10,000X.

Gómez-Estaca et al., (2012) evaluated the effect of the zein concentration on the nanoparticle size and morphology by means of the electrospraying technique. That research group reported that 1% (w/v), zein did not form nanoparticles due to the low concentration and molecular weight of zein in comparison to other polymers. Also, at 5% (w/v) zein it was

observed a spherical morphology and a compact structure with a particle size between 200 and 350 nm. However, at 10 % (w/v) zein, a morphology was reported that was similar to that obtained in this study, where nanoparticles formed biconcave discs, collapsing the particle due to increase in droplet size along with a rapid evaporation of the solvent, forming a zein concentration gradient along the droplet and the creation of a semi-solid layer of zein at the surface, therefore collapsed and shrunken particles were obtained and not the formation of compact particles. In other studies, obtention of zein nanoparticles with spherical morphology have been reported. Dai et al., (2017) obtained espherical zein-lecithin nanoparticles from of 1.0 g of zein was dissolved in 100 mL of 70% (v/v) of ethanol with an average diameter of 177.90 ± 2.55 nm. This process allowed the obtaintion of spherical nanoparticles an average diameter of 134.6 nm. Zou, van Baalen, Yang, & Scholten, (2018) reported spherical nanoparticles at a concentration of 2.5% (w/v) with an average diameter of 85 nm, while Wei, Sun, Dai, Zhan, & Gao, (2018) prepared a zein solution control with 0.2 g zein that was dissolved in 200 mL 70% (v/v) of aqueous ethanol under magnetic stirring at 600 rpm for 2 h. The results exhibited spherical nanoparticles and average diameters of zein colloidal particles of 361.90 ± 2.87 nm.

Therefore, for the encapsulation of quercetin in zein nanoparticles, a solution of 5% (w/v) of zein and a concentration of 80% (v/v) of ethanol was used.

3.3.1.2 Effect of the encapsulation of quercetin

Figure 5 shows the micrograph recorded by SEM, at a magnification of 20,000X, for each treatment of quercetin-loaded zein nanoparticles. The control treatment without quercetin demonstrated a smaller diameter (67.9 ± 11.2 nm) compared with nanoparticles with quercetin, observing that as the concentration of quercetin increased, the diameter of the

particle increased (data confirmed by the particle-size distribution). All treatments showed quercetin-loaded zein nanoparticles with homogeneous populations that were spherical, with a smooth surface. Currently, to our knowledge, there have been no previous studies that demonstrate the formation of quercetin-loaded zein nanoparticles by the electrospraying technique, but rather, by other methods, such as the solvent-antisolvent method and the desolvation method.

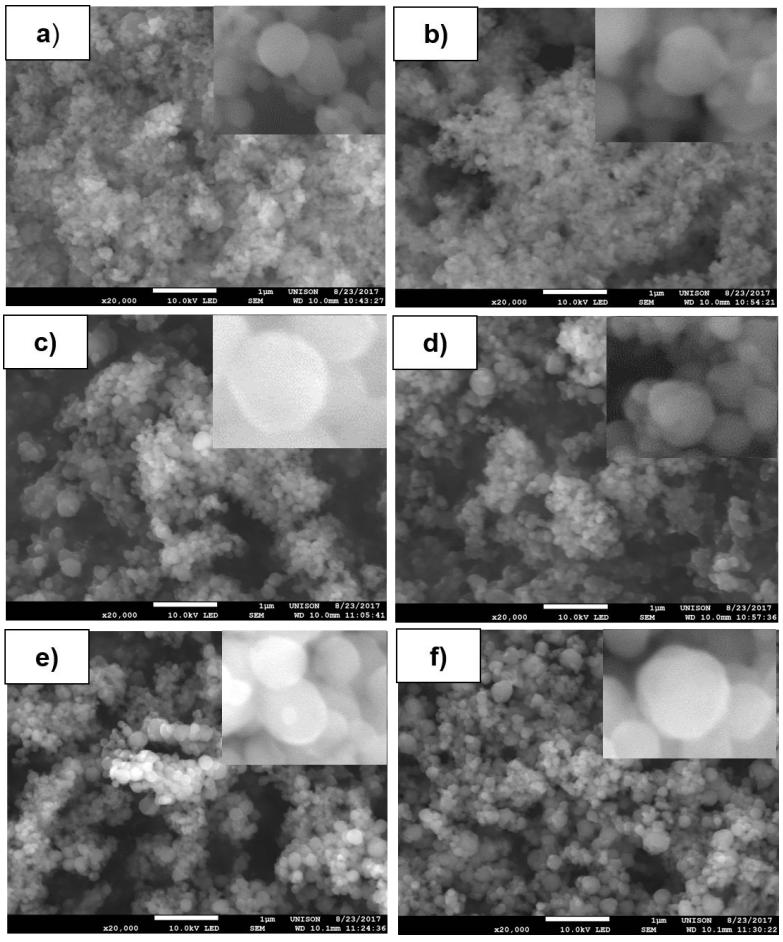

Figure 5 Micrography by SEM of a) zein nanoparticles. Zein at different quercetin concentrations, b) 1 mg mL^{-1}, c) 5 mg $mL^{-1,}$ d) 10 mg mL^{-1}, e) 15 mg mL^{-1}, and f) 20 mg mL^{-1}. Conditions: voltage of 15 kV, flow rate of 0.1 mL h^{-1} and collector distance of 15 cm. Magnification, 20,000X.

Patel, Heussen, Hazekamp, Drost & Velikov, (2012) elaborated quercetin-loaded zein nanoparticles, by means of the solvent-antisolvent (co-precipitating) method to improve the molecular stability of quercetin due to degradation by light and pH. The results were nanoparticles with an average diameter of between 130 and 161 nm. The authors observed that quercetin was trapped in the zein matrix, protecting quercetin from degradation due to the effect of pH and light.

Penalva, González-Navarro, Gamazo, Esparza & Irache, (2017) synthesized zein nanoparticles to entrap quercetin by the desolvation process. These authors evaluated the absorption, bioavailability, and anti-inflammatory effect of quercetin-loaded zein nanoparticles. Processing conditions included the elaboration of a hydroalcoholic solution containing zein, 2-HydroxyPropyl-β-CycloDextrin (HP-β-CD) and quercetin. The results revealed homogenous populations of spherical nanoparticles with a smooth surface and similar apparent size. The sizes ranged from 222-324 nm for the treatments and controls obtained and were greater than the obtained in the current study.

The difference between the studies of Patel et al., (2012) and Penalva et al., (2017) and those of this current study is that the method of obtaining nanoparticles does indeed exert an influence on the diameter of the particle, this being smaller by electrospraying, as shown later.

3.3.1.3 Average diameter and particle-size distribution of quercetin-loaded zein nanoparticles

Table 3 and Figure 6 depict the particle-size distribution and average diameter for zein control nanoparticles without quercetin and quercetin-loaded zein nanoparticles. The results

obtained were dependent on the concentration of quercetin, that is, the higher the encapsulated quercetin concentration, the greater the particle diameter obtained. In addition, the dispersity (mono- or polydispersity) of nanoparticles is related to particle size distribution and the standard deviation. The average diameter obtained for zein control nanoparticles was 67.9 ± 11.2 nm (Table 3), while for the entrapment of quercetin in the zein nanoparticle, average diameters were 70.4 ± 14.4, 84.5 ± 14.6, 91.8 ± 13.5, 99.6 ± 16.2, and 100.0 ± 17.9 nm for concentrations of quercetin of 20, 15, 10, 5, and 1 mg mL^{-1}, respectively, showing statistically significant differences among them (p <0.05) (Table 3). Penalva et al., (2017) obtained quercetin-loaded zein nanoparticles by the desolvation process, with an average diameter of 222 nm, larger than those reported by the current study. Therefore, the method for the nanoparticle synthesis is important to be considered in order to obtain small diameters of nanoparticles. Electrospraying technique allows us to obtain particles with sizes less than 100 nm. An advantage of the electrospraying technique is the application of voltage, which charges the polymer solution, breaking the surface tension of the same, forming smaller diameters and more spherical particles (Jaworek & Sobczyk, 2008; Tapia-Hernández et al., 2015; Boda, Li, & Xie, 2018). When the concentration of a bioactive compound increases in zein nanoparticles, the particle size increases. For instance, particle size of procyanidins has been reported in the range of 392 to 447 nm (Zou, Li, Percival, Bonard, & Gu, 2012), for retinol from 300.93 to 318.73 (Park, Park, & Kim, 2015), and for quercetin from 88.9 to 164 nm (Sun et al., 2015).

Table 3. Diameter, polydispersity index and efficiency of entrapment of quercetin-loaded zein nanoparticles nanoparticles at different concentrations of quercetin

Sample	Diameter (nm)	PDI	Entrapment efficiency (%)
Znp	67.9 ± 11.2^{a}	0.165	
ZQnp-1	70.4 ± 14.4^{b}	0.205	93.0 ± 2.6^{a}
ZQnp-5	84.5 ± 14.6^{c}	0.173	91.7 ± 1.7^{b}
ZQnp-10	91.8 ± 13.5^{d}	0.147	90.8 ± 1.7^{c}
ZQnp-15	99.6 ± 16.2^{e}	0.163	88.7 ± 1.0^{d}
ZQnp-20	100.0 ± 17.9^{e}	0.179	87.9 ± 1.5^{e}

Different letters (a, b, c, d, e) represent significant statistically differences by Tukey test ($p<0.05$)

Particle-size distribution (PSD) varied in all of the concentrations obtained (Figure 6). The control nanoparticle of zein showed the lowest distribution in a range of 35-85 nm, with the greatest accumulation between 55 and 75 nm (Figure 6a). Zein with 1 mg mL^{-1} of quercetin had a range distribution of 45-95 nm, but with a higher accumulation of between 55 and 85 nm, behaved like the control zein (Figure 6b). On the other hand, the concentration of zein with 5 mg mL^{-1} at a distribution within the range of 55-105 nm, with a greater accumulation between 75 and 95 nm, presents a more symmetrical distribution (Gaussian type) (Figure 6c). However, concentrations of 10, 15, and 20 mg mL^{-1} presented more asymmetrical and very broad distributions compared to the previous ones, with ranges between 55 and 125, 55 and 145, and 55 and 145, respectively (Figures 6d-6f). The amplitudes of PSD of quercetin-loaded zein nanoparticles were checked by means of the standard deviation (SD) and PDI.

The zein control presented an SD of 11. 2 nm, its distance lower than the mean, were considered as monodispersed particles, while for quercetin-loaded zein nanoparticles with 1, 5, 10, 15, and 20 mg mL^{-1} of quercetin, this was 14.4, 14.6, 13.5, 16.2, and 17.39 nm, respectively, observing at concentration of 15 and 20 mg mL^{-1}, different particle sizes, while for 1, 5, and 10 mg mL^{-1}, the particles were more homogeneous in size. Despite the dispersion in particle size was attributed to the SD, Table 3 shows the PDI of zein control and quercetin-loaded zein nanoparticles with values ≤ 0.2. Danaei et al., (2018) mention that for polymeric nanoparticles a PDI value ≤ 0.2 corresponds to monodisperse particles, therefore the particles in our study can be classified as monodisperse.

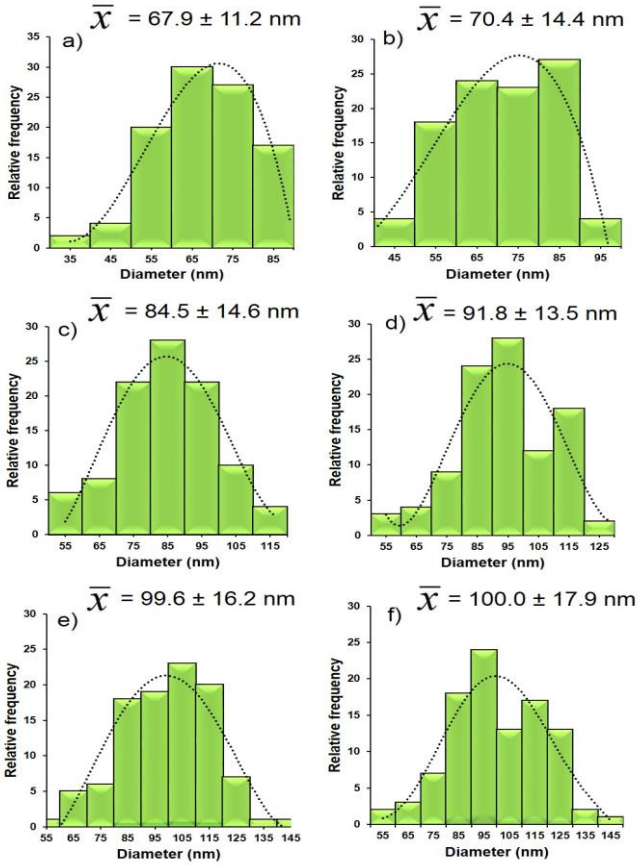

Figure 6 Particle size distribution of a) zein nanoparticles. Zein at different quercetin concentrations, b) 1 mg mL^{-1}, c) 5 mg $mL^{-1,}$ d) 10 mg mL^{-1}, e) 15 mg mL^{-1}, and f) 20 mg mL^{-1}.

3.3.2 Distribution mode of quercetin in the zein nanoparticle

Figure 7 shows micrographs by TEM of quercetin-loaded zein nanoparticles. Figure 7a and 7b present the micrograph of zein control nanoparticles, and in these, we are able to observe transparent nanoparticles, defined in the form of spheres and smooth. Figure 7c-7f depict the quercetin-loaded zein nanoparticles at 20 mg mL^{-1} of quercetin with spherical morphology but, unlike the control nanoparticles, they are not transparent and exhibit relief. In addition, in the quercetin-loaded zein nanoparticles, darkness areas throughout the particle can be observed and are attributed to the presence of quercetin. Therefore, the form in which quercetin is found in the zein nanoparticle is by entrapment. The electrospraying technique promotes the formation of nanoparticles by entrapment; when an active compound is dissolved in the same solution as that of the polymer as shown in Figure 1, interactions between both parties are promoted (as those observed in FT-IR). Chuacharoen & Sabliov (2017) encapsulated folic acid in zein nanoparticles by liquid-liquid dispersion and observed that one of the proposed mechanisms of the manner in which it interacted was by the entrapment of folic acid inside and around the particle.

3.3.3 Interaction of quercetin-loaded zein nanoparticle by FT-IR

To observe the interaction between quercetin and the zein matrix Fourier Transform-Infrared spectroscopy was used. Figure 8 shows the infrared spectra for zein powder, quercetin powder, zein nanoparticle and the quercetin-loaded zein nanoparticle at a concentration of 20 mg mL^{-1} of quercetin. Figure 8a shows the infrared spectrums for raw materials (zein and quercetin powder), where it is observed three characteristic bands corresponding to a protein. The amide I band corresponds to the vibrational stretch of -C=O at 1,666 cm^{-1}. The amide II band corresponds to the flexion vibration of the -N-H bond and the vibration of the -C-N at

1,537 cm^{-1}, whereas the -OH and -NH_2 bands correspond to the vibrational stretching bond at 3,323 cm^{-1}. The Infrared spectrum of quercetin powder (red line) shows the bands corresponding to the flexion and stretching bonds present in aromatic rings A and B and observed from 1,100 to 1,600 cm^{-1}, and where the -OH groups (hydroxyl groups) attached to the aromatic rings appear around of 1,200 to 1,400 cm^{-1} and 3,383 cm^{-1}. Figure 8b shows the infrared spectrum of zein nanoparticle (blue line) where the amide I band at 1,659 cm^{-1}, the amide II band at 1,537 cm^{-1}, and the -OH and -NH_2 bands at 3,316 cm^{-1}. These results suggest that there is a significant change in the secondary structure of zein powder to zein nanoparticle due to the effect of the solvent and the electrospray technique, mainly in the amide I and the -OH bands. Also, Figure 8b shows the infrared spectrum of quercetin-loaded zein nanoparticles (green line), where the characteristic bands are masked from 1,100 to 1,600 cm^{-1} in the zein nanoparticle, mainly in the bands corresponding to the –OH groups. The band at 3,316 cm^{-1} of zein nanoparticle decreases to 3,309 cm^{-1} in the quercetin-loaded nanoparticle, suggesting an interaction between zein and the hydroxyl of the quercetin, forming hydrogen bonds. Due to the hydrophobic nature of both molecules, hydrophobic interactions take place with the aromatic rings of quercetin and amino acids with R groups ending in alkyl groups, such as for alanine and proline present in zein.

Patel et al., (2012) observed that the phenolic stretch band of the -OH characteristic of quercetin was decreased, suggesting that hydrogen bonding is one of the main interactions. Li, Shi, Yu, Liao, & Wang, (2014) noted that the interaction of zein and quercetin occurs through of -N-H and -C=O groups, suggesting that these could act as both as proton donors and proton acceptor for the formation of hydrogen bonding. Aytac, Ipek, Durgun, & Uyar, (2018) reported some characteristic bands of quercetin similar to those found in this study,

other bands associated with aromatic rings at 3,429-3,238 cm^{-1} (OH), 1,674 cm^{-1} (C=O), 1,616 cm^{-1} (C = C), 1,359 cm^{-1} (C-OH), and 1,245 cm^{-1} (COC), and for zein, 1,656 cm^{-1} (Amide I) and 1,540 cm^{-1} (Amide II). These authors concluded that when zein and quercetin interact, it was not possible to visualize the characteristic bands of quercetin due to the intensity of the zein bands.

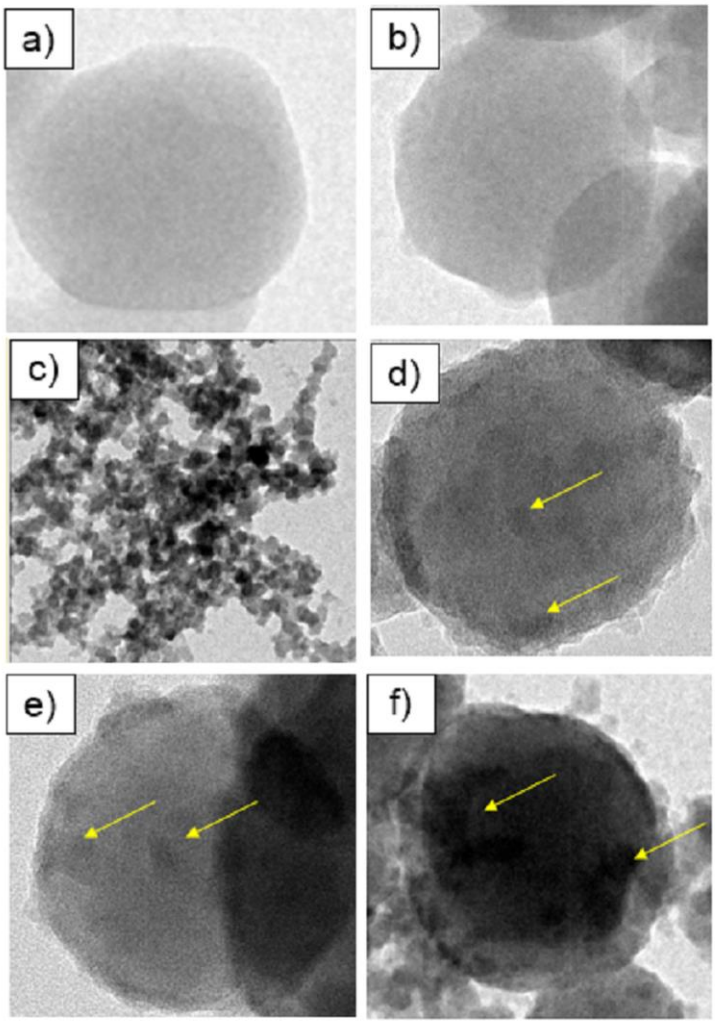

Figure 7 Micrography by TEM of a) and b) zein nanopartícles and c), d), e) f) zein-quercetin nanoparticles (quercetin concentration of 20 mg mL^{-1}).

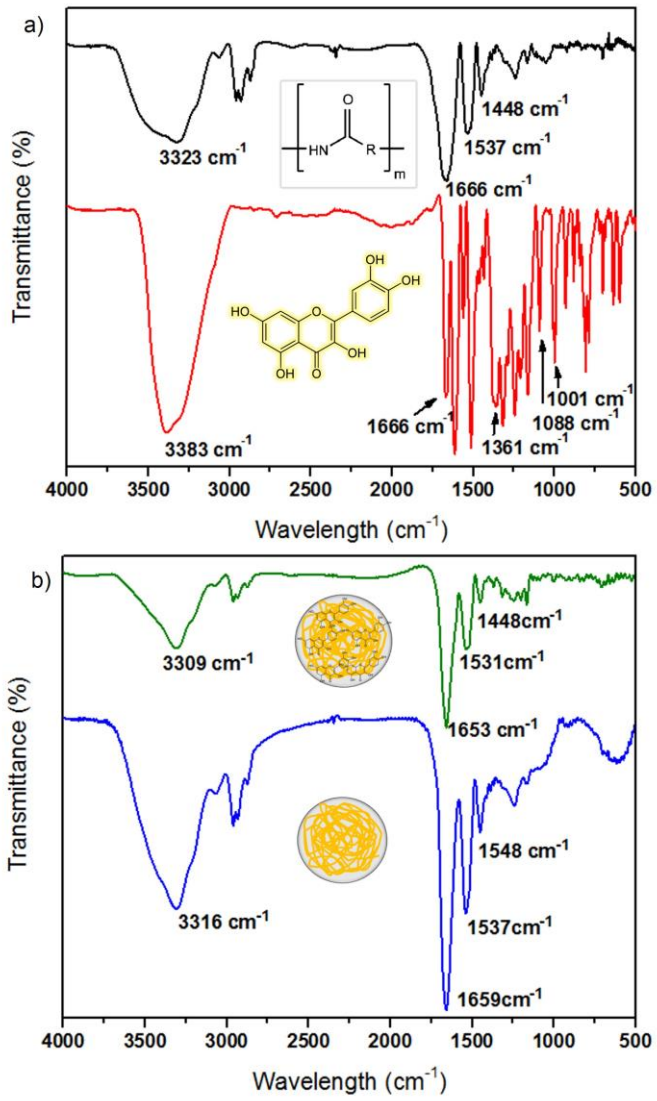

Figure 8 Infrared spectra of raw material and nanoparticles. a) zein powder in black line and quercetin powder in red line, b) zein nanoparticles in blue line and quercetin-loaded zein nanoparticles in green line (concentration of 20 mg mL^{-1}).

3.4 Efficiency entrapment

Table 3 discloses the entrapment efficiency for all of the quercetin concentrations. This parameter is defined as the amount of quercetin distributed into the zein nanoparticle (Hu, Lin, Liu, Li, & Zhao, 2012). In quercetin-loaded zein nanoparticles, the increases of the

concentration of quercetin in the process of zein nanoparticle formation the entrapment efficacy of quercetin decreases. This behavior was similar to that reported in the zein nanoparticle by Hu et al., (2012) and Liang et al., (2017). For 1, 5, 10, 15, and 20 mg mL^{-1}, entrapment efficiency was 93.0 ± 2.6, 91.7 ± 1.7, 90.8 ± 1.7, 88.7 ± 1.0, and 87.9 ± 1.5, respectively, showing statistically significant differences between them (p <0.05). Entrapment is dependent on solid-state drug solubility in the matrix material or polymer (solid dissolution or dispersion), which is related to a polymer composition, molecular weight, drug-polymer interaction, and the presence of functional groups (Mohanraj & Chen, 2006). Liang et al., (2017) elaborated epigallocatechin gallate in zein nanoparticles coated with chitosan and observed that, as the concentration of epigallocatechin gallate increased from 2 to 5 mg, entrapment efficiency decreased from 80 to 78.5% and, when increased to 8 mg, entrapment efficiency decreased up to 70%. The difference in entrapment efficiency of quercetin and epiigallocatechin gallate in zein nanoparticles is due to the high hydrophobicity of quercetin where, apart from hydrogen bonding interactions, it interacts through hydrophobic interactions, and in epigallocatechin gallate the hydrophobicity is lower.

Therefore, quercetin may be interacting by hydrogen bonds and hydrophobic interactions in zein nanoparticles with spherical and compact morphology by entrapment, and encapsulation efficiency demonstrated a dependence on the concentration of quercetin. Therefore, zein-quercetin nanoparticles are feasible for their application as a therapeutic treatment.

3.5 *In vitro* gastrointestinal release and bioavailability

Figure 9 shows the gastrointestinal release and bioavailability of free quercetin and quercetin-loaded zein nanoparticles (trapped quercetin) at quercetin concentration of 1 mg mL^{-1}. Figure 9a shows the gastric digestion phase at 30 min that gave the highest release of free quercetin

(83.9%), while that for trapped quercetin was much lower (47.6%) being the most external quercetin in the nanoparticle of zein, which was released faster. At 120 min of gastric digestion phase, this percentage increased for free quercetin to 90.4% and for trapped quercetin to 62.9%.

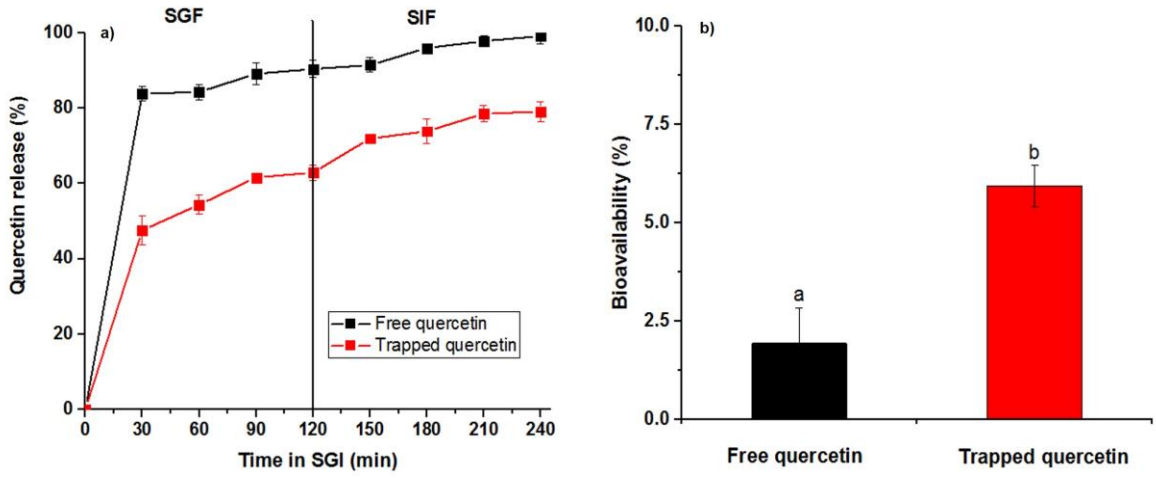

Figure 9 *In vitro* study de quercetin-loaded zein nanoparticles with a concentration of 1 mg mL^{-1} of quercetin a) gastrointestinal release and b) bioavailability. Different letters (a, b) in bioavailability represent significant statistically differences by Tukey test ($p<0.05$)

In intestinal digestion phase (after 120 min) the release of free quercetin was only 8.7%, but together with gastric digestion, 99.2% of release was achieved at 240 min. In contrast, trapped quercetin showed a greater release in intestinal digestion phase with 16.2%, and along with with the gastric digestion, reached 79.1% at 240 min being able to still released the remaining 20% at later times. Therefore, trapped quercetin in zein nanoparticles promotes that quercetin to be more bioaccessible in the intestine part compared to free quercetin.

Figure 9b shows the bioavailability of free quercetin and trapped from the digests obtained from the intestine phase. Bioavailability is defined as the fraction of an orally administered substance that is absorbed and available for physiologic activity or storage (Guo & Bruno,

2015). For free quercetin, the bioavailability was 1.9% corresponding to 5.4 μg of the initial free quercetin used for SGI. On the other hand, the bioavailability of trapped quercetin was 5.9%, corresponding to 16.7 μg. Therefore, the entrapment promotes that quercetin to be three times more bioavailable than its free form.

4. Conclusions

The rheological behavior of zein solutions at different concentrations of ethanol was observed as a Newtonian fluid by the Power Law model. Also, viscosity with respect to time and shear rate predicted stability in nanoparticle morphology. The 80% solution (v/v) of ethanol and that of 5% (w/v) of zein were the best conditions evaluated for the formation of nanoparticles. The electrospraying method provided entrapment of quercetin in the nanoparticle, obtaining quercetin-loaded zein nanoparticles with spherical and compact morphologies. Main interactions between zein and quercetin were by hydrogen bonds. For all quercitin concentrations, high entrapment efficiency was provided. Also, quercetin-loaded zein nanoparticle provides stability to quercetin during gastrointestinal digestion, promoting greater bioavailability than free quercetin. Based on the present study, and combined with the most recent reports about coaxial electrospraying and method studying the working processes more active ingredients and macromolecules extracted from foods and crops can find their ways for new potential functional applications in the form of electrosprayed particles.

Acknowledgments

José Agustíın Tapia-Hernández, M.Sc., thanks CONACYT for the scholarship granted

Ethical Statement

This study does not involve any human testing

Author Contributions

Francisco Rodríguez-Félix had overall responsibility for the project, contributed to the interpretation and discussion of the results and manuscript preparation. Carmen Lizette Del-Toro-Sánchez, Francisco Javier Cinco-Moroyoqui, Saul Ruiz-Cruz, Josué Juárez interpreted some results and edited the manuscript. Elizabeth Carvajal-Millan, Daniela Denisse Castro-Enríquez, Carlos Gregorio Barreras-Urbina and Guadalupe Amanda López-Ahumada advised on some techniques, helped in the statistical analysis and reviewed the writing. José Agustíın Tapia-Hernández designed the study, carried out overall experiment and wrote of the manuscript. All authors read and approved the final manuscript.

References

Alehosseini, A., Ghorani, B., Sarabi-Jamab, M., & Tucker, N. (2017). Principles of electrospraying: A new approach in protection of bioactive compounds in foods. Critical *Reviews in Food science and Nutrition*, 1-18. https://doi.org/10.1080/10408398.2017.1323723

Aytac, Z., Ipek, S., Durgun, E., & Uyar, T. (2018). Antioxidant electrospun zein nanofibrous web encapsulating quercetin/cyclodextrin inclusion complex. *Journal of Materials Science*, *53*(2), 1527-1539. https://doi.org/10.1007/s10853-017-1580-x

Baspinar, Y., Üstündas, M., Bayraktar, O., & Sezgin, C. (2018). Curcumin and piperine loaded zein-chitosan nanoparticles: *Development and in-vitro characterisation. Saudi Pharmaceutical Journal*, *26*(3), 323-334. https://doi.org/10.1016/j.jsps.2018.01.010

Bisharat, L., Berardi, A., Perinelli, D.R., Bonacucina, G., Casettari, L., Cespi, M., AlKhatib, H.S., & Palmieri, G.F. (2018). Aggregation of zein in aqueous ethanol dispersions: Effect on cast film properties. *International Journal of Biological macromolecules*, *106*, 360-368. https://doi.org/10.1016/j.ijbiomac.2017.08.024

Bhushani, J.A., Kurrey, N.K., & Anandharamakrishnan, C. (2017). Nanoencapsulation of green tea catechins by electrospraying technique and its effect on controlled release and in-vitro permeability. *Journal of Food Engineering*, *199*, 82-92. https://doi.org/10.1016/j.jfoodeng.2016.12.010

Boda, S.K., Li, X., & Xie, J. (2018). Electrospraying an enabling technology for pharmaceutical and biomedical applications: A review. *Journal of Aerosol Science*, *125*, 164-181. https://doi.org/10.1016/j.jaerosci.2018.04.002

Chen, Y., Ye, R., & Liu, J. (2013). Understanding of dispersion and aggregation of suspensions of zein nanoparticles in aqueous alcohol solutions after thermal treatment. *Industrial Crops and Products*, *50*, 764-770. https://doi.org/10.1016/j.indcrop.2013.08.023

Chen, Y., Ye, R., & Liu, J. (2014). Effects of different concentrations of ethanol and isopropanol on physicochemical properties of zein-based films. *Industrial Crops and Products*, *53*, 140-147. https://doi.org/10.1016/j.indcrop.2013.12.034

Chen, H., Zhang, Y., & Zhong, Q. (2015). Physical and antimicrobial properties of spray-dried zein–casein nanocapsules with co-encapsulated eugenol and thymol. *Journal of Food Engineering*, *144*, 93-102. https://doi.org/10.1016/j.jfoodeng.2014.07.021

Cheng, C.J., & Jones, O.G. (2017). Stabilizing zein nanoparticle dispersions with ι-carrageenan. *Food Hydrocolloids*, *69*, 28-35. https://doi.org/10.1016/j.foodhyd.2017.01.022

Chevalier, E., Assezat, G., Prochazka, F., & Oulahal, N. (2018). Development and characterization of a novel edible extruded sheet based on different casein sources and influence of the glycerol concentration. *Food Hydrocolloids*, *75*, 182-191. https://doi.org/10.1016/j.foodhyd.2017.08.028

Chuacharoen, T., & Sabliov, C.M. (2016). The potential of zein nanoparticles to protect entrapped β-carotene in the presence of milk under simulated gastrointestinal (GI) conditions. *LWT-Food Science and Technology*, *72*, 302-309. https://doi.org/10.1016/j.lwt.2016.05.006

Chuacharoen, T., & Sabliov, C.M. (2017). Zein nanoparticles as delivery systems for covalently linked and physically entrapped folic acid. *Journal of Nanoparticle Research*, *19*(2), 81. https://doi.org/10.1007/s11051-017-3763-4

Granato, M., Rizzello, C., Montani, M. S.G., Cuomo, L., Vitillo, M., Santarelli, R., Gonnella, R., D'Orazi, G., Faggioni, A., & Cirone, M. (2017). Quercetin induces apoptosis and autophagy in primary effusion lymphoma cells by inhibiting PI3K/AKT/mTOR and STAT3 signaling pathways. *The Journal of Nutritional Biochemistry*, *41*, 124-136. https://doi.org/10.1016/j.jnutbio.2016.12.011

Guo, Y., & Bruno, R.S. (2015). Endogenous and exogenous mediators of quercetin bioavailability. *The Journal of Nutritional Biochemistry*, *26*(3), 201-210. https://doi.org/10.1016/j.jnutbio.2014.10.008

Dai, L., Sun, C., Li, R., Mao, L., Liu, F., & Gao, Y. (2017). Structural characterization, formation mechanism and stability of curcumin in zein-lecithin composite nanoparticles fabricated by antisolvent co-precipitation. *Food Chemistry*, *237*, 1163-1171. https://doi.org/10.1016/j.foodchem.2017.05.134

Danaei, M., Dehghankhold, M., Ataei, S., Hasanzadeh Davarani, F., Javanmard, R., Dokhani, A., Khorasani, S., & Mozafari, M. (2018). Impact of particle size and polydispersity index on the clinical applications of lipidic nanocarrier systems. *Pharmaceutics*, *10*(2), 57. https://doi.org/10.3390/pharmaceutics10020057

Davidov-Pardo, G., Joye, I.J., Espinal-Ruiz, M., & McClements, D.J. (2015). Effect of maillard conjugates on the physical stability of zein nanoparticles prepared by liquid antisolvent coprecipitation. *Journal of Agricultural and Food Chemistry*, *63*(38), 8510-8518. https://doi.org/10.1021/acs.jafc.5b02699

Dhanya, R., Arya, A. D., Nisha, P., & Jayamurthy, P. (2017). Quercetin, a lead compound against type 2 diabetes ameliorates glucose uptake via AMPK pathway in skeletal muscle cell line. *Frontiers in Pharmacology*, *8*, 336. https://doi.org/10.3389/fphar.2017.00336

Donsì, F., Voudouris, P., Veen, S.J., & Velikov, K.P. (2017). Zein-based colloidal particles for encapsulation and delivery of epigallocatechin gallate. *Food Hydrocolloids*, *63*, 508-517. https://doi.org/10.1016/j.foodhyd.2016.09.039

Fu, D., & Weller, C.L. (1999). Rheology of zein solutions in aqueous ethanol. *Journal of Agricultural and Food Chemistry*, *47*(5), 2103-2108. https://doi.org/10.1021/jf9811121

Gómez-Estaca, J., Balaguer, M.P., Gavara, R., & Hernandez-Munoz, P. (2012). Formation of zein nanoparticles by electrohydrodynamic atomization: Effect of the main processing variables and suitability for encapsulating the food coloring and active ingredient curcumin. *Food Hydrocolloids*, *28*(1), 82-91. https://doi.org/10.1016/j.foodhyd.2011.11.013

Gómez-Mascaraque, L.G., Tordera, F., Fabra, M. J., Martínez-Sanz, M., & Lopez-Rubio, A. (2018). Coaxial electrospraying of biopolymers as a strategy to improve protection of bioactive food ingredients. *Innovative Food Science & Emerging Technologies, 51*, 2-11. https://doi.org/10.1016/j.ifset.2018.03.023

Hu, D., Lin, C., Liu, L., Li, S., & Zhao, Y. (2012). Preparation, characterization, and in vitro release investigation of lutein/zein nanoparticles via solution enhanced dispersion by supercritical fluids. *Journal of Food Engineering*, *109*(3), 545-552. https://doi.org/10.1016/j.jfoodeng.2011.10.025

Huang, J., Wang, Q., Sun, R., Li, T., Xia, N., & Xia, Q. (2018). A novel solid self-emulsifying delivery system (SEDS) for the encapsulation of linseed oil and quercetin: Preparation and evaluation. *Journal of Food Engineering*, *226*, 22-30. https://doi.org/10.1016/j.jfoodeng.2018.01.017

Huang, W., Hou, Y., Lu, X., Gong, Z., Yang, Y., Lu, X. J., Liu X. L. & Yu, D. G. (2019). The Process–Property–Performance Relationship of Medicated Nanoparticles Prepared by Modified Coaxial Electrospraying. *Pharmaceutics*, 11(5), 226.

Jayaraman, P., Gandhimathi, C., Venugopal, J.R., Becker, D. L., Ramakrishna, S., & Srinivasan, D.K. (2015). Controlled release of drugs in electrosprayed nanoparticles for bone tissue engineering. *Advanced Drug Delivery Reviews*, *94*. https://doi.org/10.1016/j.addr.2015.09.007

Jaworek, A.T.S.A., & Sobczyk, A.T. (2008). Electrospraying route to nanotechnology: an overview. *Journal of Electrostatics*, *66(*3-4), 197-219. https://doi.org/10.1016/j.elstat.2007.10.001

Jaworek, A., Sobczyk, A. T., & Krupa, A. (2018). Electrospray application to powder production and surface coating. *Journal of Aerosol Science*, *125*, 57-92. https://doi.org/10.1016/j.jaerosci.2018.04.006

Juárez, J., Taboada, P., Valdez, M.A., & Mosquera, V. (2008). Self-assembly process of different poly (oxystyrene)-poly (oxyethylene) block copolymers: spontaneous formation of vesicular structures and elongated micelles. *Langmuir*, *24*(14), 7107-7116. https://doi.org/10.1021/la8004568

Kim, S., & Xu, J. (2008). Aggregate formation of zein and its structural inversion in aqueous ethanol. *Journal of Cereal Science*, *47*(1), 1-5. https://doi.org/10.1016/j.jcs.2007.08.004

Kumar, R., Vijayalakshmi, S., & Nadanasabapathi, S. (2017). Health Benefits of Quercetin. *Defence Life Science Journal*, *2*(2), 142-151. https://doi.org/10.14429/dlsj.2.11359

Li, X.Y., Shi, C.J., Yu, D.G., Liao, Y.Z., & Wang, X. (2014). Electrospun quercetin-loaded zein nanoribbons. *Bio-medical Materials and Engineering*, *24*(6), 2015-2023. https://doi.org/10.3233/BME-141011

Li, X. Y., Zheng, Z. B., Yu, D. G., Liu, X. K., Qu, Y. L., & Li, H. L. (2017). Electrosprayed sperical ethylcellulose nanoparticles for an improved sustained-release profile of anticancer drug. *Cellulose*, *24*(12), 5551-5564. https://doi.org/10.1007/s10570-017-1498-0

Liang, J., Yan, H., Wang, X., Zhou, Y., Gao, X., Puligundla, P., & Wan, X. (2017). Encapsulation of epigallocatechin gallate in zein/chitosan nanoparticles for controlled applications in food systems. *Food Chemistry*, *231*, 19-24. https://doi.org/10.1016/j.foodchem.2017.02.106

Liang, Q., Ren, X., Zhang, X., Hou, T., Chalamaiah, M., Ma, H., & Xu, B. (2018). Effect of ultrasound on the preparation of resveratrol-loaded zein particles. *Journal of Food Engineering*, *221*, 88-94. https://doi.org/10.1016/j.jfoodeng.2017.10.002

Lin, J., & Zhou, W. (2018). Role of quercetin in the physicochemical properties, antioxidant and antiglycation activities of bread. *Journal of Functional Foods*, *40*, 299-306. https://doi.org/10.1016/j.jff.2017.11.018

Liu, Z.P., Zhang, Y.Y., Yu, D.G., Wu, D., & Li, H.L. (2018). Fabrication of sustained-release zein nanoparticles via modified coaxial electrospraying. *Chemical Engineering Journal*, *334*, 807-816. https://doi.org/10.1016/j.cej.2017.10.098

Mirpoor, S.F., Hosseini, S.M.H., & Nekoei, A.R. (2017). Efficient delivery of quercetin after binding to beta-lactoglobulin followed by formation soft-condensed core-shell nanostructures. *Food Chemistry*, *233*, 282-289. https://doi.org/10.1016/j.foodchem.2017.04.126

Mohanraj, V.J., & Chen, Y. (2006). Nanoparticles-a review. *Tropical journal of Pharmaceutical Research*, *5*(1), 561-573. http://dx.doi.org/10.4314/tjpr.v5i1.14634

Nabavi, S.F., Russo, G.L., Daglia, M., & Nabavi, S.M. (2015). Role of quercetin as an alternative for obesity treatment: you are what you eat!. *Food Chemistry*, *179*, 305-310. https://doi.org/10.1016/j.foodchem.2015.02.006

Nathiya, S., Durga, M., & Devasena, T. (2014). Quercetin, encapsulated quercetin and its application-a review. *International Journal of Pharmacy and Pharmaceutical Sciences*, *10*, 11, 20-26.

Neo, Y.P., Ray, S., Easteal, A.J., Nikolaidis, M.G., & Quek, S.Y. (2012). Influence of solution and processing parameters towards the fabrication of electrospun zein fibers with sub-micron diameter. *Journal of Food Engineering*, *109*(4), 645-651. https://doi.org/10.1016/j.jfoodeng.2011.11.032

Ni, S., Hu, C., Sun, R., Zhao, G., & Xia, Q. (2017). Nanoemulsions-Based Delivery Systems for Encapsulation of Quercetin: Preparation, Characterization, and Cytotoxicity Studies. *Journal of Food Process Engineering*, *40*(2), e12374. https://doi.org/10.1111/jfpe.12374

Ni, X., Wang, K., Wu, K., Corke, H., Nishinari, K., & Jiang, F. (2018). Stability, microstructure and rheological behavior of konjac glucomannan-zein mixed systems. *Carbohydrate Polymers*, *188*, 260-267. https://doi.org/10.1016/j.carbpol.2018.02.001

Nonthanum, P., Lee, Y., & Padua, G.W. (2013). Effect of pH and ethanol content of solvent on rheology of zein solutions. *Journal of Cereal Science*, *58*(1), 76-81. https://doi.org/10.1016/j.jcs.2013.04.001

Olenskyj, A.G., Feng, Y., & Lee, Y. (2017). Continuous microfluidic production of zein nanoparticles and correlation of particle size with physical parameters determined using CFD simulation. *Journal of Food Engineering*, *211*, 50-59. https://doi.org/10.1016/j.jfoodeng.2017.04.019

Paliwal, R., & Palakurthi, S. (2014). Zein in controlled drug delivery and tissue engineering. *Journal of Controlled Release*, *189*, 108-122. https://doi.org/10.1016/j.jconrel.2014.06.036

Park, C.E., Park, D.J., & Kim, B.K. (2015). Effects of a chitosan coating on properties of retinol-encapsulated zein nanoparticles. *Food Science and Biotechnology*, *24*(5), 1725-1733. https://doi.org/10.1007/s10068-015-0224-7

Patel, A.R., Heussen, P.C., Hazekamp, J., Drost, E., & Velikov, K.P. (2012). Quercetin loaded biopolymeric colloidal particles prepared by simultaneous precipitation of quercetin with hydrophobic protein in aqueous medium. *Food Chemistry*, *133*(2), 423-429. https://doi.org/10.1016/j.foodchem.2012.01.054

Penalva, R., González-Navarro, C.J., Gamazo, C., Esparza, I., & Irache, J.M. (2017). Zein nanoparticles for oral delivery of quercetin: Pharmacokinetic studies and preventive anti-inflammatory effects in a mouse model of endotoxemia. *Nanomedicine: Nanotechnology, Biology and Medicine*, *13*(1), 103-110. https://doi.org/10.1016/j.nano.2016.08.033

Porcu, E.P., Cossu, M., Rassu, G., Giunchedi, P., Cerri, G., Pourová, J., Najmanová, I., Migkos, T., Pilařová, V., Nováková, L., Mladěnka, P. & Gavini, E., (2018). Aqueous injection of quercetin: An approach for confirmation of its direct in vivo cardiovascular effects. *International Journal of Pharmaceutics*, *541*(1-2), 224-233. https://doi.org/10.1016/j.ijpharm.2018.02.036

Sharma, A., Kashyap, D., Sak, K., Tuli, H.S., & Sharma, A. K. (2018). Therapeutic charm of quercetin and its derivatives: a review of research and patents. *Pharmaceutical Patent Analyst*, *7*(1), 15-32. https://doi.org/10.4155/ppa-2017-0030

Smeets, A., Clasen, C., & Van den Mooter, G. (2017). Electrospraying of polymer solutions: study of formulation and process parameters. *European Journal of Pharmaceutics and Biopharmaceutics*, *119*, 114-124. https://doi.org/10.1016/j.ejpb.2017.06.010

Soltani, S., & Madadlou, A. (2015). Gelation characteristics of the sugar beet pectin solution charged with fish oil-loaded zein nanoparticles. *Food Hydrocolloids*, *43*, 664-669. https://doi.org/10.1016/j.foodhyd.2014.07.030

Soltani, S., & Madadlou, A. (2016). Two-step sequential cross-linking of sugar beet pectin for transforming zein nanoparticle-based Pickering emulsions to emulgels. *Carbohydrate Polymers*, *136*, 738-743. https://doi.org/10.1016/j.carbpol.2015.09.100

Sun, C., Liu, F., Yang, J., Yang, W., Yuan, F., & Gao, Y. (2015). Physical, structural, thermal and morphological characteristics of zeinquercetagetin composite colloidal nanoparticles. *Industrial Crops and Products*, *77*, 476-483. https://doi.org/10.1016/j.indcrop.2015.09.028

Tapia-Hernández, J.A., Torres-Chávez, P.I., Ramírez-Wong, B., Rascón-Chu, A., Plascencia-Jatomea, M., Barreras-Urbina, C.G., Rangel-Vázquez, N.A., & Rodríguez-Félix, F. (2015). Micro- and nanoparticles by electrospray: advances and applications in foods. *Journal of Agricultural and Food Chemistry*, *63*(19), 4699-4707. https://doi.org/10.1021/acs.jafc.5b01403

Tapia-Hernández, J.A., Rodríguez-Félix, F., & Katouzian, I. (2017). Nanocapsule formation by electrospraying. In Nanoencapsulation Technologies for the Food and Nutraceutical Industries (pp. 320-345).

Tapia-Hernández, J.A., Rodríguez-Félix, D.E., Plascencia-Jatomea, M., Rascón-Chu, A., López-Ahumada, G.A., Ruiz-Cruz, S., Barreras-Urbina, C.G., & Rodríguez-Félix, F. (2018). Porous wheat gluten microparticles obtained by electrospray: Preparation and characterization. *Advances in Polymer Technology*, *37*(6), 2314-2324. https://doi.org/10.1002/adv.21907

Tapia-Hernández, J.A., Rodríguez-Felix, F., Juárez-Onofre, J.E., Ruiz-Cruz, S., Robles-García, M.A., Borboa-Flores, J., Wong-Corral, F.J., Cinco-Moroyoqui, F.J., Castro-Enríquez, D.D., & Del-Toro-Sánchez, C.L. (2018). Zein-polysaccharide nanoparticles as matrices for antioxidant compounds: A strategy for prevention of chronic degenerative diseases. *Food Research International*, *111*, 451-471. https://doi.org/10.1016/j.foodhyd.2018.02.014

Tapia-Hernández, J.A., Del-Toro-Sánchez, C.L., Cinco-Moroyoqui, F.J., Ruiz-Cruz, S., Juárez, J., Castro-Enríquez, D.D., Barreras-Urbina, C.G., López-Ahumada, A.G., & Rodríguez-Félix, F. (2019). Gallic Acid-Loaded Zein Nanoparticles by Electrospraying Process. *Journal of Food Science*, *84*(4), 818-831. https://doi.org/10.1111/1750-3841.14486

Tapia-Hernández, J. A., Del-Toro-Sánchez, C. L., Cinco-Moroyoqui, F. J., Juárez-Onofre, J. E., Ruiz-Cruz, S., Carvajal-Millan, E., López-Ahumada G. A., Castro-Enriquez D. D.,

Barreras-Urbina C. G., & Rodríguez-Felix, F. (2019). Prolamins from Cereal By-products: Classification, Extraction, Characterization and its Applications in Micro-and Nanofabrication. *Trends in Food Science & Technology*, *90*, 111-132. https://doi.org/10.1016/j.tifs.2019.06.005

Taylor, J., Anyango, J.O., Muhiwa, P.J., Oguntoyinbo, S.I., & Taylor, J.R. (2018). Comparison of formation of visco-elastic masses and their properties between zeins and kafirins. *Food Chemistry*, *245*, 178-188. https://doi.org/10.1016/j.foodchem.2017.10.082

Terao, J. (2017). Factors modulating bioavailability of quercetin-related flavonoids and the consequences of their vascular function. Biochemical *Pharmacology*, *139*, 15-23. https://doi.org/10.1016/j.bcp.2017.03.021

Ting, Y., Chang, W.T., Shiau, D.K., Chou, P.H., Wu, M.F., & Hsu, C.L. (2017). Antiobesity efficacy of quercetin-rich supplement on diet-induced obese rats: effects on body composition, serum lipid profile, and gene expression. *Journal of Agricultural and Food Chemistry*, 66(1), 70-80. https://doi.org/0.1021/acs.jafc.7b03551

Uzun, S., Ilavsky, J., & Padua, G.W. (2017). Characterization of zein assemblies by ultra-small-angle X-ray scattering. *Soft Matter*, *13*(16), 3053-3060. https://doi.org/10.1039/C6SM02717B

Wang, Y., & Padua, G.W. (2010). Formation of zein microphases in ethanol− water. *Langmuir*, *26*(15), 12897-12901. https://doi.org/10.1021/la101688v

Wang, Y., Su, C.P., Schulmerich, M., & Padua, G. W. (2013). Characterization of core–shell structures formed by zein. *Food Hydrocolloids*, *30*(2), 487-494. https://doi.org/10.1016/j.foodhyd.2012.07.019

Wang, K., Wen, H. F., Yu, D. G., Yang, Y., & Zhang, D. F. (2018). Electrosprayed hydrophilic nanocomposites coated with shellac for colon-specific delayed drug delivery. *Materials & Design*, *143*, 248-255. https://doi.org/10.1016/j.matdes.2018.02.016

Wei, Y., Sun, C., Dai, L., Zhan, X., & Gao, Y. (2018). Structure, physicochemical stability and in vitro simulated gastrointestinal digestion properties of β-carotene loaded zein-propylene glycol alginate composite nanoparticles fabricated by emulsification-evaporation method. *Food Hydrocolloids*, *81*, 149-158. https://doi.org/10.1016/j.foodhyd.2018.02.042

Wu, Q., Needs, P.W., Lu, Y., Kroon, P.A., Ren, D., & Yang, X. (2018). Different antitumor effects of quercetin, quercetin-3′-sulfate and quercetin-3-glucuronide in human breast cancer MCF-7 cells. *Food & Function*, *9*(3), 1736-1746. https://doi.org/10.1039/C7FO01964E

Xiao, J., Nian, S., & Huang, Q. (2015). Assembly of kafirin/carboxymethyl chitosan nanoparticles to enhance the cellular uptake of curcumin. *Food Hydrocolloids*, *51*, 166-175. https://doi.org/10.1016/j.foodhyd.2015.05.012

Xue, J., Zhang, Y., Huang, G., Liu, J., Slavin, M., & Yu, L. L. (2018). Zein-caseinate composite nanoparticles for bioactive delivery using curcumin as a probe compound. *Food Hydrocolloids*, *83*, 25-35. https://doi.org/10.1016/j.foodhyd.2018.04.037

Yang, Y. Y., Zhang, M., Wang, K., & Yu, D. G. (2018). pH-sensitive polymer nanocoating on hydrophilic composites fabricated using modified coaxial electrospraying. *Materials Letters*, *227*, 93-96. https://doi.org/10.1016/j.matlet.2018.05.063

Yang, Y. Y., Zhang, M., Liu, Z. P., Wang, K., & Yu, D. G. (2018). Meletin sustained-release gliadin nanoparticles prepared via solvent surface modification on blending electrospraying. *Applied Surface Science*, *434*, 1040-1047. https://doi.org/10.1016/j.apsusc.2017.11.024

Yao, K., Chen, W., Song, F., McClements, D.J., & Hu, K. (2017). Tailoring zein nanoparticle functionality using biopolymer coatings: Impact on curcumin bioaccessibility and antioxidant capacity under simulated gastrointestinal conditions. *Food Hydrocolloids*, *79*, 262-272. https://doi.org/10.1016/j.foodhyd.2017.12.029

Yu, D. G., Zheng, X. L., Yang, Y., Li, X. Y., Williams, G. R., & Zhao, M. (2019). Immediate release of helicid from nanoparticles produced by modified coaxial electrospraying. *Applied Surface Science*, *473*, 148-155. https://doi.org/10.1016/j.apsusc.2018.12.147

Zhang, S., & Kawakami, K. (2010). One-step preparation of chitosan solid nanoparticles by electrospray deposition. *International Journal of Pharmaceutics*, *397(*1-2), 211-217.

Zhang, S., & Zhao, H. (2017). Preparation and properties of zein–rutin composite nanoparticle/corn starch films. *Carbohydrate Polymers*, *169*, 385-392. https://doi.org/10.1016/j.carbpol.2017.04.044

Zhong, Q., & Jin, M. (2009). Zein nanoparticles produced by liquid–liquid dispersion. *Food Hydrocolloids*, *23*(8), 2380-2387. https://doi.org/10.1016/j.foodhyd.2009.06.015

Zou, T., Li, Z., Percival, S.S., Bonard, S., & Gu, L. (2012). Fabrication, characterization, and cytotoxicity evaluation of cranberry procyanidins-zein nanoparticles. *Food Hydrocolloids*, *27*(2), 293-300. https://doi.org/10.1016/j.foodhyd.2011.10.002

Zou, L., Zheng, B., Zhang, R., Zhang, Z., Liu, W., Liu, C., & McClements, D.J. (2016). Enhancing the bioaccessibility of hydrophobic bioactive agents using mixed colloidal dispersions: Curcumin-loaded zein nanoparticles plus digestible lipid nanoparticles. *Food Research International*, *81*, 74-82. https://doi.org/10.1016/j.foodres.2015.12.035

Zou, Y., van Baalen, C., Yang, X., & Scholten, E. (2018). Tuning hydrophobicity of zein nanoparticles to control rheological behavior of Pickering emulsions. *Food Hydrocolloids*, *80*, 130-140. https://doi.org/10.1016/j.foodhyd.2018.02.014

CAPÍTULO V

Gallic Acid-Loaded Zein Nanoparticles by Electrospraying Process

Gallic Acid-Loaded Zein Nanoparticles by Electrospraying Process

José Agustín Tapia-Hernández, Carmen Lizette Del-Toro-Sánchez, Francisco Javier Cinco-Moroyoqui, Saúl Ruiz-Cruz, Josué Juárez, Daniela Denisse Castro-Enríquez, Carlos Gregorio Barreras-Urbina, Guadalupe Amanda López-Ahumada, and Francisco Rodríguez-Félix

Abstract: Currently, electrospraying is a novel process for obtaining the nanoparticles from biopolymers. Zein nanoparticles have been obtained by this method and used to protect both hydrophilic and hydrophobic antioxidant molecules from environmental factors. The objective of this work was to prepare and characterize gallic acid-loaded zein nanoparticles obtained by the electrospraying process to provide protection to gallic acid from environmental factors. Thus, it was related to the concentration of gallic acid in physicochemical and rheological properties of the electrosprayed solution, and also to equipment parameters, such as voltage, flow rate, and distance of the collector in morphology, and particle size. The physicochemical properties showed a relationship in the formation of a Taylor cone, in which at a low concentration of gallic acid (1% w/v), low viscosity (0.00464 ± 0.00001 Pa·s), and density (0.886 ± 0.00002 g/cm^3), as well as high electrical conductivity (369 ± 4.3 μs/cm), forms a stable cone-jet mode. The rheological properties and the Power Law model of the gallic acid-zein electrosprayed solution demonstrated Newtonian behavior ($n = 1$). The morphology and size of the particle were dependent on the concentration of gallic acid. Electrosprayed parameters with high voltage (15 kV), low flow rate (0.1 mL/hr), and short distance (10 cm) exhibited a smaller diameter and spherical morphology. FT–IR showed interaction in the gallic acid-loaded zein nanoparticle by hydrogen bonds. Therefore, the electrospraying process is a feasible technique for obtaining gallic acid-loaded zein nanoparticles and providing potential protection to gallic acid from environmental factors.

Keywords: biopolymer, electrospraying, gallic acid, nanoparticles, zein

Introduction

Nanotechnology is considered a multidisciplinary science that aids in solving current problems (de Francisco & García-Estepa, 2018; Prakash et al., 2018). It is defined as the control of matter at the atomic and molecular levels (Kargozar & Mozafari, 2018). Some fields where nanotechnology has been applied are the food industry, (Karimi, Sadeghi, & Kokini, 2017), food safety (Krishna et al., 2018), the cosmeceutical industry (Kaul, Gulati, Verma, Mukherjee, & Nagaich, 2018), water treatment (Mauter et al., 2018), and health (Tapia-Hernández et al., 2018). Within nanotechnology, nanoencapsulation is a strategy in recent years for the protection of food ingredients and nutraceuticals (Assadpour & Jafari 2018; Liang et al., 2018). Multiple technologies have been utilized to elaborate nanoencapsulates; however, some of these used heat, such as spray drying, microemulsion, microwave heating, and hot-melt extrusion (Hanada, Jermain, Lu, Su, & Williams III, 2018; Lintingre, Lequeux, Talini, & Tsapis, 2016; Montalbán et al., 2018; Shah, Malherbe, Eldridge, Palombo, & Harding, 2014). Therefore, no-heat technologies are currently found in a boom, with the electrohydrodynamic atomization (EHDA) as one of the most studied of these at present (Paximada, Echegoyen, Koutinas, Mandala, & Lagaron, 2017; Smeets, Clasen, & Van den Mooter, 2017; Tapia-Hernández et al., 2015).

Although EHDA processes (including e-jet printing, electrospraying, and electrospinning) are fast developing to the multiple-fluids ones, such as coaxial (Hai et al., 2019; Yu et al., 2019), triaxial (Liu et al., 2019; Yang et al., 2019), their microformation mechanisms are still unclear (Yang, Zhang, Liu, Wang, & Yu, 2018; Yu, Li, Williams, & Zhao, 2018). Thus, on one hand, the single-fluid electrospraying and electrospinning are still the mainstreams of these fabrication methods. On the other hand, the fundamental investigations about the influences of operational parameters on the processes and also the quality of resultant products are high desired (Wang et al., 2017; Boda, Li, & Xie, 2018; Li, Yang, Yu, Du, & Yang, 2018). Specifically, in electrospraying process, different biopolymers have been utilized for the elaboration of nanoparticles, such as polysaccharides (Eltayeb, Stride, & Edirisinghe, 2015; Sreekumar, Lemke, Moerschbacher, Torres-Giner, & Lagaron, 2017), lipids (Liu, Li, Williams, Wu, & Zhu, 2018), and proteins (Gómez-Estaca, Gavara, & Hernández-Muñoz, 2015; Gómez-Mascaraque, Tordera, Fabra, Martínez-Sanz, & Lopez-Rubio, 2018).

A biopolymer widely used for its ability to form nanomaterials is zein (Chen et al., 2018; Gaona-Sánchez et al., 2015; Liu, Zhang, Yu, Wu, & Li, 2018). Zein is defined as the major storage prolamin of the corn-grain endosperm (Xue et al., 2018). Zein is considered a hydrophobic protein due to its high content of amino acids, such as alanine (10%), leucine (20%), and proline (10%), it is insoluble in water (Lucio et al., 2017) and is generally recognized as safe by the US Food Drug Administration (Chen & Jones, 2017). Zein

JFDS-2018-2016 Submitted 12/10/2018, Accepted 1/30/2019. *Authors José Agustín Tapia-Hernández, Carmen Lizette Del-Toro-Sánchez, Francisco Javier Cinco-Moroyoqui, Daniela Denisse Castro-Enríquez, Carlos Gregorio Barreras-Urbina, Guadalupe Amanda López-Ahumada, and Francisco Rodríguez-Félix are from Dept. of Research and Postgraduate in Food (DIPA), Univ. of Sonora, Blvd. Luis Encinas y Rosales, S/N, Colonia Centro, 83000, Hermosillo, Sonora, Mexico. Author Saúl Ruiz-Cruz is from Dept. of Biotechnology and Food Science, Inst. Technol. of Sonora, 5 de febrero #818 sur, Colonia Centro, 85000, Ciudad Obregón, Sonora, Mexico. Author Josué Juárez is from Dept. of Physics, Univ. of Sonora, Blvd. Luis Encinas y Rosales, S/N, Colonia Centro, 83000, Hermosillo, Sonora, Mexico. Direct inquiries to author Rodríguez-Félix (E-mail: rodriguez_felix_fco@hotmail.com).*

doi: 10.1111/1750-3841.14486

Journal of Food Science A Publication of the Institute of Food Technologists

consists of three polypeptides: α-zein of 19 to 24 kDa (75 to 80%); β-zein of 17 to 18 kDa (10 to 15%), and γ-zein, of 27 kDa (5 to 10%) (Thapa et al., 2017). The structural model of zein consists in an elongated, rectangular, prism-like shape with three dimensions that are 16, 4.6, and 1.2 nm, respectively, and that render it possible to obtain aggregates in aqueous ethanol (Luo & Wang, 2014).

Due to its ability to form nanoparticles, zein has been used to provide protection, stability, and as a delivery system to bioactive compounds (Wang et al., 2018). Among the bioactive compounds that have been encapsulated in zein nanoparticles and their respective obtention methods of obtaining are the following: resveratrol by antisolvent precipitation (Huang et al., 2017); rutin by antisolvent precipitation (Zhang, & Han, 2018); quercetagetin by antisolvent coprecipitation (Chen et al., 2018); curcumin by antisolvent precipitation and liquid–liquid dispersion (Hu, Wang, Fernandez, & Luo, 2016; Xue et al., 2018; Zou et al., 2016); vitamin A by phase separation (Park, Park, & Kim, 2015); vitamin D3 by phase separation (Luo, Teng, & Wang, 2012); procyanidins by liquid–liquid dispersion (Zou, Li, Percival, Bonard, & Gu, 2012), Tangeretin by liquid–liquid dispersion (Chen, Zheng, McClements, & Xiao, 2014); lutein by liquid–liquid dispersion (Chuacharoen & Sabliov, 2016), and quercetin by the desolvation procedure of an hydroalcoholic solution (Penalva, González-Navarro, Gamazo, Esparza, & Irache, 2017). However, the previously noted methods by which zein nanoparticles with bioactive compounds have been obtained do not ensure that the entire solvent is removed from the nanoparticles, and an additional process is used, such as lyophilization, to obtain them in the form of powder, for which electrospraying comprises a technique that eliminates the entirety of the solvent and it can be obtained in powder in a single step.

Also, a bioactive compound related to health benefits is Gallic Acid (GA) (3,4,5-trihydroxybenzoic acid), which is considered a naturally occurring low-molecular weight triphenolic known as bioactive phenolic acid (Asfaram, Ghaedi, & Dashtian, 2017; Badhani, Sharma, & Kakkar, 2015), which is found in green tea, vegetables, and fruits (Shahamirifard, Ghaedi, Razmi, & Hajati, 2018). GA has been attributed a wide range of biological effects, including antioxidant, anti-inflammatory, antimicrobial, and antitumor (Farhoosh & Nyström, 2018; Rajan & Muraleedharan, 2017; Yao et al., 2017). In addition, the effect of GA on the reduction of chronic degenerative diseases such as diabetes (Abdel-Moneim, El-Twab, Yousef, Reheim, & Ashour, 2018; Abdel-Moneim, Yousef, El-Twab, Reheim, & Ashour, 2017), obesity (Huang, Chang, Yang, Wu, & Shen, 2018), heart disease (Jin, Piao et al., 2017; Jin, Sun et al., 2018), and cancer (Liao, Chen, Huang, & Wang, 2018; Sales et al., 2018) has been studied. However, GA exhibits poor stability at high temperatures, in oxygen, in light, and in alkaline pH, in addition to its low absorption after oral administration (Acevedo et al., 2018). Therefore, the bioactivity of GA is affected and strategies to maintain it must be applied.

Therefore, nanotechnology applied to the encapsulation of GA in biopolymer matrices, such as zein, is necessary. The objective of this work was to study the effect of the electrosprayed solution and equipment parameters on the morphology and particle size of GA-loaded zein nanoparticles obtained by means of the electrospraying process.

Materials and Methods

Chemical reagents

Zein, with a protein content of 86.06% w/w (Sigma Z 3625) and GA with a purity of ≥98.5% (Sigma G 7384) were purchased from Sigma–Aldrich (St. Louis, MO, USA), Ethanol was purchased from Fagalab (Mexico) and distilled water was also used.

Preparation of electrosprayed solutions

Zein solutions containing GA in aqueous ethanol were prepared from the methodology proposed by Bhushani, Kurrey, and Anandharamakrishnan (2017); 5% w/v zein solutions were prepared in 80% v/v aqueous ethanol with different concentrations of GA (1 to 5% w/v). In addition, a control zein solution was prepared. All solutions were homogenized using magnetic stirring for 1 hr at 25 °C.

Physicochemical characterization of electrosprayed solutions

Viscosity. Viscosity was carried out based on the methodology proposed by Bhushani et al. (2017) with modifications. Measurements were taken on Modular Compact Rheometer (MCR) equipment (Anton Paar, Germany) utilizing concentric cylinder geometry. Analysis was performed for zein nanoparticles at different concentrations of GA (1 to 5% w/v). Conditions included a constant shear rate of 50 s^{-1} at 25 °C. Determinations were made in triplicates.

Density. Density was calculated by pycnometer methods as described by Tapia-Hernández et al. (2018). First, the empty pycnometer was brought to constant weight and the measurement was denominated M1. A reference pattern was generated that consisted of a pycnometer containing water, named M2. Then, solutions of 5% w/v of zein in 80% v/v ethanol and different concentrations of GA (1 to 5% w/v) were placed in the pycnometer and weighed, this measure named M3. The density of the prepared zein solutions was determined based on Eq. (1). Determinations were conducted in triplicate.

$$\rho = \frac{M3 - M1}{M2 - M1} 1 \text{ g/cm}^3 \quad (1)$$

Electrical conductivity. Electrical conductivity was determined from the methodology described by Prietto et al. (2018). Electrical conductivity was determined for all zein solutions at different concentrations of GA (1 to 5% w/v). A HANNA Instruments conductometer, model HI 2550 (pH, ORP & EC/TDS/NaCl meter) was used. Determinations were made in triplicates.

Rheological behavior of GA-zein electrosprayed solutions

Determination of the rheological behavior of the GA-zein electrosprayed solution was from the methodology described by Martín-Alfonso, Cuadri, Berta, and Stading (2018), with modification. MCR-102 equipment (Anton Paar, Germany) with concentric cylinder geometry was used and a distance between the base and the cylinder was 1 mm. The conditions of shear rate versus shear stress included a continuous ramp of 0.1 to 100 (s^{-1}) at 25 °C with 100 points, and an interval of 2 s per point, and with a duration of 200 s per measurement. Determinations were performed in triplicate.

The data obtained in shear stress measurements were adjusted to the Power Law model and obtained rheological behavior of GA-zein electrosprayed solutions was obtained. For determination of the type of fluid (Newtonian or non-Newtonian), the following Eq. (2) was employed:

$$\tau = KY^n \quad (2)$$

where τ is the shear stress (Pa), $\dot{Y}$ is the shear rate (s^{-1}), n is the Power Law index, and K is the consistency parameter (Pa s^n). Values = 1 are considered Newtonian fluids, values <1 are considered non-Newtonian fluids, and values of >1 are fluids with a tendency to thicken.

First, the stability of the viscosity of the zein solution was determined with respect to time at different shear rates (50, 100, 150, and 200 s^{-1}). Then, with the GA-zein electrosprayed solutions, the stability of the viscosity with respect to time was measured with best shear rate evaluated in zein solutions. The conditions for all solutions were 300 s and a temperature of 25 °C. For this measurement, 50 points were used with an interval of 6 s per point.

Electrospraying process

First, 5 mL of control zein and GA-zein electrosprayed solutions were transferred into a plastic syringe with a needle of 0.8-mm diameter. Then, the syringe was set in a pump (KD Scientific, Holliston, MA, USA) to regulate the flow of the polymer solution. The voltage was applied using a high-voltage power source (model CZE 1000R, Spellman, Hauppauge, NY, USA). A 10 cm × 10 cm aluminum plate was utilized for nanoparticle collection. For this experiment, a factorial design with four variables was employed (GA concentration, applied voltage, flow rate, and collector distance).

All of the GA-zein electrosprayed solutions were applied at two voltages (10 and 15 kV), at two flow rates (0.5 and 0.1 mL/hr), and at two collector distances (5 and 15 cm). Table 1 presents the runs that were evaluated in the electrospray process. Figure 1 depicts schematically the obtention of the GA-loaded zein nanoparticles through the electrospraying process.

Characterization of nanoparticles

Scanning electron microscopy (SEM). The morphological characterization of the material obtained was conducted using Scanning Electron Microscopy (SEM). AJEOL model 5410LV microscope was used. The samples were coated with gold and an acceleration voltage of 25 kV and a magnification of 10000× were utilized.

From the micrographs by SEM, particle size was measured for all of the formulations of GA-loaded zein nanoparticles using the ImageJ software program. One hundred nanoparticles were counted and their average diameter was obtained.

Fourier transform–infrared spectroscopy (FT–IR). To observe the interactions among the components of the material obtained, FT–IR was performed using a PerkinElmer Frontier spectrometer. For the analysis, a potassium bromide (kBr) pellet was fabricated with a nanoparticle powder sample. The measurement derived from a spectrum scan ranges from 4000 to 500 cm^{-1} in transmittance mode.

Table 1–Electrospray process conditions utilized to obtain GA-loaded zein nanoparticles.

Sample	GA (% w/v)	Voltage (kV)	Flow rate (mL/hr)	Distance (cm)
1	1	10	0.1	10
2	1	15	0.1	10
3	2	10	0.1	10
4	2	15	0.1	10
5	3	10	0.1	10
6	3	15	0.1	10
7	4	10	0.1	10
8	4	15	0.1	10
9	5	10	0.1	10
10	5	15	0.1	10
11	1	15	0.5	10
12	2	15	0.5	10
13	3	15	0.5	10
14	4	15	0.5	10
15	5	15	0.5	10
16	1	15	0.1	15
17	2	15	0.1	15
18	3	15	0.1	15
19	4	15	0.1	15
20	5	15	0.1	15
Control	0	15	0.1	15

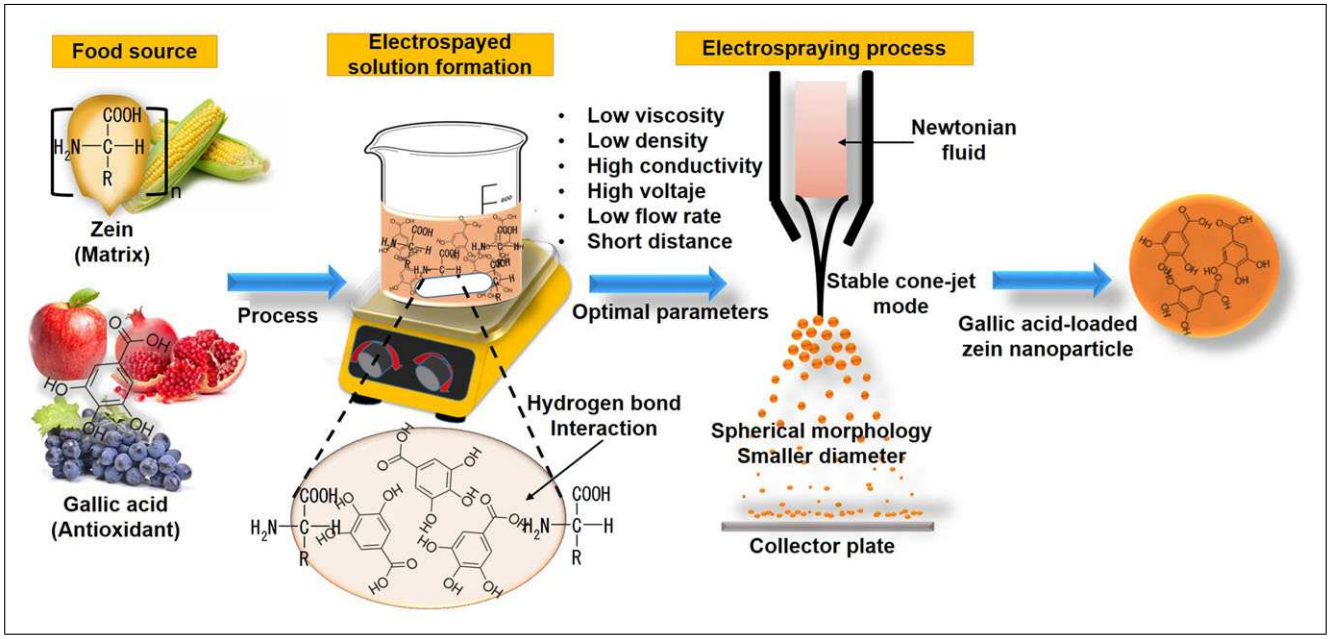

Figure 1–Schematic representation of the obtention of the GA-loaded zein nanoparticles by the electrospraying process.

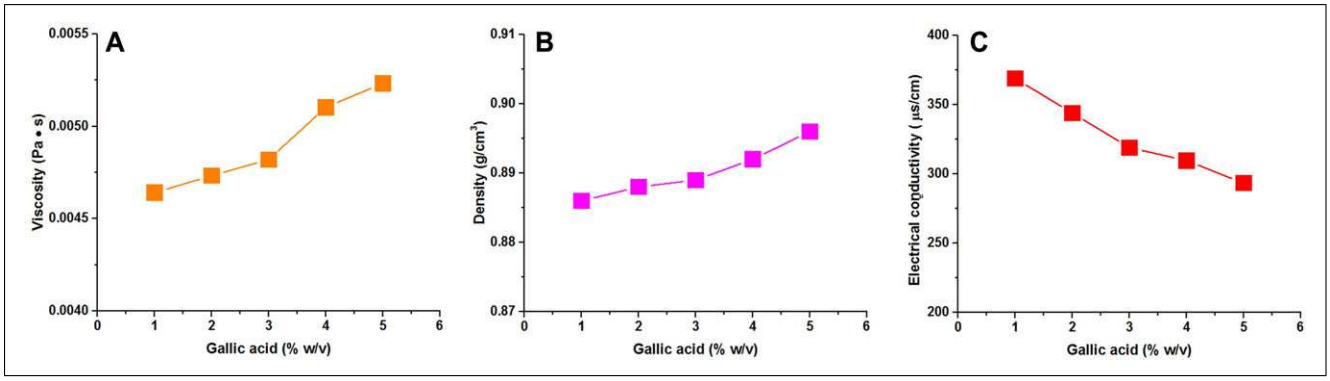

Figure 2–Effect of the physicochemical properties in the GA-zein electrosprayed solution on different concentrations of GA, (A) viscosity, (B) density, and (C) electrical conductivity.

Experimental design and statistical analysis

For the encapsulation of GA in zein nanoparticles by the electrospraying process, a factorial design of 5 × 2 × 2 × 2 was employed. The variables included GA concentration with five levels (1, 2, 3, 4, and 5%), applied voltage with two levels (10 and 15 kV), flow rate with two levels (0.1 and 0.5 mL/hr), and collector distance with two levels (10 and 15 cm). Also, descriptive statistics was employed for the determination of means and standard deviations (SDs) from the triplicates.

Results and Discussion

Effect of the physicochemical parameters of GA-zein electrosprayed solutions in the Taylor cone formation

Effect of viscosity. The physicochemical parameters of the GA-zein electrosprayed solution, such as viscosity, density, and electrical conductivity, are shown in Figure 2 and were dependent on the concentration of GA at 5% w/v of zein and 80% v/v aqueous ethanol. Viscosity exhibited upward behavior as the concentration of GA increased from 1 to 5% w/v; however, the increase was minimal between the concentrations. Viscosity for the solution of 1% w/v was 0.00464 ± 0.00001 Pa·s, while that of the 2% solution w/v) was of 0.00473 ± 0.00001 Pa·s. The difference between the viscosity of 1 and 2% w/v was minimal with 0.00009 Pa·s; on the other hand, the 3% solution (w/v) revealed a viscosity of 0.00482 Pa·s and a difference compared with the 2% solution of 0.00009 Pa·s. However, the solutions that showed the greatest variation were those of 4 and 5% (w/v) of zein with 0.0051 ± 0.00001 and 0.00523 ± 0.00001 Pa·s, where the 4% solution obtained a variation of 0.00028 ± 0.00001 with respect to the viscosity of 3% (w/v) and a variation of 0.00013 Pa·s with respect to the viscosity of 5% w/v. Viscosity is related with the cone-jet mode; for example, an appropriate viscosity forms a stable cone-jet mode with controlled deposition (controlled morphology and particle size) (Luo, Loh, Stride, & Edirisinghe, 2012; Smeets, Clasen, & Van den Mooter, 2017). Figure 3 presents the effect of the viscosity on the formation of a stable or unstable Taylor cone mode. A stable cone-jet mode is considered when the liquid is discharged from the tip of the nozzle in the form of a regular, axisymmetric cone with a thin jet at its apex, stretching along the nozzle's axis (Jaworek & Krupa, 1999).

In the electrospraying process, if it increases the concentration of the components, larger particles are obtained, while on increasing the voltage, the viscosity decreases and smaller particles are obtained (Ghayempour & Mortazavi, 2013; Tapia-Hernández, Rodríguez-Félix, & Katouzian, 2017). Figure 4 depicts the impact of particle size due to the increase in viscosity by the increase in the concentration of GA where, at a lower concentration (1% w/v) of GA, there was lower viscosity with stable cone-jet mode and smaller particle diameter. On the other hand, the morphology did not present variation in all GA concentrations, where spherical particles were obtained. Similar results were reported by Neo et al. (2013), where the authors studied the effect of the addition of GA on the viscosity of fiber-forming GA-zein electrosprayed solutions. The solutions contained between 5 and 20% w/v of GA and, as the concentration increased, the viscosity increased from 204.67 ± 44.9 mPa·s for 5% to 263.08 ± 56.8 mPa·s for 20% w/v.

Effect of density. The density of the GA-zein electrosprayed solution at different concentrations of GA is illustrated in Figure 2. The density demonstrated same behavior as the viscosity wherein, as the concentration of GA increases, the density increases. The concentration of 1% w/v of GA showed a density of 0.886 ± 0.00002 g/cm^3, while the concentration of 2, 3, and 4% w/v exhibited a concentration of 0.888 ± 0.0002, 0.889 ± 0.00004, and 0.892 ± 0.0001 g/cm^3. The difference among the electrosprayed solutions was 0.002 g/cm^3, this is a minimal increase. However, the electrosprayed solution with the highest increase of density was 5% w/v with 0.896 ± 0.0002 g/cm^3 and a difference of 0.004 g/cm^3 with respect to the electrosprayed solution of 4% w/v. The density is proportional to the polymer concentration and viscosity and possesses a crucial impact on the development of the Taylor cone. At a higher density, the Taylor cone tends to form big particles, while at a lower density, Taylor cone shifts to a stable cone-jet mode or cone-multijet mode with smaller particles (Jaworek & Sobczyk, 2008) (Figure 3). In GA-zein electrosprayed solution, at a lower concentration of GA, a lower density (≤0.886 ± 0.00002 g/cm^3), and a stable cone jet are obtained, resulting in smaller particle sizes with spherical and monodisperse morphology, as depicted in Figure 3.

Effect of electrical conductivity. Another important parameter in the formation of nanoparticles from GA-zein electrosprayed solutions is the electrical conductivity and, unlike the viscosity and density, this was inversely proportional to the concentration of GA. Figure 2 presents the results of electrical conductivity for different concentrations of GA. Electrical conductivities were 369 ± 4.3, 344 ± 4, 319 ± 1, 309.7 ± 3, and 293.3 ± 2.1 µs/cm for the GA-zein electrosprayed solution with 1, 2, 3, 4, and 5% w/v of GA, respectively. The differences among all of the concentrations ranged from 25 to 10 µs/cm. Electrical conductivity is defined as the ability a material possesses to allow the electric charge to pass through it, in this case, a polymeric material (Tapia-Hernández et al., 2015). The electrical conductivity of the

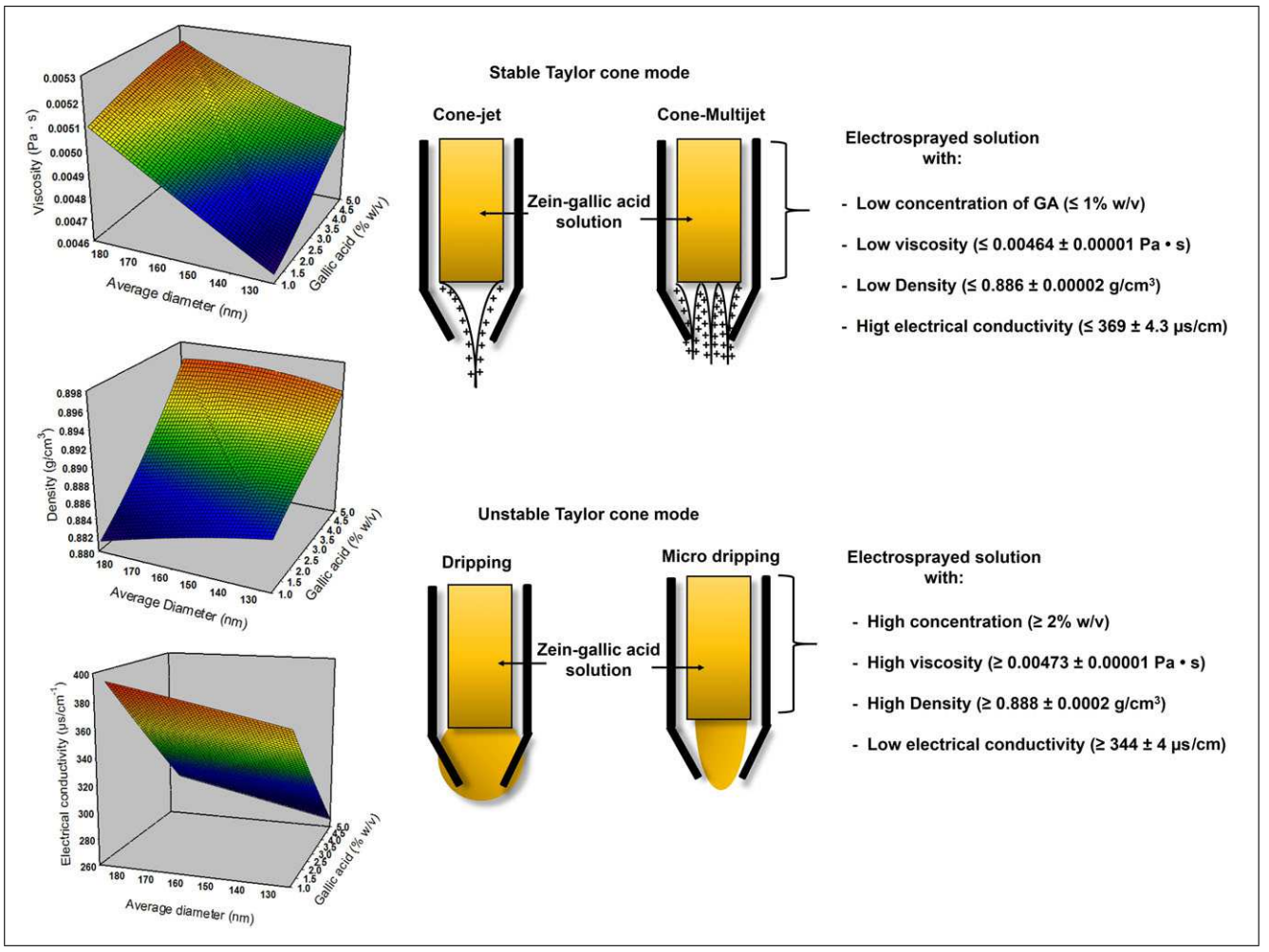

Figure 3–Schematic representation of the influence of the physicochemical parameters of the GA-zein electrosprayed solution in the Taylor cone formation.

electrosprayed solution is the parameter that determines the amount of the charge that a liquid may acquire while passing through the nozzle. Figure 3 shows that a electrosprayed solution is charged quickly, resulting in a stable cone-jet mode with smaller and uniform-size particles, but an insulator electrosprayed solution receives a very small amount of charge or no charge, resulting in unstable cone-jet mode formation, bigger particles with a large variation, and deposition of uneven particles (Faraji, Sadri, Hokmabad, Jadidoleslam, & Esmaeilzadeh, 2017; Khan, Nazir, & Maan, 2017). In this study, the electrosprayed solution with a lower concentration of GA (1% w/v) had high electrical conductivity (369 ± 4.3 µs/cm), which is related to the smaller particle size and to the similar morphology obtained and is demonstrated in Figure 4. The electrical conductivity of the GA-zein electrosprayed solution is influenced by the type and concentration of the components, the solvent, and the availability of ionizable compounds (do Evangelho et al., 2018).

Effect of the GA concentration. GA-loaded zein nanoparticles with different concentrations of GA (1 to 5% w/v) were obtained and are illustrated in Figure 4. Significant differences were revealed in the particle size: as the concentration of GA increased, the particle diameter increased. With concentration of 1% w/v, the smallest particle diameter with 126.5 ± 17.12 nm was obtained, which was very similar to that of the zein control, that is, 123.9 ± 16.5 nm. The concentration of 2% w/v showed a particle diameter of 131.8 ± 32.7 nm with a spherical morphology but with a high polydispersity. The concentration of 3% w/v demonstrated a particle diameter of 132.4 ± 22.9 nm but, unlike, the previous two solutions, it presented morphology with biconcave structures due to the rapid evaporation of the solvent. On the other hand, concentrations of 4 and 5% w/v showed higher average diameters with 168.4 ± 34.7 and 186 ± 30.3 nm, with spherical morphology, but they presented high polydispersity. The polydispersity can be observed as reflected in the Standard Deviations (SDs), where the concentration of 1% w/v was that with the lowest polydispersity among particle sizes, very similar to control nanoparticles.

For an electrosprayed solution, the particle size can be controlled in two ways: either by varying the concentration of the polymer in solution or by changing the liquid flow rate, since the particle diameter increases monotonically with both parameters (Almería & Gómez 2014). This effect of the concentration is due to the fact that a higher polymer concentration has a higher viscosity; therefore, larger particles will be formed (increased GA concentration), while solutions with a lower polymer concentration (decreased GA concentration) have a lower viscosity and particles with smaller diameters are obtained (Bhushani et al., 2017). Also, chain entanglements are related to the GA-zein concentration, where

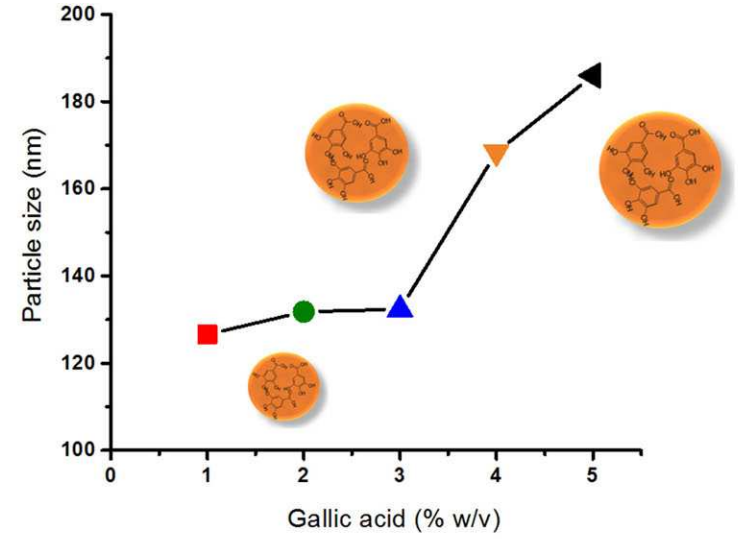

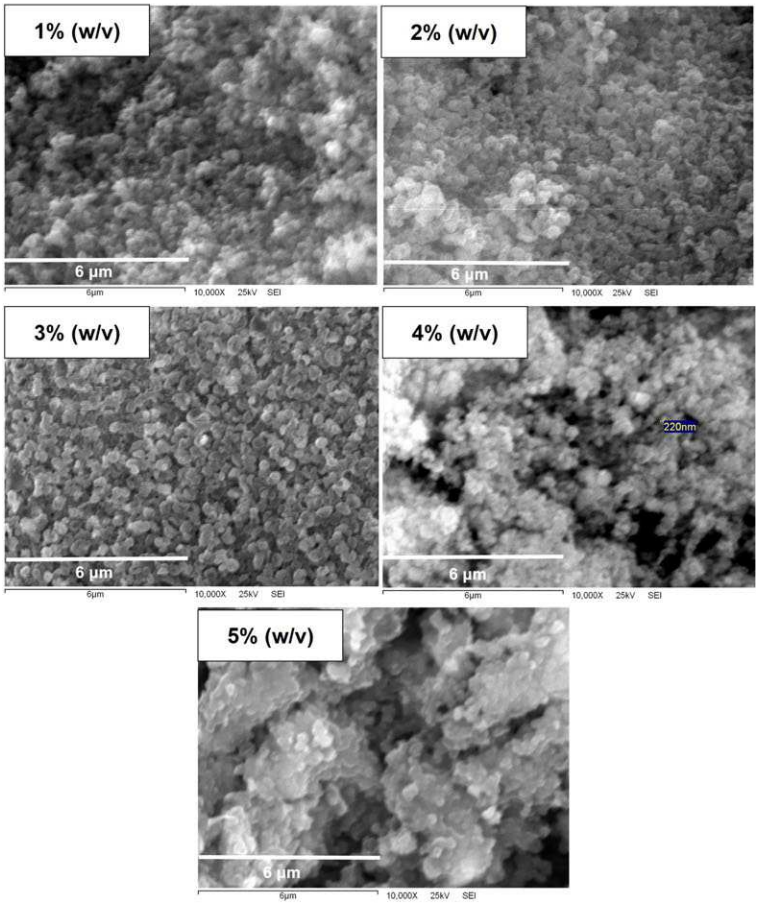

Figure 4–Effect of the GA concentration on the particle size and morphology of GA-loaded zein nanoparticles. Conditions: voltage of 15 kV; flow rate of 0.1 mL/hr, and collector distance of 10 cm.

low concentrations (5% zein and 1% GA), there are fewer entanglement possibilities for the polymer chains, where the operating regime is known as the semidilute unentangled regime. In this state, the concentration is sufficiently large for chains to overlap, but not sufficient to obtain a significant degree of entanglement at higher concentrations; the same available hydrodynamic volume is occupied by more polymer chains, introducing chain entanglements (Bock, Woodruff, Hutmacher, & Dargaville, 2011).

Effect of rheological behavior

Figure 5 shows the rheogram of the GA-zein electrosprayed solution at different GA concentrations (1 to 5% w/v). First, the total change shear stress can be observed from the shear rate ramp of 0.1 to 100 s^{-1} where, as the concentration of GA increases, the shear stress increases at 100 s^{-1} with 0.491 ± 0.012, 0.472 ± 0.005, 0.493 ± 0.005, 0.504 ± 0.005, 0.534 ± 0.009, and 0.541 ± 0.018 Pa for 1, 2, 3, 4, and 5% w/v of GA incorporated

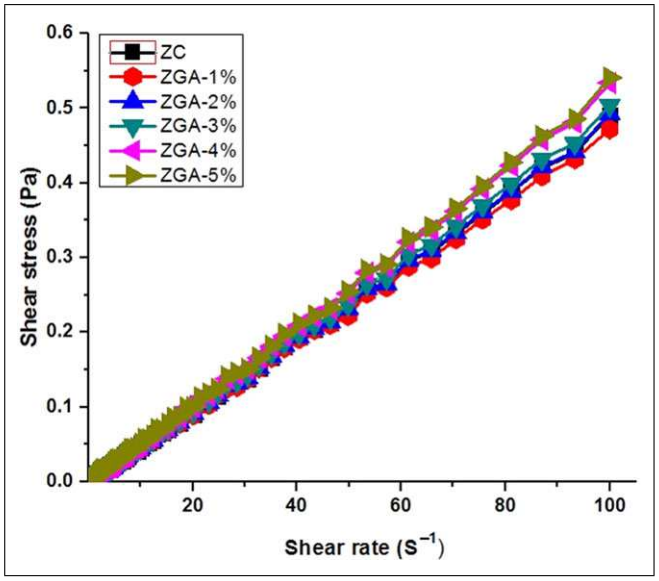

Figure 5–Rheogram of shear rate versus shear stress of GA-zein electrosprayed solution at different concentrations of GA with a continuous ramp of 0.1 to 100 s^{-1}.

Table 2–Power Law parameter of the GA-zein electrosprayed solution at different concentrations of GA.

	Ethanol (% v/v)	Zein (% w/v)	GA (% w/v)	Power law parameter	
Sample				N	R^2
1	80	5	1	1.04 ± 0.003	0.99
2	80	5	2	1.05 ± 0.004	0.99
3	80	5	3	1.06 ± 0.002	0.99
4	80	5	4	1.04 ± 0.003	0.99
5	80	5	5	1.05 ± 0.006	0.99

into 5% of zein in 80% v/v of ethanol. From the data obtained of shear rate versus shear stress, the Power Law model was applied and the results are shown in Table 2. All of the electrosprayed solutions at different concentrations of GA and at 5% w/v of zein showed a Power Law index (n) of around 1 and an $R^2 = 0.99$, with data ranging from 0.1 to 100 s^{-1}. This result is characteristic of Newtonian fluids, that is to say, the viscosity remains constant with respect to the change of shear rate increase. Similar results were reported by Soltani and Madadlou (2015), where for a solution of zein at 0.2% w/v in 80% v/v of ethanol demonstrated a Power Law index of $n = 1$, behaving as Newtonian fluids. Bhushani et al. (2017) reported a zein electrosprayed solution at 5% w/v of zein in aqueous ethanol that behaved as Newtonian fluids.

Figure 6 shows the rheogram of time versus viscosity of zein and the GA-zein electrosprayed solution. Figure 6A illustrates the viscosity behavior of zein solutions with 5% w/v at a shear rate of 25, 50, 100, 150, and 200 s^{-1}, observing that a shear rate of 50 s^{-1} showed the smallest change in viscosity in a ramp of 0 to 300 s, while the other shear rates obtained great amplitude among the viscosities. Figure 6B reported the viscosity for the different GA-zein electrosprayed solutions at a shear rate of 50 s^{-1}, observing that this was dependent on the GA concentration within a range of 0.0046 to 0.0052 Pa s. On analyzing the SD obtained from the viscosities (50 points analyzed) in a ramp of 0 to 300 s, it is concluded that with 1% w/v of GA, it obtained the least change with 0.004641 ± 0.000012 Pa s, while others obtained a major change with 0.0047336 ± 0.000015, 0.0048208 ± 0.000015,

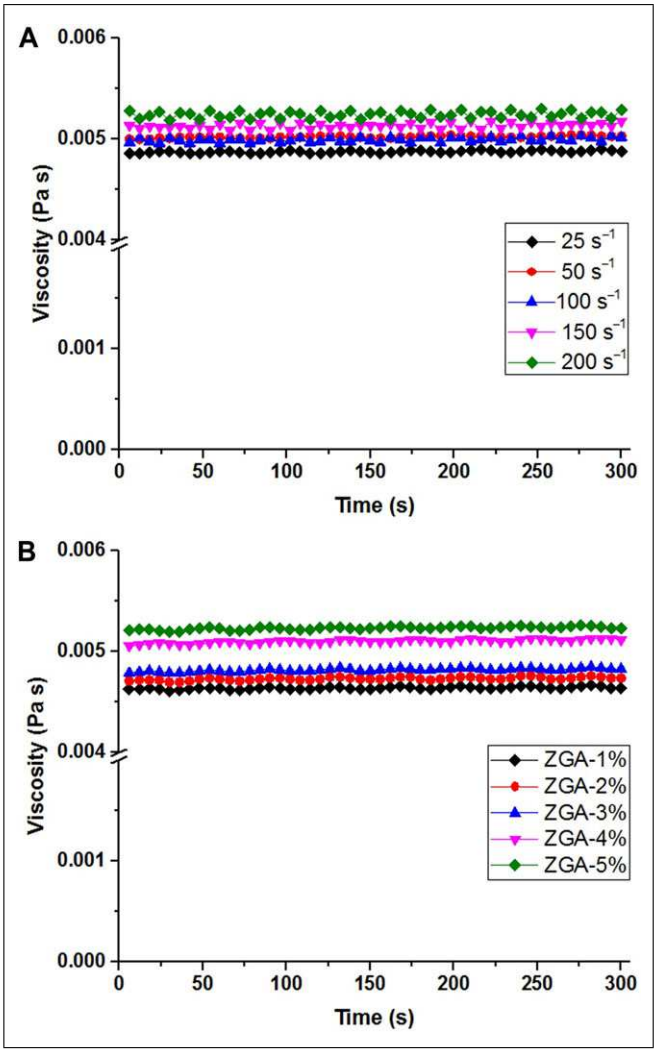

Figure 6–Rheogram of time versus viscosity of GA-zein electrosprayed solution at different concentrations of GA with continuous ramp of 0 to 300 s^{-1}.

0.0051038 ± 0.000018, and 0.0052334 ± 0.000015 Pa s for 2, 3, 4, and 5% w/v, respectively. With these results, it may be concluded that 1% w/v of GA is more stable for the formation of nanoparticles with a similar morphology and monodisperse particles during the electrospray process and as corroborated in Figure 4. When an electrosprayed solution possesses less viscosity and less change in viscosity with respect to time, thus, better stability, it remains constant during the electrospray technique and tends to form more uniform and monodispersed particles (Jain, Sood, Bora, Vasita, & Katti, 2014; Tapia-Hernández et al., 2018).

Effect of equipment parameters on morphology and particle size

Effect of voltage. Figure 7 depicts the effect of the voltage at 10 and 15 kV and its influence on particle diameter and morphology. First, at a voltage of 10 kV, diameters of 150 ± 31.5, 188.3 ± 30.8, 244.2 ± 26.2, 295.5 ± 32.3, and 306.3 ± 35.8 nm and a voltage of 15 kV, there were 134.2 ± 11.5, 171.9 ± 15.5, 195.4 ± 21.2, 226.2 ± 20.5, and 253.2 ± 31.5 nm for concentrations of 1, 2, 3, 4, and 5% w/v of GA in zein nanoparticles, observing that as the voltage is increased, smaller diameters of particles are obtained in each GA. Voltage is a parameter that represents the driving

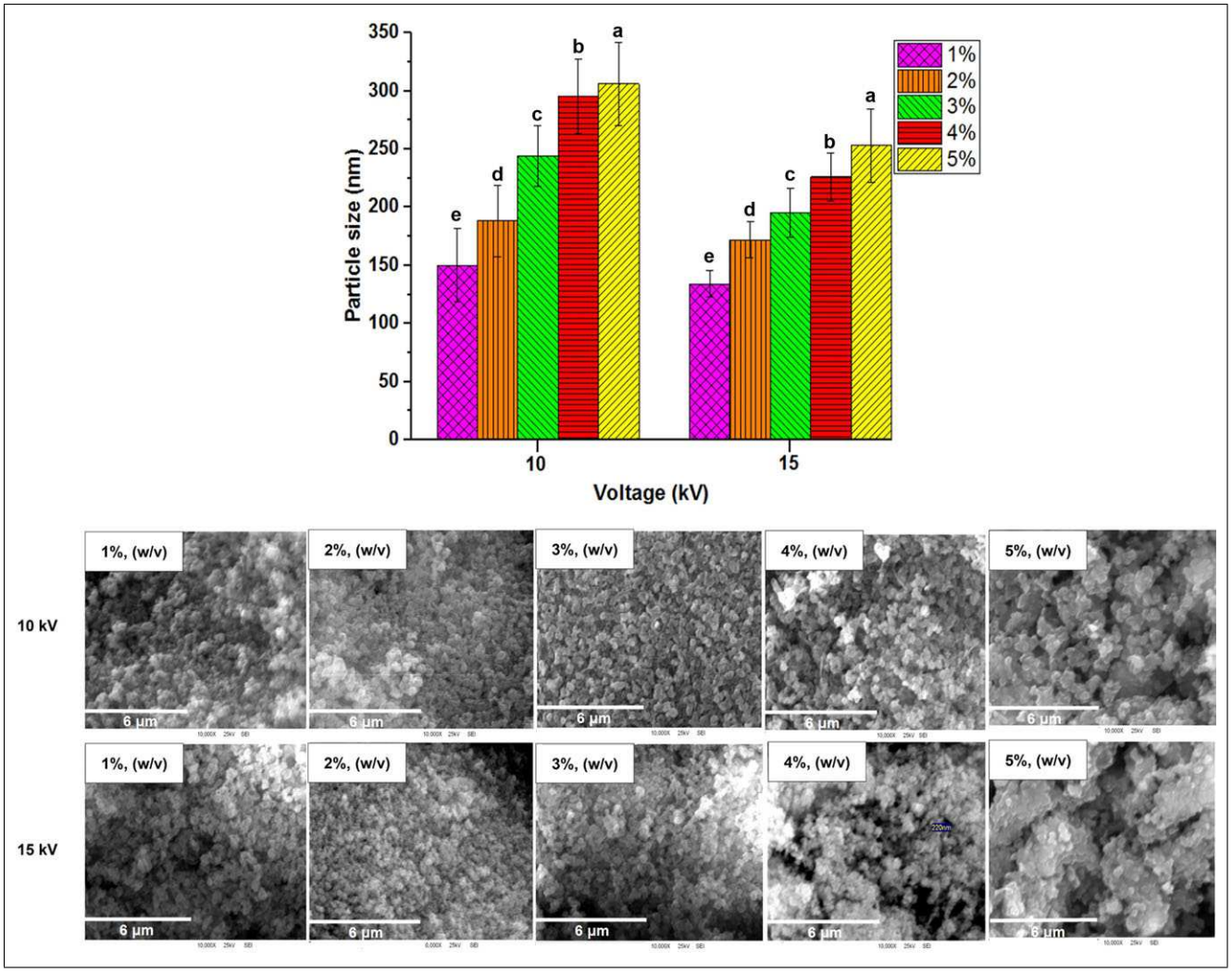

Figure 7–Effect of voltage (10 and 15 kV) on the particle size and morphology of GA-loaded zein nanoparticles at different concentrations of GA (1 to 5% p/v). Conditions: flow rate of 0.1 mL/hr and a collector distance of 10 cm. Error bars correspond to the standard deviation and different letters (a, b, c, d, e) represent significant statistically differences by Tukey test ($P < 0.05$).

force and it is determined by the electrical conductivity of the polymer matrix in solution, that is, a polymer matrix with high electrical conductivity occupies less voltage to break the surface tension of the solution and form particles smaller in diameter (Tapia-Hernández et al., 2015). Figure 8 presents GA-loaded zein nanoparticles obtained at high (15 kV) and low (10 kV) voltage. At high voltage values, it aids in obtaining a smaller particle diameter with spherical morphology and one that is more monodispersed, unlike low voltage, with irregular morphology and polydispersity (Boda et al., 2018). A similar study was carried out by Baspinar, Üstündas, Bayraktar, and Sezgin (2018), who elaborated zein and curcumin-loaded zein nanoparticles and evaluated the effect of voltage on morphology and particle size. The voltages used were 15, 17.5, 20, and 22.5 kV. These authors reported that in zein nanoparticles when the voltage is increased, the morphology was not affected compared with nanoparticles that are obtained at 15 kV. However, with curcumin-loaded zein nanoparticles at a ratio of 1:10, the particle diameter decreased from 339 nm (17.5 kV), to 328 nm (20 kV), and further to 322 nm (22.5 kV) with similar morphology and particle-size distribution. The voltage effect of the current study with GA-loaded zein nanoparticles is similar to that reported for curcumin-loaded zein nanoparticles by Baspinar.

Effect of flow rate. Figure 9 depicts the effect of flow rate on the morphology and particle size of GA-loaded zein nanoparticles at different concentrations of GA. Two flow rates, 0.1 and 0.5 mL/hr, were used. The flow rate was the parameter that most influenced the diameter of the particles and polydispersity, corroborated in the SD. First, at a flow rate of 0.1 mL/hr, average diameters were 134.2 ± 11.5, 171.9 ± 15.5, 195.4 ± 21.2, 226.2 ± 20.5, and 253.2 ± 31.5 nm, while for a flow rate of 0.5 mL/hr, average diameters were 1225.1 ± 53.2, 1292.6 ± 65.6, 1326.4 ± 78.6, 1358.6 ± 81.3, and 1459.2 ± 83.4 nm. The increase in flow rate reflects a considerable particle-size increase and vice versa (Figure 8). When high flow rates are utilized, it can lead to the nonrupture of surface tension and unstable particle fission because the solvent is not completely volatilized, in addition, to that the formation of large drops in the Taylor cone is provided, producing high polydispersity with high voltage additionally is required (Castillo, Martin, Rodriguez-Perez, Higuera, & Garcia-Ybarra, 2018; Smeets et al., 2017). However, when a low flow rate is utilized, stable particle fission is obtained. In addition, the solvent

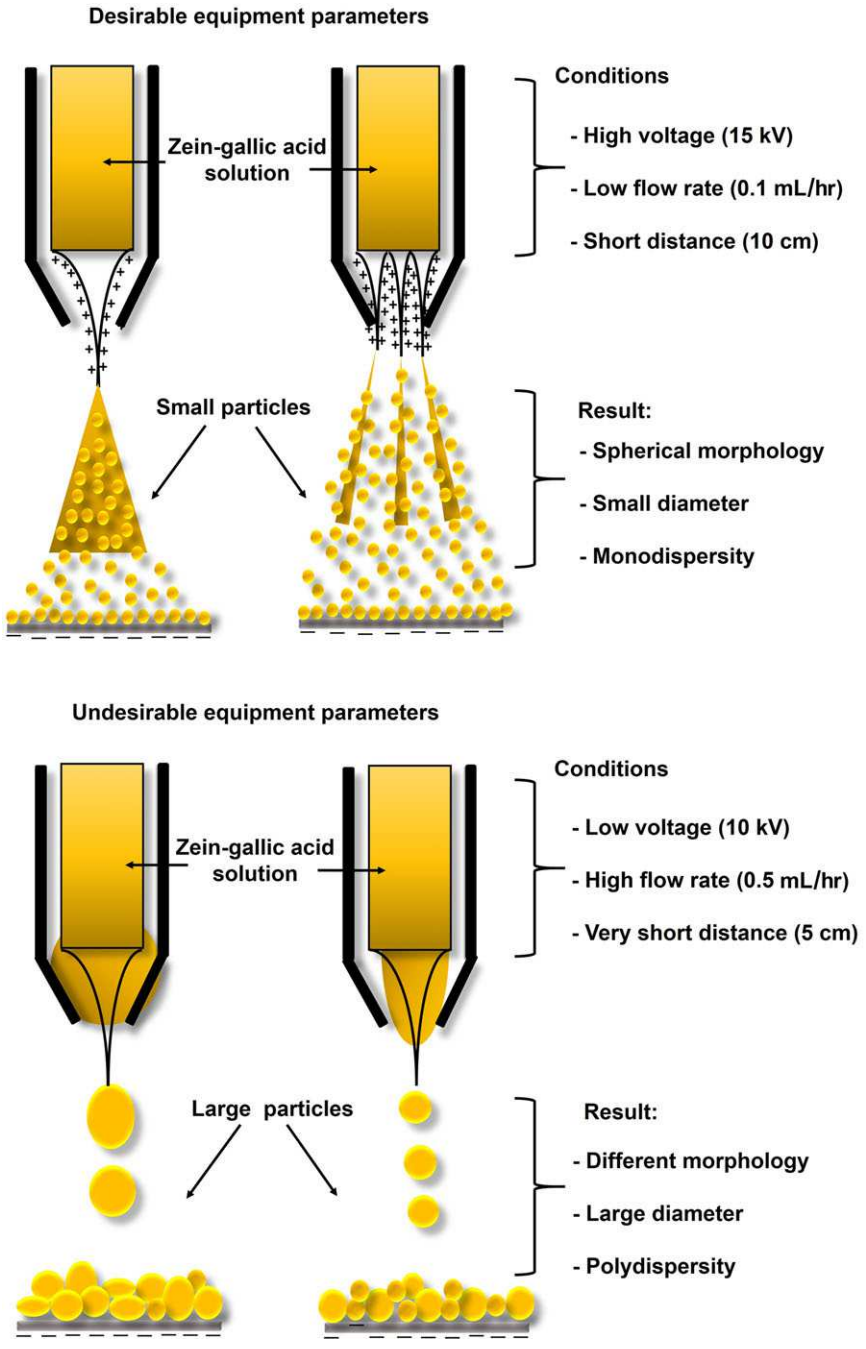

Figure 8–Schematic representation of the influence of equipment parameters of GA-loaded zein nanoparticles on particle size and morphology.

is volatilized and the Taylor cone with jet mode is obtained, producing low polydispersity, spherical morphology, and smaller particle size (Gañán-Calvo, López-Herrera, Herrada, Ramos, & Montanero, 2018; Smeets et al., 2017).

Other researchers reported the influence of flow rate on morphology and the size of nanoparticles from biopolymers by the electrospraying process and reveal two behaviors: (1) high flow rate and (2) low flow rate. High flow rate is considered in an electrosprayed solution at 0.5 mL/hr or higher, with broad and biconcave morphology particles with high particle size, and rapid solvent evaporation. However, low flow rate is considered at less than 0.5 mL/hr, where uniform particles, round in morphology and apparently compact, with a very smooth surface with smaller particle size and low solvent evaporation, are found (Gómez-Estaca et al., 2015; Mai et al., 2017, Tapia-Hernández et al., 2018).

Effect of collector distance. Figure 10 illustrates the effect of collector distance on particle size at two different distances: 10 and 15 cm. At a distance of 10 cm, average diameters were 150 ± 31.5, 188.3 ± 30.8, 244.2 ± 26.2, 295.5 ± 32.3, and 306.3 ± 35.8 nm, and at a distance of 15 cm, these were 174.2 ± 23.5, 203.8 ± 18.2, 265.1 ± 27.3, 312.7 ± 33.2, and 332.9 ± 30.1 nm for concentrations of 1, 2, 3, 4, and 5% w/v, respectively. Studies report that needle distance of the collector and solvent evaporation exert a significant impact on particle size and distribution with three behaviors as follows: the first behavior, were at short distance (<10 cm) and high solvent evaporation, a

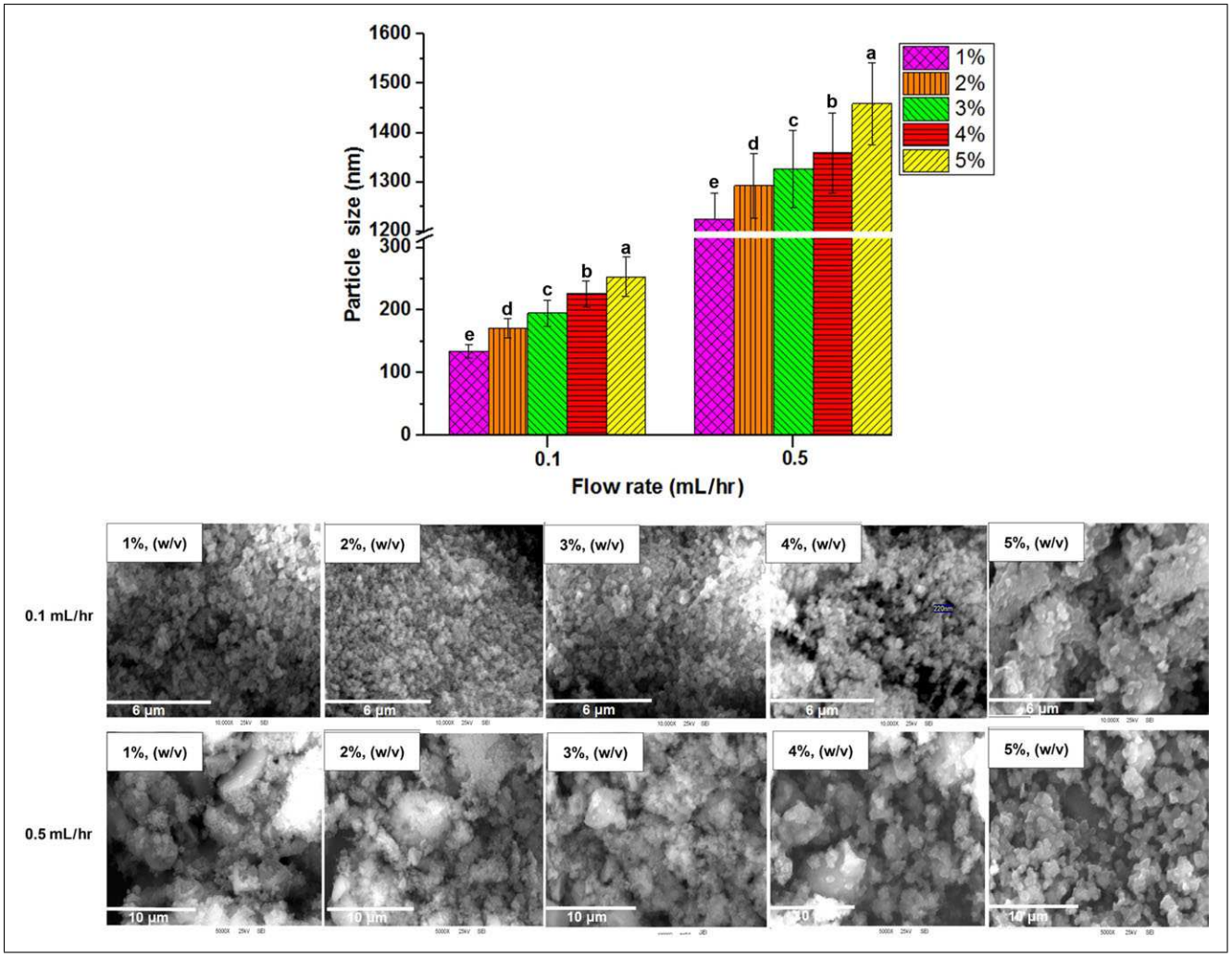

Figure 9–Effect of the flow rate (0.1 and 0.5 mL/hr) on the particle size and morphology of GA-loaded zein nanoparticles at different concentrations of GA (1 to 5% p/v). Conditions: voltage of 15 kV and collector distance of 10 cm. Error bars correspond to the standard deviation and different letters (a, b, c, d, e) represent significant statistically differences by Tukey test ($P < 0.05$).

smaller diameter is obtained; the second, if the collector distance is very short (5 cm), it will not be possible to evaporate all of the solvent; thus, the particle will be unstable and the size will be larger (Costamagna et al., 2017; Ghayempour, & Mortazavi, 2013), and, in the third behavior, if the collector distance is long (>10 cm) with low solvent evaporation, it can volatilize the solvent and the polymer particle encourages fission (Chen et al., 2017; Tapia-Hernández et al., 2017). Similar studies that have reported distances of 10 cm for zein nanoparticles were those of do Evangelho et al. (2018) and Gómez-Mascaraque et al. (2018).

Interaction of GA-loaded zein nanoparticles by FT–IR

Figure 11 and Table 3 reveal the infrared spectra and main functional groups of the raw material, the zein nanoparticle, and the GA-loaded zein nanoparticle. First, the main bands of GA are presented in Figure 11A, where bands at 3500 and 3280 cm^{-1} correspond to the vibrational stretching bond of OH, the hydroxyl groups present in positions 3, 4, and 5 of the aromatic ring. In addition, three bands are presented at 1613, 1537, and 1428 cm^{-1}, due to the stretching and bending bonds of -C=C and C-H of the aromatic ring. Four bands are also presented at 1318, 1263, 1222, and 1037 cm^{-1}, corresponding to the flexion bond of the -C-H of aromatic ring and the -O-H of the phenol alcohol. Finally, three bands are presented at 1023, 899, and 866 cm^{-1} of the stretching and flexion bonds of carboxyl -C-O. Figure 11B presents the infrared spectrum for zein powder, where the characteristic bands corresponding to a protein are observed, amide band I corresponds to the vibratory stretching of -C=O at 1668 cm^{-1}, amide band II corresponds to the vibration of flexion of the -NH bond and the vibration of the CN at 1537 cm^{-1}, amide band III corresponds to a complex mixture of displacement at 1455 cm^{-1} and the band of -OH and -NH corresponds to the vibrational stretch bond at 3.328 cm^{-1}. Also, bands are presented at 2964 and 2875 cm^{-1}, corresponding to the vibrational stretching of the C-H of the aliphatic groups.

Figure 11C demonstrates the infrared spectrum for zein nanoparticles with the four characteristic bands that were exhibited in zein powder, but with rightward shifts: amide band I at 1661 cm^{-1}, amide band II at 1537 cm^{-1}, amide band III at 1455 cm^{-1}, and the -OH band and N-H at 3321 cm^{-1}. These differences are due to the conformational rearrangement of zein when it passes from raw material into a nanoparticle, due to the solvent and the electrospraying process, increasing mainly hydrogen-bonding interactions. Figure 11D presents the infrared spectrum of the GA-loaded zein nanoparticle, with an amide band I at 1654 cm^{-1}, an amide II band at 1537 cm^{-1}, an amide band

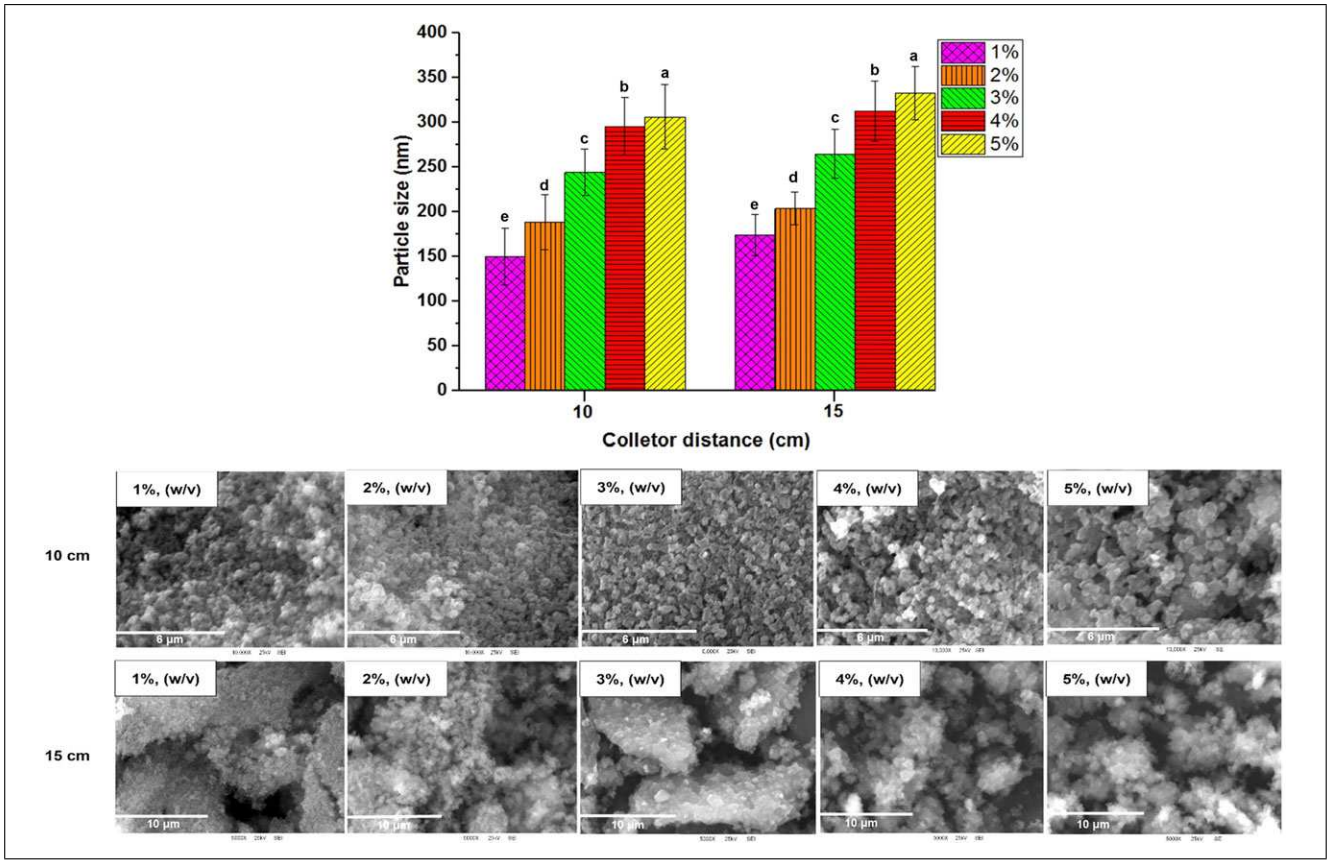

Figure 10–Effect of the collector distance (10 and 15 cm) on the particle size and morphology of GA-loaded zein nanoparticles at different concentrations of GA (1 to 5% p/v). Conditions: voltage of 10 kV and flow rate of 0.1 mL/hr. Error bars correspond to the standard deviation and different letters (a, b, c, d, e) represent significant statistically differences by Tukey test ($P < 0.05$).

Table 3–Principal functional groups of the materials under study.

		Wavenumber (cm^{-1})			
Functional groups	**Type of vibration**	**GA**	**Zein powder**	**Zein nanoparticle**	**GA-L-Zein-np***
O-H	Stretching	3500			
O-H/N-H	Stretching		3328	3321	3314
O-H	Stretching	3280			
C-H	Stretching		2964	2964	2964
C-H	Stretching		2875	2875	2875
Amide I C=O	Stretching		1668	1661	1654
C-C/C-H	Stretching and flexion	1613			
Amide II N-H/C-N	Flexion		1537	1537	1537
C-C/C-H	Stretching and flexion	1537			
Amide III			1455	1455	1448
C-C/C-H	Stretching and flexion	1428			
C-C/C-H	Stretching and flexion	1386			
C-H/O-H	Flexion	1318			
C-H/O-H	Flexion	1263			
C-H/O-H	Flexion	1222			1222
C-O	Stretching and flexion	1037			1037
C-O	Stretching and flexion	899			
C-O	Stretching and flexion	866			

*GA-L-Zein-np = gallic acid-loaded zein nanoparticle.

III at 1448 cm^{-1}, and the band of -OH and -NH at 1314 cm^{-1}. In addition, two new bands presented at 1222 and 1037 cm^{-1}, corresponding to -CH and -OH of the aromatic ring of GA. Similarly, bands at 2964 and 2875 cm^{-1} presented for zein particle and GA-loaded zein nanoparticles. Displacements of zein bands are due to the formation of hydrogen-bond interactions with GA.

Another study that reports the interaction of GA with zein by FT–IR was that of Neo et al. (2013), these authors elaborated GA-loaded zein fibers. First, the authors reported that the amide band I present in zein nanofibers at 1644 cm^{-1} was traversed at 1646 and 1649 cm^{-1}, when the fibers from the GA-loaded zein interaction were formed at 10 and 20% w/v of GA. In addition,

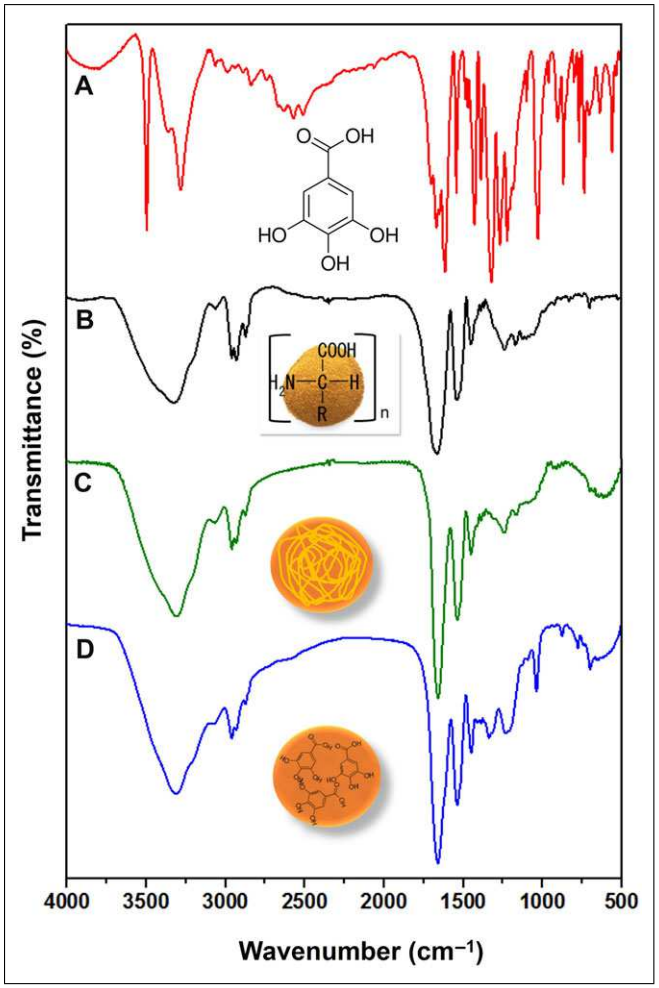

Figure 11–Infrared spectra of (A) GA powder, (B) zein powder, (C) zein nanoparticle, and (D) GA-loaded zein nanoparticle.

the majority of GA bands are not shown, due to the intensity of the zein bands. The band of GA disappears at 3491 cm^{-1}, corresponding to the vibrational stretching of the O-H of the hydroxyl groups. The authors reported that the synthesis of GA-loaded zein fiber exhibited structural changes in both components. Therefore, interactions between both components at the molecular level have shown promising results, favoring the stability of the fibers.

Conclusions

Electrospraying is a feasible technique for the elaboration of GA-loaded zein nanoparticles. In addition, the physicochemical and rheological parameters comprise are important and complementary ones during the electrospinning process for predicting Taylor cone and fluid type. Low viscosity, density, and high electrical conductivity were necessary to obtain stable cone-jet mode, and Newtonian behavior is required to predict the stability of the electrosprayed solution and to obtain the desired morphology. Equipment parameters, such as high voltage, low flow rate, and short collector distance, are necessary to obtain particles with spherical morphology and a smaller size in GA-loaded zein nanoparticles. FT–IR revealed conformational changes from zein powder into nanoparticle and GA-loaded zein nanoparticle; also, the main interactions formed were hydrogen bonds. Therefore, the electrospraying process can be used for obtaining biopolymeric nanoparticles, such as matrices, and provides potential protection to antioxidant compounds from environmental factors.

Acknowledgments

José Agustín Tapia-Hernández, M.Sc., thanks CONACYT for the scholarship granted.

Ethical Statement

This study does not involve any human testing.

Author Contributions

José Agustín Tapia-Hernández designed the study, carried out overall experiment and wrote of the manuscript. Carmen Lizette Del-Toro-Sánchez, Francisco Javier Cinco-Moroyoqui, Saúl Ruiz-Cruz, Josué Juárez interpreted some results and edited the manuscript. Daniela Denisse Castro-Enríquez, Carlos Gregorio Barreras-Urbina and Guadalupe Amanda López-Ahumada advised on some techniques, helped in the statistical analysis and reviewed the writing Francisco Rodriguez-Félix had overall responsibility for the project, contributed to the interpretation and discussion of the results and manuscript preparation. All authors read and approved the final manuscript.

Conflicts of Interest

The authors declare that they do not have any conflicts of interest.

References

Abdel-Moneim, A., El-Twab, S. M. A., Yousef, A. I., Reheim, E. S. A., & Ashour, M. B. (2018). Modulation of hyperglycemia and dyslipidemia in experimental type 2 diabetes by gallic acid and p-coumaric acid: The role of adipocytokines and PPARγ. *Biomedicine and Pharmacotherapy*, *105*, 1091–1097.

Abdel-Moneim, A., Yousef, A. I., El-Twab, S. M. A., Reheim, E. S. A., & Ashour, M. B. (2017). Gallic acid and p-coumaric acid attenuate type 2 diabetes-induced neurodegeneration in rats. *Metabolic Brain Disease*, *32*(4), 1279–1286.

Acevedo, F., Hermosilla, J., Sanhueza, C., Mora-Lagos, B., Fuentes, I., Rubilar, M., . . . Alvarez-Lorenzo, C. (2018). Gallic acid loaded PEO-core/zein-shell nanofibers for chemopreventive action on gallbladder cancer cells. *European Journal of Pharmaceutical Sciences*, *119*, 49–61.

Almería, B., & Gomez, A. (2014). Electrospray synthesis of monodisperse polymer particles in a broad (60 nm–2 μm) diameter range: Guiding principles and formulation recipes. *Journal of Colloid and Interface Science*, *417*, 121–130.

Asfaram, A., Ghaedi, M., & Dashtian, K. (2017). Rapid ultrasound-assisted magnetic microextraction of gallic acid from urine, plasma and water samples by HKUST-1-MOF-Fe3O4-GA-MIP-NPs: UV–vis detection and optimization study. *Ultrasonics Sonochemistry*, *34*, 561–570.

Assadpour, E., & Jafari, S. M. (2018). A systematic review on nanoencapsulation of food bioactive ingredients and nutraceuticals by various nanocarriers. *Critical Reviews in Food Science and Nutrition*, *8*, 1–47.

Badhani, B., Sharma, N., & Kakkar, R. (2015). Gallic acid: A versatile antioxidant with promising therapeutic and industrial applications. *RSC Advances*, *5*(35), 27540–27557.

Baspinar, Y., Üstündas, M., Bayraktar, O., & Sezgin, C. (2018). Curcumin and piperine loaded zein-chitosan nanoparticles: Development and in-vitro characterisation. *Saudi Pharmaceutical Journal*, *26*(3), 323–334.

Bhushani, J. A., Kurrey, N. K., & Anandharamakrishnan, C. (2017). Nanoencapsulation of green tea catechins by electrospraying technique and its effect on controlled release and in-vitro permeability. *Journal of Food Engineering*, *199*, 82–92.

Bock, N., Woodruff, M. A., Hutmacher, D. W., & Dargaville, T. R. (2011). Electrospraying, a reproducible method for production of polymeric microspheres for biomedical applications. *Polymers*, *3*(1), 131–149.

Boda, S. K., Li, X., & Xie, J. (2018). Electrospraying an enabling technology for pharmaceutical and biomedical applications: A review. *Journal of Aerosol Science*, *125*, 164–181.

Castillo, J. L., Martin, S., Rodriguez-Perez, D., Higuera, F. J., & Garcia-Ybarra, P. L. (2018). Nanostructured porous coatings via electrospray atomization and deposition of nanoparticle suspensions. *Journal of Aerosol Science*, *125*, 148–163.

Chen, J., Zheng, J., McClements, D. J., & Xiao, H. (2014). Tangeretin-loaded protein nanoparticles fabricated from zein/β-lactoglobulin: Preparation, characterization, and functional performance. *Food Chemistry*, *158*, 466–472.

Chen, Q., Liu, Y., Wang, T., Wu, J., Zhai, X., Li, Y., . . . Zhao, X. (2017). Chitosan–PVA monodisperse millimeter-sized spheres prepared by electrospraying reduce the thromboembolic risk in hemorrhage control. *Journal of Materials Chemistry B*, *5*(20), 3686–3696.

Cheng, C. J., & Jones, O. G. (2017). Stabilizing zein nanoparticle dispersions with ι-carrageenan. *Food Hydrocolloids*, *69*, 28–35.

Chen, S., Sun, C., Wang, Y., Han, Y., Dai, L., Abliz, A., & Gao, Y. (2018). Quercetagetin-loaded composite nanoparticles based on zein and hyaluronic acid: Formation, characterization and physicochemical stability. *Journal of Agricultural and Food Chemistry*, *66*(28), 7441–7450.

Chen, S., Xu, C., Mao, L., Liu, F., Sun, C., Dai, L., & Gao, Y. (2018). Fabrication and characterization of binary composite nanoparticles between zein and shellac by anti-solvent co-precipitation. *Food and Bioproducts Processing*, *107*, 88–96.

Chuacharoen, T., & Sabliov, C. M. (2016). Stability and controlled release of lutein loaded in zein nanoparticles with and without lecithin and pluronic F127 surfactants. *Colloids and Surfaces A: Physicochemical and Engineering Aspects*, *503*, 11–18.

Costamagna, M. S., Gómez-Mascaraque, L. G., Zampini, I. C., Alberto, M. R., Pérez, J., López-Rubio, A., & Isla, M. I. (2017). Microencapsulated chañar phenolics: A potential ingredient for functional foods development. *Journal of Functional Foods*, *37*, 523–530.

de Francisco, E. V., & García-Estepa, R. M. (2018). Nanotechnology in the agrofood industry. *Journal of Food Engineering*, *238*, 1–11.

do Evangelho, J. A., Crizel, R. L., Chaves, F. C., Prietto, L., Pinto, V. Z., de Miranda, M. Z., . . . da Rosa Zavareze, E. (2018). Thermal and irradiation resistance of folic acid encapsulated in zein ultrafine fibers or nanocapsules produced by electrospinning and electrospraying. *Food Research International*. https://doi.org/10.1016/j.foodres.2018.08.019

Eltayeb, M., Stride, E., & Edirisinghe, M. (2015). Preparation, characterization and release kinetics of ethylcellulose nanoparticles encapsulating ethylvanillin as a model functional component. *Journal of Functional Foods*, *14*, 726–735.

Faraji, S., Sadri, B., Hokmabad, B. V., Jadidoleslam, N., & Esmaeilzadeh, E. (2017). Experimental study on the role of electrical conductivity in pulsating modes of electrospraying. *Experimental Thermal and Fluid Science*, *81*, 327–335.

Farhoosh, R., & Nyström, L. (2018). Antioxidant potency of gallic acid, methyl gallate and their combinations in sunflower oil triacylglycerols at high temperature. *Food Chemistry*, *244*, 29–35.

Gañán-Calvo, A. M., López-Herrera, J. M., Herrada, M. A., Ramos, A., & Montanero, J. M. (2018). Review on the physics electrospray: From electrokinetics to the operating conditions of single and coaxial Taylor cone-jets, and AC electrospray. *Journal of Aerosol Science*, *125*, 32–56.

Gaona-Sánchez, V. A., Calderon-Dominguez, G., Morales-Sanchez, E., Chanona-Perez, J. J., Velazquez-De La Cruz, G., Mendez-Mendez, J. V., . . . Farrera-Rebollo, R. R. (2015). Preparation and characterisation of zein films obtained by electrospraying. *Food Hydrocolloids*, *49*, 1–10.

Ghayempour, S., & Mortazavi, S. M. (2013). Fabrication of micro–nanocapsules by a new electrospraying method using coaxial jets and examination of effective parameters on their production. *Journal of Electrostatics*, *71*(4), 717–727.

Gómez-Estaca, J., Gavara, R., & Hernández-Muñoz, P. (2015). Encapsulation of curcumin in electrosprayed gelatin microspheres enhances its bioaccessibility and widens its uses in food applications. *Innovative Food Science & Emerging Technologies*, *29*, 302–307.

Gómez-Mascaraque, L. G., Tordera, F., Fabra, M. J., Martínez-Sanz, M., & Lopez-Rubio, A. (2018). Coaxial electrospraying of biopolymers as a strategy to improve protection of bioactive food ingredients. *Innovative Food Science & Emerging Technologies*. https://doi.org/10.1016/j.ifset.2018.03.023

Hai, T., Wan, X., Yu, D. G., Wang, K., Yang, Y., & Liu, Z. P. (2019). Electrospun lipid-coated medicated nanocomposites for an improved drug sustained-release profile. *Materials and Design*, *162*, 70–79.

Hanada, M., Jermain, S. V., Lu, X., Su, Y., & Williams III, R. O. (2018). Predicting physical stability of ternary amorphous solid dispersions using specific mechanical energy in a hot melt extrusion process. *International Journal of Pharmaceutics*, *548*(1), 571–585.

Hu, S., Wang, T., Fernandez, M. L., & Luo, Y. (2016). Development of tannic acid cross-linked hollow zein nanoparticles as potential oral delivery vehicles for curcumin. *Food Hydrocolloids*, *61*, 821–831.

Huang, D. W., Chang, W. C., Yang, H. J., Wu, J. S. B., & Shen, S. C. (2018). Gallic acid alleviates hypertriglyceridemia and fat accumulation via modulating glycolysis and lipolysis pathways in perirenal adipose tissues of rats fed a high-fructose diet. *International Journal of Molecular Sciences*, *19*(1), 254.

Huang, X., Dai, Y., Cai, J., Zhong, N., Xiao, H., McClements, D. J., & Hu, K. (2017). Resveratrol encapsulation in core-shell biopolymer nanoparticles: Impact on antioxidant and anticancer activities. *Food Hydrocolloids*, *64*, 157–165.

Jaworek, A., & Krupa, A. (1999). Classification of the modes of EHD spraying. *Journal of Aerosol Science*, *30*(7), 873–893.

Jaworek, A. T. S. A., & Sobczyk, A. T. (2008). Electrospraying route to nanotechnology: An overview. *Journal of Electrostatics*, *66*(3–4), 197–219.

Jain, A. K., Sood, V., Bora, M., Vasita, R., & Katti, D. S. (2014). Electrosprayed inulin microparticles for microbiota triggered targeting of colon. *Carbohydrate Polymers*, *112*, 225–234.

Jin, L., Piao, Z. H., Sun, S., Liu, B., Ryu, Y., Choi, S.Y., . . . Jeong, M. H. (2017). Gallic acid attenuates pulmonary fibrosis in a mouse model of transverse aortic contraction-induced heart failure. *Vascular Pharmacology*, *99*, 74–82.

Jin, L., Sun, S., Ryu, Y., Piao, Z. H., Liu, B., Choi, S. Y., . . . Jeong, M. H. (2018). Gallic acid improves cardiac dysfunction and fibrosis in pressure overload-induced heart failure. *Scientific Reports*, *8*(1), 9302.

Karimi, M., Sadeghi, R., & Kokini, J. (2017). Pomegranate as a promising opportunity in medicine and nanotechnology. *Trends in Food Science & Technology*, *69*, 59–73.

Kargozar, S., & Mozafari, M. (2018). Nanotechnology and nanomedicine: Start small, think big. *Materials Today: Proceedings*, *5*(7), 15492–15500.

Kaul, S., Gulati, N., Verma, D., Mukherjee, S., & Nagaich, U. (2018). Role of nanotechnology in cosmeceuticals: A review of recent advances. *Journal of Pharmaceutics*. https://doi.org/10.1155/2018/3420204

Khan, M. K. I., Nazir, A., & Maan, A. A. (2017). Electrospraying: A novel technique for efficient coating of foods. *Food Engineering Reviews*, *9*(2), 112–119.

Krishna, V. D., Wu, K., Su, D., Cheeran, M. C., Wang, J. P., & Perez, A. (2018). Nanotechnology: Review of concepts and potential application of sensing platforms in food safety. *Food Microbiology*, *75*, 47–54.

Li, J. J., Yang, Y. Y., Yu, D. G., Du, Q., & Yang, X. L. (2018). Fast dissolving drug delivery membrane based on the ultra-thin shell of electrospun core-shell nanofibers. *European Journal of Pharmaceutical Sciences*, *122*, 195–204.

Liang, Q., Ren, X., Zhang, X., Hou, T., Chalamaiah, M., Ma, H., & Xu, B. (2018). Effect of ultrasound on the preparation of resveratrol-loaded zein particles. *Journal of Food Engineering*, *221*, 88–94.

Liao, C. C., Chen, S. C., Huang, H. P., & Wang, C. J. (2018). Gallic acid inhibits bladder cancer cell proliferation and migration via regulating fatty acid synthase (FAS). *Journal of Food and Drug Analysis*, *26*(2), 620–627.

Liu, K., Li, H., Williams, G. R., Wu, J., & Zhu, L. M. (2018). pH-responsive liposomes self-assembled from electrosprayed microparticles, and their drug release properties. *Colloids and Surfaces A: Physicochemical and Engineering Aspects*, *537*, 20–27.

Liu, Z. P., Zhang, Y. Y., Yu, D. G., Wu, D., & Li, H. L. (2018). Fabrication of sustained-release zein nanoparticles via modified coaxial electrospraying. *Chemical Engineering Journal*, *334*, 807–816.

Liu, X., Yang, Y., Yu, D. G., Zhu, M. J., Zhao, M., & Williams, G. R. (2019). Tunable zero-order drug delivery systems created by modified triaxial electrospinning. *Chemical Engineering Journal*, *356*, 886–894.

Lintingre, E., Lequeux, F., Talini, L., & Tsapis, N. (2016). Control of particle morphology in the spray drying of colloidal suspensions. *Soft Matter*, *12*(36), 7435–7444.

Lucio, D., Martínez-Ohárriz, M. C., Jaras, G., Aranaz, P., González-Navarro, C. J., Radulescu, A., & Irache, J. M. (2017). Optimization and evaluation of zein nanoparticles to improve the oral delivery of glibenclamide. In vivo study using *C. elegans*. *European Journal of Pharmaceutics and Biopharmaceutics*, *121*, 104–112.

Luo, C. J., Loh, S., Stride, E., & Edirisinghe, M. (2012). Electrospraying and electrospinning of chocolate suspensions. *Food and Bioprocess Technology*, *5*(6), 2285–2300.

Luo, Y., Teng, Z., & Wang, Q. (2012). Development of zein nanoparticles coated with carboxymethyl chitosan for encapsulation and controlled release of vitamin D3. *Journal of Agricultural and Food Chemistry*, *60*(3), 836–843.

Luo, Y., & Wang, Q. (2014). Zein-based micro- and nano-particles for drug and nutrient delivery: A review. *Journal of Applied Polymer Science*, *131*(16).

Mai, Z., Chen, J., He, T., Hu, Y., Dong, X., Zhang, H., . . . Zhou, W. (2017). Electrospray biodegradable microcapsules loaded with curcumin for drug delivery systems with high bioactivity. *RSC Advances*, 7(3), 1724–1734.

Martín-Alfonso, J. E., Cuadri, A. A., Berta, M., & Stading, M. (2018). Relation between concentration and shear-extensional rheology properties of xanthan and guar gum solutions. *Carbohydrate Polymers*, *181*, 63–70.

Mauter, M. S., Zucker, I., Perreault, F., Werber, J. R., Kim, J. H., & Elimelech, M. (2018). The role of nanotechnology in tackling global water challenges. *Nature Sustainability*, *1*(4), 166–175.

Montalbán, M. G., Carissimi, G., Lozano-Pérez, A. A., Cenis, J. L., Coburn, J. M., Kaplan, D. L., & Víllora, G. (2018). Biopolymeric nanoparticle synthesis in ionic liquids. In *Recent Advances in Ionic Liquids*. London, UK: IntechOpen.

Neo, Y. P., Ray, S., Jin, J., Gizdavic-Nikolaidis, M., Nieuwoudt, M. K., Liu, D., & Quek, S. Y. (2013). Encapsulation of food grade antioxidant in natural biopolymer by electrospinning technique: A physicochemical study based on zein–gallic acid system. *Food Chemistry*, *136*(2), 1013–1021.

Park, C. E., Park, D. J., & Kim, B. K. (2015). Effects of a chitosan coating on properties of retinol-encapsulated zein nanoparticles. *Food Science and Biotechnology*, *24*(5), 1725–1733.

Paximada, P., Echegoyen, Y., Koutinas, A. A., Mandala, I. G., & Lagaron, J. M. (2017). Encapsulation of hydrophilic and lipophilized catechin into nanoparticles through emulsion electrospraying. *Food Hydrocolloids*, *64*, 123–132.

Penalva, R., González-Navarro, C. J., Gamazo, C., Esparza, I., & Irache, J. M. (2017). Zein nanoparticles for oral delivery of quercetin: Pharmacokinetic studies and preventive anti-inflammatory effects in a mouse model of endotoxemia. *Nanomedicine: Nanotechnology, Biology and Medicine*, *13*(1), 103–110.

Prakash, B., Kujur, A., Yadav, A., Kumar, A., Singh, P. P., & Dubey, N. K. (2018). Nanoencapsulation: An efficient technology to boost the antimicrobial potential of plant essential oils in food system. *Food Control*, *89*, 1–11.

Prietto, L., Pinto, V. Z., El Halal, S. L. M., de Morais, M. G., Costa, J. A. V., Lim, L. T., . . . Zavareze, E. D. R. (2018). Ultrafine fibers of zein and anthocyanins as natural pH indicator. *Journal of the Science of Food and Agriculture*, *98*(7), 2735–2741.

Rajan, V. K., & Muraleedharan, K. (2017). A computational investigation on the structure, global parameters and antioxidant capacity of a polyphenol, Gallic acid. *Food Chemistry*, *220*, 93–99.

Sales, M. S., Roy, A., Antony, L., Banu, S. K., Jeyaraman, S., & Manikkam, R. (2018). Octyl gallate and gallic acid isolated from *Terminalia bellarica* regulates normal cell cycle in human breast cancer cell lines. *Biomedicine & Pharmacotherapy*, *103*, 1577–1584.

Shah, R. M., Malherbe, F., Eldridge, D., Palombo, E. A., & Harding, I. H. (2014). Physicochemical characterization of solid lipid nanoparticles (SLNs) prepared by a novel microemulsion technique. *Journal of Colloid and Interface Science*, *428*, 286–294.

Shahamirifard, S. A., Ghaedi, M., Razmi, Z., & Hajati, S. (2018). A simple ultrasensitive electrochemical sensor for simultaneous determination of gallic acid and uric acid in human urine and fruit juices based on zirconia-choline chloride-gold nanoparticles-modified carbon paste electrode. *Biosensors and Bioelectronics*, *114*, 30–36.

Smeets, A., Clasen, C., & Van den Mooter, G. (2017). Electrospraying of polymer solutions: Study of formulation and process parameters. *European Journal of Pharmaceutics and Biopharmaceutics*, *119*, 114–124.

Soltani, S., & Madadlou, A. (2015). Gelation characteristics of the sugar beet pectin solution charged with fish oil-loaded zein nanoparticles. *Food Hydrocolloids*, *43*, 664–669.

Sreekumar, S., Lemke, P., Moerschbacher, B. M., Torres-Giner, S., & Lagaron, J. M. (2017). Preparation and optimization of submicron chitosan capsules by water-based electrospraying for food and bioactive packaging applications. *Food Additives & Contaminants: Part A*, *34*(10), 1795–1806.

Tapia-Hernández, J. A., Torres-Chávez, P. I., Ramírez-Wong, B., Rascón-Chu, A., Plascencia-Jatomea, M., Barreras-Urbina, C. G., . . . Rodríguez-Félix, F. (2015). Micro-and nanoparticles by electrospray: Advances and applications in foods. *Journal of Agricultural and Food Chemistry*, *63*(19), 4699–4707.

Tapia-Hernández, J. A., Rodríguez-Felix, F., Juárez-Onofre, J. E., Ruiz-Cruz, S., Robles-García, M. A., Borboa-Flores, J., . . . Del-Toro-Sánchez, C. L. (2018). Zein-polysaccharide nanoparticles as matrices for antioxidant compounds: A strategy for prevention of chronic degenerative diseases. *Food Research International*, *111*, 451–471.

Tapia-Hernández, J. A., Rodríguez-Félix, F., & Katouzian, I. (2017). Nanocapsule formation by electrospraying. In *Nanoencapsulation Technologies for the Food and Nutraceutical Industries* (pp. 320–345). Amsterdam, Netherlands: Elsevier.

Tapia-Hernández, J. A., Rodríguez-Félix, D. E., Plascencia-Jatomea, M., Rascón-Chu, A., López-Ahumada, G. A., Ruiz-Cruz, S., & Rodríguez-Félix, F. (2018). Porous wheat gluten

microparticles obtained by electrospray: Preparation and characterization. *Advances in Polymer Technology*, *37*(6), 2314–2324.

Thapa, R. K., Nguyen, H. T., Jeong, J. H., Shin, B. S., Ku, S. K., Choi, H. G., . . . Kim, J. O. (2017). Synergistic anticancer activity of combined histone deacetylase and proteasomal inhibitor-loaded zein nanoparticles in metastatic prostate cancers. *Nanomedicine: Nanotechnology, Biology and Medicine*, *13*(3), 885–896.

Wang, M., Fu, Y., Chen, G., Shi, Y., Li, X., Zhang, H., & Shen, Y. (2018). Fabrication and characterization of carboxymethyl chitosan and tea polyphenols coating on zein nanoparticles to encapsulate β-carotene by anti-solvent precipitation method. *Food Hydrocolloids*, *77*, 577–587.

Xue, J., Zhang, Y., Huang, G., Liu, J., Slavin, M., & Yu, L. L. (2018). Zein-caseinate composite nanoparticles for bioactive delivery using curcumin as a probe compound. *Food Hydrocolloids*, *83*, 25–35.

Yang, Y., Li, W., Yu, D. G., Wang, G., Williams, G. R., & Zhang, Z. (2019). Tunable drug release from nanofibers coated with blank cellulose acetate layers fabricated using tri-axial electrospinning. *Carbohydrate Polymers*, *203*, 228–237.

Yang, Y. Y., Zhang, M., Liu, Z. P., Wang, K., & Yu, D. G. (2018). Meletin sustained-release gliadin nanoparticles prepared via solvent surface modification on blending electrospraying. *Applied Surface Science*, *434*, 1040–1047.

Yao, Y., Wu, M., Huang, Y., Li, C., Pan, X., Zhu, W., & Huang, Y. (2017). Appropriately raising fermentation temperature beneficial to the increase of antioxidant activity and gallic acid content in Eurotium cristatum-fermented loose tea. *LWT—Food Science and Technology*, *82*, 248–254.

Yu, D. G., Li, J. J., Williams, G. R., & Zhao, M. (2018). Electrospun amorphous solid dispersions of poorly water-soluble drugs: A review. *Journal of Controlled Release*, *292*, 91–100.

Yu, D. G., Zheng, X. L., Yang, Y., Li, X. Y., Williams, G. R., & Zhao, M. (2019). Immediate release of helicid from nanoparticles produced by modified coaxial electrospraying. *Applied Surface Science*, *473*, 148–155.

Zhang, S., & Han, Y. (2018). Preparation, characterisation and antioxidant activities of rutin-loaded zein-sodium caseinate nanoparticles. *PloS One*, *13*(3), e0194951.

Zou, T., Li, Z., Percival, S. S., Bonard, S., & Gu, L. (2012). Fabrication, characterization, and cytotoxicity evaluation of cranberry procyanidins-zein nanoparticles. *Food Hydrocolloids*, *27*(2), 293–300.

Zou, L., Zheng, B., Zhang, R., Zhang, Z., Liu, W., Liu, C., . . . McClements, D.J. (2016). Enhancing the bioaccessibility of hydrophobic bioactive agents using mixed colloidal dispersions: Curcumin-loaded zein nanoparticles plus digestible lipid nanoparticles. *Food Research International*, *81*, 74–82.

CONCLUSIONES

Los residuos del cártamo, en especial la mezcla hoja-tallo, son una fuente de CF que confieren alta actividad antioxidante. Las propiedades fisicoquímicas y reológicas de las soluciones poliméricas de zeína-CF son atributos que predicen el comportamiento del cono de Taylor, obteniendo un cono estable, de tipo chorro. La distribución del tamaño de partícula, diámetro promedio e índice de polidispersidad de los nanoencapsulados, es dependiente de la concentración del extracto de cártamo encapsulado. Finalmente, se puede concluir que la nanoencapsulación de los CF del cártamo en matrices de zeína, promueve la protección a cambios de pH y enzimas, simulando su paso durante el tracto gastrointestinal, aumentado su biodisponibilidad en un sistema *in vitro*, lo que abre nuevas líneas de investigación para que en estudios posteriores se analicen las diversas formas de aplicación, ya sean en la industria alimentaria y/o farmacéutica.